Compressive Stress Enhances Coordinated Migration of Mammary Carcinoma Cells

by

Janet M. Tse

B.S. Chemical Engineering
University of California, Berkeley (2002)

M.S. Chemical Engineering Practice
Massachusetts Institute of Technology (2006)

SUBMITTED TO THE DEPARTMENT OF CHEMICAL ENGINEERING
IN PARTIAL FULFILLMENT OF THE REQUIREMENTS FOR THE DEGREE OF

DOCTOR OF SCIENCE IN CHEMICAL ENGINEERING
AT THE
MASSACHUSETTS INSTITUTE OF TECHNOLOGY

February 2010

Signature of Author:_____
Department of Chemical Engineering
January 19, 2010

Certified by:_____
Rakesh K. Jain
Andrew Werk Cook Professor of Tumor Biology, Harvard Medical School
Thesis Supervisor

Certified by:_____
Robert S. Langer
Institute Professor
Thesis Supervisor

Accepted by:_____
William M. Deen
Professor of Chemical Engineering
Chairman, Committee for Graduate Students

Compressive Stress Enhances Coordinated Migration of Mammary Carcinoma Cells

by

Janet M. Tse

Submitted to the Department of Chemical Engineering on January 6, 2010
in Partial Fulfillment of the Requirements for the Degree of
Doctor of Science in Chemical Engineering

ABSTRACT

Cancer research has traditionally focused on genetic and biochemical changes during tumor progression. Uncontrolled cell proliferation of a solid tumor in a confined space not only creates well-studied oxidative stress (hypoxia), but also generates growth-induced mechanical stress (compression). However, the importance of such compressive stress in tumor biology has been largely ignored. Our lab has previously shown that compressive stress influences tumor spheroid growth and stimulates production of extracellular matrix molecules. Others have also demonstrated the importance of matrix rigidity in tumor development and enhanced tumor cell adhesion by hydrostatic pressure. Yet whether growth-induced compressive stress can enhance caner cell migration and invasion remains unclear.

The focus of this thesis is to evaluate the effect of anisotropic compressive stress on cancer cell motility. To mimic growth-induced compressive stress experienced by cancer cells *in vivo*, we developed an *in vitro* compression device for compressing a monolayer of cancer cells with precisely-defined normal forces. Here we show, for the first time, that externally-applied compressive stress resulted in faster migration of some mammary carcinoma cell lines. Independent of multi-cellular micro-organization, compression induced migration of mammary carcinoma cells in a coordinated sheet, initiated by "leader cells" – single cells at the leading edge of the sheet, extending long filopodia. Accompanied by redistribution of fibronectin deposition, compression enhanced cell-matrix adhesion and stabilized cell distension, thereby promoting coordinated cell migration. Using a stochastic model to simulate 2-D collective cell migration, cell distension and uniform cell migration were found to be crucial factors for effective collective migration. Our finding on compression-induced coordinated migration of mammary carcinoma cells has significant implications for *in vivo* situations where epithelial cancer cells form a "coordinated" invading mass guided by "leader" cells. Our work suggests that compressive stress generated by proliferating cancer cells can distort their shape, enhance cell-substrate adhesion and stimulate formation of leader cells responsible for collective cell migration. This discovery could open the door to characterization of novel pathways driven by mechanical-stress and improved strategies for cancer treatment.

Thesis Supervisor: Rakesh K. Jain
Title: Andrew Werk Cook Professor of Tumor Biology, Harvard Medical School

Thesis Supervisor: Robert S. Langer
Title: Institute Professor

Biographical Sketch

EDUCATION

2006	Massachusetts Institute of Technology, M.S., Chemical Engineering Practice
2002	University of California at Berkeley, B.S (*High Honors*) in Chemical Engineering

PROFESSIONAL EXPERIENCE

06/00-12/00	Undergraduate Researcher, Department of Chemical Engineering UC Berkeley, Berkeley, CA Advisor: Dr. Douglas S. Clark
01/01-12/02	Undergraduate Researcher, Department of Chemical Engineering UC Berkeley, Berkeley, CA Advisor: Dr. Jay D. Keasling
06/01-08/01	Research Intern Roche Bioscience, Palo Alto, CA
06/02-08/02	Research Intern, Drug Eluting Stent Unit Guidant Corporation, Santa Clara, CA
01/03-08/03	Chemical Engineer, Drug Eluting Stent Unit Guidant Corporation, Santa Clara, CA
02/04-present	Research Fellow, Edwin L. Steele Laboratory Massachusetts General Hospital, Charlestown, MA Advisors: Drs. Rakesh K. Jain and Robert S. Langer
02/05-03/05	Practice School, MIT Chemical Engineering Novartis Pharmaceuticals, Suffern, NY
04/05-05/05	Practice School, MIT Chemical Engineering General Mills, Golden Valley, MN
09/07-01/08	Teaching Assistant: Chemical/Biological Engineering Laboratory Department of Chemical Engineering, MIT, Cambridge, MA

HONORS AND AWARDS

Xerox Technical Minority Scholarship (2000-2001)
Elected to Tau Beta Pi (2001)
Robert T. Haslam Chemical Engineering Fellowship (2003)
Honorable Mention, National Science Foundation Graduate Research Fellowship (2003)

PUBLICATIONS

Cheng, G., **Tse, J**., Jain, R.K., Munn, L.L. *Micro-environmental mechanical stress controls tumor spheroid size and morphology by suppressing proliferation and inducing apoptosis in cancer cells*. PLoS One, 4(2): e4632, 2009.

J.M. Tse, G. Cheng, J.A. Tyrrell, S.A. Wilcox-Adelman, Y. Boucher, R.K. Jain, L.L. Munn, "Compression-induced cell distension and adhesion stimulate coordinated migration of mammary carcinoma cells." Submitted.

CONFERENCE PRSENTATIONS

"Mechanical stress-induced invasion of cancer cells: regulation of cell-cell contact and cell-substrate adhesion." Annual Meeting of the Biomedical Engineering Society, Pittsburgh, PA, October 2009.

"Mechanical stress induces cancer cell alignment and migration." Annual Meeting of the Biomedical Engineering Society, St. Louis, MO, October 2008.

Acknowledgements

I would like to start by thanking my thesis advisor Dr. Rakesh K. Jain for his support. His belief in my abilities has been palpable. He encourages me and pushes me to reach my full potential. He has provided me with countless opportunities to work on an exciting project and train myself to be a scientist and an engineer. His support for me has been boundless and I am deeply grateful. I would also like to specially thank one of my committee members Dr. Lance L. Munn for guiding me through my thesis project. His guidance, support and energy are inspirational. I am grateful to him for being unfailingly generous with his time. I would also like to thank Dr. Yves Boucher for his guidance during my first year in the lab.

I would also like to thank my co-advisor Dr. Robert S. Langer, my thesis committee members Drs. William W. Deen, Roger D. Kamm and Subra Suresh. They have provided me with invaluable advice and encouragement. I would also like to thank the MIT Chemical Engineering Department for opening many educational avenues and building solid and rigorous foundation for my career.

My friends in the Steele Lab have always been generous with their time and talents, and have been patient with me as I learned many new things. They have truly been a source of encouragement and I thank them for this. In particular, I would like to thank Sung-Suk Chae for his generous time when I consulted him for guidance and advice in molecular biology experiments. I would also like to thank Wilson Mok, Patrick Au, Josh Tam, Jonathan Song, Temitope Sodunke, Gang Cheng and my fellow graduate students: Benjamin Diop and Vikash Chauhan for all their supports. When I was frustrated about my experiments, they would cheer me up and encourage me to be positive and move forward. They have all been generous with their time, and have been my good listeners. Thank you for making the lab a really enjoyable place and keeping me company on many a late night. I don't know if I would be able to survive the frustration without fun and entertainment provided by them.

Finally, I would like to thank my family. Although I cannot recall a single conversation in which I discussed my research with any of them, they instilled in me the principles of hard work, persistence, patience and striving for excellence. These were essential traits for me to complete this thesis. I have never appropriately expressed to my parents the appreciation I feel for the sacrifices they have made for me. Especially, they gave up everything they had established in Hong Kong and moved to the United States simply for providing my brother and me with a better education. I hope that by dedicating this thesis to them I can begin to make up for that.

Table of Contents

List of Figures

List of Tables

Chapter 1: Introduction and background

Portions of the chapter have been taken from:

G. Cheng, **J. Tse**, R.K. Jain, L.L. Munn, "Micro-environment mechanical stress controls tumor spheroid size and morphology by suppressing proliferation and inducing apoptosis in cancer cells." PLoS One. 2009; 4(2): e4632.

Introduction

Cancer is the second leading cause of death in the United States, accounting for nearly 25% of total deaths [1]. The American Cancer Society estimates that about 565,650 Americans will die of cancer and 1.44 million new cancer cases will be diagnosed [1].

Cancer is a disease characterized by uncontrolled growth of abnormal cells, which have undergone DNA mutation. The most commonly mutated gene in human tumors is p53, which is a tumor suppressor gene promoting arrest in G1 and G2 checkpoints of the cell cycle, apoptosis, and DNA repair in response to damaged DNA [2]. The accumulation of DNA mutations promotes the development of cancers, not all of which form solid tumors. For instance, leukemias are cancers of white blood cells, which do not form solid tumors, but circulate in the blood vessels. However, over 85% of human cancers form solid tumors, such as carcinomas, sarcomas and adenocarcinomas [1].

These solid tumors transform over time from a benign cell mass into an invasive phenotype. Eventually, those malignant tumor cells spread to other parts of the body (metastasis) and become fatal. Cancer research has historically focused primarily on studying the role of genetic and biochemical changes in tumor progression. For instance, it is well established that intratumoral hypoxia (cancer cells starved of oxygen) activates certain genes, which promotes cancer cell motility and invasion. However, in growing solid tumors, cancer cells also experience compressive stress generated by uncontrolled cell proliferation in a confined space[3,4]. While it has been long known that mechanical

stimuli are essential for normal physiological processes such as tissue remodeling and maintenance [5-7], endothelial cell biology[8,9], and morphogenesis [10,11], the role of such compressive mechanical force (transmitted through pericellular matrix and cells) in cancer progression has not been widely investigated.

The importance of mechanical stress in tumor biology is being recognized increasingly. Our lab has previously shown that compressive stress influences tumor spheroid growth [3,4] and stimulates production of extracellular matrix molecules [12]. Others have also demonstrated the importance of matrix rigidity in tumor development [13-15] and enhanced tumor cell adhesion by hydrostatic pressures[16-18]. Yet whether growth-induced compressive stress can impose selection pressure for cancer cells with enhanced migratory and invasive potentials remains unclear.

The focus of this thesis is to evaluate the effect of anisotropic compressive stress on cancer cell motility. Here we show, for the first time, that externally-applied compressive stress results in faster migration of mammary carcinoma cells. Unlike geometry-driven migration in the control cultures, compression induces migration of 67NR mammary carcinoma cells in a coordinated sheet, initiated by "leader cells" – single cells at the leading edge of the sheet, extending long filopodia. Accompanied by redistribution of fibronectin deposition, applied compression enhances cell-matrix adhesion and stabilizes cell distension independent of actomyosin contractility. Our finding on the coordinated migration of 67NR mammary carcinoma cells induced by compressive stress has significant implications for *in vivo* situations where epithelial cancer cells form an

"coordinated" invading mass guided by "leader" cells [19]. They suggest that mechanical stress accumulated during tumor growth can enhance cell-substrate adhesion and trigger formation of leader cells during multicellular invasion.

Specific Aims

Hypothesis: Compressive stress generated by tumor growth promotes a more migratory phenotype in cancer cells

Specific Aim 1: Investigate the effect of compressive stress on cancer cell motility (Chapter 2).

Normal cells have regulated rates of proliferation, but cancer cells grow uncontrollably in a confined matrix [2]. Previous findings of collapsed intratumoral vessels [20] suggest that compressive stress is generated from proliferating cancer cells. While intratumoral hypoxia has been shown to be a selection pressure for aggressive cancer cells [21], whether externally-applied compressive stress induces similar selective pressure has yet to be studied. Our findings would open the door to a new class of targets for blocking mechanical stress pathways.

Specific Aim 1a: Develop an in vitro compression device for simulation of compressive stress experienced by tumor cells in vivo.

In order to simulate the compressive stress generated by rapid cell proliferation at the tumor margin *in vivo*, an *in vitro* compression device was developed to apply a desired normal force (anisotropic stress) to compress a cell monolayer. In this system, there were no nutrient limitations, hydrostatic force, or oxidative stress.

Specific Aim 1b: Screen for the effect of compressive stress on migration potential of various cancer cell lines.

To determine the effect of compressive stress on tumor malignancy, various cancer cell lines established from different tissues, such as breast, colon and kidney, were subjected to compressive stress and their migration potential were assessed with scratch-wound assay. A normal mammary epithelial cell line was also used for comparison.

Specific Aim 1c: Examine the cytoskeletal components of cancer cells in response to compression.

Mechanical stress has been shown to influence organization of cytoskeleton[22,23], which provides structural support and cell shape. As recent studies showed the importance of mechanical stress in breast tumor development[14,24], we investigated the cytoskeletal changes of mammary epithelial cells in response to mechanical compression. Hence, we stained the mammary carcinoma cell lines that demonstrated enhanced cell migration under compression in Aim 1b as well as the normal mammary epithelial cells for actin filaments and microtubules.

Specific Aim 1d: Determine whether compression-induced migration results from changes in gene transcription.

Mechanical stress propagated to a cell nucleus through matrix attachment and cytoskeletal filaments induces gene transcription [25-28]. While hypoxia has been shown to activate genes that stimulate cell migration and invasion such as CXCR4 and Met, mechanical stress has also been shown recently to induce Twist gene expression in *Drosophila* embryo [10] and Twist facilitates metastasis in mice [29]. To identify

compressive-stress-regulated genes in cancer cells, gene expression studies of 67NR mammary carcinoma cell line exhibiting the most prominent changes in migration potential in Aim 1b, were performed with DNA microarrays related to tumor metastasis and extracellular matrix (ECM) and adhesion molecules.

Specific Aim 2: Determine the effect of compressive stress on leader-cell formation and migration (Chapter 3).

Coordinated cell migration (collective cell migration) is prevalent in many epithelial cancers (as well as morphogenesis and tissue regeneration), and differs from single cell migration in that cells remain connected as they move, which results in a migrating sheet guided by "leader" cells[19,30]. While mechanical cues are critical in physiological processes involving collective migration, little is known about the effect of mechanical stress on leader-cell formation during collective migration. Our studies provide novel insights into how mechanical stimulation triggers coordinated migration in cancer.

Specific Aim 2a: Characterize the leader cells in the control and compressed cultures.

67NR mammary carcinoma cell line demonstrated coordinated migration behavior (such as migration in a sheet guided by leader cells) in Aim 1b. Using the *in vitro* scratch-wound assay, which is a useful tool to study collective migration, we stained the cells for actin filament and then quantified the difference in leader-cell formation between the control and compressed cultures. Moreover, we quantified the nuclear offset (an indicator for cell polarization) and cell size/length.

Specific Aim 2b: Evaluate the effect of compressive stress on geometry-driven migration.

Geometric cues (such as individual cell shape and multi-cellular micro-organization) can modulate cell proliferation [31] and direct the formation of lamellipodia and filopodia [32]. To determine whether geometric cues influence coordinated cell migration with or without compressive stress, we used microfabrication to control the organization of sheet of 67NR mammary carcinoma cells and then quantified the difference in migration rate and shape change of the cell pattern between the control and compressed cultures.

Specific Aim 2c: Examine the role of Rac1 and Cdc42 in compression-induced protrusions and migration.

Rac1 and Cdc42 – members of Rho family small guanosine triphosphate (GTP)-binding proteins (GTPases) – regulate cell shape, cell polarity and formation of protrusions, thereby affecting cell migration[33-35]. Hence, we measured the effect of compressive stress on activation of Rac1 and Cdc42 activity in 67NR mammary carcinoma cells. To determine the significance of Rac 1 and Cdc42 in compression-induced protrusions and migration, we perturbed the activity level of those Rho GTPases proteins using a molecular approach and performed the scratch-wound compression experiment. We quantified the migration rate of the control and compressed cells, and stained the cells for actin filaments to visualize their protrusions.

Specific Aim 3: Determine the effect of compressive stress on cell adhesion and migration (Chapter 4)

For migration to occur, any newly-formed protrusions have to be stabilized by attaching to the substrate surface. In addition, one of the hallmarks characterizing collective cell migration is the preserved cell-cell contact during movement [19,30]. While the

mechanisms of collective migration are less well understood, an understanding of the effect of mechanical stimulation on cell adhesion, including cell-cell and cell-matrix adhesions, during coordinated movement would enable us to define strategies to interfere with cancer cell migration.

Specific Aim 3a: Evaluate the role of cadherin-mediated cell-cell contacts in compression-induced migration

In coordinated migration, most of the adhesive cell-cell couplings are cadherin-mediated but some involve integrin-ECM interactions[36]. To determine whether E-cadherin expression plays a role in compression-associated migration, we treated E-cadherin-expressing normal mammary epithelial cells (MCF10A) and mammary carcinoma cells (MCF7) with an anti-E-cadherin antibody and determined their migration rate with scratch-wound assay in the presence or absence of compressive stress. In addition, we performed ectopic expression of E-cadherin in 67NR mammary carcinoma cells and quantified their motility in response to compression.

Specific Aim 3b: Quantify and characterize the effect of compressive stress on cell-matrix adhesion

Other than cell-cell coadhesion, cell-substrate interaction also plays an important role in modulating cell migration behavior. Therefore, we quantified the difference in the cell-matrix adhesion strength of 67NR mammary carcinoma cells between the control and compressed cultures using a shear detachment assay, and identified the ECM molecule accountable for compression-induced cell-matrix adhesion. Then, we determined the effect of compressive stress on the synthesis and spatial distribution of the determined ECM molecule with quantitative PCR and confocal immunofluorescence microscopy,

respectively. As cell-matrix adhesion involves formation of adhesion sites, immunostaining of focal adhesion-associated molecules such as focal adhesion kinase (FAK) and vinculin were also performed.

Specific Aim 3c: Assess the role of integrin signaling in compression-induced migration

Cell-matrix interaction involves integrin signaling[37,38]. Hence, we identified the integrin subunit involved in compression-induced migration of 67NR mammary carcinoma cells with integrin-blocking antibodies. We also determined the effect of compressive stress on the expression and spatial distribution of the integrin and its associated protein, paxillin, with Western blot and confocal immunofluorescence microscopy, respectively.

Specific Aim 3d: Determine the effect of actomyosin contractility on compression-induced migration.

Cell-matrix adhesion gives rise to intracellular contractile force mediated by actomyosin machinery, which is essential for maturation of focal contacts and stress fiber formation [39]. We examined the requirement of actin-myosin activity in compression-induced migration using molecular (such as dominant-negative RhoA retrovirus) and pharmacological (such as Rho kinase inhibitor Y-27632, myosin light-chain kinase inhibitor ML-7) approaches and quantified the migration rate with scratch-wound assay.

Specific Aim 4: Develop a preliminary and simple stochastic model to explain the experimental data on compression-induced coordinated migration (Chapter 5)

Our experimental observations on compression-induced coordinated migration of 67NR mammary carcinoma cells (Chapters 2-4) led us to propose that (1) dynamic coordination

of free-cell perimeter (related to the formation rate of protrusions) and cell-cell interactions would affect cell migration behavior; and (2) externally-applied stress could perturb the protrusion/migration rate. However, definitive experiments to test this hypothesis are elusive. A mathematical model has yet to be developed to describe the relative significance of free-cell perimeter and cell-cell contact on collective cell migration. Such a model would provide us with insights into the physical underpinnings governing the collective migration induced by compressive stress.

Specific Aim 4a: Simulate cell migration behavior observed in stress-free experiments

Based on our experimental observations under stress-free conditions, we developed a stochastic model to simulate 2-dimensional collective migration of cells initially arranged in a square geometry. Each cell is composed of multiple blocks such that their protrusion rates and cell-cell interactions can be determined separately according to the local microenvironment. Then a force balance - incorporating protrusive force (due to formation of protrusions) and cell-cell interactions - is performed to determine the direction of protrusion and migration.

Specific Aim 4b: Investigate the relative importance of various model parameters, such as free-cell perimeter, cell protrusion length and number of protrusions, in compression-induced coordinated cell migration.

Using the model developed in Aim 4a, we changed one model parameter at a time to determine what model parameter could be influenced by compression. By comparing the simulated migration patterns with our experimental observations of compressed cultures, the model provides an estimate of which critical parameters in the force balance are influenced by compressive stress.

Background

Role of mechanical force in normal tissue development and function

Cells are continuously exposed to a variety of mechanical stimuli including hydrostatic pressure, shear, compression and tension. Various lines of investigation have revealed that mechanical stresses play a critical role in normal physiological processes.

I. Force and embryogenesis/differentiation

During embryo development, the normal morphogenic movements generate compressive stress that affects the physical shape of the embryo. To mimic these developmental compressive forces, *Drosophila* (fruit flies) embryo was deformed by external uniaxial mechanical compression. The externally-applied force was shown to drive nuclear translocation of the transcriptional factor Armadillo and activate Twist expression, which controls the shape in the early *Dropsophila* embryo[10].

Mechanical forces are also important to normal tissue-specific development. For example, the major mechanical stimulus to the fetal lung growth is stretch induced by fetal breathing movements[40,41]. Abnormal forces exerted on lung tissues contribute to many pathological conditions such as pulmonary hypoplasia. Other examples are mechanical stretch-induced hypertrophic responses in cardiac myocytes[42], and hemodynamic forces as regulators for vascular endothelial gene expression[43].

II. Tissue maintenance and modeling

A balance of forces is required to maintain homeostasis in tissues, including bone[5,7] and cartilage [6,44]. For instance, exercise affects joint loading, and thus increases the proteoglycan content of articular cartilage, whereas reduced mobility leads to loss of

proteoglycan content and exacerbates arthritis-associated joint degeneration[45,46]. In addition, microgravity directly affects bone formation and resorption, contributing to severe loss of bone mass during space flight [47]. Similarly, while laminar shear stress induced by blood flow allows normal artery maturation, turbulent shear stress may lead to atherosclerosis[48].

Furthermore, mechanical forces of the same type can produce different responses depending on the magnitude, duration and application mode of loading. One specific example is the effect of compressive stress on the extracellular biosynthesis of chondrocytes. *In vitro* studies have shown that static compression on chondrocyte-seeded constructs or cartilage explants inhibits extracellular-matrix (ECM) biosynthesis [44] while dynamic compression stimulates ECM biosynthesis [49].

Experimental models for applying mechanical stimulation to living cells

Two main types of mechanical cues have been studied in the area of cell mechanobiology: (I) matrix stiffness and composition, and (II) external force application. Numerous novel experimental models have been developed to simulate various physical forces on cells *in vitro*.

I. Matrix stiffness and composition

3D culture systems made of cell-modifiable prefabricated ECM have been commonly used to study epithelial morphogenesis and malignant transformation[15,50]. Matrigel is critical for normal epithelial morphogenesis, but it is very soft with a modulus virtually identical to normal mammary tissue. Therefore, to explore the role of matrix stiffness in mammary tissue behavior, epithelial cells are cultured in Matrigel mixed with different

concentrations of collagen I for the desired the mechanical property[15]. In addition to the biologically-derived ECM, synthetic materials such as polyacrylamide gels functionalized with ligand of choice (e.g. fibronectin) have been used to illustrate the effect of substrate stiffness on cell phenotype [50,51].

II. Engineered devices for force application

The cellular response to mechanical stimulation depends on the type of force applied, the magnitude, frequency and duration of the applied stimuli. To modulate the temporal, spatial and intensity of physical forces applied to cells, various experimental devices have been developed (Fig. 1.1) and can be categorized into two approaches.

The first approach focuses on the response of individual cells directed to mechanical stimuli (Fig. 1.1A-D). For example, atomic force microscopy (Fig. 1.1A)[52] and magnetic twisting cytometry (Fig. 1.1B)[53] apply pico- to nano-Newton forces locally to a portion of the cell membrane. Micropipette aspiration (Fig. 1.1C) and optical trapping (Fig. 1.1D) deform an entire cell by applying suction through a micropipette placed on the surface of the cell[54], and directing the beads attached to the cell to move away or closer[55], respectively. It should be noted that these techniques, with appropriate analysis of deformation, can be used to probe the viscoelastic properties of cellular components[52,56,57].

While the previous techniques use sophisticated devices to apply precise forces to individual cells, cell-cell communication under mechanical stimulation is not considered. Therefore, another approach applies controlled forces to cell monolayers or 3D cultures (*ex vivo* explant culture or cells embedded in tissue-engineered scaffolds), which mimic

the forces that each cell would experience within their physiological microenvironment (tissues) (Fig.1.1E-H). For instance, flow chambers have been used to apply shear stresses to endothelial cells (Fig. 1.1E). Application of static or cyclic, axial or biaxial strains has been applied to monolayers of cells plated on a deformable membrane (Fig. 1.1F-H) in various organ models such as lung[41,58,59]. Systems for application of compression and hydrostatic pressures have also been developed to study ECM biosynthesis of chondrocytes[44,60], and cancer cell adhesion [16,61,62], respectively.

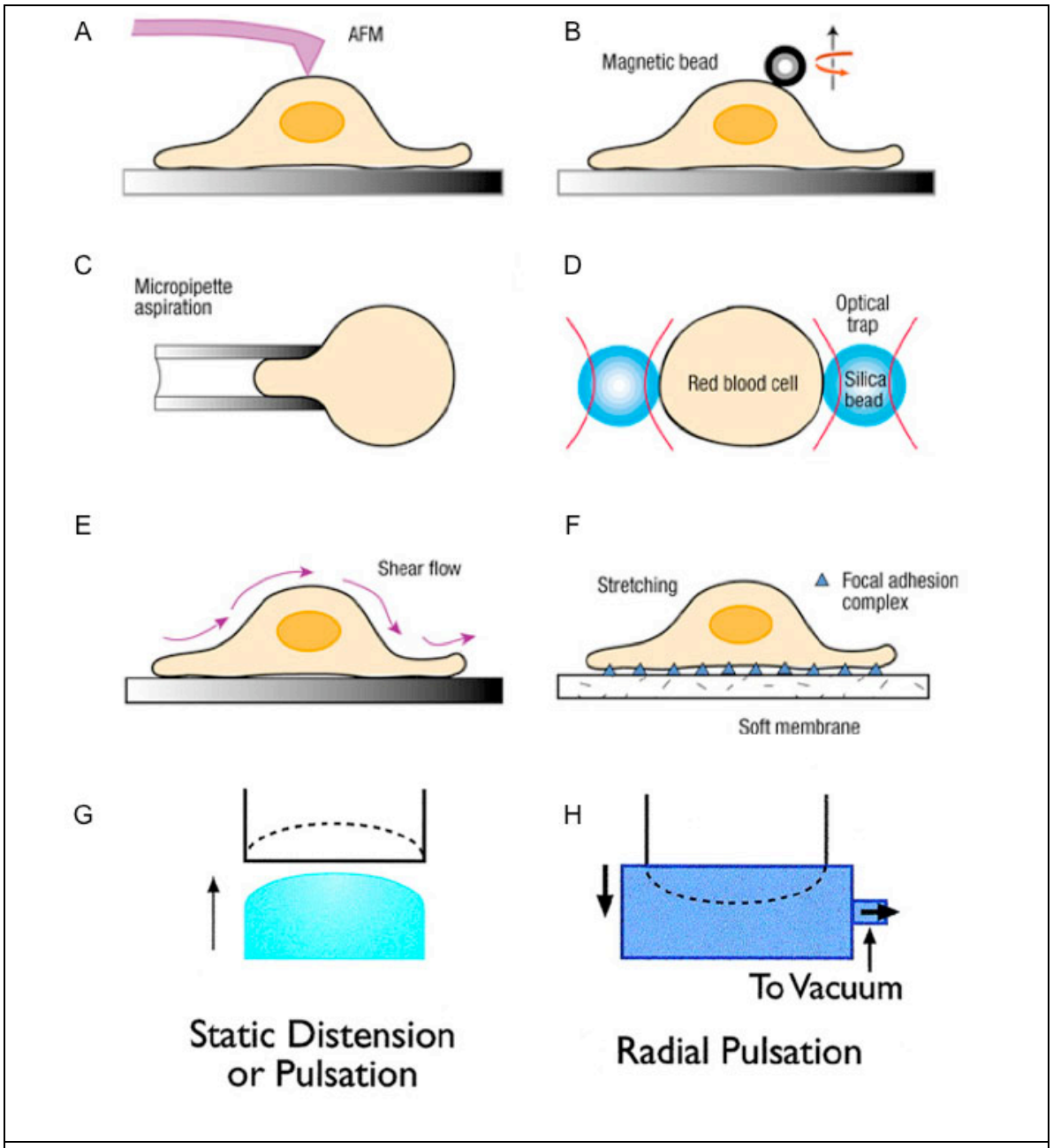

Figure 1.1. Schematic representations of different experimental techniques used to apply mechanical stimulation to living cells. A, Atomic force microscopy: a sharp tip at the free end of a flexible cantilever generates a local deformation on the cell surface. **B,** Magnetic twisting cytometry: magnetic beads with functionalized surfaces are attached to a cell and a magnetic field imposes a twisting moment on the beads, thereby deforming a

portion of the cell. **C,** Micropipette aspiration: a cell is deformed by applying suction through a micropipette. **D,** Optical trapping: a trap is used with two microbeads attached to the opposite ends of a cell. **E,** Shear flow: a parallel-plate flow channel applies shear stress to cells cultured as a monolayer. **F,** Uniaxial stretch: cells are cultured on a thin-sheet polymer substrate, such as silicone, which is stretched uniaxially to deform cells. **G, H,** Biaxial stretch: cells are cultured on an elastic membrane that is pushed upward (**G**) or pulled downward by negative pressure **(H)**. (Figures reproduced and modified from refs. [41,57])

Mechanical models of mechanotransduction

Cells sense and convert mechanical cues into biochemical responses, such as activation of gene transcriptions [63]. Two similar mechanical paradigms – tensegrity[64-66] and adhesion-mediated mechanosensing[67,68]- have been described to explain how cells respond to mechanical stress involving actin cytoskeleton.

Cells do not simply contain viscous cytoplasm surrounded by a plasma membrane, they also contain cytoskeleton – a cellular "skeleton" contained with the cytoplasm- to provide structural support for maintaining cell shape and enabling cellular motion. The tensegrity model suggests that cells exist in a "pre-stress" state, in which their intracellular tension generated in the actin cytoskeleton is balanced by internal microtubule struts and external ECM adhesions. Thus, cellular response to external mechanical loading can vary with the level of intracellular tension in the cell. More importantly, since cell surface-ECM adhesion receptors such as integrins are linked intracellularly to actin cytoskeleton, the

tensegrity theory indicates that mechanical signals that are transmitted across integrin receptors can be transduced into a chemical response through distortion-dependent changes in cytoskeletal structure either locally at the site of receptor binding or distally at other locations inside the cell [69,70] (Fig. 1.2). Similarly, adhesion-mediated mechanosensing model suggests that mechanical stimuli transmitted via actin filaments to mechanosensitive layer of focal adhesions triggers the growth of focal adhesions in the direction of the intracellular tension[67].

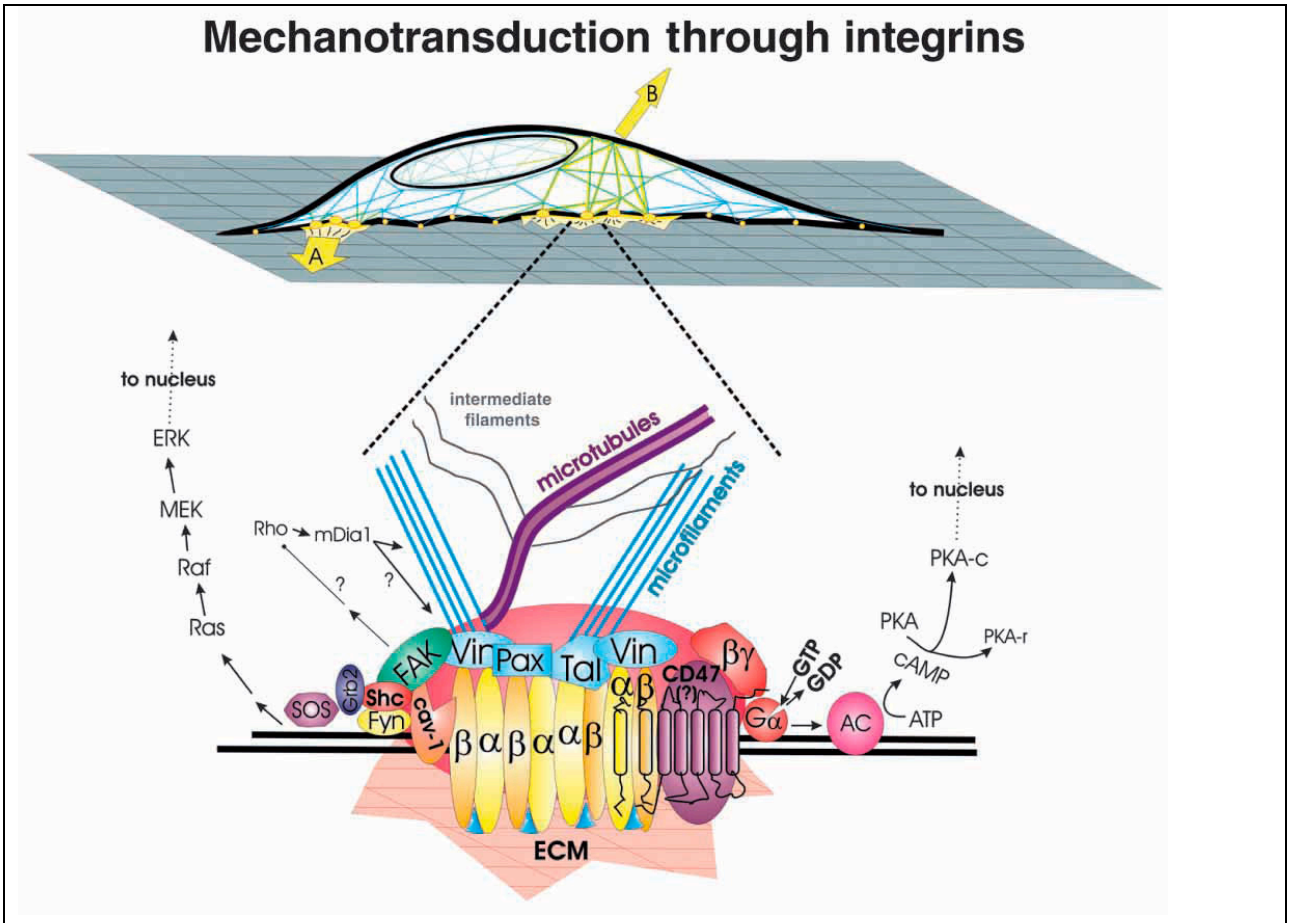

Figure 1.2. Schematic diagram of how forces applied via ECM (A) or directly to the cell surface (B) transmit across integrins and focal adhesions to induce a biochemical response, respectively. Forces (A) concentrated within the focal adhesion can stimulate clustering of

dimeric (α,β) integrin receptors and induce recruitment of focal adhesion proteins (e.g. vinculin (Vin), paxillin (Pax), talin (Tal)) that connect to cytoskeletal structures (actin filaments and microtubules), thereby activating integrin-associated signaling cascades, such as focal adhesion kinase (FAK). Cell distortion induced by forces (B) increase intracellular tension, which is transmitted to focal adhesions through the cytoskeleton. (Figure reproduced from ref. [65])

Mechanical stress and cancer biology

Historically, research in cancer biology has been focused in genetic or molecular changes in the tumor cells and their cellular responses to extrinsic soluble cues such as growth factors and cytokines. Only in recent years, the importance of mechanical stress in tumor biology has been increasingly appreciated. Indeed, cancer cells in tumors have been shown to experience (i) matrix stiffening due to abundant deposit of collagenous fibers synthesized by activated stromal myofibroblasts[71], (ii) increased interstitial pressure due to a leaky vasculature and poor lymphatic drainage[72,73], and (iii) increased compressive stress due to the expanding tumor mass[3,4]. As cancer cells escape from the tumor and get into blood vessels or lymphatic system, increased hydrostatic pressures enhance tumor cell adhesion to epithelium or extracellular matrix[16-18].

Previous studies have shown the importance of matrix rigidity in tumor development and tumor progression [13-15,74], whereas increased interstitial pressures present significant challenges to drug delivery[75-77] and influence tumor cell proliferation[78]. As for growth-induced compressive stress, little is known about the dynamics of such stress accumulation in tumors or its mechanical impact on tumor pathophysiology. Growth-

induced compressive stress (solid stress) is mechanical compression transmitted through the structural elements of the interstitium and the cells. It is unlikely affected by interstitial fluid pressures, which is transmitted through intra- and extracellular fluids, under physiological conditions. There have been no physical ways to measure solid stress reliably in tumors *in vivo* and the heterogeneity of a tumor makes the spatial quantification of solid stress within the tumor and its surrounding matrix even more challenging.

However, our lab has presented evidence of compressive stress generated by tumor cells in a mouse model that collapsed intratumor blood vessels opened again after killing cancer cells surrounding them [20] (Fig.1.3). A case report also showed that a young adult had visual loss due to the tumor-induced intracranial extrinsic compression of the optic nerve [79].

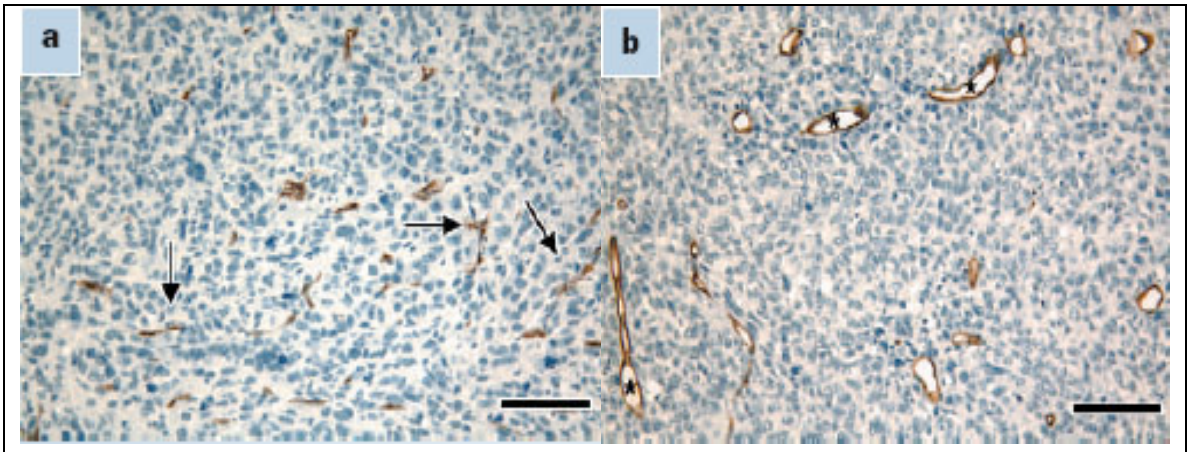

Figure 1.3. Compressive stress generated by cancer cells collapses blood vessels. In a mouse model, collapsed blood vessels (arrows in panel a) have an open lumen (asterisks in panel b) after relieving compressive forces generated by cancer cells. Scale bars, 50

μm. (Figure reproduced from ref [20])

To better understand the mechanical impact on tumors, our lab has previously demonstrated that the growth of tumor spheroids in agarose gel is inhibited by increasing gel stiffness[3] and the growth-induced mechanical stress distribution controls tumor spheroid shape[4], as shown in Figure 1.4. Similarly, using multiple-particle tracking, an invading brain tumor spheroid in Matrigel (containing polymer beads as reference markers) has also been shown to exert mechanical pressure and significant traction on its microenvironment[80].

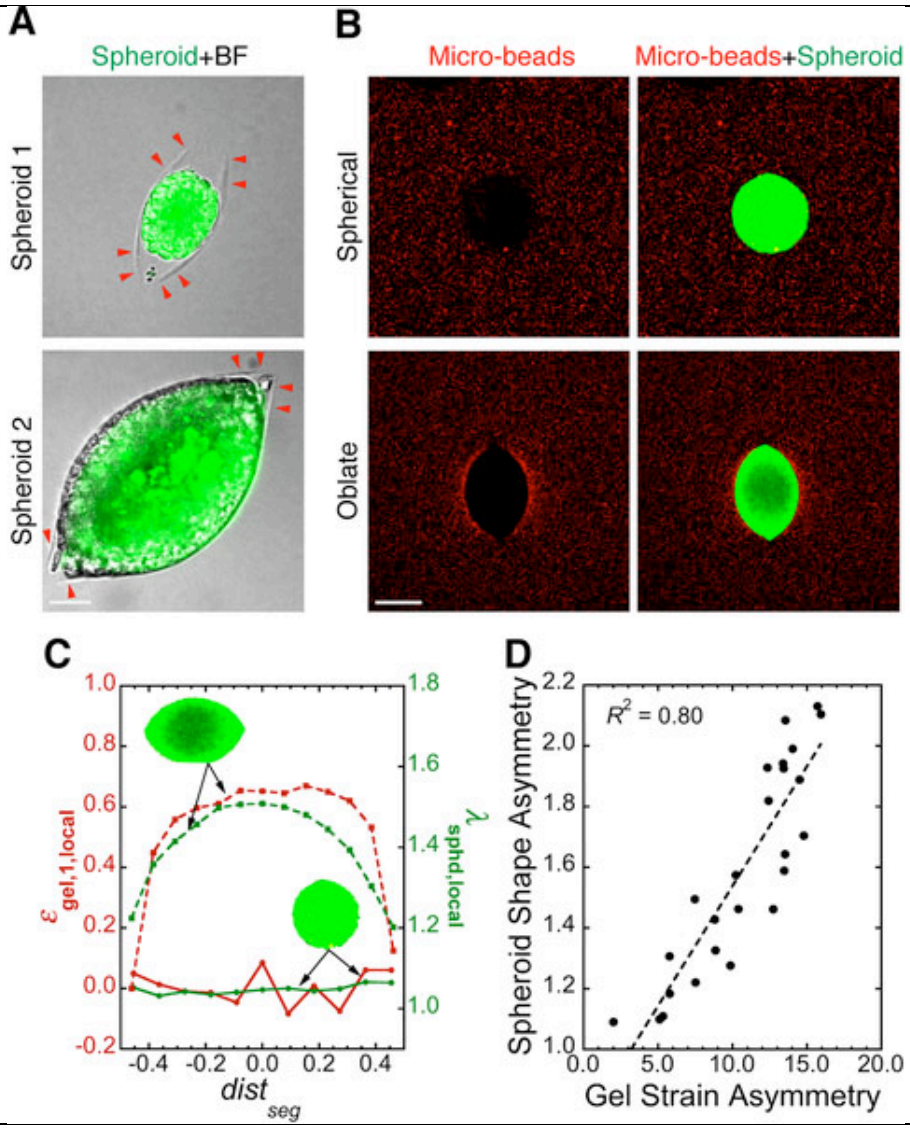

Figure 1.4. Growth-induced mechanical stress distribution controls tumor spheroid shape. A, Agarose gel can fail under tension from growing tumor spheroids (green). Red arrowheads indicate the edge of planar cracks in the agarose gel (BF: bright-field image taken in Nomarski mode). Scale bar = 50 μm. **B,** Spheroids (green) of different shapes and their surrounding stress fields visualized by micro-beads (red). Scale bar = 150 μm. **C,** Relationship between local strain in agarose gel ($\varepsilon_{gel,1,local}$) and local spheroid deformation ($dist_{seg}$) for the spheroids (green, inset) shown in **A**. $dist_{seg}$ is the distance of spheroid segments from spheroid center normalized over the length of the major axis. **D,**

Correlation between the asymmetry in spheroid shape and in the corresponding strain in the surrounding agarose gel, showing that spheroids are more deformed along the direction of higher stress. Each data point is for one spheroid. *R* is the linear regression coefficient ($p<0.0001$). (Figure reproduced from ref[4])

In addition, mathematical models have been recently developed to determine the level of compressive stress induced by tumor growth [81,82]. Using mechanical properties of the tumor and its surrounding tissue, the model predicts equal radial and circumferential stresses at the necrotic center of the spheroid but higher circumferential stress than radial stress near the spheroid boundary (i.e. tumor's advancing front with rapid cell proliferation)[81]. Table 1.1 summarizes key studies of mechanical stress in tumor biology.

Growth-induced compressive stress and tumor malignancy?

As mentioned above, cancer cells experience different kind of mechanical stresses. In this thesis, we focused on whether growth-induced compressive stress increases cancer cell motility, because such compressive stress might impose similar selection pressure as demonstrated by oxidative stress[21].

Proliferating tumors rapidly outgrow their blood supply, leaving the cancer cells starved of oxygen – a condition known as hypoxia (oxidative stress). Meanwhile, cancer cells also experience compressive stress generated by uncontrolled cell proliferation in a confined space. Growth-induced compressive stress inhibits the growth of tumor

spheroids in agarose [3,4], whereas a tumor with regions beyond the limits of oxygen diffusion can neither expand beyond a few cubic millimeters in size without an adequate oxygen supply [83]. It is well-established that intratumoral hypoxia (oxidative stress) selects for cancer cells with enhanced migratory and invasive potentials, involving the activation of genes such as Met and CXCR4[21,84-87]. However, little is known about the effect of growth-induced compressive stress on tumor malignancy.

Our lab has previously shown that such compressive stress stimulates hyaluronan synthesis in tumor spheroids [12], of which higher concentrations have been associated with malignant tumors [88-90]. Moreover, other studies have shown that mechanical compression induces Twist gene expression in *Drosophila* embryo [10] and Twist facilitates metastasis in mice [29]. Taken together, we hypothesized that compressive stress generated by tumor growth promotes a more migratory phenotype in cancer cells.

Year	Type of Mechanical Stress*	Studies	Refs
1997	III	Growth-induced stress suppresses tumor spheroid growth	[3]
1999	III	Neoplastic cell density can affect blood vessel diameter	[91]
2000, 2004, 2006, 2008, 2009	II	Increased extracellular hydrostatic pressure enhances cancer cell adhesion	[16-18,61,92-94]
2002	III	Solid stress facilitates spheroid formation	[12]
2003	III	Multiple particle tracking is developed to measure mechanical stress exerted by the brain tumor to Matrigel	[80]
2003	III	A linear poroelasticity model is developed to estimate growth-induced stress	[81]
2004	III	Cancer cells compress intratumor vessels	[20]
2004	II	Shear stress enhances colon cancer cell adhesion	[95]

2004, 2005	I	Matrix rigidity induces malignant phenotypes	[15,24]
2006	II	High tumor interstitial fluid pressure can contribute to increased tumor proliferation	[78]
2009	I	Matrix crosslinking forces tumor progression	[74]
2009	III	Local mechanical stress controls tumor spheroid size and shape	[4]

Table 1.1. Studies of mechanical stress in tumor biology. (*I: Matrix rigidity; II: Fluid pressure (shear/static); III: Solid stress generated by expanding tumor mass)

Cell migration

Cell migration is an important process for many physiological processes such as tissue development, immune response, and cancer metastasis [96,97]. Some cells migrate as individuals (single-cell migration) but many cell types will remain connected and move in groups (collective cell migration) under physiological conditions such as wound repair and even cancer invasion [19].

Single-cell migration has been well-studied and is a highly integrated multistep process, which can be described as follows[96,98]: (i) the cell polarizes and extends lamellipodial/filopodial protrusions (generally driven by actin polymerization) in the direction of migration guided by external cues such as soluble gradients; (ii) the cell makes adhesions to ECM via adhesion receptors such as integrins to stabilize the protrusions and generate traction on the substrate; (iii) the cell retracts its rear after disassembly of rear adhesions so that it can translocate its cell body forward.

In the classical view of metastasis – a process of tumor cells spreading to other parts of the body, transformation of epithelial-like tumor cells to become mesenchymal is thought to be required for them to migrate as single cells[99]. However, it becomes more

prominent that tumor cells can also invade the surrounding environment in clusters or strands [100]- another mode of movement, termed as collective/coordinated cell migration. Collective cell movement still retains the principles of single-cell migration, but the main difference is that the cells remain coupled by cell-cell coadhesions (which can be mediated by cadherins [101]or integrins[36]) during collective cell movement and the moving group is usually guided by multiple "leader" cells[19,30,102]. These leader cells at the edge of a group may be polarized by distinct free edge versus cell-cell contact edge within the physically connected sheets of cells[102].

Several *in vitro* and *in vivo* experimental systems exist to study collective cell migration[19,103]. The most common 2D *in vitro* model is scratch-wound assay: an artificial wound generated by mechanical removal of cells from a central region across a confluent monolayer of cells of epithelial cells [33,104]. The assay allows cell-cell and cell-matrix interactions to be studied during the wound closure. In this thesis, we have used scratch-wound assay to quantify the difference in the migration potential of epithelial cancer cells between the control and compressed cultures.

References

1. Jemal, A., R. Siegel, E. Ward, Y. Hao, J. Xu, T. Murray, and M.J. Thun. 2008. Cancer statistics, 2008. *CA Cancer J Clin*. 58:71-96.
2. Lodish, H., A. Berk, P. Matsudaira, C. Kaiser, M. Krieger, M.P. Scott, S.L. Zipursky, and J. Darnell. 2004. Molecular cell biology. W.H. Freeman and Company. 973 pp.
3. Helmlinger, G., P.A. Netti, H.C. Lichtenbeld, R.J. Melder, and R.K. Jain. 1997. Solid stress inhibits the growth of multicellular tumor spheroids. *Nat Biotechnol*. 15:778-83.

4. Cheng, G., J. Tse, R.K. Jain, and L.L. Munn. 2009. Micro-environmental mechanical stress controls tumor spheroid size and morphology by suppressing proliferation and inducing apoptosis in cancer cells. *PLoS ONE*. 4:e4632.
5. Burr, D.B., A.G. Robling, and C.H. Turner. 2002. Effects of biomechanical stress on bones in animals. *Bone*. 30:781-6.
6. Grodzinsky, A.J., M.E. Levenston, M. Jin, and E.H. Frank. 2000. Cartilage tissue remodeling in response to mechanical forces. *Annu Rev Biomed Eng*. 2:691-713.
7. Nagatomi, J., B.P. Arulanandam, D.W. Metzger, A. Meunier, and R. Bizios. 2002. Effects of cyclic pressure on bone marrow cell cultures. *J Biomech Eng*. 124:308-14.
8. Chien, S. 2006. Mechanical and chemical regulation of endothelial cell polarity. *Circ Res*. 98:863-5.
9. Yao, Y., A. Rabodzey, and C.F. Dewey, Jr. 2007. Glycocalyx modulates the motility and proliferative response of vascular endothelium to fluid shear stress. *Am J Physiol Heart Circ Physiol*. 293:H1023-30.
10. Farge, E. 2003. Mechanical Induction of Twist in the Drosophila Foregut/Stomodeal Primordium. *Current Biology*. 13:1365-1377.
11. Nerurkar, N.L., A. Ramasubramanian, and L.A. Taber. 2006. Morphogenetic adaptation of the looping embryonic heart to altered mechanical loads. *Dev Dyn*. 235:1822-9.
12. Koike, C., T.D. McKee, A. Pluen, S. Ramanujan, K. Burton, L.L. Munn, Y. Boucher, and R.K. Jain. 2002. Solid stress facilitates spheroid formation: potential involvement of hyaluronan. *Br J Cancer*. 86:947-53.
13. Butcher, D.T., T. Alliston, and V.M. Weaver. 2009. A tense situation: forcing tumour progression. *Nat Rev Cancer*. 9:108-22.
14. Kumar, S., and V.M. Weaver. 2009. Mechanics, malignancy, and metastasis: the force journey of a tumor cell. *Cancer Metastasis Rev*. 28:113-27.
15. Paszek, M.J., N. Zahir, K.R. Johnson, J.N. Lakins, G.I. Rozenberg, A. Gefen, C.A. Reinhart-King, S.S. Margulies, M. Dembo, D. Boettiger, D.A. Hammer, and V.M. Weaver. 2005. Tensional homeostasis and the malignant phenotype. *Cancer Cell*. 8:241-254.
16. Basson, M.D., C.F. Yu, O. Herden-Kirchoff, M. Ellermeier, M.A. Sanders, R.C. Merrell, and B.E. Sumpio. 2000. Effects of increased ambient pressure on colon cancer cell adhesion. *J Cell Biochem*. 78:47-61.
17. Downey, C., K. Alwan, V. Thamilselvan, L. Zhang, Y. Jiang, A.K. Rishi, and M.D. Basson. 2006. Pressure stimulates breast cancer cell adhesion independently of cell cycle and apoptosis regulatory protein (CARP)-1 regulation of focal adhesion kinase. *Am J Surg*. 192:631-5.
18. Craig, D.H., C.P. Gayer, K.L. Schaubert, Y. Wei, J. Li, Y. Laouar, and M.D. Basson. 2009. Increased extracellular pressure enhances cancer cell integrin-binding affinity through phosphorylation of beta1-integrin at threonine 788/789. *Am J Physiol Cell Physiol*. 296:C193-204.
19. Friedl, P., and D. Gilmour. 2009. Collective cell migration in morphogenesis, regeneration and cancer. *Nat Rev Mol Cell Biol*. 10:445-57.
20. Padera, T.P., B.R. Stoll, J.B. Tooredman, D. Capen, E. di Tomaso, and R.K. Jain. 2004. Pathology: cancer cells compress intratumour vessels. *Nature*. 427:695.

21. Bernards, R. 2003. Cancer: cues for migration. *Nature*. 425:247-8.
22. Dartsch, P.C., and E. Betz. 1989. Response of cultured endothelial cells to mechanical stimulation. *Basic Res Cardiol*. 84:268-81.
23. Li, J., S. Zhang, J. Chen, T. Du, Y. Wang, and Z. Wang. 2009. Modeled microgravity causes changes in the cytoskeleton and focal adhesions, and decreases in migration in malignant human MCF-7 cells. *Protoplasma*.
24. Paszek, M.J., and V.M. Weaver. 2004. The tension mounts: mechanics meets morphogenesis and malignancy. *J Mammary Gland Biol Neoplasia*. 9:325-42.
25. Alenghat, F.J., and D.E. Ingber. 2002. Mechanotransduction: All Signals Point to Cytoskeleton, Matrix, and Integrins. *Science's STKE*. 2002:pe6-.
26. Ingber, D.E. 2003. Tensegrity II. How structural networks influence cellular information processing networks. *J Cell Sci*. 116:1397-408.
27. Ingber, D.E. 2003. Tensegrity I. Cell structure and hierarchical systems biology. *J Cell Sci*. 116:1157-73.
28. Wang, N., J.P. Butler, and D.E. Ingber. 1993. Mechanotransduction across the cell surface and through the cytoskeleton. *Science*. 260:1124-7.
29. Yang, J., S.A. Mani, J.L. Donaher, S. Ramaswamy, R.A. Itzykson, C. Come, P. Savagner, I. Gitelman, A. Richardson, and R.A. Weinberg. 2004. Twist, a Master Regulator of Morphogenesis, Plays an Essential Role in Tumor Metastasis. *Cell*. 117:927-939.
30. Ilina, O., and P. Friedl. 2009. Mechanisms of collective cell migration at a glance. *J Cell Sci*. 122:3203-8.
31. Nelson, C.M., R.P. Jean, J.L. Tan, W.F. Liu, N.J. Sniadecki, A.A. Spector, and C.S. Chen. 2005. Emergent patterns of growth controlled by multicellular form and mechanics. *Proc Natl Acad Sci U S A*. 102:11594-9.
32. Brock, A., E. Chang, C.C. Ho, P. LeDuc, X. Jiang, G.M. Whitesides, and D.E. Ingber. 2003. Geometric determinants of directional cell motility revealed using microcontact printing. *Langmuir*. 19:1611-7.
33. Nobes, C.D., and A. Hall. 1999. Rho GTPases control polarity, protrusion, and adhesion during cell movement. *J Cell Biol*. 144:1235-44.
34. Machacek, M., L. Hodgson, C. Welch, H. Elliott, O. Pertz, P. Nalbant, A. Abell, G.L. Johnson, K.M. Hahn, and G. Danuser. 2009. Coordination of Rho GTPase activities during cell protrusion. *Nature*. 461:99-103.
35. Ridley, A.J. 2001. Rho GTPases and cell migration. *J Cell Sci*. 114:2713-22.
36. Casey, R.C., K.M. Burleson, K.M. Skubitz, S.E. Pambuccian, T.R. Oegema, Jr., L.E. Ruff, and A.P. Skubitz. 2001. Beta 1-integrins regulate the formation and adhesion of ovarian carcinoma multicellular spheroids. *Am J Pathol*. 159:2071-80.
37. Berrier, A.L., and K.M. Yamada. 2007. Cell-matrix adhesion. *J Cell Physiol*. 213:565-73.
38. Zamir, E., and B. Geiger. 2001. Molecular complexity and dynamics of cell-matrix adhesions. *J Cell Sci*. 114:3583-90.
39. Chrzanowska-Wodnicka, M., and K. Burridge. 1996. Rho-stimulated contractility drives the formation of stress fibers and focal adhesions. *J Cell Biol*. 133:1403-15.
40. Kitterman, J.A. 1996. The effects of mechanical forces on fetal lung growth. *Clin Perinatol*. 23:727-40.

41. Liu, M., A.K. Tanswell, and M. Post. 1999. Mechanical force-induced signal transduction in lung cells. *Am J Physiol*. 277:L667-83.
42. Sadoshima, J., and S. Izumo. 1997. The cellular and molecular response of cardiac myocytes to mechanical stress. *Annu Rev Physiol*. 59:551-71.
43. Resnick, N., H. Yahav, L.M. Khachigian, T. Collins, K.R. Anderson, F.C. Dewey, and M.A. Gimbrone, Jr. 1997. Endothelial gene regulation by laminar shear stress. *Adv Exp Med Biol*. 430:155-64.
44. Chen, A.C., and R.L. Sah. 1998. Effect of static compression on proteoglycan biosynthesis by chondrocytes transplanted to articular cartilage in vitro. *J Orthop Res*. 16:542-50.
45. Bird, J.L., D. Platt, T. Wells, S.A. May, and M.T. Bayliss. 2000. Exercise-induced changes in proteoglycan metabolism of equine articular cartilage. *Equine Vet J*. 32:161-3.
46. Haapala, J., M.J. Lammi, R. Inkinen, J.J. Parkkinen, U.M. Agren, J. Arokoski, I. Kiviranta, H.J. Helminen, and M.I. Tammi. 1996. Coordinated regulation of hyaluronan and aggrecan content in the articular cartilage of immobilized and exercised dogs. *J Rheumatol*. 23:1586-93.
47. Tamma, R., G. Colaianni, C. Camerino, A. Di Benedetto, G. Greco, M. Strippoli, R. Vergari, A. Grano, L. Mancini, G. Mori, S. Colucci, M. Grano, and A. Zallone. 2009. Microgravity during spaceflight directly affects in vitro osteoclastogenesis and bone resorption. *FASEB J*. 23:2549-54.
48. Davies, P.F., A. Remuzzi, E.J. Gordon, C.F. Dewey, Jr., and M.A. Gimbrone, Jr. 1986. Turbulent fluid shear stress induces vascular endothelial cell turnover in vitro. *Proc Natl Acad Sci U S A*. 83:2114-7.
49. Kisiday, J.D., M. Jin, M.A. DiMicco, B. Kurz, and A.J. Grodzinsky. 2004. Effects of dynamic compressive loading on chondrocyte biosynthesis in self-assembling peptide scaffolds. *Journal of Biomechanics*. 37:595-604.
50. Lopez, J.I., J.K. Mouw, and V.M. Weaver. 2008. Biomechanical regulation of cell orientation and fate. *Oncogene*. 27:6981-93.
51. Ulrich, T.A., E.M. de Juan Pardo, and S. Kumar. 2009. The Mechanical Rigidity of the Extracellular Matrix Regulates the Structure, Motility, and Proliferation of Glioma Cells. *Cancer Res*. 69:4167-4174.
52. Mathur, A.B., A.M. Collinsworth, W.M. Reichert, W.E. Kraus, and G.A. Truskey. 2001. Endothelial, cardiac muscle and skeletal muscle exhibit different viscous and elastic properties as determined by atomic force microscopy. *Journal of Biomechanics*. 34:1545-1553.
53. Pommerenke, H., E. Schreiber, F. Durr, B. Nebe, C. Hahnel, W. Moller, and J. Rychly. 1996. Stimulation of integrin receptors using a magnetic drag force device induces an intracellular free calcium response. *Eur J Cell Biol*. 70:157-64.
54. Hochmuth, R.M. 2000. Micropipette aspiration of living cells. *J Biomech*. 33:15-22.
55. Gan, Y. 2007. Invited review article: a review of techniques for attaching micro- and nanoparticles to a probe's tip for surface force and near-field optical measurements. *Rev Sci Instrum*. 78:081101.

56. Bausch, A.R., F. Ziemann, A.A. Boulbitch, K. Jacobson, and E. Sackmann. 1998. Local Measurements of Viscoelastic Parameters of Adherent Cell Surfaces by Magnetic Bead Microrheometry. *Biophys. J.* 75:2038-2049.
57. Bao, G., and S. Suresh. 2003. Cell and molecular mechanics of biological materials. *Nat Mater*. 2:715-25.
58. Vanderploeg, E.J., S.M. Imler, K.R. Brodkin, A.J. Garcia, and M.E. Levenston. 2004. Oscillatory tension differentially modulates matrix metabolism and cytoskeletal organization in chondrocytes and fibrochondrocytes. *J Biomech*. 37:1941-52.
59. Wall, M.E., P.S. Weinhold, T. Siu, T.D. Brown, and A.J. Banes. 2007. Comparison of cellular strain with applied substrate strain in vitro. *J Biomech*. 40:173-81.
60. Ragan, P.M., V.I. Chin, H.H. Hung, K. Masuda, E.J. Thonar, E.C. Arner, A.J. Grodzinsky, and J.D. Sandy. 2000. Chondrocyte extracellular matrix synthesis and turnover are influenced by static compression in a new alginate disk culture system. *Arch Biochem Biophys*. 383:256-64.
61. van Zyp, J.V., W.C. Conway, D.H. Craig, N.V. van Zyp, V. Thamilselvan, and M.D. Basson. 2006. Extracellular pressure stimulates tumor cell adhesion in vitro by paxillin activation. *Cancer Biol Ther*. 5:1169-78.
62. Flanigan, T.L., D.H. Craig, C.P. Gayer, and M.D. Basson. 2009. 35: Increased Extracellular Pressure and Integrin Phosphorylation Independently Influence Fibroblast Migration. *Journal of Surgical Research*. 151:187-187.
63. Khachigian, L.M., N. Resnick, M.A. Gimbrone, Jr., and T. Collins. 1995. Nuclear factor-kappa B interacts functionally with the platelet-derived growth factor B-chain shear-stress response element in vascular endothelial cells exposed to fluid shear stress. *J Clin Invest*. 96:1169-75.
64. Ingber, D.E. 2008. Tensegrity and mechanotransduction. *J Bodyw Mov Ther*. 12:198-200.
65. Ingber, D.E. 2003. Tensegrity II. How structural networks influence cellular information processing networks. *J Cell Sci*. 116:1397-408.
66. Ingber, D.E. 2003. Tensegrity I. Cell structure and hierarchical systems biology. *J Cell Sci*. 116:1157-73.
67. Bershadsky, A., M. Kozlov, and B. Geiger. 2006. Adhesion-mediated mechanosensitivity: a time to experiment, and a time to theorize. *Curr Opin Cell Biol*. 18:472-81.
68. Bershadsky, A.D., N.Q. Balaban, and B. Geiger. 2003. Adhesion-dependent cell mechanosensitivity. *Annu Rev Cell Dev Biol*. 19:677-95.
69. Ingber, D.E. 1997. Tensegrity: the architectural basis of cellular mechanotransduction. *Annu Rev Physiol*. 59:575-99.
70. Ingber, D. 1991. Integrins as mechanochemical transducers. *Curr Opin Cell Biol*. 3:841-8.
71. Shao, Z.-M., M. Nguyen, and S. Barsky. 2000. Human breast carcinoma desmoplasia is PDGF initiated. *Oncogene*. 19:4337-4345.
72. Less, J.R., M.C. Posner, Y. Boucher, D. Borochovitz, N. Wolmark, and R.K. Jain. 1992. Interstitial hypertension in human breast and colorectal tumors. *Cancer Res*. 52:6371-4.

73. Boucher, Y., and R.K. Jain. 1992. Microvascular pressure is the principal driving force for interstitial hypertension in solid tumors: implications for vascular collapse. *Cancer Res*. 52:5110-4.
74. Levental, K.R., H. Yu, L. Kass, J.N. Lakins, M. Egeblad, J.T. Erler, S.F. Fong, K. Csiszar, A. Giaccia, W. Weninger, M. Yamauchi, D.L. Gasser, and V.M. Weaver. 2009. Matrix crosslinking forces tumor progression by enhancing integrin signaling. *Cell*. 139:891-906.
75. Jain, R.K. 1989. Delivery of novel therapeutic agents in tumors: physiological barriers and strategies. *J Natl Cancer Inst*. 81:570-6.
76. Jain, R.K. 1994. Barriers to drug delivery in solid tumors. *Sci Am*. 271:58-65.
77. Minchinton, A.I., and I.F. Tannock. 2006. Drug penetration in solid tumours. *Nat Rev Cancer*. 6:583-92.
78. Hofmann, M., M. Guschel, A. Bernd, J. Bereiter-Hahn, R. Kaufmann, C. Tandi, H. Wiig, and S. Kippenberger. 2006. Lowering of tumor interstitial fluid pressure reduces tumor cell proliferation in a xenograft tumor model. *Neoplasia*. 8:89-95.
79. Hogan, M.C., A. Lee, L.A. Solberg, and S.D. Thomâe. 2002. Unusual presentation of multiple myeloma with unilateral visual loss and numb chin syndrome in a young adult. *Am J Hematol*. 70:55-9.
80. Gordon, V.D., M.T. Valentine, M.L. Gardel, D. Andor-Ardo, S. Dennison, A.A. Bogdanov, D.A. Weitz, and T.S. Deisboeck. 2003. Measuring the mechanical stress induced by an expanding multicellular tumor system: a case study. *Experimental Cell Research*. 289:58-66.
81. Roose, T., P.A. Netti, L.L. Munn, Y. Boucher, and R.K. Jain. 2003. Solid stress generated by spheroid growth estimated using a linear poroelasticity model small star, filled. *Microvasc Res*. 66:204-12.
82. Sarntinoranont, M., F. Rooney, and M. Ferrari. 2003. Interstitial stress and fluid pressure within a growing tumor. *Ann Biomed Eng*. 31:327-35.
83. Hanahan, D., and J. Folkman. 1996. Patterns and Emerging Mechanisms of the Angiogenic Switch during Tumorigenesis. *Cell*. 86:353-364.
84. Buchler, P., H.A. Reber, R.S. Lavey, J. Tomlinson, M.W. Buchler, H. Friess, and O.J. Hines. 2004. Tumor hypoxia correlates with metastatic tumor growth of pancreatic cancer in an orthotopic murine model1. *Journal of Surgical Research*. 120:295-303.
85. Le, Q.T., N.C. Denko, and A.J. Giaccia. 2004. Hypoxic gene expression and metastasis. *Cancer Metastasis Rev*. 23:293-310.
86. Rofstad, E.K., and T. Danielsen. 1999. Hypoxia-induced metastasis of human melanoma cells: involvement of vascular endothelial growth factor-mediated angiogenesis. *Br J Cancer*. 80:1697-707.
87. Zhang, L., and R.P. Hill. 2004. Hypoxia Enhances Metastatic Efficiency by Up-Regulating Mdm2 in KHT Cells and Increasing Resistance to Apoptosis. *Cancer Res*. 64:4180-4189.
88. Auvinen, P., R. Tammi, J. Parkkinen, M. Tammi, U. Agren, R. Johansson, P. Hirvikoski, M. Eskelinen, and V.-M. Kosma. 2000. Hyaluronan in Peritumoral Stroma and Malignant Cells Associates with Breast Cancer Spreading and Predicts Survival. *Am J Pathol*. 156:529-536.

89. Kim, H.-R., M.A. Wheeler, C.M. Wilson, J. Iida, D. Eng, M.A. Simpson, J.B. McCarthy, and K.M. Bullard. 2004. Hyaluronan Facilitates Invasion of Colon Carcinoma Cells in Vitro via Interaction with CD44. *Cancer Res*. 64:4569-4576.
90. Lipponen, P., S. Aaltomaa, R. Tammi, M. Tammi, U. Agren, and V.-M. Kosma. 2001. High stromal hyaluronan level is associated with poor differentiation and metastasis in prostate cancer. *European Journal of Cancer*. 37:849-856.
91. Griffon-Etienne, G., Y. Boucher, C. Brekken, H.D. Suit, and R.K. Jain. 1999. Taxane-induced apoptosis decompresses blood vessels and lowers interstitial fluid pressure in solid tumors: clinical implications. *Cancer Res*. 59:3776-82.
92. Thamilselvan, V., and M.D. Basson. 2004. Pressure activates colon cancer cell adhesion by inside-out focal adhesion complex and actin cytoskeletal signaling. *Gastroenterology*. 126:8-18.
93. Conway, W.C., J.V.d.V.v. Zyp, V. Thamilselvan, M.F. Walsh, D.L. Crowe, and M.D. Basson. 2006. Paxillin modulates squamous cancer cell adhesion and is important in pressure-augmented adhesion. *Journal of Cellular Biochemistry*. 98:1507-1516.
94. Downey, C., D.H. Craig, and M.D. Basson. 2008. Pressure activates colon cancer cell adhesion via paxillin phosphorylation, Crk, Cas, and Rac1. *Cell Mol Life Sci*. 65:1446-57.
95. Thamilselvan, V., A. Patel, J. van der Voort van Zyp, and M.D. Basson. 2004. Colon cancer cell adhesion in response to Src kinase activation and actin-cytoskeleton by non-laminar shear stress. *J Cell Biochem*. 92:361-71.
96. Ridley, A.J., M.A. Schwartz, K. Burridge, R.A. Firtel, M.H. Ginsberg, G. Borisy, J.T. Parsons, and A.R. Horwitz. 2003. Cell migration: integrating signals from front to back. *Science*. 302:1704-9.
97. Friedl, P., and B. Weigelin. 2008. Interstitial leukocyte migration and immune function. *Nat Immunol*. 9:960-9.
98. Lauffenburger, D.A., and A.F. Horwitz. 1996. Cell migration: a physically integrated molecular process. *Cell*. 84:359-69.
99. Thiery, J.P. 2002. Epithelial-mesenchymal transitions in tumour progression. *Nat Rev Cancer*. 2:442-54.
100. Christiansen, J.J., and A.K. Rajasekaran. 2006. Reassessing epithelial to mesenchymal transition as a prerequisite for carcinoma invasion and metastasis. *Cancer Res*. 66:8319-26.
101. Ewald, A.J., A. Brenot, M. Duong, B.S. Chan, and Z. Werb. 2008. Collective epithelial migration and cell rearrangements drive mammary branching morphogenesis. *Dev Cell*. 14:570-81.
102. Rorth, P. 2009. Collective cell migration. *Annu Rev Cell Dev Biol*. 25:407-29.
103. Friedl, P., Y. Hegerfeldt, and M. Tusch. 2004. Collective cell migration in morphogenesis and cancer. *Int J Dev Biol*. 48:441-9.
104. Liang, C.-C., A.Y. Park, and J.-L. Guan. 2007. In vitro scratch assay: a convenient and inexpensive method for analysis of cell migration in vitro. *Nat. Protocols*. 2:329-333.

Chapter 2: Migration potential of cancer cells in response to applied compressive stress

Portions of the chapter have been taken from:

G. Cheng, **J. Tse**, R.K. Jain, L.L. Munn, "Micro-environment mechanical stress controls tumor spheroid size and morphology by suppressing proliferation and inducing apoptosis in cancer cells." PLoS One. 2009; 4(2): e4632.

J.M. Tse, G. Cheng, J.A. Tyrrell, S.A. Wilcox-Adelman, Y. Boucher, R.K. Jain, L.L. Munn, "Compression-induced cell distension and adhesion stimulate coordinated migration of mammary carcinoma cells." Submitted.

Introduction

In addition to biochemical stimuli, cells can also respond to a wide range of mechanical cues, which are vital for normal physiological processes such as endothelial cell biology[1,2], tissue maintenance [3,4] and morphogenesis [5,6]. In growing solid tumors, it is well established that cancer cells experience oxidative stress (hypoxia) due to a deprivation of oxygen supply, but compressive stress generated by uncontrolled cell proliferation in a confined space has not been widely investigated. Our lab has previously shown that the compressive stress produced by a growing tumor is sufficient to collapse blood and lymphatic vessels in animal models[7]. While intratumor hypoxia has been shown to be a selection pressure for cancer cells with enhanced migratory and invasive potentials, involving the activation of genes such as Met and CXCR4[8], whether compressive stress can impose similar selection pressure remains unclear.

Previous *in vitro* studies have demonstrated that mechanical stress can influence proliferation and apoptosis of tumor spheroids [9,10], induce malignant phenotypes [11-13] and enhance tumor cell adhesion[14-16]. All of these studies involved *isotropic* stresses (uniform in all directions), which were carried out either by growing cancer cells in 3D gels with defined mechanical stiffness or by applying hydrostatic pressures over a culture of cells. However, tumors experience *anisotropic* (causing cell distortion) compressive stress while growing in confined heterogeneous microenvironments *in vivo* [17]. Hence, little is known about the direct effect of such cell-deforming stress on cancer cell migration.

In response to mechanical distortion, cytoskeleton – actin microfilaments, intermediate filaments and microtubules - plays an important role in providing structural support. To ensure cell shape stability, actin microfilaments and intermediate filaments act as tension cables while microtubules act as compression struts to provide mechanical force balance[18]. In addition, the microtubule-actin filament crosstalk helps stabilizing the polarity in migrating cells. Actin initiates the polarization process, whereas microtubules maintain the stability of the polarized organization [19].

In this study, we hypothesized that anisotropic compressive stress could alter cytoskeletal structures, stimulate tumor cell migration and thus promote a more invasive phenotype leading to metastasis. In order to address this notion, we developed an *in vitro* compression system to apply direct and anisotropic compressive stress to a monolayer of cells and assess its effect on cancer cell motility with scratch-wound assay. Here we show, for the first time, that continuously-applied compressive stress at a moderate level can increase migration of some cancer cell lines. Specifically, mechanical stress stimulates coordinated migration of 67NR mammary carcinoma cells with formation of actin stress fibers and elongation of microtubules. Additionally, we have examined any possible gene transcription induced by compressive stress using microarrays.

Materials and Methods

Cell cultures

A total of 8 tumor cell lines originated from mammary, colon or renal tissues were used in this study. The human mammary carcinoma cell lines MCF-7, MDA-MB-231 were obtained from American Type Culture Collection (ATCC) while the murine 4T1 and 67NR were kindly provided by Dr. Fred R. Miller at Wayne State University [20]. The human renal carcinoma cell lines SN12C and SN12L1 were kind gifts of Dr. Isiah J. Fidler from the University of Texas M.D. Anderson Hospital and Tumor Institute at Houston[21]. The human colon cancer cell lines were LS174T and LiM6 (obtained from Dr. R. Bresalier, Henry Ford Hospital, Detroit, Michigan). The immortalized mammary epithelial cell line MCF10A was obtained from ATCC. The 293ET packaging cells were a kind gift from Dr. Brian Seed (Massachusetts General Hospital, Boston). All cell lines were cultured in Dulbecco's Modified Eagle Medium (DMEM) supplemented with 10% fetal bovine serum (FBS), except for murine mammary carcinoma cells [20], human renal carcinoma cells [22], and MCF10A [23] cultured as described. All cells were incubated at 37°C with 5%CO_2.

Retrovirus packaging and transduction

The enhanced green florescent protein (EGFP) retrovirus vector, PBMN-I-EGFP was kindly provided by Dr. Gary Nolan (Stanford, CA). For retrovirus packaging, the plasmids of PBMN-I-EGFP, Gag-pol, and VSVG (15 μg, 7 μg, and 5 μg, respectively) were mixed and co-transfected into 293ET cells with lipofectamine 2000 (Invitrogen, Carlsbad, CA) per manufacturer's protocol. After overnight incubation, the 293ET cells were washed with PBS and then given Dulbecco's Modified Eagle Medium 10% fetal bovine serum. The next day, the supernatant containing retrovirus was collected and fresh

media was added; this step was repeated three more times. After the supernatant was collected, it was passaged through a 0.45 μm filter (Whatman, Brentford, UK) and was either used immediately for infection or kept at –80°C. For the transduction of all cancer cell lines and normal mammary epithelial cells, the supernatant was first diluted 1:1 with fresh DMEM and supplemented with polybrene (8 μg/ml). The diluted supernatant was then added to a subconfluent monolayer of cells and allowed to incubate for 16 hours. Fresh DMEM medium was exchanged at the end of the incubation period and this step was repeated 2 to 3 times on consecutive days. After 2 to 3 rounds of infection, cell sorting was performed to select the EGFP cells if less than 90% of the cells expressed EGFP.

In vitro compression device

A schematic diagram of the *in vitro* compression device is shown in Figure 2.1. A piston of adjustable weights applies a constant force to an agarose disk in contact with cells growing on a transwell membrane with 0.4um-pores that permit nutrient and oxygen diffusion but prevent cell transmigration. For control samples, the transwell inserts had the agarose disk, but no piston.

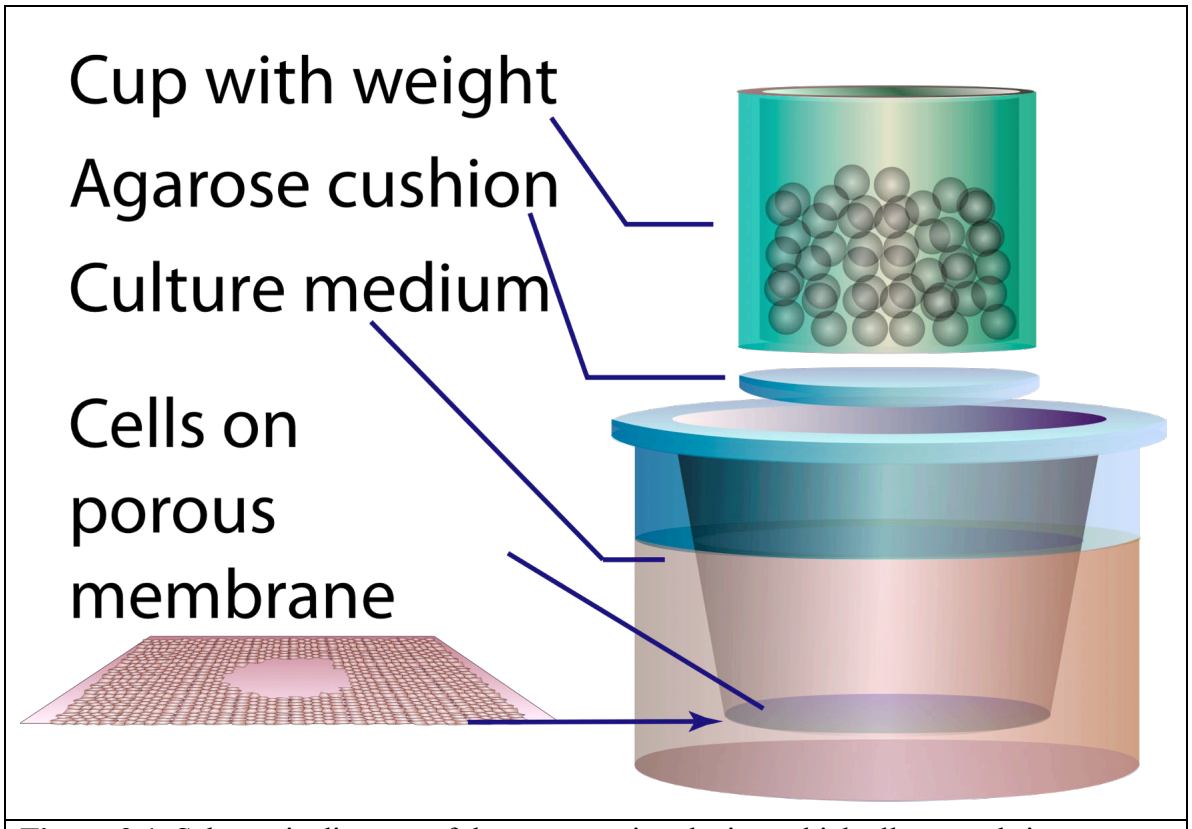

Figure 2.1. Schematic diagram of the compression device, which allows real-time monitoring of cell migration exposed to a constant loading force.

In vitro scratch wound-compression experiment

To assess cancer cell migration, cells were allowed to grow to confluence on uncoated transwell inserts. Using a p-200 pipette tip the monolayer was scraped to denude a circular area of ~1000 µm in diameter. The wound closure was monitored microscopically under stress-free or a compressive stress of 5.8mmHg (unless specified) and migration was determined as the change in wound area covered by cells 16 hr after wounding. Each experiment was repeated three times, and results were averaged.

WST-1 Cell Proliferation Assay

The cells were plated at 30% confluence on transwell membranes. After overnight compression with the *in vitro* compression device, the number of metabolically active cells in the culture was assessed using Cell Proliferation Reagent WST-1 (Roche Applied Sciences, Indianapolis, IN) according to the manufacturer's instructions. Each experiment was repeated three times, and results were averaged.

Immunofluorescence microscopy for cytoskeletal structures

The 67NR cells after *in vitro* scratch wound-compression experiment were fixed with 4% paraformaldehyde in cytoskeletal buffer[24], permeabilized and blocked with 5% normal horse serum containing 0.2% Triton X-100. The cells were then incubated with Alexa Fluor-546 phalloidin (1:200; Molecular Probe) for 20 min at room temperature for visualization of actin filaments. As for staining of microtubules, the fixed cells were incubated with anti-alpha-tubulin antibody (1:1500; Sigma) for 1 hr at room temperature. The cells were mounted in Vectashield Mounting Medium containing nuclear dye DAPI and then visualized with an Olympus FluoView 500 confocal microscope system (Olympus, Center Valley, PA).

Time-lapse live-cell fluorescent microscopy

To visualize real-time *in vitro* cell migration and wound closure, confluent cells growing on transwell inserts were scraped with a p-200 pipette tip. Cells, either compressed or uncompressed, were monitored with an inverted microscope (Olympus IX 70, Center Valley, PA). Fluorescent images were obtained at 30-min intervals over a period of 16 hr. The cultures were kept at 37°C in a custom-built micro-incubator supplied with 5% CO_2.

Toluidine blue staining of 67NR cell morphology

At the end of the time-lapse experiment, the 67NR cells were fixed with 4% paraformaldehyde in phosphate buffered saline (PBS) for 20mins, followed by PBS washes. Then, the cells were stained with filtered 0.1% toluidine blue solution prepared in 0.1% sodium borate for 3 minutes, followed by washes with distilled water. Finally, the section was mounted with Faramount aqueous mounting medium (Dako, Carpintera, CA) and visualized by light microscopy.

Quantification of cell alignment

Confluent cells on transwell inserts were scraped with a p-200 pipette tip and then compressed for 16 hr using the *in vitro* compression device with the uncompressed condition as the control. After 16-hr compression, images of the wound leading edge were captured with an inverted microscope (Olympus IX70, Center Valley, PA) and a montage of the whole wound was generated using NIH ImageJ 1.4J. To determine the effect of compressive stress on cell alignment, we calculated an alignment correlation index using Matlab (Mathworks, Natick, MA). The cell alignment correlation index (CACI) is a value in the range [0,1], defined as: CACI= Mean ($|\vec{a} \cdot \vec{b}|$), where $\vec{a}$ is the unit vector normal to the wound perimeter and $\vec{b}$ is the unit vector along the transversal axis of a cell.

Live/dead viability assay

At the end of the *in vitro* scratch wound-compression experiment, the cells were labeled with a mixture of 2uM calcein-AM and 4uM ethidium homodimer-1 (Invitrogen) in PBS for 20 mins at 37°C. The labeled cells were then rinsed with PBS twice to remove any excess labeling solution. Images of live cells (labeled with calcein-AM) and dead cells (labeled with ethidium homodimer-1) were captured with an inverted microscope (Olympus IX70, Center Valley, PA). Using ImageJ software, percent of dead cells was calculated as pixel area covered by ethidium homodimer-1 staining relative to the total staining (calcein-AM + ethidium homodimer-1 staining), multiplied by 100%.

Compression followed by stress release experiment

The *in vitro* scratch wound-compression experiment was first performed with line wounds created. After 16 hours, the piston was removed from the compressed cultures. Images of the wound were then captured with an inverted microscope (Olympus IX70) 21 hrs and 46 hrs after removal of the piston. Migration rate was determined as the change in distance traveled by the leading front of the cell sheet between the two consecutive time points.

Microarray analysis

The tumor metastasis and extracellular matrix and adhesion molecules oligo GEArray (SABiosciences, Frederick, MD) were used to determine the effect of compression on the expression of metastasis- and adhesion- related genes. Total RNA was isolated from control and compressed 67NR cells cultured in full-growth medium at the indicated times using the Trizol reagent (Invitrogen) according to the manufacturer's protocol and then

treated with the RNeasy Mini Kit (Qiagen, Valencia, CA). cRNA was then synthesized from 0.5ug total RNA using TrueLabeling-AMP 2.0 (SABiosciences) according the manufacturer's instructions. The synthesized cRNA was then hybridized with the microarray membranes and signals were detected following the manufacturer's protocol.

Results

Development of in vitro compression model

Cancer cells collectively experience significant compressive stress at the tumor margin, where rapid cell proliferation occurs[25,26]. In this study, we wanted to develop a simple platform to study the relationship between anisotropic compression and cell migration without confounding variables, such as, hypoxia, present in three-dimensional culture. Therefore, we developed a device for compressing a monolayer of cells on 0.4um-porous membrane reproducibly and uniformly with precisely defined normal stresses using a weighted piston (Fig. 2.1) and assessed the cell motility with scratch-wound assay. The 2-D scratch-wound assay allows cell-cell and cell-matrix interactions that cancer cells would typically experience within a solid tumor to be studied during cell migration[27]. Between the cell monolayer and the piston surface was a 1-mm-thick "cushion" layer of 1% inert agarose gel, with which the cells could not interact. A fluid flow was induced when we initially applied the compressive stress to the system but it became steady-state (i.e. no fluid flow) shortly afterward. To determine if fluid flow resulted from compressing the agarose gel would affect oxygen and nutrient access to the cells by diffusion through the 0.4um-porous membrane, thereby affecting cell migration behavior, a Peclet number calculation was performed below:

$Pe_i = \frac{Lv}{D_i}$, where L is the membrane thickness (10um), v is the velocity of the fluid flow and D_i is the diffusion coefficient of species i.

To determine the velocity of the fluid flow (v), we estimated v from Darcy's Law:

$v = -K\nabla P = -K\frac{\Delta P}{\Delta l}$,

where K is the hydraulic conductivity of 1% agarose gel (~10^{-5} cm^2 $mmHg^{-1}$ sec^{-1} estimated from the ref [28]), Δl is the thickness of the agarose gel (1mm) where pressure drop (ΔP = 5.8mmHg) took place. Thus, v was determined to be $5.8x10^{-4}$ cm sec^{-1}.

With $D_{glucose\ in\ water}$ = 6.8 x 10^{-6} cm^2 sec^{-1} and $D_{O2\ in\ H2O}$ = 2.7 x 10^{-5} cm^2 sec^{-1}[29], we got $Pe_{glucose}$ = 8.5 x 10^{-2} and Pe_{O2} = 2.1 $x10^{-2}$, respectively. Since the calculated Pe values for both glucose and oxygen are much smaller than 1, we could assume that the fluid flow through the pores caused by compressing the agarose gel was insignificant, as compared to diffusion through the porous membranes. Unlike other systems that use air pressure [30,31] or hydrostatic pressure[32], our two-compartment model ensures a constant and sufficient nutrient and oxygen supply to the culture by diffusion through the porous membrane substrate. In addition, the membrane can be modified by pre-coating with relevant proteins such as fibronectin, and the spatial arrangement of the cells can be controlled by patterning them on desired geometries using micro-contact printing techniques.

Before the above system was developed for our study, we have also attempted two other *in vitro* compression models. However, applying external stress using those systems caused complications, which could lead to data mis-interpretations. For example, in one system, when we compressed a monolayer of cells on an 8.0um-porus membrane and assessed the ability of cell transmigration by quantifying the number of cells migrating through the pores to the underside of the membrane, we found that the cells could readily extrude through them under compression (Fig. 2.2). While attempting to resolve such issue, we had a thin layer (500-1000um) of collagen I gel at a concentration of 2mg/mL (typical literature value used for invasion assays) on top of an 8um-porous membrane and then seeded a monolayer of cancer cells on the surface of the collagen gel. We determined the invasion potential of cancer cells under compression by measuring the number of cells invading through the collagen gel and passing through the porous membrane. However, compared to the uncompressed gel, the gel under compression was collapsed and more compacted, significantly hindering cell motility.

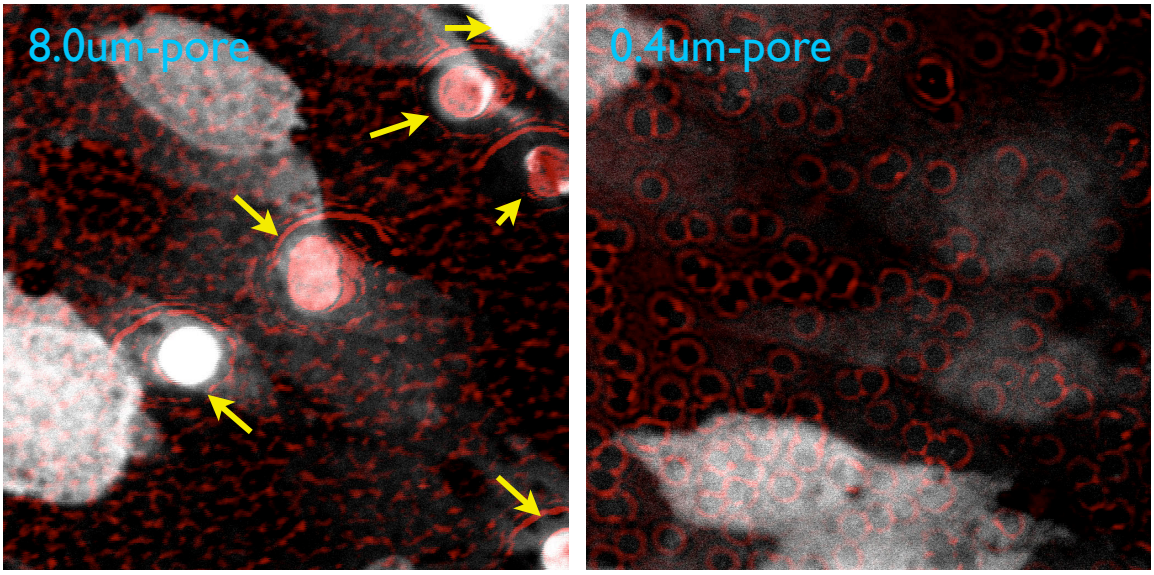

Figure 2.2. Forced cell extrusion by compression occurs on the 8um-porous membranes, but not on the 0.4um ones. The 67NR cells (in white) were plated on 8um- and 0.4um- porous membrane, respectively, and then exposed to a compressive stress of 5.8mmHg for 1 hr. The cells were fixed for confocal microscopy and images were taken at the plane of the porous membrane. The yellow arrows indicate that part of the cell body co-localizes with the circular pores, suggesting forced cell-extrusion caused by compression.

After the *in vitro* compression system was developed, we visualized cells under non-transparent piston, which blocked the transmission of visible light, by making the cells fluorescent. At first, we used Calcein AM, a widely used green fluorescent cell marker, to label 67NR mammary carcinoma cells because the labeling process is simple and fast. However, the green fluorescent color did not last long enough for a 16-20 hr experiment. In addition, after the labeled 67NR cells were exposed to fluorescent light for imaging, we noticed that the cells started to round up, indicating an apparent cytotoxicity issue resulted from the cell-specific adverse reaction of Calcein AM with the fluorescent light. Therefore, we transduced all the cancer cell lines used in this study with retroviral particles containing enhanced green-fluorescent protein (eGFP). These fluorescent proteins have been widely used for the purpose of cell visualization and long-term tracking because of its low cytotoxicity.

Applied compressive stress enhances migration of some cancer cell lines

Since little is known about the effect of compressive stress on cancer cell motility, we first screened a number of cancer cell lines that would form solid tumors *in vivo*. Using

the device in Figure 2.1, we subjected various established cancer cell lines originating from different tissue organs such as breast (MCF7, 67NR, 4T1 and MDA-MB-231), renal (SN12C and SN12L1) and colon (LS174T and LiM6) to compressive stress, assessed their morphology in real-time and measured migration rates via scratch-wound assay (throughout this paper, "wound" refers to the denuded area in our 2D cultures where cells have been removed or excluded). Figure 2.3 shows that compressive stress increased the migration potential of multiple cancer cell lines, including renal carcinoma and mammary carcinoma cell lines. Notably, among all breast cancer cell lines, mechanical stress enhanced the motility of both highly aggressive 4T1 and MDA-MB-231 cells, as well as 67NR cells, which have undergone partial epithelial-mesenchymal-transition[33]. In contrast, compressive stress reduced the migration of the normal mammary epithelial MCF10A (insert) and the non-invasive, well-differentiated MCF7 cell line, which retain certain features of normal mammary epithelium[34].

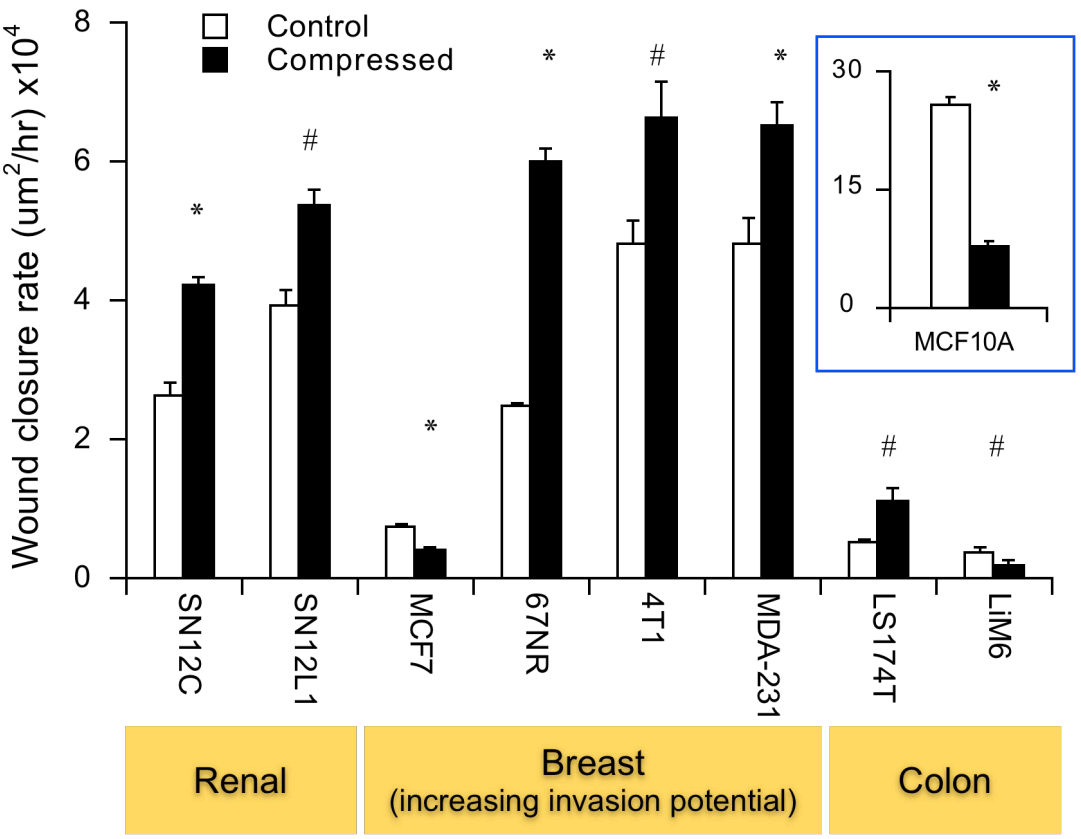

Figure 2.3. Compressive stress induces faster cell migration in multiple cancer cell lines, particularly more aggressive breast cancer cell lines. Average migration rate obtained from the scratch-wound assay for eight different cancer cell lines originating from various tissue organs (kidney, breast and colon) and normal mammary epithelial cells (insert: MCF10A) subjected to stress-free (control) or a compressive stress of 5.8mmHg for 16 hrs using the device described in **Figure 2.1** (n=9; *P<0.005 compared with their individual control; #P<0.05 compared with their individual control). Error bars represent s.e.m.

In general, wound closure results from a combination of cell proliferation and cell migration. To exclude the possibility that the stress increases cell proliferation rates, thus indirectly influencing wound closure, we quantified cell viability and proliferation with the WST-1 assay (Fig. 2.4). In the various cell lines, compression caused either no change or decreased proliferation. Notably, while the compression-induced wound closure rate was higher in the more aggressive breast cancer cell lines (Fig. 2.3), compressive stress did not affect cell proliferation in more aggressive breast cancer cell lines (Fig. 2.4). This result suggests that compression can promote migration of mammary carcinoma cell lines independent of any effect on cell proliferation.

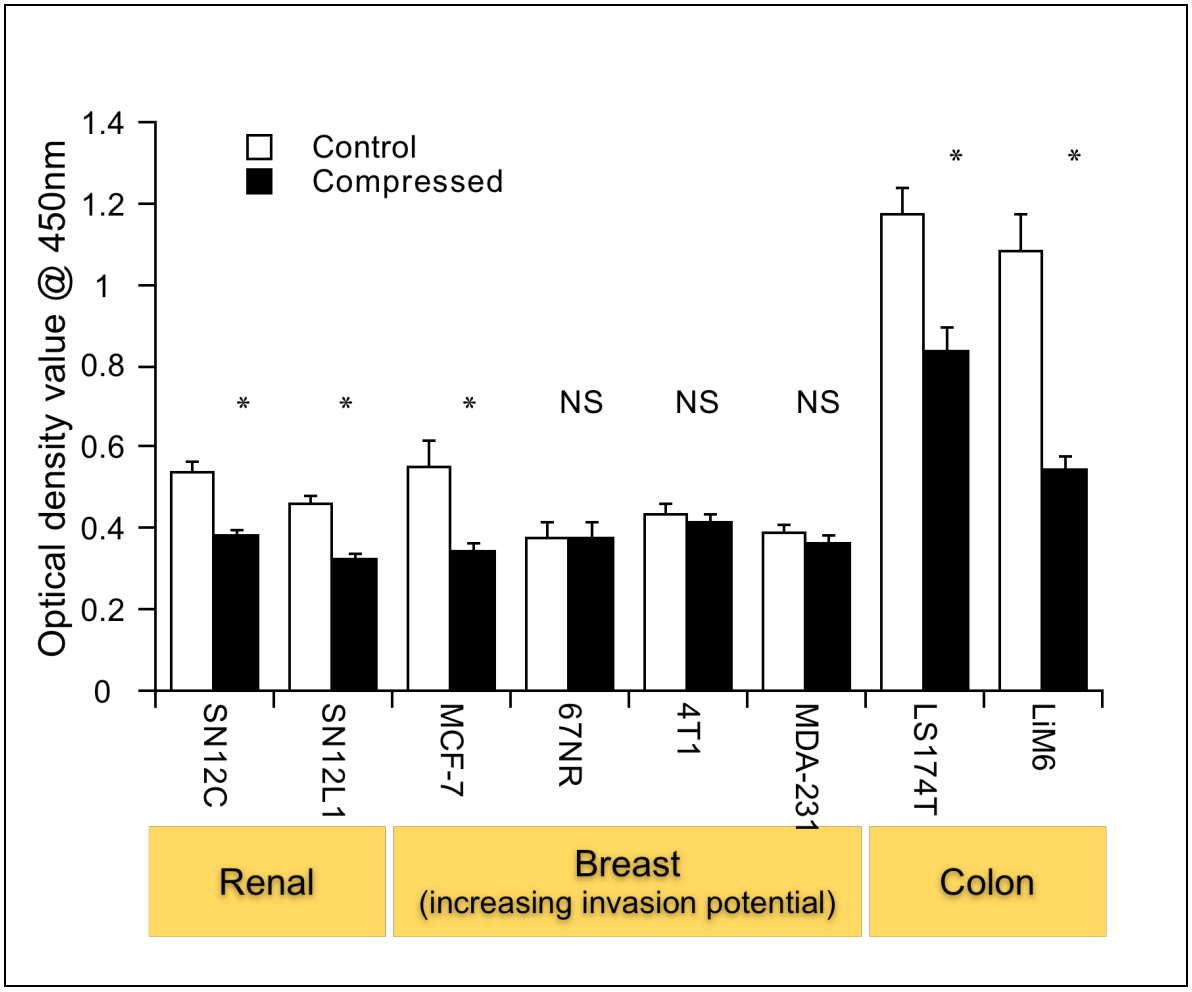

Figure 2.4. Compressive stress causes no change or decreased cell proliferation. Cell proliferation/viability results obtained from the WST-1 assay for eight cancer cell lines (shown in Figure 2.3) subjected to stress-free (control) or a compressive stress of 5.8mmHg for 16 hrs using the device described in **Figure 2.1** (n=9; NS=not significant; *P<0.05 compared with their individual control).

Mammary carcinoma cells and normal cells show differential changes in cytoskeleton organization in response to mechanical compressive stress

Mechanical stress is expected to play an important role in progression of breast carcinomas, as matrix stiffness has been shown to regulate malignant transformation of mammary epithelial cells [11,35]. Thus, we focused our study on the role of compressive stress in mammary carcinoma cells. Figure 2.5 displays distinct patterns of the wound periphery in the control and compressed cultures of MCF10A normal mammary epithelial cells, 67NR mammary carcinoma cells and highly aggressive 4T1 mammary epithelial cells, respectively. While MCF10A and 4T1 cells did not exhibit any discernible changes in leading-edge pattern between the control and compressed cultures, the compressed 67NR cells surrounding the leading edge of the wound exhibited directional orientation more readily than the control cells.

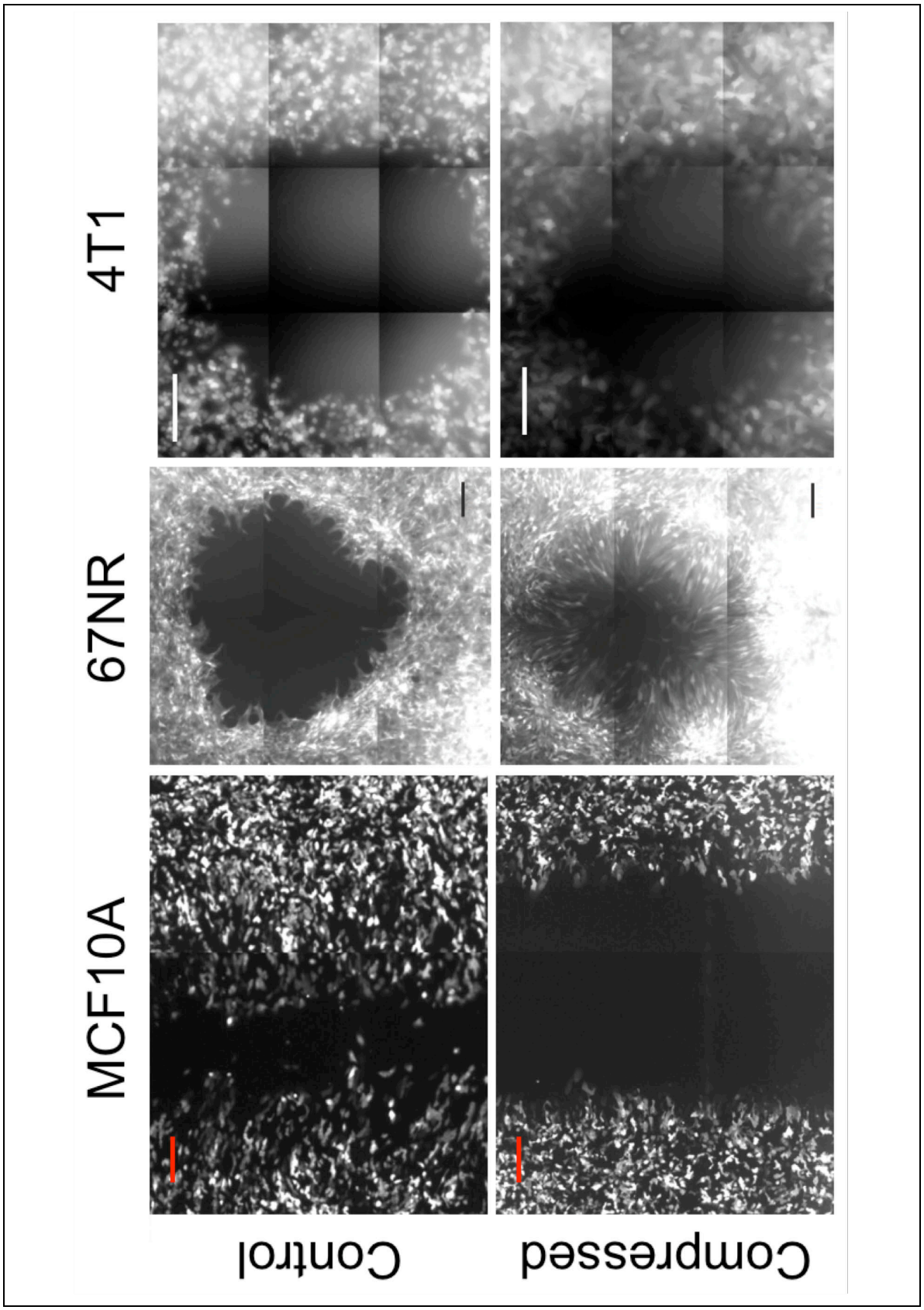
4T1
67NR
MCF10A
Control
Compressed

Figure 2.5. Compressive stress differentially influences cell migration behavior. Representative images (from 3-4 independent experiments) of control and compressed cells (MCF10A, 67NR and 4T1) closing the "wound" after 16 hrs (but 6hrs for 4T1). The compressed MCF10A migrated much slower than the control cells while both the compressed 67NR and 4T1 cells migrated faster than their respective control cells (wound closure rates are shown in Fig. 2.3). In particular, compressing 67NR cells induced more cells at the leading edge to show directional alignment perpendicular to the cell-denuded areas. Scale bar, 200um.

As mechanical stimulation can influence cytoskeleton organization[36,37], which provide structural support and shape for cells, we performed immunostaining of phalloidin for actin filaments (Fig. 2.6) and alpha-tubulin for microtubules (Fig. 2.7), which have been viewed as tension cables and compression struts, respectively[38,39], in those three cell lines. The Cy3-phalloidin staining shows that the marginal actin filaments (indicated by yellow arrows) appeared less pronounced and revealed a less intense fluorescence staining in the leading edge of the compressed MCF10A and 4T1 cultures (Fig. 2.6). Moreover, prominent actin filaments (stress fibers) were induced within the cytoplasm in the compressed cultures of 67NR and 4T1 cells, suggesting that tension of the actin cytoskeleton was raised. Moreover, those actin filaments were clearly oriented in correlation to cell elongation and orientation in the compressed 67NR cultures.

4T1
67NR
MCF10A
Control
Compressed

Figure 2.6. Compressive stress induces cytoskeletal actin rearrangement. Immunostaining of phallodin for actin microfilaments (Cy3; red) of MCF10A, 67NR and 4T1 cells at the periphery of the cell-denuded area. Compressive stress reduces marginal actin filaments in MCF10A and 4T1 leading cells (indicated by yellow arrows) and enhances stress fiber formation within cytoplasm in 67NR and 4T1 cell lines. In particular, actin filaments of the compressed 67NR cells are clearly oriented in correlation to cell elongation and orientation (n=8-16; scale bar, 10um).

In addition to re-organization of actin cytoskeleton, mechanical stress appeared to modulate the microtubule network in 67NR and 4T1 cells (Fig. 2.7), which exhibited enhanced migration under compression. In the uncompressed 67NR and 4T1 cultures, the microtubule staining was more diffuse, which could correspond to either free tubulin subunits or numerous but very short microtubules. By contrast, in the compressed 67NR cultures, the microtubule network and distribution appeared to extend longer preferentially in the direction of migration; while in the 4T1 cultures, compressive stress induced a dendritic network of microtubules in the lamellipodia of the cells. In addition, their microtubules displayed a small wavelength curvature, indicating that they buckled under compressive loads. When compressive stress increased the tension of the actin cytoskeleton, microtubule buckling would also increase[18]. As opposed to 67NR and 4T1 mammary carcinoma cells, externally-applied stress did not cause any significant overall changes in the microtubule network in the MCF10A normal mammary epithelial cells (Fig. 2.7), which showed suppressed motility under compression. In both the control and compressed cultures, microtubules in MCF10A cells originated around the nuclei and

ran radially through the cytoplasm without a preferential alignment and terminating near the cell periphery. It should be noted that the vast network of microtubules in the uncompressed MCF10A cultures could contribute to their superior motility (compared to the uncompressed 67NR and 4T1 cells), as demonstrated in the *in vitro* scratch-wound assay (Fig. 2.3). These findings, coupled with phalloidin staining, suggest that (1) compression-induced cell motility could be initiated by increased tension in actin cytoskeleton, thereby inducing formation of stress fibers; (2) the elevated tension within the compressed cells induces formation of microtubule network to ensure mechanical stability[19,39].

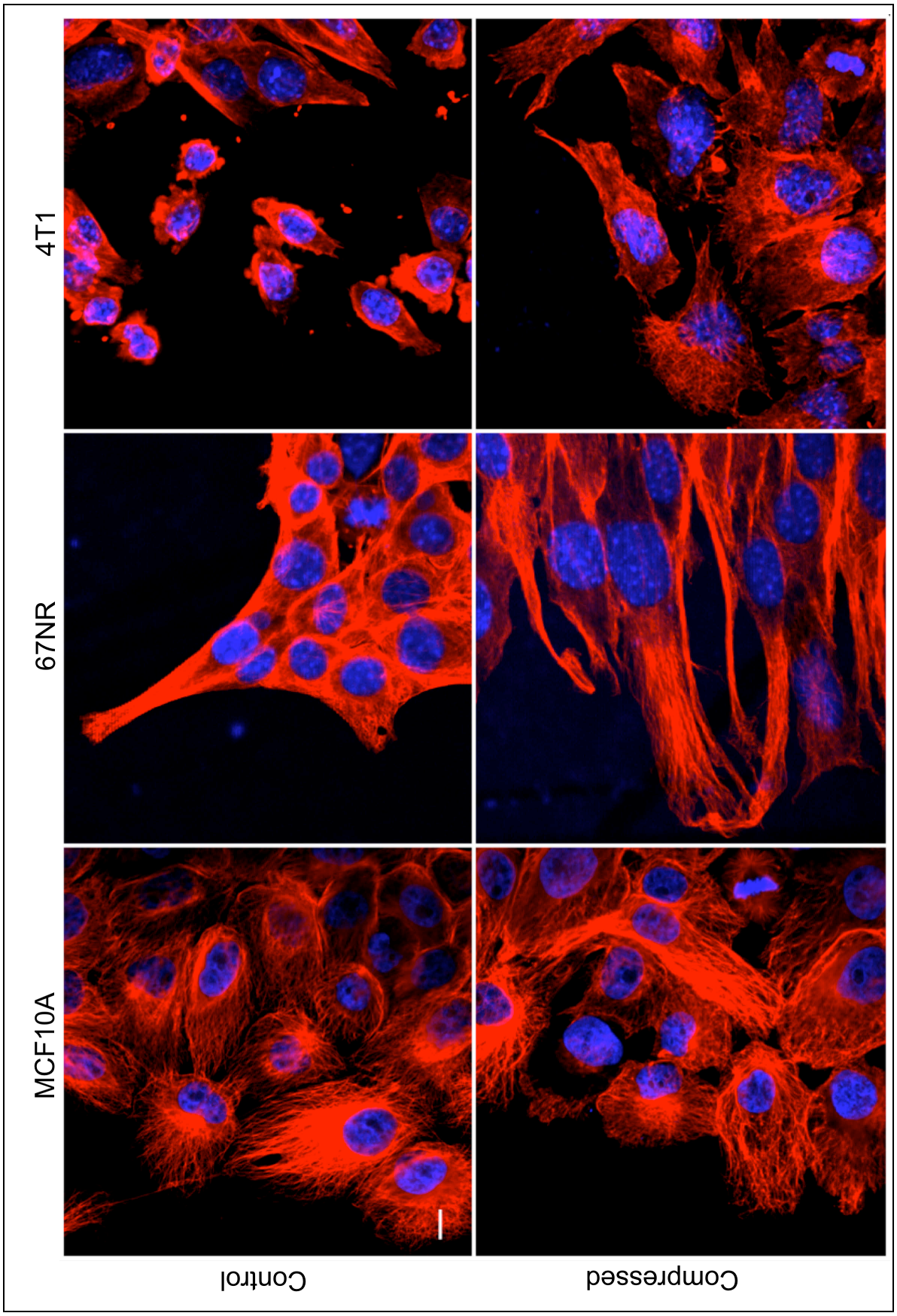
4T1
67NR
MCF10A
Control
Compressed

Figure 2.7. Compressive stress alters microtubule organization in cancer cells. Visualization of b-tubulin (Cy3; red) in MCF10A, 67NR and 4T1 cells at the periphery of the cell-denuded area. The uncompressed MCF10A cells have microtubules radiating throughout the cytoplasm from the perinuclear area toward the cell periphery, and compressive stress results in formation and/or re-arrangement of microtubule network in the two cancer cell lines (67NR and 4T1) without dramatically altering the organization in the "normal" MCF10A cells (n=8-16; scale bar, 10um).

Compressive stress stimulates directional migration of 67NR mammary carcinoma cells in a coordinated cell sheet

The 67NR mammary carcinoma cells have shown the most pronounced cytoskeletal changes and enhanced cell motility in response to mechanical compression (Fig.2.3 and Figs. 2.5-2.7). We, therefore, selected 67NR cell line as our model for subsequent study of compression-induced migration. To investigate the effect of compressive stress on 67NR cell migration behavior, we first visualized the migration process using time-lapse fluorescent microscopy (Fig. 2.8A). In the absence of compression (control), the cells extended in random directions and clustered at the wound periphery. In contrast, compressed 67NR cells demonstrated a clear persistence and directionality in their movement at the leading edge of the cell sheet, and preferentially aligned perpendicular to the wound periphery with the leading edges extending into the open area (Fig. 2.8B).

A

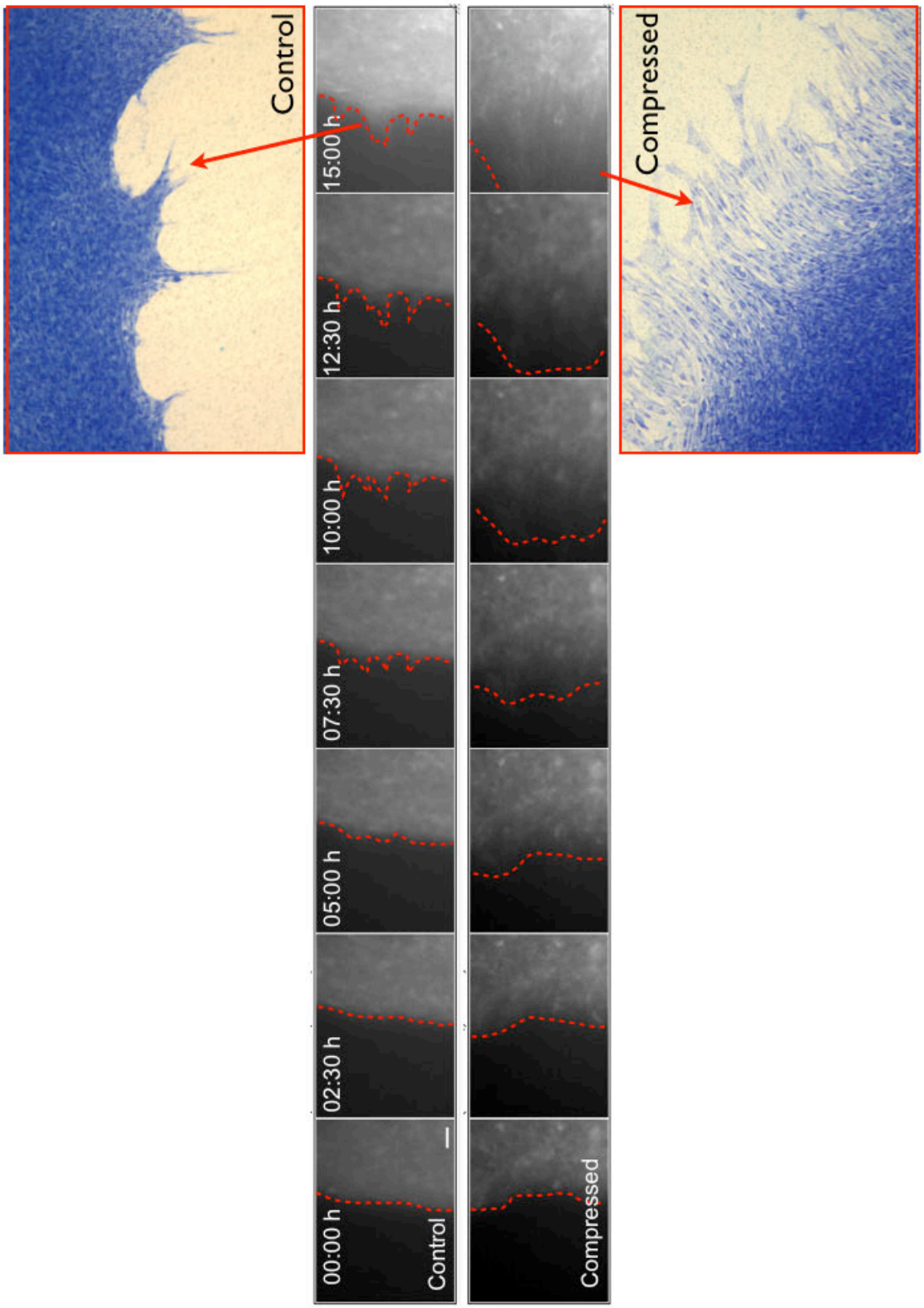
Control
Compressed
15:00 h
12:30 h
10:00 h
07:30 h
05:00 h
02:30 h
00:00 h
Control
Compressed

B

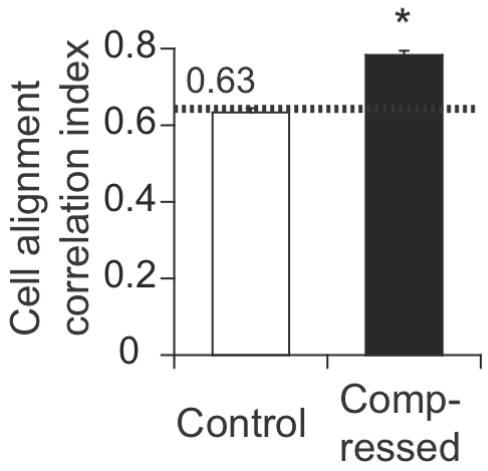

Figure 2.8. Compressive induces directional migration of 67NR cells in a coordinated manner. A, Representative snapshots of specified time points from time-lapse fluorescent microscopy of 67NR cells subjected to stress-free (control) or a compressive stress of 5.8mmHg. The inserts display the toluidine blue staining of 67NR cell morphology at the end of the time-lapse experiment. The compressed cells at the leading edge of the cell sheet show a clear persistence and directionality in the movement, but uncompressed cells move in random directions, generating a spiky edge of the cell sheet (scale bar, 50um). **B,** Quantitative analysis represented by a cell alignment correlation index to determine cell orientation of the 67NR cells at the wound periphery after 16-hr exposure to stress-free (control) or a compressive stress of 5.8mmHg. An index value of 1 indicates that the cells align perpendicular to the cell-denuded areas, while a value of 0 indicates orientation parallel to the wound periphery. Random cell alignment would result in an index of 0.63 according to theory. Uncompressed (control) samples had randomly-oriented cells, but compression induced directed elongation into the denuded region (n=7; *P<0.005). Error bars represent s.e.m.

Sustained and moderate applied compressive stress is required for enhanced cell motility

We previously exposed 67NR mammary carcinoma cells to a moderate stress level (5.8mmHg) similar to that found in the native breast tumor microenvironment[13] and observed increased migration of some cancer cells. We next investigated if higher stresses would enhance migration even more. (To ensure that the mere presence of pores on the membranes was not accountable for compression-induced migration in 67NR cells, we showed in Appendix Figure A1 that similar response was also observed on non-porous surfaces). By titrating the compressive force, we determined that compressive stress on 67NR carcinoma cells beyond 5.8mmHg triggered apoptosis and only 40% of cells remained viable at 58mmHg[10](Fig. 2.9A). In addition, the motility of viable 67NR cells was diminished by stresses greater than 5.8 mmHg (Fig. 2.9B). In fact, the wound closure was adversely affected by higher stresses and was completely inhibited at 58mmHg. Hence, this result suggests that moderate level of mechanical stress enhances cancer cell motility, while too high stresses trigger cell death.

A

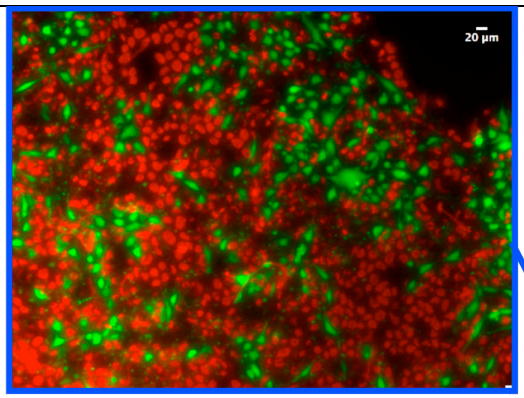
20 µm

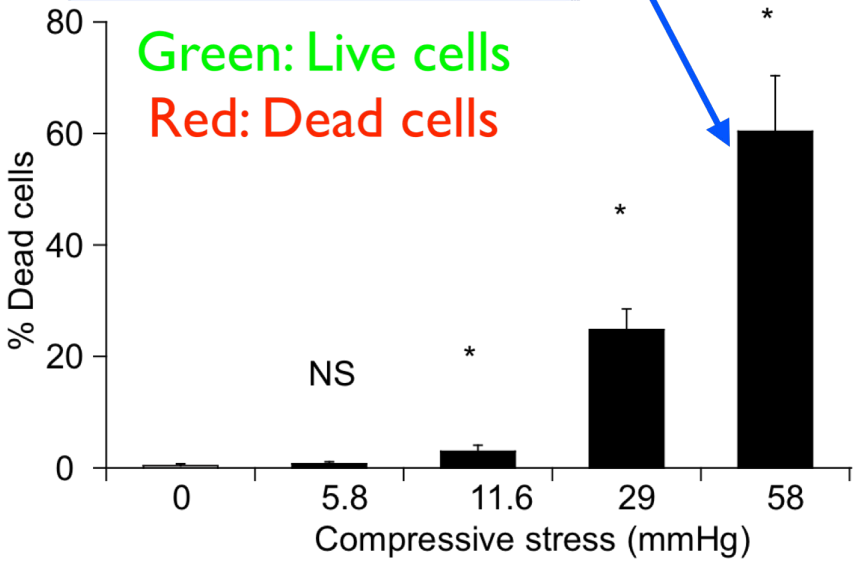
Green: Live cells
Red: Dead cells
% Dead cells
80
60
40
20
0
NS
*
*
*
0
5.8
11.6
29
58
Compressive stress (mmHg)

B

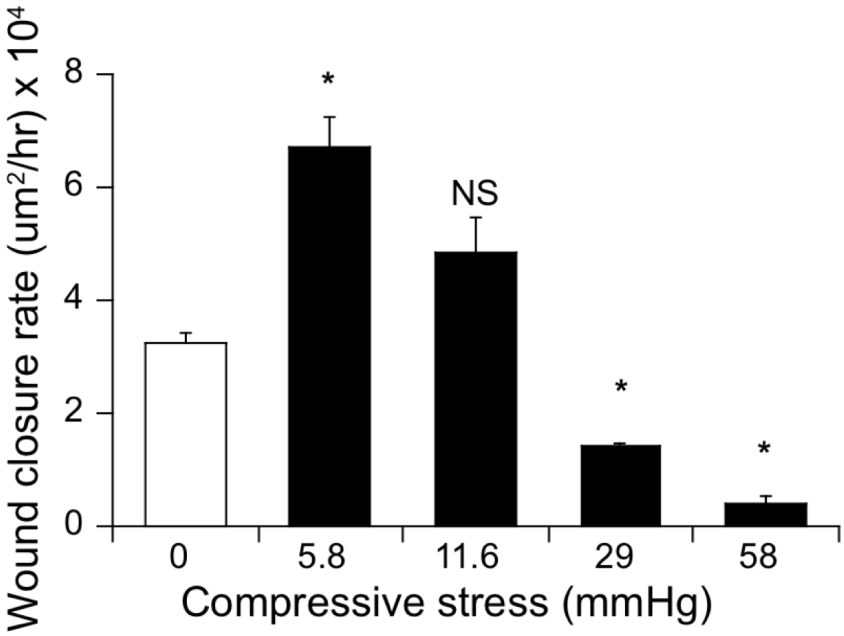
Wound closure rate (um²/hr) x 10⁴
8
6
4
2
0
*
NS
*
*
0
5.8
11.6
29
58
Compressive stress (mmHg)

Figure 2.9. Moderate stress enhances 67NR cell motility without a significant decrease in cell viability. Cell viability (**A**) and average migration rate obtained from the scratch-wound assay (**B**) for 67NR cells subjected to different specified levels of compressive stress for 16 hrs using the device described in **Figure 2.1.** The insert in **A** shows a representative image of viability of cells subjected to a compressive stress of 58mmHg, where live and dead cells were labelled with calcein-AM (green) and ethidium homodimer-1 (red), respectively (n=6-12; NS=not significant; *P<0.05 compared with the control – 0mmHg). Error bars represent s.e.m.

We then tested whether continuous compressive stress is required for enhanced cell migration. We first performed the same *in vitro* scratch wound-compression experiment with 67NR cells and they exhibited enhanced cell migration under compression as expected. Then, we removed the piston from the compressed cultures and determined the wound closure rates after stress release. We found that continuous compression was necessary for enhanced migration: 67NR cells pre-conditioned with a compressive stress of 5.8mmHg migrated slower after stress removal than continuously compressed cells (Fig. 2.10). Taken together, these results show that moderate levels of continuously-applied compressive stress are necessary to induce more aggressive cell motility.

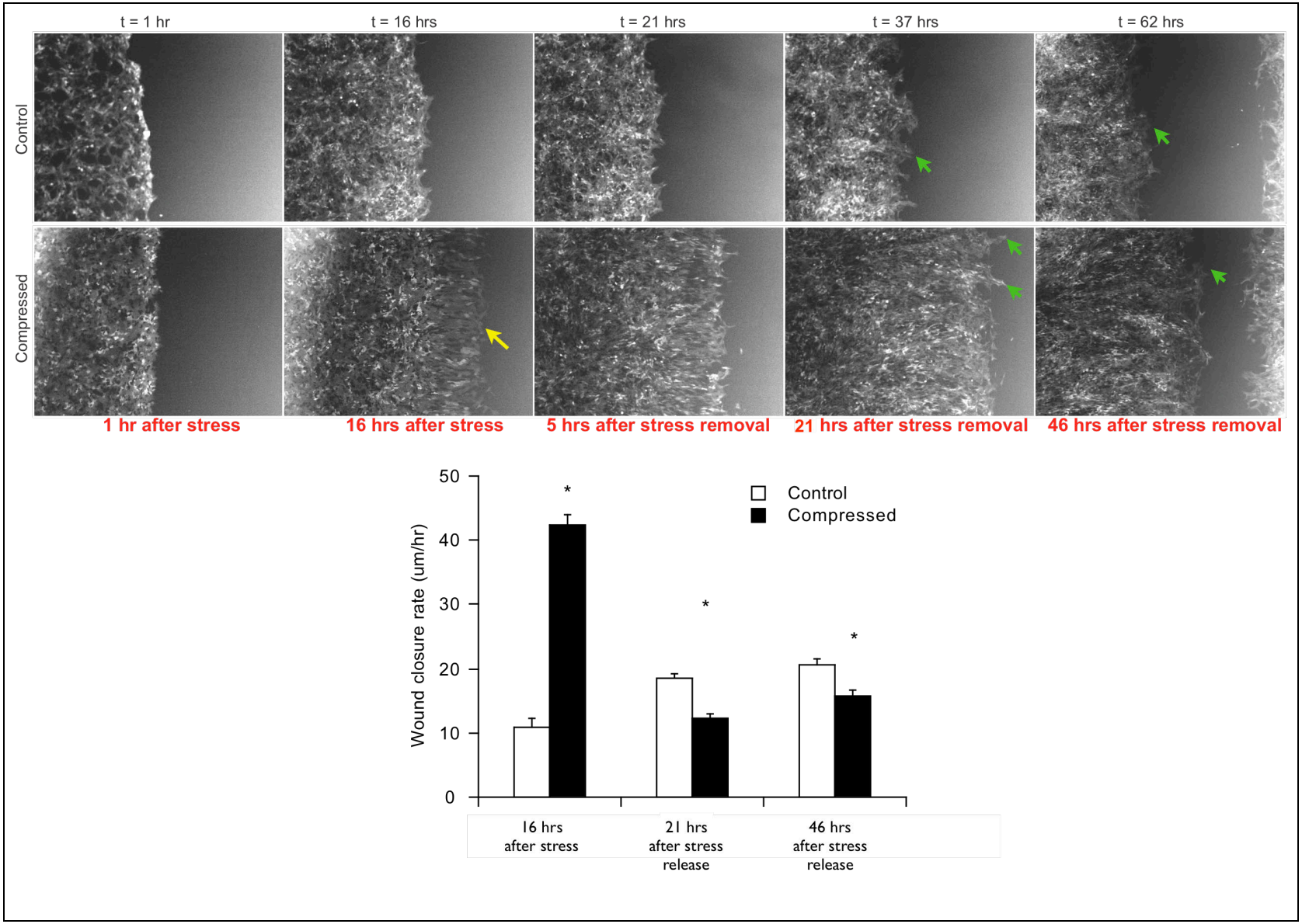
t = 1 hr
t = 16 hrs
t = 21 hrs
t = 37 hrs
t = 62 hrs
Control
Compressed
1 hr after stress
16 hrs after stress
5 hrs after stress removal
21 hrs after stress removal
46 hrs after stress removal
Wound closure rate (um/hr)
50
40
30
20
10
0
Control
Compressed
*
*
*
16 hrs after stress
21 hrs after stress release
46 hrs after stress release

Figure 2.10. Continuous compressive stress is required to maintain enhanced cell migration. The top panel shows the representative images of control and 5.8mmHg-compressed 67NR cells closing the "wound" after 16 hrs, followed by stress (piston) removed from the compressed cells. The compressed cells at the leading edge exhibited directional migration (yellow arrow). However, after stress was removed, some of the leading-front cells started clustering together as control cells (green arrows). The bottom panel shows the corresponding average migration rate of 67NR cells with and without compression (n=9; *P<0.005 compared with the control). The compressed cells migrated slower after stress removal than continuously compressed cells. Error bars represent s.e.m.

Could compression-induced cell migration be a result of gene expression change?

Cells can sense mechanical forces and transduce them via cytoskeletal network into changes in intracellular biochemical signaling and gene expression[39,40]. Moreover, it has been shown that mechanical stress induces Twist gene expression in *Drosophila* embryo [5] and Twist facilitates metastasis in mice [41]. Hence, compression-induced cytoskeletal changes in 67NR cells (Figs. 2.6 and 2.7) could affect gene expression to produce migratory phenotypes. To test this possibility, we compressed the cells and then collected total RNA for microarray analysis. Using pathway-focused DNA microarrays (SABiosciences), we specifically measured transcriptional changes in genes associated with tumor metastasis and extracellular matrix and adhesion molecules. Figure 2.11 displays the raw images of microarray expression data (A: Tumor metastasis array; B: Extracellular matrix and adhesion molecules array) for both the control and compressed

cultures. Their respective genes tables are shown in Appendix Figure A2. We showed that compression did not induce any significant changes in the expression of genes related to tumor metastasis, including Twist, and hypoxia-activated genes such as CXCR4 and Met (Fig. 2.11A). The expression data for the extracellular matrix (ECM) and adhesion molecules array initially suggested that a few genes could be influenced by compression (Fig. 2.11B). However, after quantitative PCR verification (a more reliable detection method than microarray), only the expression changes for beta-catenin (adhesion molecule) and TIMP-1 (extracellular matrix protease inhibitor) were reproducible but their small changes (less than 2-fold) detected by quantitative PCR were questionable. Since quantitative PCR is a highly sensitive detection method, 2-fold change is considered practically insignificant (based on consultation with Dr. Sung-Suk Chae, a post-doc with expertise in molecular biology). Thus, our findings indicate that compressive stress applied to 67NR cells unlikely affect the expression levels of those ~150 genes we examined.

However, it should be noted that beta-catenin can function as an oncogene when it is translocated to the nucleus, and high beta-catenin activity significantly correlates with poor prognosis of breast cancer patients[42]. Therefore, in spite of insignificant changes in beta-catenin expression, we examined its localization in the 67NR control and compressed cultures. Using confocal immunofluorescence microscopy, we, however, determined that neither did compressive stress induce any nuclear localization of beta-catenin (Appendix Fig. A3).

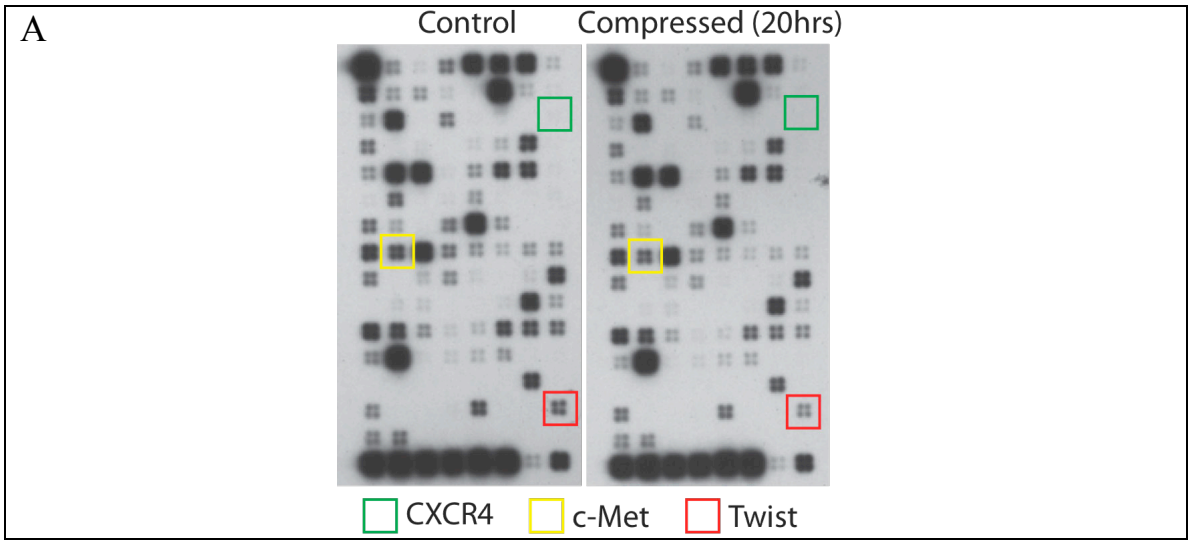
A
Control
Compressed (20hrs)
CXCR4
c-Met
Twist

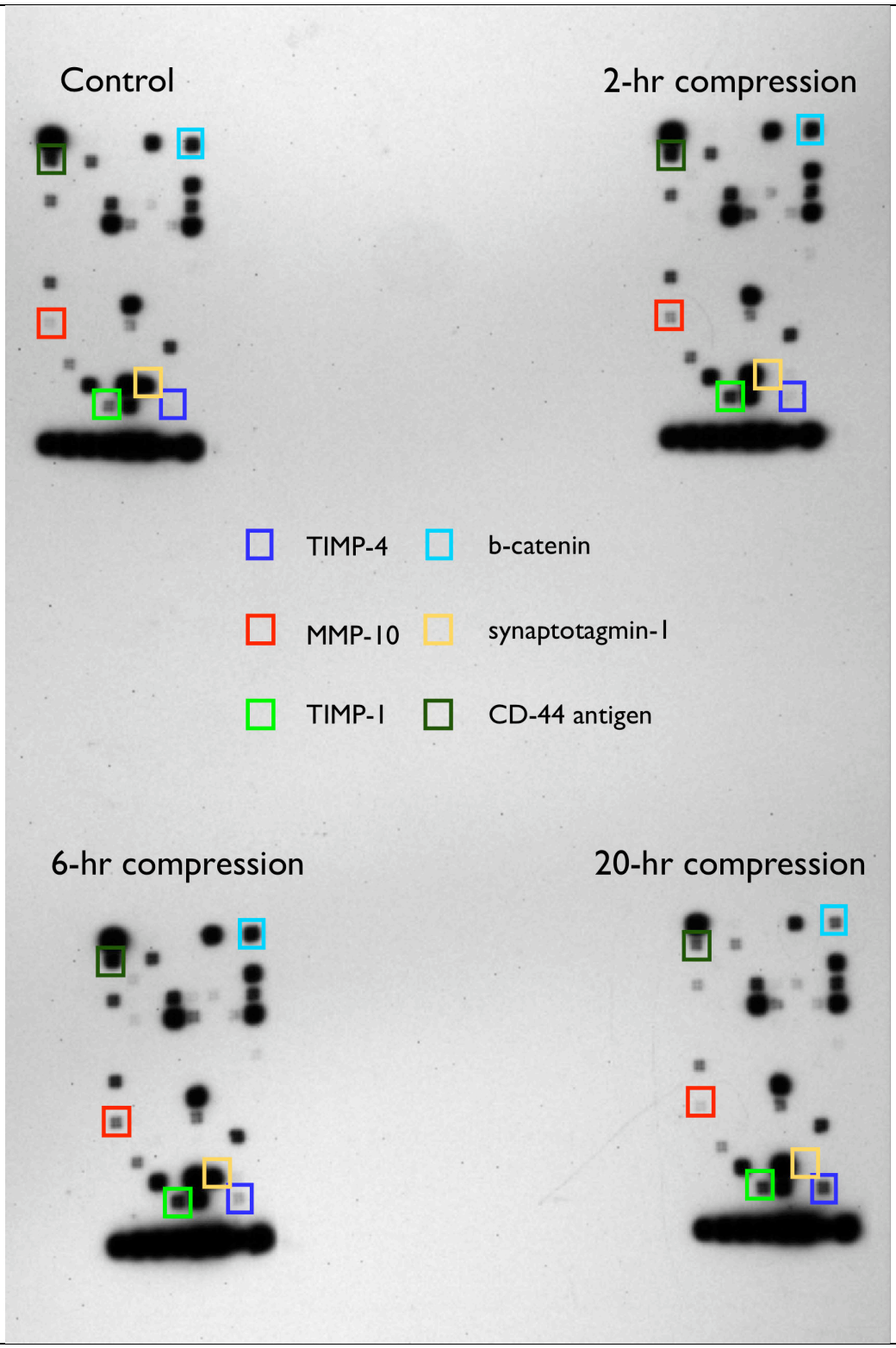

Figure 2.11. Compressive stress unlikely influence the genes associated with tumor metastasis or extracellular matrix and adhesion molecules arrays. A, B, Microarray

data using total RNA pooled together from 3 samples of uncompressed (control) or compressed (5.8mmHg) 67NR cells. Samples were collected at the indicated times. **A,** Tumor metastasis microarray: No significant changes were observed in the various tumor metastasis-related genes, including CXCR4, Met and Twist. **B,** Extracellular matrix and adhesion molecules microarray: The genes (inscribed in squares) appeared to have expression change in the compressed cultures. However, after quantitative PCR verification, only beta-catenin and TIMP-1 showed consistent results (data not shown), but the changes detected by quantitative PCR was less than 2-fold, which is generally considered insignificant for the highly sensitive quantitative PCR detection method. The bottom row of the microarrays represents various house-keeping genes for normalization.

Discussion

Cancer cell migration is a key event during metastasis and most of its research focuses on gene expression [41,43] and soluble gradients[44,45]. In solid tumors, cancer cells actively proliferate in a confined matrix at the expense of host tissue, thus experiencing substantial growth-induced compressive stress. While previous *in vitro* studies have demonstrated that matrix rigidity can influence tumor growth and development [9-13], the direct effect of mechanical compression on cancer cell migration has not been studied. In the present study, we developed an *in vitro* compression model utilizing a simple piston device and provided the first evidence that continuously-applied compressive stress can enhance migration of some cancer cells. In particular, compression stimulates directional migration of 67NR mammary carcinoma cells in a coordinated manner.

Our findings showed that cancer cells exhibited divergent responses to mechanical stress. While faster migration was observed in multiple cancer cell lines subjected to continuous compression, some exhibited reduced motility. As mechano-responsiveness is cell and tissue specific[12], differences in gene expression and phenotypic properties among cancer cells could influence their mechanosensitivity. For instance, the fact that 4T1 mammary carcinoma cells display greater inherent cell-substrate adhesion and migration potential than 67NR cells [46] could affect the transduction of mechanical stimuli into other cellular signals. In addition, rheological properties of the cells can also affect their mechanosensitivity. The cytoskeleton of cancer cells appears more irregular and compliant (with fewer filamentous actin, intermediate filaments and microtubules) than that of normal epithelial cells [47]. Thus, cancer cells generally have higher deformability than normal epithelial cells, implying that both cancerous and normal cells could impart distinct mechano-responses. Indeed, consistent with other studies on mechanical stimulation of epithelial cells[48,49], the motility of normal mammary epithelial MCF10A cells was impaired under compression in our study, while other mammary carcinoma cells (except for the MCF7 cell line with certain features of normal mammary epithelial cells) showed compression-induced migration.

However, increasing stresses does not augment cancer cell motility, but trigger cell death and restrain motility of viable cells. We speculate that compression increases cell-matrix adhesion, thereby enhancing cell migration (confirmed in Chapter 4). As there is a bell-shaped relationship between cell migration speed and substrate concentration (adhesion

strength)[50,51], the over-compressed 67NR mammary carcinoma cells might adhere too strongly to the surface and thus have difficulty in breaking the adhesion with the substrate in the trailing back. For optimal cancer invasion *in vivo*, our results suggest a feedback regulation of stress-dependent matrix degradation and/or apoptosis as a defensive cellular response against stress. Hence, some cancer cells could respond to growth-generated compressive stress by increasing migration.

Based on our microarray analysis of about ~150 genes related to tumor metastasis and ECM and adhesion molecules, we determined that compressive stress unlikely affected expression of those genes. Two possible explanations are: (1) the small sampling of genes (less than 1% of the whole genome) could simply miss the potential mechanically-sensitive genes; and (2) compression-induced migration involved regulation of signaling pathways rather than gene transcriptions. To address the first possibility, we could have performed the genomic profiling experiment of the control and compressed cultures. However, the transcriptional changes might also be confined to a limited number of cells such as leader cells. Nevertheless, the requirement of continuous compression for enhanced cell motility implies that the latter explanation could be more probable, and it suggests that (1) compression did not likely cause any permanent genetic mutations in cancer cells; and (2) any compression-induced changes were reversible and these modifications could be, but not limited to, cell shape distortion, size and activation of signaling pathways.

Indeed, when the mechanical stress was removed, the migration potential of pre-compressed 67NR cells that previously demonstrated increased cell motility plummeted significantly (Fig. 2.10). Cell shape is dynamically stabilized through a mechanical force balance in which the microtubules and ECM adhesions resist and balance the tension of the actin cytoskeleton[38,39]. The immunofluorescent staining of cytoskeletal structure in 67NR cells shows that applied compression-induced cell distortion increases formation of stress fibers, an indicator of increased cytoskeletal tension, which is accompanied by elongation of microtubules to resist the cell distension. Hence, any additional mechanical disturbance (such as stress removal) would upset the force balance, resulting in re-arrangement of cytoskeletal structure (and cell shape) to restore the mechanical stability. As cell shape can govern various cellular processes such as proliferation and directional protrusions[52,53], sustained stress is essential to maintain the compression-induced migratory phenotype. Furthermore, Tschumperlin et al. [54] revealed that compressive stress shrunk the lateral intercellular space, leading to an increase local concentration of soluble factors that were sufficient to trigger molecular signaling. This finding suggests that similar phenomenon could have happened in our system. Thus, constant stress is required to enhance autocrine or paracrine mechanisms that could contribute to increased cell motility.

In conclusion, continuous compressive stress enhances migration of mammary carcinoma cells. It is possible that the reorganization of cytoskeleton by compressive stress is sufficient to drive internal polarization for directional migration of 67NR cells, independent of any changes in gene transcription. Indeed, a recent report has also

demonstrated persistent and fast migration of cancer cells when they were mechanically confined in channels of size comparable to cell size [55]. Coordinated migration of 67NR mammary carcinoma cells induced by compressive stress in an *in vitro* scratch-wound assay has relevance to *in vivo* situations when cancer cells form an "coordinated" invading mass guided by "leader" cells - another mode of cell movement termed as collective/coordinated cell migration, which has been demonstrated by most epithelial cancers in histopathological sections [56]. Furthermore, it should be noted that compressive stress did not affect migration of normal fibroblasts (CRL-2575; Appendix Fig. A4) that constitute the majority of stroma, but it has been previously reported to regulate the production of extracellular matrix[57]. Several studies have shown that matrix rigidity can transform cells to malignant phenotypes [11,58]. Thus, while most studies focus on molecular pathways of collective cell migration[56,59], an intriguing possibility, supported by our study, is that the initial step of collective tumor migration could be triggered by compressive stress in the growing tumor.

References

1. Chien, S. 2006. Mechanical and chemical regulation of endothelial cell polarity. *Circ Res*. 98:863-5.
2. Yao, Y., A. Rabodzey, and C.F. Dewey, Jr. 2007. Glycocalyx modulates the motility and proliferative response of vascular endothelium to fluid shear stress. *Am J Physiol Heart Circ Physiol*. 293:H1023-30.
3. Burr, D.B., A.G. Robling, and C.H. Turner. 2002. Effects of biomechanical stress on bones in animals. *Bone*. 30:781-6.
4. Grodzinsky, A.J., M.E. Levenston, M. Jin, and E.H. Frank. 2000. Cartilage tissue remodeling in response to mechanical forces. *Annu Rev Biomed Eng*. 2:691-713.
5. Farge, E. 2003. Mechanical Induction of Twist in the Drosophila Foregut/Stomodeal Primordium. *Current Biology*. 13:1365-1377.

6. Nerurkar, N.L., A. Ramasubramanian, and L.A. Taber. 2006. Morphogenetic adaptation of the looping embryonic heart to altered mechanical loads. *Dev Dyn*. 235:1822-9.
7. Padera, T.P., B.R. Stoll, J.B. Tooredman, D. Capen, E. di Tomaso, and R.K. Jain. 2004. Pathology: cancer cells compress intratumour vessels. *Nature*. 427:695.
8. Bernards, R. 2003. Cancer: cues for migration. *Nature*. 425:247-8.
9. Helmlinger, G., P.A. Netti, H.C. Lichtenbeld, R.J. Melder, and R.K. Jain. 1997. Solid stress inhibits the growth of multicellular tumor spheroids. *Nat Biotechnol*. 15:778-83.
10. Cheng, G., J. Tse, R.K. Jain, and L.L. Munn. 2009. Micro-environmental mechanical stress controls tumor spheroid size and morphology by suppressing proliferation and inducing apoptosis in cancer cells. *PLoS ONE*. 4:e4632.
11. Paszek, M.J., N. Zahir, K.R. Johnson, J.N. Lakins, G.I. Rozenberg, A. Gefen, C.A. Reinhart-King, S.S. Margulies, M. Dembo, D. Boettiger, D.A. Hammer, and V.M. Weaver. 2005. Tensional homeostasis and the malignant phenotype. *Cancer Cell*. 8:241-254.
12. Lopez, J.I., J.K. Mouw, and V.M. Weaver. 2008. Biomechanical regulation of cell orientation and fate. *Oncogene*. 27:6981-93.
13. Butcher, D.T., T. Alliston, and V.M. Weaver. 2009. A tense situation: forcing tumour progression. *Nat Rev Cancer*. 9:108-22.
14. Downey, C., D.H. Craig, and M.D. Basson. 2008. Pressure activates colon cancer cell adhesion via paxillin phosphorylation, Crk, Cas, and Rac1. *Cell Mol Life Sci*. 65:1446-57.
15. Craig, D.H., C.P. Gayer, K.L. Schaubert, Y. Wei, J. Li, Y. Laouar, and M.D. Basson. 2009. Increased extracellular pressure enhances cancer cell integrin-binding affinity through phosphorylation of beta1-integrin at threonine 788/789. *Am J Physiol Cell Physiol*. 296:C193-204.
16. Koike, C., T.D. McKee, A. Pluen, S. Ramanujan, K. Burton, L.L. Munn, Y. Boucher, and R.K. Jain. 2002. Solid stress facilitates spheroid formation: potential involvement of hyaluronan. *Br J Cancer*. 86:947-53.
17. Gevertz, J.L., G.T. Gillies, and S. Torquato. 2008. Simulating tumor growth in confined heterogeneous environments. *Phys Biol*. 5:36010.
18. Ingber, D.E. 1997. Tensegrity: the architectural basis of cellular mechanotransduction. *Annu Rev Physiol*. 59:575-99.
19. Li, R., and G.G. Gundersen. 2008. Beyond polymer polarity: how the cytoskeleton builds a polarized cell. *Nat Rev Mol Cell Biol*. 9:860-73.
20. Aslakson, C.J., and F.R. Miller. 1992. Selective events in the metastatic process defined by analysis of the sequential dissemination of subpopulations of a mouse mammary tumor. *Cancer Res*. 52:1399-405.
21. Naito, S., A.C. von Eschenbach, and I.J. Fidler. 1987. Different growth pattern and biologic behavior of human renal cell carcinoma implanted into different organs of nude mice. *J Natl Cancer Inst*. 78:377-85.
22. Bockhorn, M., S. Roberge, C. Sousa, R.K. Jain, and L.L. Munn. 2004. Differential gene expression in metastasizing cells shed from kidney tumors. *Cancer Res*. 64:2469-73.

23. Sodunke, T.R., K.K. Turner, S.A. Caldwell, K.W. McBride, M.J. Reginato, and H.M. Noh. 2007. Micropatterns of Matrigel for three-dimensional epithelial cultures. *Biomaterials*. 28:4006-16.
24. Putnam, A.J., J.J. Cunningham, B.B. Pillemer, and D.J. Mooney. 2003. External mechanical strain regulates membrane targeting of Rho GTPases by controlling microtubule assembly. *Am J Physiol Cell Physiol*. 284:C627-39.
25. Roose, T., P.A. Netti, L.L. Munn, Y. Boucher, and R.K. Jain. 2003. Solid stress generated by spheroid growth estimated using a linear poroelasticity model small star, filled. *Microvasc Res*. 66:204-12.
26. Sarntinoranont, M., F. Rooney, and M. Ferrari. 2003. Interstitial stress and fluid pressure within a growing tumor. *Ann Biomed Eng*. 31:327-35.
27. Liang, C.-C., A.Y. Park, and J.-L. Guan. 2007. In vitro scratch assay: a convenient and inexpensive method for analysis of cell migration in vitro. *Nat. Protocols*. 2:329-333.
28. Johnson, E.M., and W.M. Deen. 1996. Hydraulic Permeability of Agarose Gels. *AIChE Journal*. 42:1220.
29. Hannoun, B., and G. Stephanopoulos. 1986. Diffusion coefficents of glucose and ethanol in cell-free and cell-occupied calcium alginate membranes. *Biotechnology and Bioengineering*. 28:829-835.
30. van Zyp, J.V., W.C. Conway, D.H. Craig, N.V. van Zyp, V. Thamilselvan, and M.D. Basson. 2006. Extracellular pressure stimulates tumor cell adhesion in vitro by paxillin activation. *Cancer Biol Ther*. 5:1169-78.
31. Onoue, N., J. Nawata, T. Tada, D. Zhulanqiqige, H. Wang, K. Sugimura, Y. Fukumoto, K. Shirato, and H. Shimokawa. 2008. Increased static pressure promotes migration of vascular smooth muscle cells: involvement of the Rho-kinase pathway. *J Cardiovasc Pharmacol*. 51:55-61.
32. Manome, Y., N. Saeki, H. Yoshinaga, M. Watanabe, and S. Mizuno. 2003. A culture device demonstrates that hydrostatic pressure increases mRNA of RGS5 in neuroblastoma and CHC1-L in lymphocytic cells. *Cells Tissues Organs*. 174:155-61.
33. Lou, Y., O. Preobrazhenska, U. auf dem Keller, M. Sutcliffe, L. Barclay, P.C. McDonald, C. Roskelley, C.M. Overall, and S. Dedhar. 2008. Epithelial-mesenchymal transition (EMT) is not sufficient for spontaneous murine breast cancer metastasis. *Dev Dyn*. 237:2755-68.
34. van Deurs, B., Z.Z. Zou, P. Briand, Y. Balslev, and O.W. Petersen. 1987. Epithelial membrane polarity: a stable, differentiated feature of an established human breast carcinoma cell line MCF-7. *J Histochem Cytochem*. 35:461-9.
35. Paszek, M.J., and V.M. Weaver. 2004. The tension mounts: mechanics meets morphogenesis and malignancy. *J Mammary Gland Biol Neoplasia*. 9:325-42.
36. Dartsch, P.C., and E. Betz. 1989. Response of cultured endothelial cells to mechanical stimulation. *Basic Res Cardiol*. 84:268-81.
37. Li, J., S. Zhang, J. Chen, T. Du, Y. Wang, and Z. Wang. 2009. Modeled microgravity causes changes in the cytoskeleton and focal adhesions, and decreases in migration in malignant human MCF-7 cells. *Protoplasma*.
38. Ingber, D.E. 2003. Tensegrity I. Cell structure and hierarchical systems biology. *J Cell Sci*. 116:1157-73.

39. Ingber, D.E. 2008. Tensegrity-based mechanosensing from macro to micro. *Prog Biophys Mol Biol*. 97:163-79.
40. Nicolas, A., B. Geiger, and S.A. Safran. 2004. Cell mechanosensitivity controls the anisotropy of focal adhesions. *Proc Natl Acad Sci U S A*. 101:12520-5.
41. Yang, J., S.A. Mani, J.L. Donaher, S. Ramaswamy, R.A. Itzykson, C. Come, P. Savagner, I. Gitelman, A. Richardson, and R.A. Weinberg. 2004. Twist, a Master Regulator of Morphogenesis, Plays an Essential Role in Tumor Metastasis. *Cell*. 117:927-939.
42. Lin, S.Y., W. Xia, J.C. Wang, K.Y. Kwong, B. Spohn, Y. Wen, R.G. Pestell, and M.C. Hung. 2000. Beta-catenin, a novel prognostic marker for breast cancer: its roles in cyclin D1 expression and cancer progression. *Proc Natl Acad Sci U S A*. 97:4262-6.
43. Chan, D.A., and A.J. Giaccia. 2007. Hypoxia, gene expression, and metastasis. *Cancer Metastasis Rev*. 26:333-9.
44. Green, C.E., T. Liu, V. Montel, G. Hsiao, R.D. Lester, S. Subramaniam, S.L. Gonias, and R.L. Klemke. 2009. Chemoattractant signaling between tumor cells and macrophages regulates cancer cell migration, metastasis and neovascularization. *PLoS One*. 4:e6713.
45. Kriebel, P.W., V.A. Barr, E.C. Rericha, G. Zhang, and C.A. Parent. 2008. Collective cell migration requires vesicular trafficking for chemoattractant delivery at the trailing edge. *J Cell Biol*. 183:949-61.
46. Eckhardt, B.L., B.S. Parker, R.K. van Laar, C.M. Restall, A.L. Natoli, M.D. Tavaria, K.L. Stanley, E.K. Sloan, J.M. Moseley, and R.L. Anderson. 2005. Genomic analysis of a spontaneous model of breast cancer metastasis to bone reveals a role for the extracellular matrix. *Mol Cancer Res*. 3:1-13.
47. Suresh, S. 2007. Biomechanics and biophysics of cancer cells. *Acta Biomater*. 3:413-38.
48. Savla, U., and C.M. Waters. 1998. Mechanical strain inhibits repair of airway epithelium in vitro. *Am J Physiol Lung Cell Mol Physiol*. 274:L883-892.
49. Desai, L.P., K.E. Chapman, and C.M. Waters. 2008. Mechanical stretch decreases migration of alveolar epithelial cells through mechanisms involving Rac1 and Tiam1. *Am J Physiol Lung Cell Mol Physiol*. 295:L958-965.
50. DiMilla, P.A., J.A. Stone, J.A. Quinn, S.M. Albelda, and D.A. Lauffenburger. 1993. Maximal migration of human smooth muscle cells on fibronectin and type IV collagen occurs at an intermediate attachment strength. *J Cell Biol*. 122:729-37.
51. Palecek, S.P., J.C. Loftus, M.H. Ginsberg, D.A. Lauffenburger, and A.F. Horwitz. 1997. Integrin-ligand binding properties govern cell migration speed through cell-substratum adhesiveness. *Nature*. 385:537-40.
52. Ingber, D.E. 2005. Mechanical control of tissue growth: function follows form. *Proc Natl Acad Sci U S A*. 102:11571-2.
53. Parker, K.K., A.L. Brock, C. Brangwynne, R.J. Mannix, N. Wang, E. Ostuni, N.A. Geisse, J.C. Adams, G.M. Whitesides, and D.E. Ingber. 2002. Directional control of lamellipodia extension by constraining cell shape and orienting cell tractional forces. *FASEB J*. 16:1195-204.

54. Tschumperlin, D.J., G. Dai, I.V. Maly, T. Kikuchi, L.H. Laiho, A.K. McVittie, K.J. Haley, C.M. Lilly, P.T. So, D.A. Lauffenburger, R.D. Kamm, and J.M. Drazen. 2004. Mechanotransduction through growth-factor shedding into the extracellular space. *Nature*. 429:83-6.
55. Irimia, D., and M. Toner. 2009. Spontaneous migration of cancer cells under conditions of mechanical confinement. *Integrative Biology*. 1:489-556.
56. Friedl, P., and D. Gilmour. 2009. Collective cell migration in morphogenesis, regeneration and cancer. *Nat Rev Mol Cell Biol*. 10:445-57.
57. Chiquet, M., A.S. Renedo, F. Huber, and M. Fluck. 2003. How do fibroblasts translate mechanical signals into changes in extracellular matrix production? *Matrix Biol*. 22:73-80.
58. Kumar, S., and V.M. Weaver. 2009. Mechanics, malignancy, and metastasis: the force journey of a tumor cell. *Cancer Metastasis Rev*. 28:113-27.
59. Daly, A.J., L. McIlreavey, and C.R. Irwin. 2008. Regulation of HGF and SDF-1 expression by oral fibroblasts--implications for invasion of oral cancer. *Oral Oncol*. 44:646-51.

Chapter 3: Role of compressive stress in leader-cell formation and migration

Portions of the chapter have been taken from:

J.M. Tse, G. Cheng, J.A. Tyrrell, S.A. Wilcox-Adelman, Y. Boucher, R.K. Jain, L.L. Munn, "Compression-induced cell distension and adhesion stimulate coordinated migration of mammary carcinoma cells." Submitted.

Introduction

Unrestrained growth of cancer cells at the tumor margin inevitably generates compressive stress, as demonstrated in a mouse model [1,2]. However, the role of such stress in tumor progression remains unclear. In the previous chapter (Chapter 2), we have shown that externally-applied stress enhances migration of some cancer cell lines. Specifically, compression stimulates coordinated migration of 67NR mammary carcinoma cells in the *in vitro* scratch-wound assay.

Coordinated cell migration (collective cell migration) differs from single cell migration in that cells remain connected as they move, which results in a migrating sheet guided by "leader" cells[3,4]. The leader cells in the front row display polarized morphology including active membrane extension (protrusions), detect extracellular guidance and generate greater cytoskeletal dynamics than follower cells in the cohort[5]. Whereas leader cells at the leading edge are often less ordered and mesenchymal-like, cells at the rear tend to form more tightly packed assemblies[3]. Cell polarization can arise from perceived spatial, temporal or concentration stimulus gradients[6-8]. For example, the leader cells can polarize in response to a chemoattractant and re-organize their actin cytoskeleton for movement by generating a protrusive force at the leading edge. In the *in vitro* scratch-wound assay (an example of coordinated/collective movement), the cells sense the free space left by the scratch and the interactions with their neighbors. In absence of concentration stimulus gradients, these directional cues trigger the front row of the cells to polarize and restrict protrusive activity to the free space (leading edge).

Following cell polarization, cells actively extend the plasma membrane at the cell front and form protrusions driven by local actin polymerization. Membrane protrusions at the leading edge include lamellipodia, filopodia and other various structures[6,7]. Lamellipodia are broad, flat, sheet-like structures with actin cross-linked into a two-dimensional mesh network. By contrast, filopodia are thin, cylindrical, needle-like projections with actin filaments grouped into rope-like bundles [6], and they extend much faster than lamellipodia[9]. These membrane protrusions control the direction of cohort movement.

Most work on induction of cell polarization in the direction of collective migration has focused on the role of gradients of chemokines such as stromal cell-derived factor 1 (SDF1; also known as CXCL12) and members of the fibroblast growth factor (FGF). These factors activate members of the Rho GTPases - Rac and Cdc42-which induce formation of lamellipodia and filopodia [10,11], thus promoting directional cell migration. Recent findings show that direct mechanical distortion of cell shape promotes directional control of lamellipodia extensions where Rac activation is concentrated[12,13]. By contrast, other studies demonstrate that external mechanical tension decreases Rac activation and thus lamellipodia formation[14,15]. While those studies have focused on protrusions of singles cells, little is known about the role of mechanical stimulation in directional control of membrane protrusions of leader cells in the collective cell movement.

In this chapter, we investigated the determinant of compression-induced 67NR collective cell migration, and in particular, the effect of externally-applied stress on formation of leader cells and membrane protrusions. We determined that compressive stress stimulated the leader-cell formation with filopodial protrusions, of which the process was independent of Rac and Cdc42 activation. Utilizing micro-contact printing technology to pattern 67NR cells in defined geometries, we instead identified a mechanism responsible for compression-modulated formation of a population of "leader cells" which appear to orchestrate the coordinated migration.

Materials and Methods

Cell cultures

The murine mammary carcinoma cell line 67NR, kindly provided by Dr. Fred R. Miller at Wayne State University [16], had been transduced with the enhanced green fluorescent protein (EFGP) retrovirus described earlier in the Materials and Methods of Chapter 2. The cells were cultured in high-glucose DMEM (Sigma D5671) supplemented with 10% fetal bovine serum (FBS) and 1% non-essential amino acid (Gibco), and were incubated at 37°C with 5%CO_2.

In vitro scratch wound-compression experiment

To assess cancer cell migration under compression, the same *in vitro* compression device described in Chapter 2 (Fig. 2.1) was used, and cell migration was assessed with scratch-wound assay. Briefly, 67NR-GFP cells were allowed to grow to confluence on uncoated transwell inserts. Using a p-200 pipette tip the monolayer was scraped to denude a

circular area of ~1000 μm in diameter. The wound closure was monitored microscopically under stress-free or a compressive stress of 5.8mmHg and migration was determined as the change in wound area covered by cells 16 hr after wounding (unless specified). In this chapter, other than *in vitro* wound-scratch assay, cell micro-contact printing method (described below) was also performed to assess cell migration on different geometries.

Cell micro-contact printing

We patterned 67NR mammary carcinoma cells in defined geometries using micro-contact printing. For circles and rosettes, the fibronectin (and cells) were *excluded* from the shapes; for squares, the fibronectin (and cells) were *confined* to the shape. The fabrication of polydimethylsiloxane (PDMS) stamps used for micro-contact printing has been previously described [17-19]. In brief, a template used in the molding of stamps was fabricated with UV photolithography. To fabricate a PDMS stamp with defined features, the prepolymer mixed with a curing agent (10:1 ratio) was poured onto a template and cured to crosslink the polymer. The PDMS stamp with defined pattern was then pre-coated with a 1:2 mixture of 50ug/mL rhodamine-conjugated fibronectin (Cytoskeleton Inc, Denver, CO) and 50ug/mL non-conjugated fibronectin (BD Biosciences, San Jose, CA) for 1 hr at room temperature. For fibronectin to transfer onto the transwell membranes efficiently, the transwell inserts were pre-treated with plasma oxidation for 30 seconds. In order to reduce non-specific cell adhesion, transwell membranes were blocked with 3% BSA (Sigma) for 1 hr at room temperature prior to seeding 67NR cells in serum free medium. Any floating cells were removed after 1 hr and full-growth

medium was then added. The cells were allowed to attach overnight and cell compression experiments were performed the next day. The cell patterns were monitored microscopically under stress-free or a compressive stress of 5.8mmHg and migration was determined as the distance travelled by cells over a 20-hr period.

Immunofluorescence microscopy

To visualize the actin cytoskeleton, the 67NR cells after *in vitro* scratch wound-compression experiment were fixed with 4% paraformaldehyde in phosphate buffered saline (PBS), permeabilized and blocked with 5% normal horse serum containing 0.2% Triton X-100. The cells were then incubated with Alexa Fluor-546 phalloidin (1:200, Molecular Probe) for 20 min at room temperature. The cells were mounted in Vectashield Mounting Medium containing nuclear dye DAPI and then visualized with an Olympus FluoView 500 confocal microscope system (Olympus, Center Valley, PA).

Quantification of leader-cell frequency

Confluent 67NR cells on transwell inserts were scraped with a p-200 pipette tip and then compressed for 16 hours with the *in vitro* compression device. The 67NR cells were then stained with actin-phalloidin and counterstained with DAPI. The 67NR cells at wound leading edges were imaged with a laser scanning confocal microscope for analysis with ImageJ 1.4J software. The fraction of leader cells was calculated as the number of leader cells relative to the total number of perimeter cells. Perimeter cells were defined as any cell bordering the periphery of the cell-denuded area. "Leader cells" were defined as those with leading edge protrusions (filopodia) along the longest axis of the cell invading

toward the open wound area. To be classified as a leader cell, the cell must have at least one protrusion longer than 5um, and the longest protrusion must have free perimeter on both sides, for at least some of its length.

Quantification of cell morphology

The 67NR cells at the wound periphery were stained for actin-phalloidin, counterstained with DAPI and imaged with a laser scanning confocal microscope. The confocal images were then analyzed with ImageJ 1.4J software to determine the projected cell area (cell-substrate contact area), whole length and frontal length of leader cells and the nuclear offset index. The projected cell area was calculated as the total cell area bounded by phalloidin staining divided by the number of DAPI-stained nuclei. To compare the projected cell area of the leading edge and internal monolayer, the cells at the wound edge were considered as "leading edge", while the cells that were a few rows away from the wound edge were considered as "internal monolayer". The whole cell length is measured transversely from the leading tip of the leader cell to the opposite end, while frontal length is measured transversely from its leading tip to its nucleus. The nuclear offset index (a measure of leader cell polarization) was determined as frontal length relative to the whole cell length.

Quantification of cell pattern shape change

67NR mammary carcinoma cells were patterned on square islands (500mm X 500mm), using micro-contact printing. The cells were then cultured in the compression device with or without a piston (compressed or uncompressed respectively) for 16-20 hrs. Fluorescent

images of the cell patterns were captured with an inverted microscope (Olympus IX 70, Center Valley, PA) at the beginning (t_0) and the end (t_{end}) of the compression period. To quantify the effect of cell pattern geometry on leader-cell formation, images were analyzed with NIH ImageJ 1.40f to determine the shape change index (SCI), defined as: $SCI = \frac{(b_{tend} - b_{t0})/b_{t0}}{(a_{tend} - a_{t0})/a_{t0}}$, where a_i and b_i are the height (shortest) and diagonal of the cell pattern, respectively.

Measurement of Rac1 activity

The 67NR cells were seeded at 30% confluency in full-growth medium and then serum-starved the next day for 16 hours. After serum starvation, the cells were either stress-free or compressed at 5.8 mmHg for the indicated duration. Cell lysates were then collected and active Rac1 level was determined by two different methods: (1) Rac1 pull-down followed by Western blot, and (2) ELISA-based Rac activation assay. For Rac1 pull-down assay, Rac1 Activation Assay Biochem Kit (Cytoskeleton, Inc.) was used to extract active Rac1 according to the manufacturer's instruction. The pull-down proteins and total proteins (without pull-down) were analyzed by Western Blot for active Rac1 and total Rac1, respectively.

For ELISA-based Rac activation assay, Rac1 activity in uncompressed and compressed cells was also measured with Rac G-LISA Activation Assay (Cytoskeleton, Inc), following the manufacturer's instructions. Briefly, equal amount of protein from collected cell lysates was incubated in Rac-GTP affinity plate (binding active Rac) for

30mins. Then antibody detection reagent was added, and signal was developed with colorimetric methods.

Measurement of Cdc42 activity by pull-down assay

The 67NR cells were seeded at 30% confluence in full-growth medium and then serum-starved the next day for 16 hours. After serum starvation, the cells were either stress-free or compressed at 5.8 mmHg for the indicated duration. Then, the cells were washed in ice-cold phosphate-buffered saline, incubated for 5 min on ice in the radio immunoprecipitation assay (RIPA) lysis buffer, and then centrifuged for 5 min at 10,000 *g* at 4°C. Aliquots of total protein samples were taken from the sample supernatant to determine protein concentration. Equal amount of protein was incubated with PAK-PBD GST fusion proteins (Cytoskeleton, Inc), bound to glutathione-coupled Sepharose beads at 4°C for 1 hour. The beads and proteins bound to the fusion protein were washed three times in an excess of RIPA lysis buffer, eluted in Laemmli sample buffer (60 mM Tris, pH 6.8, 5% beta-mercaptoethanol, 10% glycerin, 0.1% bromphenol blue) and then boiled at 100°C for 5 mins. These pull-down and total protein samples were analyzed for active Cdc42 and total Cdc42, respectively, by Western blotting using a polyclonal rabbit antibody against Cdc42 (Cell Signaling Technology). Beta-actin was used as a loading control.

Transient transfection

The day before transfection, 67NR cells were freshly plated at 70% confluence in 6-well plates. Transient transfections with different Rac1-related, Cdc42-related or control

plasmids (8ug/well) were performed using Lipofectamine 2000 (20ul/well; Invitrogen) according to the manufacturer's instruction. All the plasmids were purchased from Addgene (Cambridge, MA) and they were pcDNA3-eGFP-Rac1-T17N (Plasmid 12982; Rac1 dominant negative), pcDNA3-eGFP-Rac1-Q61L (Plasmid 12981; Rac1 constitutively active), pcDNA3-eGFP-Cdc42-T17N (Plasmid 12976; Cdc42 dominant negative), pcDNA3-eGFP-Cdc42-Q61L (Plasmid 12986; Cdc42 constitutively active), and pcDNA3-eGFP (Plasmid 13031; control). After overnight incubation at 37°C, the transfected cells (expressing eGFP) were used to perform *in vitro* scratch wound-compression experiment.

Statistical analysis

Quantitative data are shown as mean ± s.e.m., and $P \leq 0.05$ was considered significant in unpaired, two-tailed Student's t-tests.

Results

Compressive stress enhances leader-cell formation

In the previous chapter (Chapter 2), we showed that compression induced a directionality and persistence in the movement of 67NR cells at the leading edge of the cell sheet. The top panel of Figure 3.1A illustrates that in the absence of compression (control), the cells extended in random directions and clustered at the wound periphery after 16 hours. In contrast, compressed 67NR cells preferentially aligned perpendicular to the wound periphery with the leading edges extending into the open area. Using Alexa546-phalloidin to visualize F-actin in migrating 67NR cells, we found that actin alignment

was more pronounced in compressed cells (Fig. 3.1A, bottom). More importantly, there was a striking difference in the formation of "leader cells" between the control and compressed cultures. Leader cells (marked by yellow triangles in Fig. 3.1A, bottom) are defined as individual cells at the wound periphery that extend protrusions into the denuded area while maintaining connections with neighboring cells. The number of leader cells was nearly doubled when the 67NR cells were exposed to mechanical compression (Fig. 3.1B).

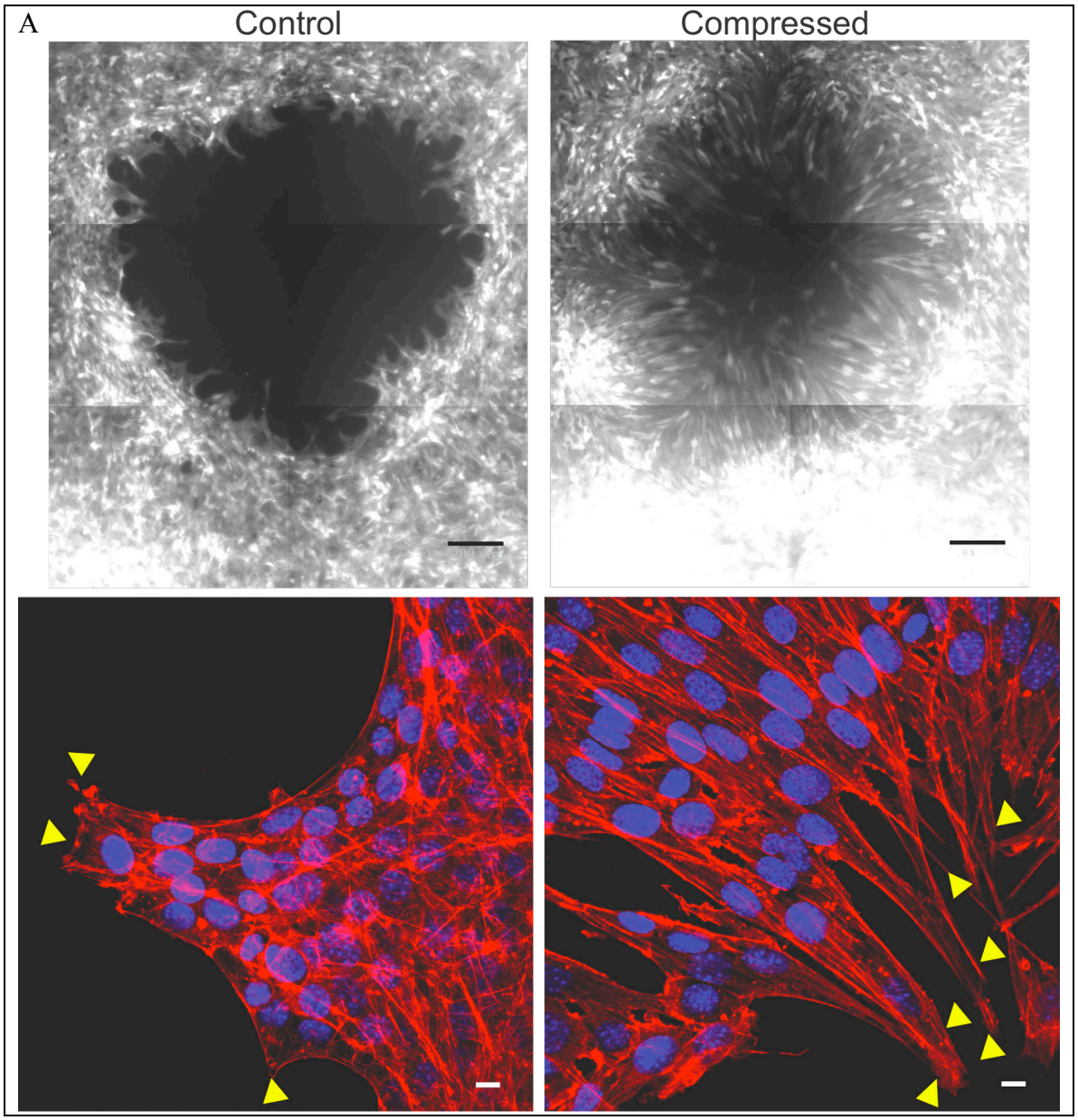
A
Control
Compressed

B

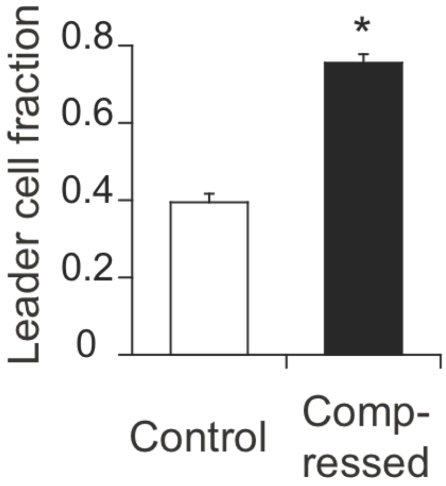

Figure 3.1. Externally-applied stress enhances leader-cell formation. A, Representative images (from 3-4 independent experiments) of control (left side) and compressed 67NR cells (right side) closing the "wound" after 16 hrs. The top panel shows the wound closure of 67NR-GFP cells under 16-hr stress-free (control) or compressive stress of 5.8mmHg, visualized by fluorescent microscopy. The cells were then fixed for phalloidin staining for actin microfilaments (bottom panel; red: actin microfilaments; blue: nuclei) and imaged by confocal microscopy. The compressed cells at the leading edge showed directional alignment (top) and contained elongated actin filaments (red; bottom) perpendicular to the cell-denuded areas. Examples of leader cells, defined as individual cells at the wound margin that extend protrusions into the denuded area, were indicated by the yellow triangles. Scale bar, 200um (top) and 10um (bottom). **B,** The fraction of cells around the denuded periphery that were phenotypically determined to be leader cells was dramatically higher in the 16-hr compressed samples. Leader cells are defined as those cells at the wound margin that extend protrusions into denuded area (n=12; *P<0.005 compared with control). For a more detailed definition of

leader cells, please see Methods and Materials. Error bars represent s.e.m.

Next, we assessed the size, shape and polarization of the leader cells in compressed and control cultures. Although leader cells were always polarized in both conditions (Fig. 3.2A), those under compression had larger projected cell-substrate contact areas (Fig. 3.2B). Furthermore, when the total cell length and frontal length (measured from the nucleus to the leading tip of the cell) of the leader cells were quantified, we found that the whole cell length distribution of the leader cells in the compressed cultures was shifted toward longer cells (Fig. 3.3A). More importantly, the leader cells in compressed culture had more extended filopodial protrusions, as indicated by a longer frontal length (Fig.3.3B). Filopodial protrusion functions as a sensor of local environment and as a mechanical device in "probing" the surrounding environment. These long filopodia would increase the extent of free-cell perimeter - the portion of cell periphery not associated with neighboring cells, open to free space - available for new matrix adhesions, thereby enhancing leader-cell formation, and the directionality and motility of the leader cells. Enhanced protrusions have also been observed in another cell line (LS174T, human colon carcinoma cells) under compression (Appendix Fig. B1).

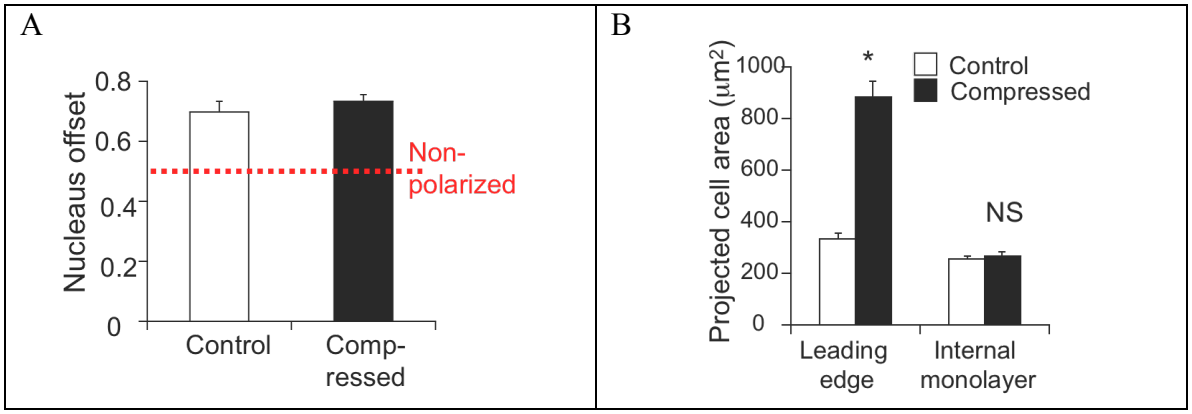

Figure 3.2. Both control and compressed 67NR cells at the leading edge of the "wound" are polarized but the compressed ones have larger projected cell-substrate contact area. A, Average nucleus offset of leader cells in both control (n= 107 cells) and compressed (n= 177cells) cultures. Nucleus offset was determined as the ratio of the frontal length, measured from the leading tip of the cell to its nucleus, to the total cell length, obtained by extending a line from the leading tip through the nucleus to the trailing edge of the cell. A nucleus offset greater than 0.5 implies cell polarization as the nucleus is located closer to the rear end of the cell (NS=not significant). **B,** Average projected cell areas of the control and compressed 67NR cells at the leading edge of the "wound" and those in the internal monolayer, far from the edge, (n=7-8. NS=not significant; *P<0.005 compared with the control in the same group). Error bars represent s.e.m.

A

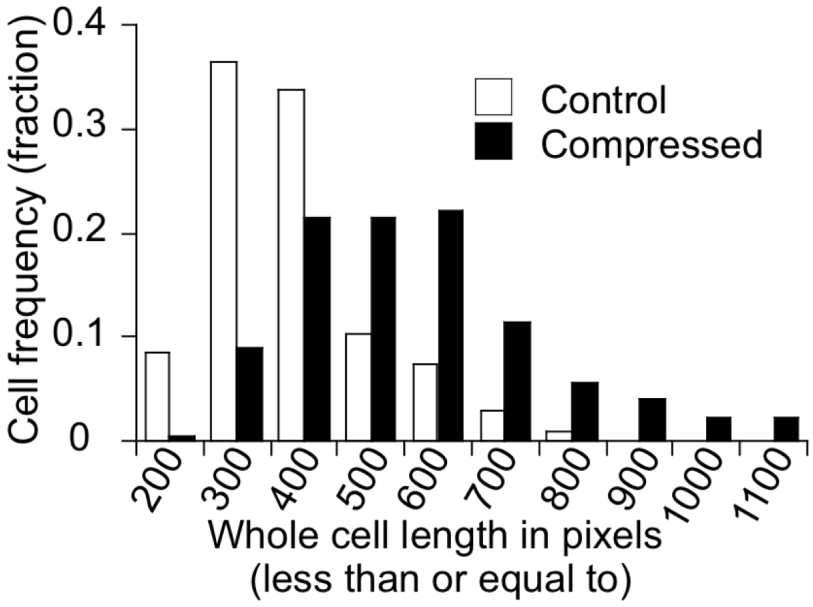

B

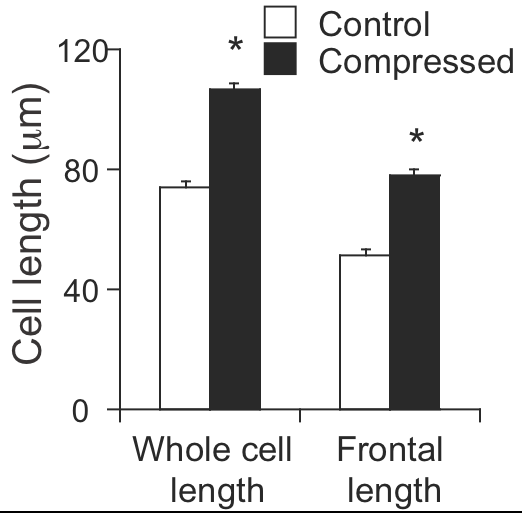

Figure 3.3. Compressive stress induces 67NR cell extension and filopodial protrusions. A, Histogram of leader cell lengths in the control (n = 107 cells) and compressed (n = 177 cells) cultures. **B,** Comparison of average cell lengths in control and compressed samples. Frontal length (filopodial protrusion length) was measured from the leading tip of the cell to its nucleus (*P<0.005 compared with the control). Error bars represent s.e.m.

ACS-induced cell extrusion compensates for geometry-driven leader-cell formation

To evaluate whether leader-cell formation could be related to the free cell perimeter, we controlled cell-cell spatial organization by seeding 67NR cells on fibronectin-coated adhesive patterns generated by micro-contact printing. Fluorescent images of the fibronectin-coated patterns created with polydimethylsiloxane (PDMS) stamps are shown in Appendix Figure B2. By patterning the cells on different polygonal-shaped geometries, we were able to alter the extent of free-cell perimeter (compared to that associated with neighboring cells) and then monitor their migration behaviors. For instance, while the cells around the periphery of the circle have roughly the same extent of free perimeter,

the cells at the corners of a square have more free cell perimeter than those on the edges of the pattern. To validate the system, we first patterned cells surrounding a circular void (analogous to the scratch-wound assay geometry). In agreement with the results obtained in the circular scratch cultures (Chapter 2, Fig. 2.1 and Fig. 3.1), compression resulted in leader-cell formation (Fig. 3.4A) and faster wound closure (Fig. 3.4B), as opposed to slower wound closure and infrequent leader-cell formation in the uncompressed circle pattern.

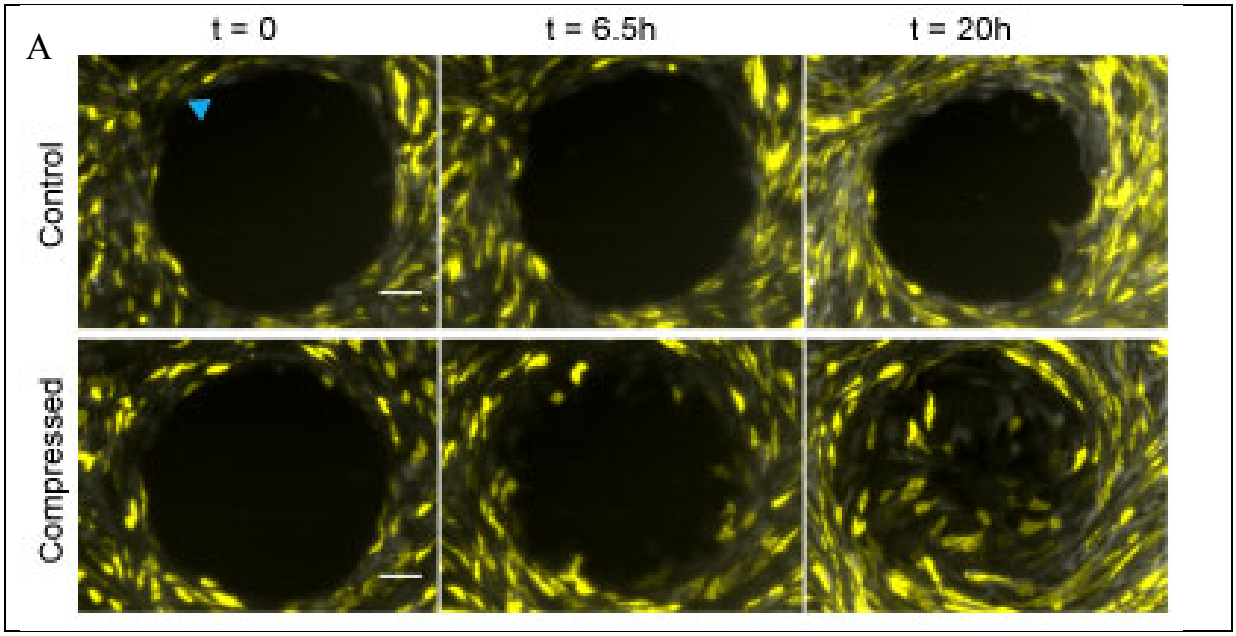

B

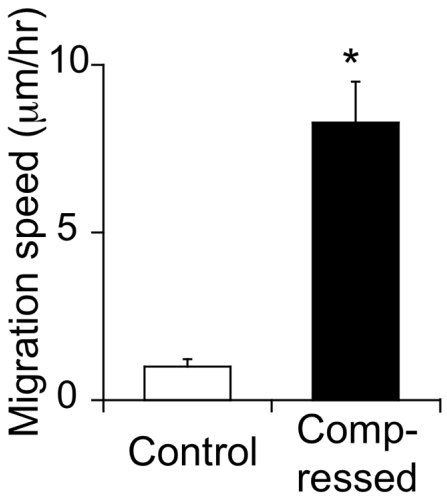

Figure 3.4. Compression-induced leader cells and enhanced cell migration were reproduced in circular patterns created by cell micro-contact printing. A, Representative images of morphological changes and cell migration when 67NR cell monolayers (yellow and gray) were patterned into circles and subjected to either stress-free (control) or a compressive stress of 5.8mmHg using the device in Figure 2.1. Filled blue triangles represent edge cells (with free cell perimeter, defined as the fraction of cell periphery not associated with neighboring cells and free to open space, less than 25%) (n=6-8; scale bar,100um). The compressed cultures show significantly more leader cells than that in control culture. **B,** Average migration rate of control and compressed cells in circle patterns (n=6-7; *P<0.005). Error bars represent s.e.m.

Next, we patterned 67NR cells in a square geometry such that the cells at the four square corners have higher free-cell perimeter than other edge cells. Similar to the results from the compressed circular-void cultures, applied compression facilitated leader-cell

formation uniformly at all positions around the square. In contrast, the uncompressed 67NR cells cultured on square islands preferentially protruded at the square corners (Fig. 3.5A). Figure 3.5B depicts the quantitative analysis with a shape change index describing the extent of square distortion due to cell movement. The geometry-driven leader-cell formation in uncompressed cultures indicates that local cell-cell spatial arrangement affecting free-cell perimeter can influence cell migration behavior, while ACS-induced leader-cell formation is independent of cell micro-organization.

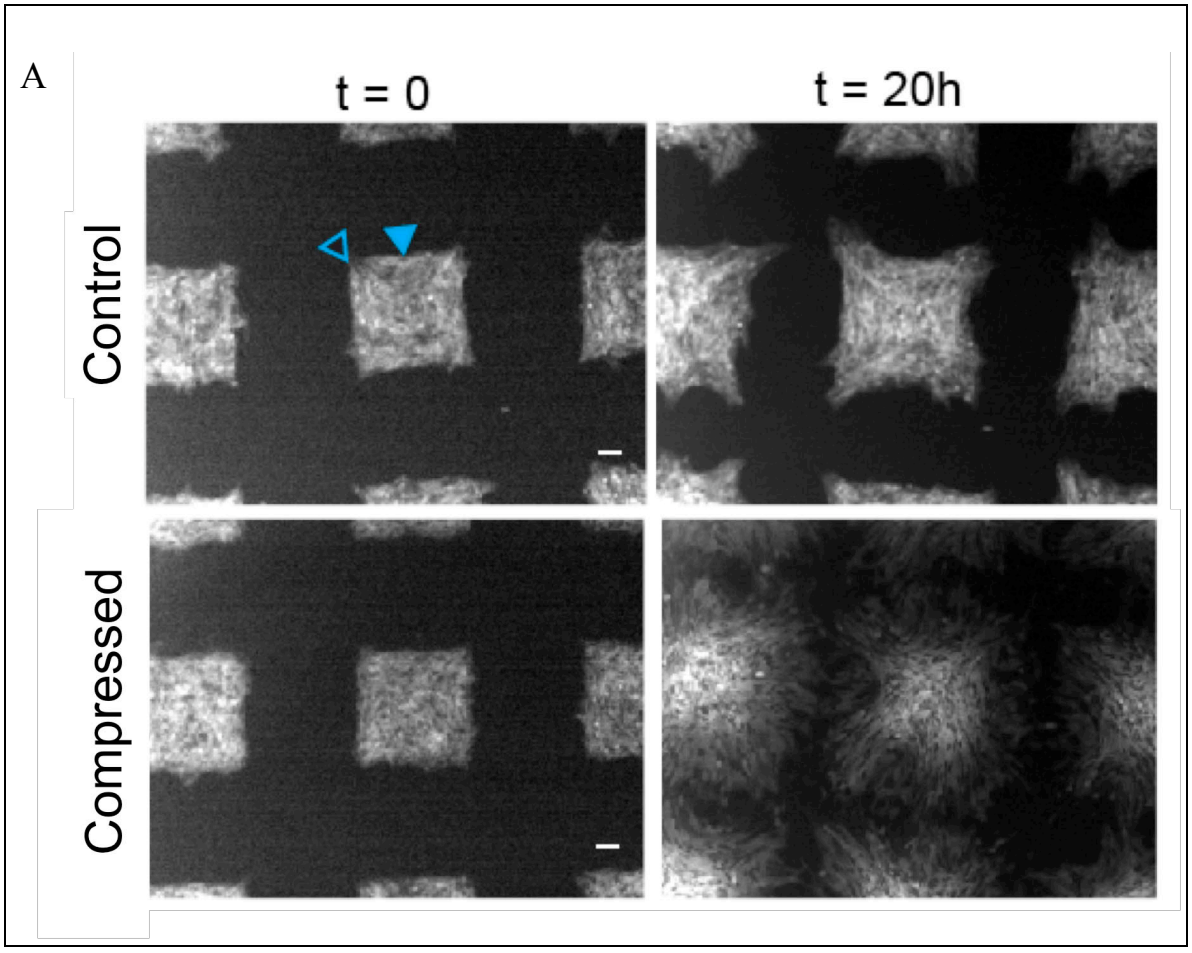

B

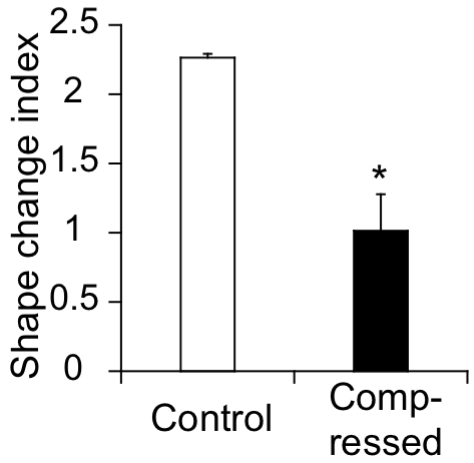

Figure 3.5. Compressive stress induces leader-cell formation independent of geometry-driven polarization. A, Representative images of morphological changes and cell migration when 67NR cell monolayers (gray) were patterned into squares and subjected to either stress-free (control) or a compressive stress of 5.8mmHg using the device in Figure 2.1. Filled and open triangles represent edge cells (with free cell perimeter less than 25%) and corner cells (with free cell perimeter of at least or more than 25%), respectively (n=6-8; scale bar,100um). **B,** 500 X 500 μm square patterns distort due to cell migration, and this can be quantified using a shape change index. For compressed cells, the index is ~1 suggesting that the square pattern expands uniformly around the boundary; in contrast, control samples had much higher indices, indicating that the shape expanded preferentially along the diagonals (n=8; *P<0.005). Error bars represent s.e.m.

Finally, we forced 67NR cells to extend by patterning them in a rosette configuration (see the fibronectin-coated pattern in Appendix Figure B2) with potential leader cells pre-

defined at the rosette tips (Fig. 3.6A). The cells at the points of the rosette have, on average, much greater extent of free perimeter than those at the square corners. Consistent with the findings from the circular-void and square patterns, there was no preferential location for enhanced leader-cell formation with compression (Figs. 3.6A and 3.6B), while in uncompressed cultures, extension of leader cells from these tips was more frequent than from the smooth edges of the pattern (Fig. 3.6C). Taken together, these findings suggest that (1) the spatial organization of cells in uncompressed cultures influences free-cell perimeter, resulting in distinctive patterns of localized leader-cell formation; and (2) exogenous force is able to induce leader cells, independent of cell micro-organization by causing an increase in free-cell perimeter and cell-substrate contact.

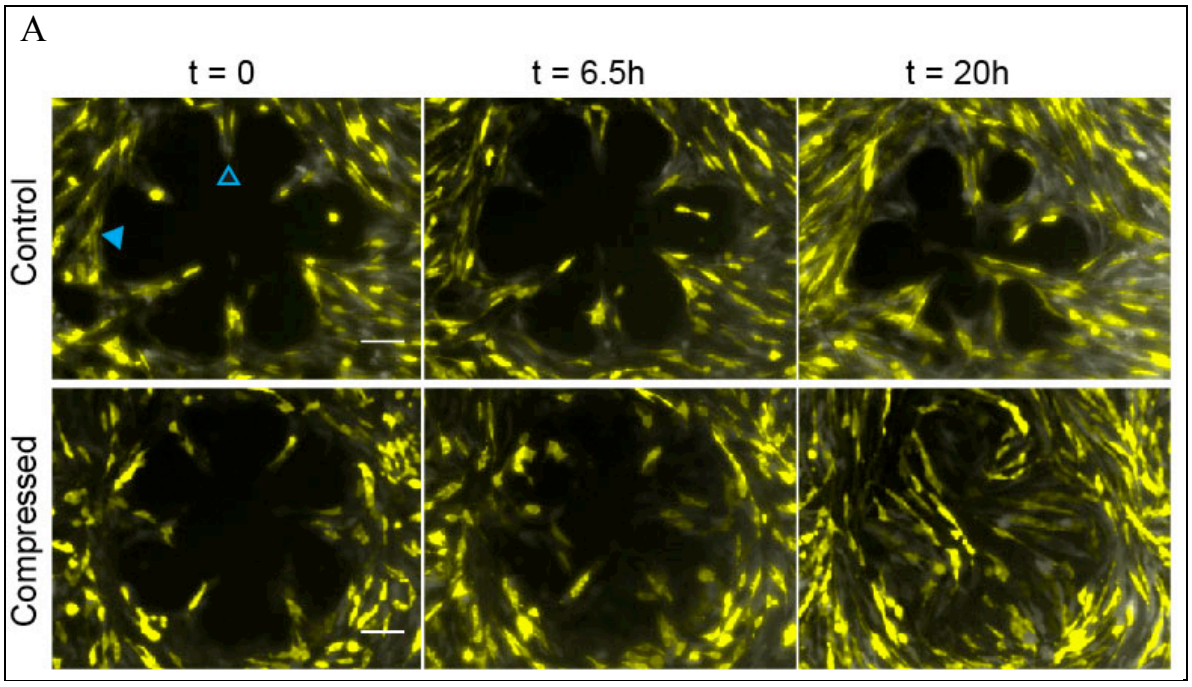

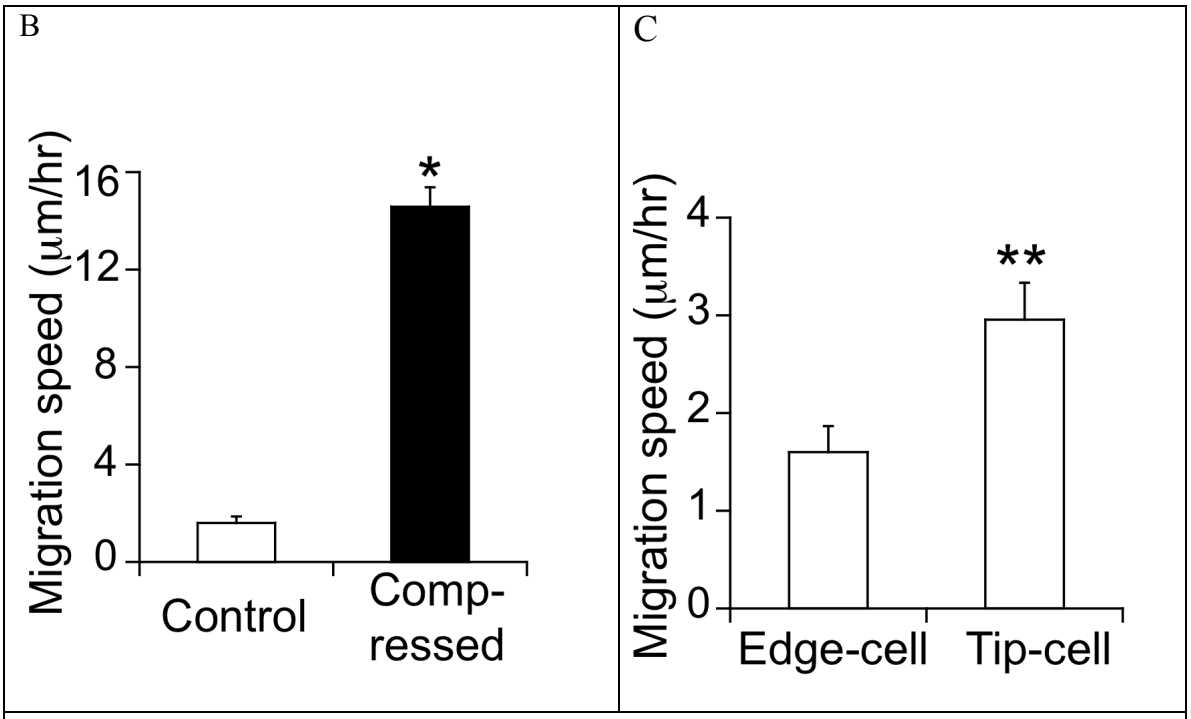

Figure 3.6. Free-cell perimeter determines leader-cell formation: geometry-driven in uncompressed cultures vs. cell distension-induced by compressed cultures. A, Representative images of morphological changes and cell migration when 67NR cell monolayers (yellow and gray) were patterned into rosettes and subjected to either stress-free (control) or a compressive stress of 5.8mmHg using the device in Figure 2.1. Filled and open triangles represent edge cells (with free cell perimeter less than 25%) and tip cells –potential leader cells predefined at the rosette tips- (with free cell perimeter more than 50%), respectively (n=6-8; scale bar, 100um). There was no preferential location for enhanced leader cell formation with compression, while in uncompressed cultures, extension of leader cells from these tips was more frequent than from the smooth edges of the pattern. **B,** Average migration speed of compressed cells is higher than that of control cells in rosette patterns, due to an increase in leader-cell formation (n=13-17; *P<0.005). **C,** Average migration speed of tip-cells is higher than that of edge-cells in the uncompressed cultures, suggesting that induction of leader cells increases their cell motility (n=13-17; **P<0.05 compared with edge cells). Error bars represent s.e.m.

Compression-induced formation of filopodial protrusion is Rac-activation-independent

We have shown that formation of leader cells with filopodial protrusions was induced in the compressed cultures (Figs. 3.1A and 3.3B). To become leader cells, they polarize and extend protrusions to detect the surrounding microenvironment. Studies have shown that Rac1 and Cdc42 - members of Rho family small guanosine triphosphate (GTP)-binding proteins (GTPases) as versatile modulators of cell shape that act on actin cytoskeleton - regulate cell polarity and the formation of protrusions [20-22]. In addition, mechanical stress (e.g. shear stress, stretching) can influence the activity of Rho-GTPases[14,23,24]. We first investigated whether compression increases Rac1 activity. Considering the fact that GTPase activation is usually a rapid and dynamic response (e.g. growth factor-induced activation within minutes), we measured Rac1 activation at various time points throughout the course of compression. Using Rac pull-down assay followed by Western blot analysis and more sensitive Enzyme-Linked Immunosorbent Assay (ELISA), we determined that compression did not have any significant effect on Rac activity level (Figs. 3.7A and 3.7B). Even when we suppressed Rac1 activity by introducing mutant Rac proteins (RacT17N) for competitive inhibition[25], compression-induced formation of leader cells with filopodial protrusions was not abolished (Fig. 3.7C). Collectively, these findings suggest that Rac1 is not involved in formation of leader cells or filopodial protrusions induced by mechanical compression.

A

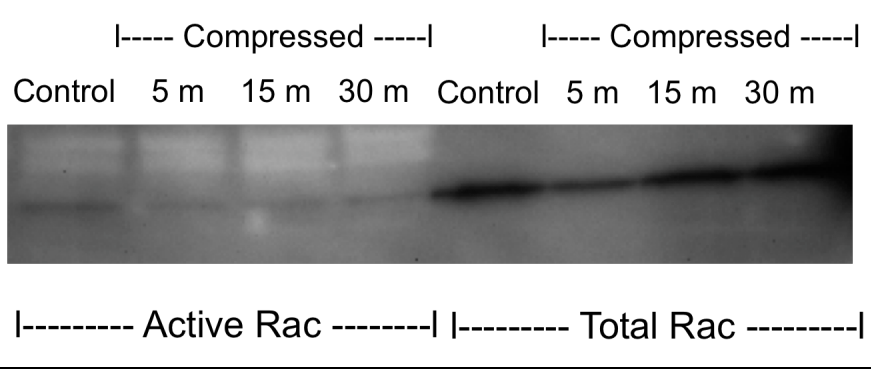
I----- Compressed -----I
I----- Compressed -----I
Control 5 m 15 m 30 m Control 5 m 15 m 30 m
I--------- Active Rac --------I I--------- Total Rac ---------I

B

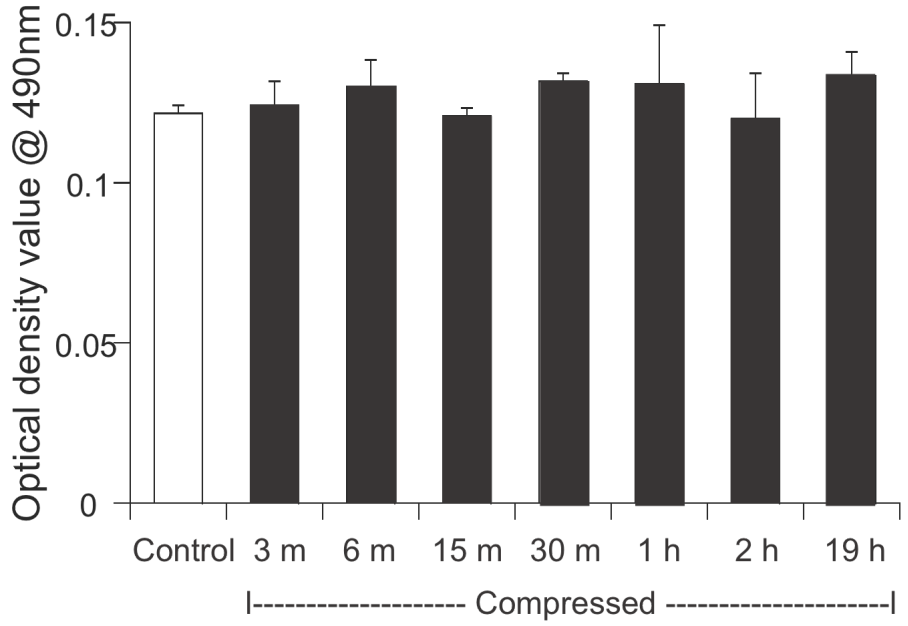
Optical density value @ 490nm
0.15
0.1
0.05
0
Control 3 m 6 m 15 m 30 m 1 h 2 h 19 h
I---------- Compressed ----------I

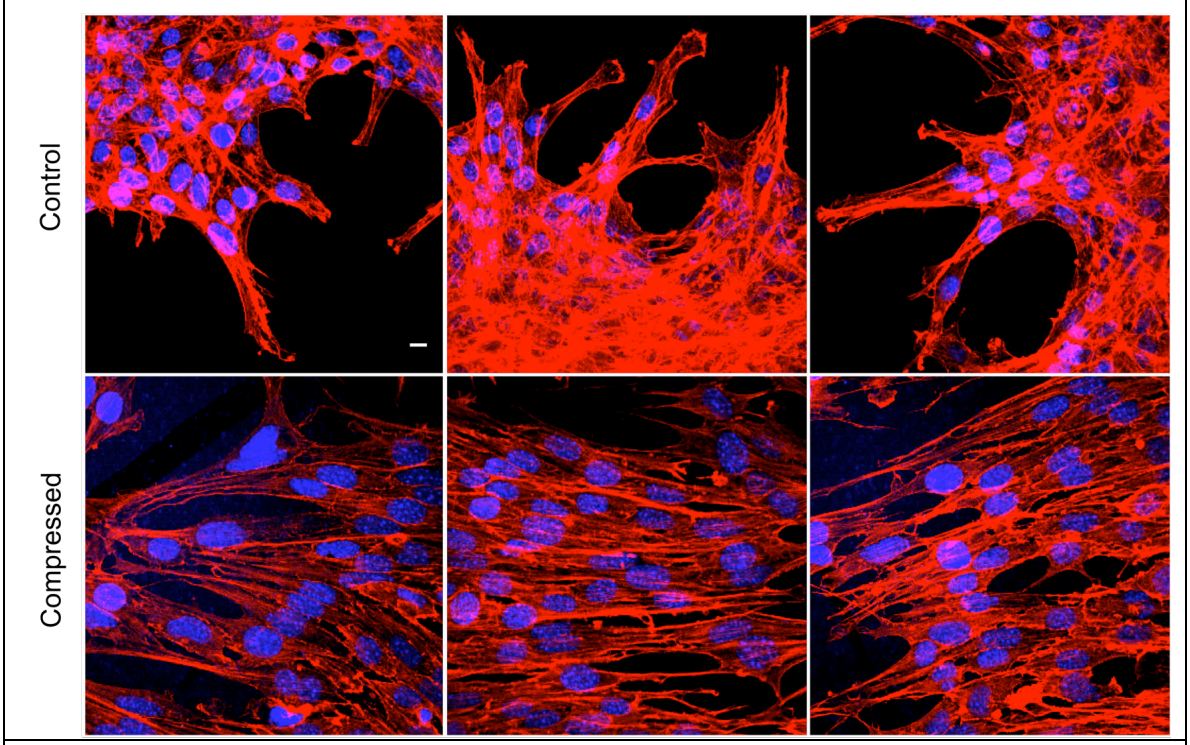

Figure 3.7. Rac activity is not required for compression-induced protrusions. The level of Rac activation in the control and compressed 67NR samples for the indicated duration was analyzed by Western blot (**A**) and Enzyme-Linked Immunosorbent Assay (ELISA) (**B**), respectively, in two independent experiments. The 67NR cells were serum-starved overnight and then compressed in serum-free medium for the indicated duration. **A,** For each condition, equal amount of cell lysate (pooled from three individual samples) was incubated with PAK-PBD GST fusion proteins for 1 hr and bound, active GTP-Rac molecules were analyzed by Western blot. **B,** Equal amount of cell lysate from each sample was directly used for ELISA following the manufacturer's protocol. Both assays show that there is no significant difference in Rac activation level between the control and compressed samples. Error bars represent s.d. **C,** Representative images of phalloidin staining for actin microfilaments of 67NR leader cells at the wound edge. 67NR cells

were transfected with empty vector (wild-type), dominant negative Rac-T17N plasmid or constitutively active Rac-Q61L plasmid and subjected to stress-free or a compressive stress of 5.8mmHg for 16 hrs (n = 8). Compression-induced formation of leader cells with filopodial protrusion was still observed under perturbation of Rac activity. Scale bar, 10um.

Next we investigated the effect of externally-applied compressive stress on Cdc42 activity. Previous studies have shown that expression of constitutively active Cdc42 induces filopodial formation, but dominant negative Cdc42 prevents filopodial formation[20,26]. In addition, a significant body of evidence has indicated a crucial role for Cdc42 in cell migration[8,27]. However, the involvement of Cdc42 activation in mechanical stress-induced filopodial formation and cell migration remains unclear, while Cdc42 has been shown to mediate the polarity of fibroblasts under mechanical shear stress[28]. Similar to other Rho-GTPases, Cdc42 activation is also rapid and dynamic in response to stimulation and can return the baseline level within hours. Hence, we focused on the measurement of Cdc42 activity during early times of compression (from 5mins to 90mins). Using Cdc42 pull-down assay followed by Western blot analysis, we determined that mechanical stress appeared to decrease Cdc42 activity (Fig. 3.8), suggesting that Cdc42 activation is not required for compression-induced migration behavior including enhanced migration and leader-cell formation with filopodial protrusion. Indeed, expression of constitutively active Cdc42 (Cdc42-Q61L) reduced the migration rate of compression-induced leader cells (Fig. 3.9A) in spite of no significant effect on compression-induced filopodial formation, as determined by confocal immunofluorescence microscopy (Fig. 3.9B). Next, though contradictory to previous

studies, we wondered if compression-induced response is resulted from reduced Cdc42 activity. In agreement with literatures[21,29], inhibiting Cdc42 activity by expressing dominant negative Cdc42-T17N did not promote leader-cell formation or filopodial formation but reduced migration in the control (uncompressed cultures). However, filopodia were still observed in the compressed leader cells with slower motility (Fig. 3.9). The reduced motility observed in the dominant-negative compressed mutants did not reconcile with our Western blot results that compressed cultures with enhanced cell migration had reduced Cdc42 activity. One possible explanation is that spatial distribution of Cdc42 activity is more important than the average expression level measured from the Western blot analysis, because up-regulated Cdc42 activity is usually found at the leading edge of the cell during cell migration [7]. While both mutants (Cdc42-T17N and Cdc42-Q61L) in the uncompressed cultures behaved in accordance with literatures [30,31], they did not follow any norm under compression. Taken together, our findings suggest that (1) compressive stress affects the Cdc42 signaling pathway, and (2) Cdc42 is not essential for compression-induced formation of leader cells with filopodial protrusions.

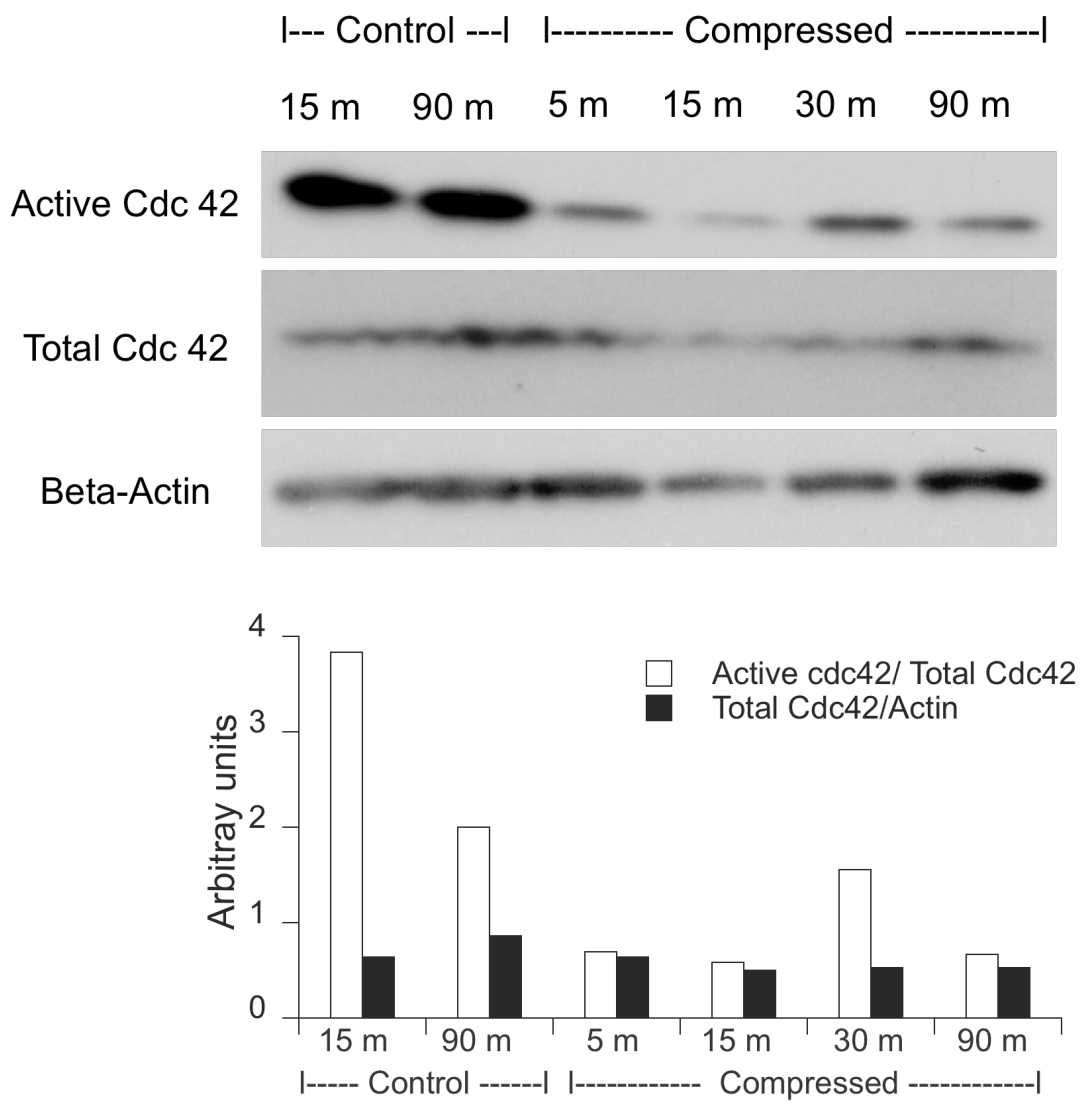

Figure 3.8. Compressive stress tends to reduce Cdc42 activity despite enhanced protrusions. The level of Cdc42 activation in the control and compressed 67NR samples for the indicated duration was analyzed by Western blot. The 67NR cells were serum-starved overnight and then compressed in serum-free medium for the indicated duration. For each condition, equal amount of cell lysate (pooled from three individual samples) was incubated with PAK-PBD GST fusion proteins for 1 hr and bound, active GTP-Cdc42 molecules were analyzed by Western blot. Beta-actin was used as a loading

control. There is no significant difference in total Cdc42 between the control and compressed cultures. However, the level of Cdc42 activation is found lower in compressed cultures than in the controls, suggesting that Cdc42 activation is not required for compression-induced protrusions.

A

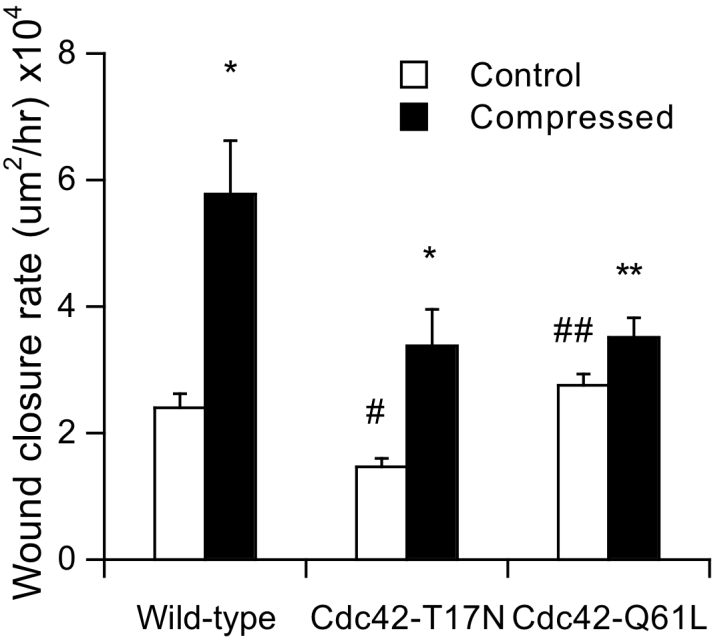

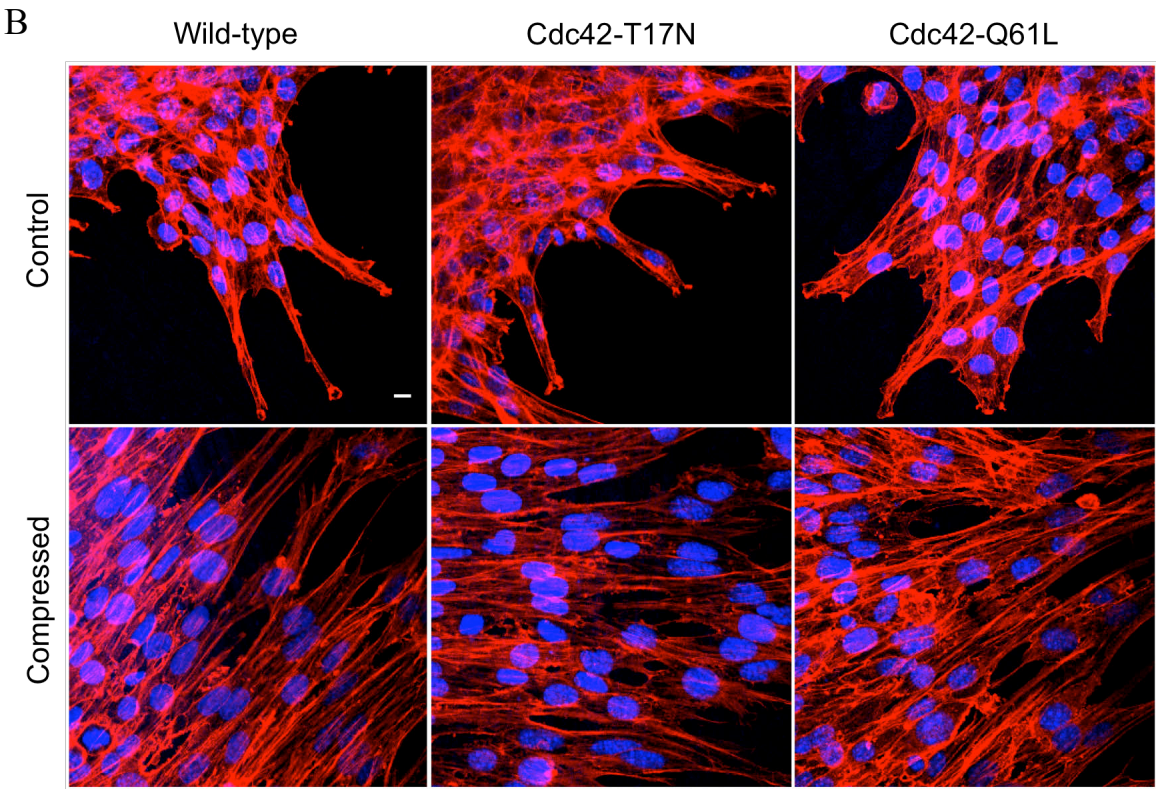

Figure 3.9. Perturbation of Cdc42 activity reduces compression-induced cell movement but not formation of leader cells with filopodial protrusions. A, B, 67NR cells were transfected with empty vector (wild-type), dominant negative Cdc42-T17N plasmid or constitutively active Cdc42-Q61L, and then subjected to stress-free or a compressive stress of 5.8mmHg for 16 hrs. **A,** Average migration rate obtained from the scratch-wound assay for 67NR cells transfected with indicated plasmids and subjected to stress-free or a compressive stress of 5.8mmHg for 16 hrs (n = 4-6; *P<0.05 compared with their respective control; **Not significant compared with its respective control; #P<0.05 compared with the wild-type control; ##Not significant compared with the wild-type control). Error bars represent s.e.m. **B,** Representative images of phalloidin staining for actin microfilaments of different transfected 67NR leader cells at the wound edge. Perturbation of Cdc42 activity does not affect leader-cell formation induced by compression. Scale bar, 10um.

Discussion

Uncontrolled proliferation of cancer cells inevitably generates mechanical, compressive stresses. We showed in Chapter 2 that this stress can enhance migration of some cancer cell lines. Among them, 67NR mammary carcinoma cells demonstrated coordinated cell migration (collective migration)[3], in which some cells in the cell sheet were polarized into "leader" cells that extend protrusions in the direction of migration and guide "followers" at their rear (Fig. 2.8). In this chapter, using 67NR mammary carcinoma cells as a model, we investigated the effect of compression stress on leader-cell formation and formation of protrusions, resulting in enhanced cell migration. We found that a subpopulation of mammary carcinoma cells at the periphery of a discontinuous sheet can undergo a phenotypic transformation, becoming leader cells that migrate to fill open space. Under conditions of chronically-applied compressive stress, this phenotype becomes ubiquitous at the leading edge. In uncompressed cultures, the process of leader-cell formation depends on the geometry of the cell-neighbor contact and the extent of free-cell perimeter. However, applied compression, which enhances spreading of cells at the edge of the culture and promotes filopodial formation, precludes the need for the geometry-driven polarization, making it possible for any cell with free perimeter to transform into a leader cell.

Indeed, leader cells have been identified in collective migration during cancer cell invasion, vascular sprouting, epidermal wound closure and embryogenesis [3,4]. They form protrusions and drive the leading edge of the cell cohort forward. In our study, as opposed to the geometry-induced leader cells formed in uncompressed cultures, we

observed from a time-lapse movie of the compressed cultures that the first row of 67NR leader cells contained filopodia and appeared to lead the cell sheet. While the force generated by leader cells is sufficient to pull and coordinate migration persistence of five to ten cells behind the leading edge[5], follower cells in some 2D cell sheet models can also develop polarized protrusions in basolateral regions of moving cell sheets, which help maintain the coordinated translocation[32]. Thus, it is not clear to us whether the follower cells in the compressed cultures, though tethering to the leader cells, generated their own force for movement, or they were passively dragged forward by the leader cells. Furthermore, another possibility is that each individual cell in collective migration, regardless of whether they are leader cells or followers, engages in a global tug-and-war involving local force generation[33]. With recently-developed technique called Fourier-transform traction microscopy[33], traction force distribution within an advancing cell sheet can be determined to unveil which mechanism is responsible for the compression-induced collective motion.

The most distinct feature of compression-induced leader cells is that the compressed cells are much elongated and, most importantly, have long filopodia. Filopodia have been described as “antennae” or “tentacles” that cells use to probe their microenvironment[34], and have thus been related to cancer cell invasion[35]. In addition, activated integrins (cell-matrix receptors) were reported to accumulate in filipodia, thus readily promoting cell adhesion with matrix and enhance migration. Those integrin-containing filopodia form the initial adhesion sites, to which other signaling and adhesion molecules such as talin, focal adhesion kinase (FAK) and paxillin are recruited, transitioning into mature

adhesion sites[36,37]. Our finding that compression induces formation of leader cells containing filopodia suggests that growth-induced compressive stress in tumor could induce malignant phenotypes in cancer cells, enhancing their motility and eventually metastasis.

Our results showed that compression-induced formation of leader cells with filopodial protrusions still occurred after inhibition of Rac1 or Cdc42 activity, suggesting that neither activation of Rho GTPases is required for compression-induced migration behavior. Previous work has shown that Rho GTPases Rac and Cdc42 regulates cell protrusions at the leading edge and outward deformation of the plasma membrane: Rac controls extension of lamellipodia and Cdc42 controls extension of filopodia [20,21,38,39]. Hence, it might explain why Rac activation is not involved in filopodial formation stimulated by compression. However, our finding that inhibition of Cdc42 activation did not prevent filopodial formation in compressed leader cells contradicts with previous studies [20,26]. It could imply that Cdc42 may not be the only RhoGTPase to induce filopodial formation. Indeed, a recent study also reported that Cdc42 is not essential for filopodial formation in fibroblastoid cells [40]. Beside Cdc42, other Rho GTPases such as Rif [41], TCL [42] and Wrch-1 [43] were suggested to induce filopodia. Among them, dominant negative Cdc42 did not block filopodial formation induced by Rif [34,41]. Thus, other Rho GTPases might be responsible for compression-induced leader-cell formation with filopodial protrusions.

Other than the molecular mechanisms regulated by Rho GTPase, another possibility to explain compression-induced leader-cell formation is that the externally-applied stress changes the internal mechanical stress by cell distortion. Using the microfabrication to control the organization of sheets of cells, we demonstrated that emergence of leader cells corresponded to the tips or corners of the uncompressed monolayers, while externally-applied compression induced leader cell formation everywhere around the edge of the pattern. Multicellular micro-organization of defined shapes and sizes generated by microfabrication has also been previously shown to direct patterns of cell proliferation[44]. In that study, Nelson *et. al.* (2005) have measured the traction forces over the entire monolayer using arrays of micro-mechanical force sensors, and determined that regions of concentrated growth corresponded to regions of high tractional stress generated within the sheet. A distinct tensional stress pattern can be generated within a cell monolayer as a result of isotropic cell contraction. To keep the pattern of the cell monolayer stable, the tensional stresses generated in the cytoskeleton of each cell have to balance with cell-cell and cell-ECM attachment sites. Thus, the cells will spontaneously remodel their shape and internal cytoskeletal structure to minimize local stresses and strains, as they pull against those cell-cell and cell-ECM attachment sites [45]. Depending on the cell's position and the overall shape of the monolayer, tensional stress generated within each cell varies. Using similar mechanical basis, the highest tensional stress could be resulted in the cells at the corners/tips of the square/rosette patterns used in our experiment because they have more free-cell perimeter than that of edge cells to interact with ECM for cell-matrix adhesions. Indeed, cells have been shown previously to extend protrusions preferentially from the concentrated regions of tensional

stress such as corners of the square pattern [12,13]. Hence, leader-cell formation is geometry-driven in the control, uncompressed cultures. However, as compression distended every cell around the edge of the monolayer pattern, the cell distortion (cell extension) toward open space increased the cell-ECM contact area for adhesion, thereby increasing the magnitude of contractile force generated in the cells [46,47] and inducing leader-cell formation independent of initial cell micro-organization.

In conclusion, while other studies have shown that matrix rigidity can transform cells to malignant phenotypes [48-51], we have demonstrated, for the first time, that mechanical compression-induced cell distension can lead to enhancement of coordinated cancer cell motility via formation of leader cells with filopodial protrusions without stiffening of extracellular matrix. This result suggests that the growth-induced compressive stress experienced by proliferating cancer cells could distort their cell shapes and induce them to become leader cells responsible for collective invasion as observed in many epithelial cancers [3]. Furthermore, our results provide novel insight into how physical determinants trigger coordinated migration, which could be relevant in other physiological processes, such as vascular sprouting and wound healing.

References

1. Griffon-Etienne, G., Y. Boucher, C. Brekken, H.D. Suit, and R.K. Jain. 1999. Taxane-induced Apoptosis Decompresses Blood Vessels and Lowers Interstitial Fluid Pressure in Solid Tumors: Clinical Implications. *Cancer Res*. 59:3776-3782.
2. Padera, T.P., B.R. Stoll, J.B. Tooredman, D. Capen, E. di Tomaso, and R.K. Jain. 2004. Pathology: cancer cells compress intratumour vessels. *Nature*. 427:695.
3. Friedl, P., and D. Gilmour. 2009. Collective cell migration in morphogenesis, regeneration and cancer. *Nat Rev Mol Cell Biol*. 10:445-57.
4. Ilina, O., and P. Friedl. 2009. Mechanisms of collective cell migration at a glance. *J Cell Sci*. 122:3203-8.
5. Vitorino, P., and T. Meyer. 2008. Modular control of endothelial sheet migration. *Genes Dev*. 22:3268-81.
6. Lauffenburger, D.A., and A.F. Horwitz. 1996. Cell migration: a physically integrated molecular process. *Cell*. 84:359-69.
7. Ridley, A.J., M.A. Schwartz, K. Burridge, R.A. Firtel, M.H. Ginsberg, G. Borisy, J.T. Parsons, and A.R. Horwitz. 2003. Cell migration: integrating signals from front to back. *Science*. 302:1704-9.
8. Etienne-Manneville, S., and A. Hall. 2002. Rho GTPases in cell biology. *Nature*. 420:629-35.
9. Argiro, V., M.B. Bunge, and M.I. Johnson. 1985. A quantitative study of growth cone filopodial extension. *J Neurosci Res*. 13:149-62.
10. Maddala, R., V.N. Reddy, D.L. Epstein, and V. Rao. 2003. Growth factor induced activation of Rho and Rac GTPases and actin cytoskeletal reorganization in human lens epithelial cells. *Mol Vis*. 9:329-36.
11. Yang, F.C., S.J. Atkinson, Y. Gu, J.B. Borneo, A.W. Roberts, Y. Zheng, J. Pennington, and D.A. Williams. 2001. Rac and Cdc42 GTPases control hematopoietic stem cell shape, adhesion, migration, and mobilization. *Proc Natl Acad Sci U S A*. 98:5614-8.
12. Brock, A., E. Chang, C.C. Ho, P. LeDuc, X. Jiang, G.M. Whitesides, and D.E. Ingber. 2003. Geometric determinants of directional cell motility revealed using microcontact printing. *Langmuir*. 19:1611-7.
13. Parker, K.K., A.L. Brock, C. Brangwynne, R.J. Mannix, N. Wang, E. Ostuni, N.A. Geisse, J.C. Adams, G.M. Whitesides, and D.E. Ingber. 2002. Directional control of lamellipodia extension by constraining cell shape and orienting cell tractional forces. *FASEB J*. 16:1195-204.
14. Katsumi, A., J. Milanini, W.B. Kiosses, M.A. del Pozo, R. Kaunas, S. Chien, K.M. Hahn, and M.A. Schwartz. 2002. Effects of cell tension on the small GTPase Rac. *J Cell Biol*. 158:153-64.
15. Putnam, A.J., J.J. Cunningham, B.B. Pillemer, and D.J. Mooney. 2003. External mechanical strain regulates membrane targeting of Rho GTPases by controlling microtubule assembly. *Am J Physiol Cell Physiol*. 284:C627-39.
16. Aslakson, C.J., and F.R. Miller. 1992. Selective events in the metastatic process defined by analysis of the sequential dissemination of subpopulations of a mouse mammary tumor. *Cancer Res*. 52:1399-405.

17. Alom Ruiz, S., and C.S. Chen. 2007. Microcontact printing: A tool to pattern. *Soft Matter*:168-177.
18. Kane, R.S., S. Takayama, E. Ostuni, D.E. Ingber, and G.M. Whitesides. 1999. Patterning proteins and cells using soft lithography. *Biomaterials*. 20:2363-76.
19. Chen, C.S., J.L. Alonso, E. Ostuni, G.M. Whitesides, and D.E. Ingber. 2003. Cell shape provides global control of focal adhesion assembly. *Biochem Biophys Res Commun*. 307:355-61.
20. Nobes, C.D., and A. Hall. 1999. Rho GTPases control polarity, protrusion, and adhesion during cell movement. *J Cell Biol*. 144:1235-44.
21. Machacek, M., L. Hodgson, C. Welch, H. Elliott, O. Pertz, P. Nalbant, A. Abell, G.L. Johnson, K.M. Hahn, and G. Danuser. 2009. Coordination of Rho GTPase activities during cell protrusion. *Nature*. 461:99-103.
22. Ridley, A.J. 2001. Rho GTPases and cell migration. *J Cell Sci*. 114:2713-22.
23. Poh, Y.C., S. Na, F. Chowdhury, M. Ouyang, Y. Wang, and N. Wang. 2009. Rapid activation of Rac GTPase in living cells by force is independent of Src. *PLoS One*. 4:e7886.
24. Wojciak-Stothard, B., and A.J. Ridley. 2003. Shear stress-induced endothelial cell polarization is mediated by Rho and Rac but not Cdc42 or PI 3-kinases. *J Cell Biol*. 161:429-39.
25. Gardiner, E.M., K.N. Pestonjamasp, B.P. Bohl, C. Chamberlain, K.M. Hahn, and G.M. Bokoch. 2002. Spatial and temporal analysis of Rac activation during live neutrophil chemotaxis. *Curr Biol*. 12:2029-34.
26. Kozma, R., S. Ahmed, A. Best, and L. Lim. 1995. The Ras-related protein Cdc42Hs and bradykinin promote formation of peripheral actin microspikes and filopodia in Swiss 3T3 fibroblasts. *Mol Cell Biol*. 15:1942-52.
27. Fukata, M., M. Nakagawa, and K. Kaibuchi. 2003. Roles of Rho-family GTPases in cell polarisation and directional migration. *Curr Opin Cell Biol*. 15:590-7.
28. Lee, J.S., M.I. Chang, Y. Tseng, and D. Wirtz. 2005. Cdc42 mediates nucleus movement and MTOC polarization in Swiss 3T3 fibroblasts under mechanical shear stress. *Mol Biol Cell*. 16:871-80.
29. Yang, L., L. Wang, and Y. Zheng. 2006. Gene targeting of Cdc42 and Cdc42GAP affirms the critical involvement of Cdc42 in filopodia induction, directed migration, and proliferation in primary mouse embryonic fibroblasts. *Mol Biol Cell*. 17:4675-85.
30. Johnson, D.I. 1999. Cdc42: An essential Rho-type GTPase controlling eukaryotic cell polarity. *Microbiol Mol Biol Rev*. 63:54-105.
31. Evers, E.E., G.C. Zondag, A. Malliri, L.S. Price, J.P. ten Klooster, R.A. van der Kammen, and J.G. Collard. 2000. Rho family proteins in cell adhesion and cell migration. *Eur J Cancer*. 36:1269-74.
32. Farooqui, R., and G. Fenteany. 2005. Multiple rows of cells behind an epithelial wound edge extend cryptic lamellipodia to collectively drive cell-sheet movement. *J Cell Sci*. 118:51-63.
33. Trepat, X., M.R. Wasserman, T.E. Angelini, E. Millet, D.A. Weitz, J.P. Butler, and J.J. Fredberg. 2009. Physical forces during collective cell migration. *Nature Physics*. 5:426-430.

34. Mattila, P.K., and P. Lappalainen. 2008. Filopodia: molecular architecture and cellular functions. *Nat Rev Mol Cell Biol*. 9:446-54.
35. Vignjevic, D., M. Schoumacher, N. Gavert, K.P. Janssen, G. Jih, M. Lae, D. Louvard, A. Ben-Ze'ev, and S. Robine. 2007. Fascin, a novel target of beta-catenin-TCF signaling, is expressed at the invasive front of human colon cancer. *Cancer Res*. 67:6844-53.
36. Galbraith, C.G., K.M. Yamada, and J.A. Galbraith. 2007. Polymerizing actin fibers position integrins primed to probe for adhesion sites. *Science*. 315:992-5.
37. Partridge, M.A., and E.E. Marcantonio. 2006. Initiation of attachment and generation of mature focal adhesions by integrin-containing filopodia in cell spreading. *Mol Biol Cell*. 17:4237-48.
38. Keely, P., L. Parise, and R. Juliano. 1998. Integrins and GTPases in tumour cell growth, motility and invasion. *Trends Cell Biol*. 8:101-6.
39. Krugmann, S., I. Jordens, K. Gevaert, M. Driessens, J. Vandekerckhove, and A. Hall. 2001. Cdc42 induces filopodia by promoting the formation of an IRSp53:Mena complex. *Curr Biol*. 11:1645-55.
40. Czuchra, A., X. Wu, H. Meyer, J. van Hengel, T. Schroeder, R. Geffers, K. Rottner, and C. Brakebusch. 2005. Cdc42 is not essential for filopodium formation, directed migration, cell polarization, and mitosis in fibroblastoid cells. *Mol Biol Cell*. 16:4473-84.
41. Ellis, S., and H. Mellor. 2000. The novel Rho-family GTPase rif regulates coordinated actin-based membrane rearrangements. *Curr Biol*. 10:1387-90.
42. Abe, T., M. Kato, H. Miki, T. Takenawa, and T. Endo. 2003. Small GTPase Tc10 and its homologue RhoT induce N-WASP-mediated long process formation and neurite outgrowth. *J Cell Sci*. 116:155-68.
43. Tao, W., D. Pennica, L. Xu, R.F. Kalejta, and A.J. Levine. 2001. Wrch-1, a novel member of the Rho gene family that is regulated by Wnt-1. *Genes Dev*. 15:1796-807.
44. Nelson, C.M., R.P. Jean, J.L. Tan, W.F. Liu, N.J. Sniadecki, A.A. Spector, and C.S. Chen. 2005. Emergent patterns of growth controlled by multicellular form and mechanics. *Proc Natl Acad Sci U S A*. 102:11594-9.
45. Ingber, D.E. 2005. Mechanical control of tissue growth: function follows form. *Proc Natl Acad Sci U S A*. 102:11571-2.
46. Tan, J.L., J. Tien, D.M. Pirone, D.S. Gray, K. Bhadriraju, and C.S. Chen. 2003. Cells lying on a bed of microneedles: an approach to isolate mechanical force. *Proc Natl Acad Sci U S A*. 100:1484-9.
47. Wang, N., E. Ostuni, G.M. Whitesides, and D.E. Ingber. 2002. Micropatterning tractional forces in living cells. *Cell Motil Cytoskeleton*. 52:97-106.
48. Ulrich, T.A., E.M. de Juan Pardo, and S. Kumar. 2009. The Mechanical Rigidity of the Extracellular Matrix Regulates the Structure, Motility, and Proliferation of Glioma Cells. *Cancer Res*. 69:4167-4174.
49. Paszek, M.J., and V.M. Weaver. 2004. The tension mounts: mechanics meets morphogenesis and malignancy. *J Mammary Gland Biol Neoplasia*. 9:325-42.
50. Wells, R.G. 2005. The Role of Matrix Stiffness in Hepatic Stellate Cell Activation and Liver Fibrosis. *Journal of Clinical Gastroenterology*. 39:S158-S161.

51. Paszek, M.J., N. Zahir, K.R. Johnson, J.N. Lakins, G.I. Rozenberg, A. Gefen, C.A. Reinhart-King, S.S. Margulies, M. Dembo, D. Boettiger, D.A. Hammer, and V.M. Weaver. 2005. Tensional homeostasis and the malignant phenotype. *Cancer Cell*. 8:241-254.

Chapter 4: Role of compressive stress in cell adhesion and migration

Portions of the chapter have been taken from:

J.M. Tse, G. Cheng, J.A. Tyrrell, S.A. Wilcox-Adelman, Y. Boucher, R.K. Jain, L.L. Munn, "Compression-induced cell distension and adhesion stimulate coordinated migration of mammary carcinoma cells." Submitted.

Introduction

Uncontrolled cell proliferation of a solid tumor in a confined space generates mechanical compressive stress, which can influence the tumor cells and modify their interactions with neighboring cells and the extracellular matrix (ECM). In the previous chapter (Chapter 3), while we have shown that externally-applied stress enhances cancer cell migration via formation of leader cells with filopodial protrusions, the newly-formed protrusions have to be stabilized by attaching to the substrate surface in order for cell migration to occur. Previous studies have shown that shear stress[1,2] or extracellular pressure [3-6] can modulate tumor cell adhesion to the endothelium or extracellular matrix in vitro, respectively. The ability of cells to transduce mechanical signals is governed by two types of cell adhesion: integrin-mediated cell-ECM adhesion, and cadherin-mediated cell-cell contacts[7].

Cell-matrix interactions are mainly mediated by integrins. Integrins are heterodimeric receptors composed of two noncovalently associated subunits, denoted α and β, which both span the plasma membrane. Some integrin subunits are ubiquitously expressed (e.g. integrin b1), while others are tissue-, cell- or stage- specific (e.g. integrin b2 exclusively expressed on leukocytes) [8]. There are 24 distinct integrin receptors that bind various ECM ligands with different affinities.

The extracellular matrix (ECM) is a complex mixture of matrix molecules, such as fibronectin, collagens, and laminins, each of which has specific effects on cellular

processes. Among them, fibronectin is recognized by at least ten cell-surface receptors of the integrin family, and thus a potential ligand for most cell types[9]. One of the main binding sites in fibronectin is the amino acid sequence Arg-Gly-Asp (RGD), a widely occurring cell adhesive motif recognized by about half of all known integrins such as integrins a5b1, aIIb3, avb1 and avb3. For some of the integrins such as integrin a5b1, the synergy site PHSRN is required to act with the RGD site for high affinity binding [10].

Integrin-mediated adhesion signaling is bidirectional because it involves both "outside-in" and "inside-out" signals. Outside-in signals regulate cell response to ECM adhesion, while inside-out signals regulate integrin affinity for ECM ligands. During outside-in signaling, the engagement of integrins with ECM induces the clustering of integrin receptors, which in turn recruit different signaling proteins, such as talin and focal adhesion kinase (FAK)[11]. For example, the phosphorylation of FAK on Y397 leads to localized increases in levels of tyrosine-phosphorylated proteins (e.g.paxillin-pY118) and cytoskeletal protein (e.g. vinculin) that links with actin cytoskeleton involving actomyosin contraction. The *endogenous cellular tension* thus regulates the formation of dynamic adhesion structures such as focal complexes and focal adhesions[12-14]. Conversely, during inside-out signaling, endogenous tension can directly induce changes in integrin conformation and activation that alters its ligand-binding activity or can be transmitted through integrin receptors to the ECM and the resultant *exogenous tension* can alter matrix rigidity[12,13].

Together with integrin-mediated cell-substrate adhesion, cell-cell adhesion (either cadherin-based or integrin-ligand interaction) is also critical in regulating cell migration.

For example, both of these adhesions are found to regulate collective migration observed in tumor invasion and metastasis, such as breast cancers [15,16]. The cell-cell adhesions at the rear sides of the tumor cells keep them moving in a cohort led by a "path-finding" cell. On the other hand, it has also been demonstrated that cell invasion can be suppressed by the forced expression of E-cadherin, a calcium-dependent transmembrane protein responsible for cell-cell adhesion[17].

Compression-induced cell extrusion might have induced leader-cell formation and cell migration, either by decreased cell-cell adhesion relative to the uncompressed cells, or by increased number of cell attachment sites to the substrate matrix (ECM). In this chapter, we investigated the effect of externally-applied compressive stress on cell adhesion (cadherin-based and integrin-ECM based), primarily using 67NR mammary carcinoma cell line as a model, which expresses high levels of integrin b1 subunit, low levels of the av subunit, but not of b3 integrin [18]. Our results showed that independent of cadherin-based cell-cell cohesion, compression significantly up-regulated integrin b1- (and myosin-) mediated cell-matrix adhesion by increasing cell-fibronectin contact area, thereby promoting cell migration.

Materials and Methods

Cell cultures

The human mammary carcinoma cell line MCF-7 was obtained from American Type Culture Collection (ATCC) while the murine mammary carcinoma cell line 67NR was kindly provided by Dr. Fred R. Miller at Wayne State University [19]. The immortalized mammary epithelial cell line MCF10A were obtained from ATCC. All the cell lines were

transduced with the enhanced green fluorescent protein (EFGP) retrovirus described earlier in the Materials and Methods of Chapter 2. All cell lines were cultured in DMEM supplemented with 10% fetal bovine serum (FBS), except for murine mammary carcinoma cells and MCF10A, which were cultured as described previously [19,20]. All cells were incubated at 37°C with 5% CO_2.

In vitro scratch wound-compression experiment

To assess cancer cell migration under compression, the same in vitro compression device described in Chapter 2 (Fig. 2.1) was used, and cell migration was assessed with scratch-wound assay. Briefly, 67NR cells were allowed to grow to confluence on uncoated transwell inserts. Using a p-200 pipette tip the monolayer was scraped to denude a circular area of ~1000 μm in diameter or a line of ~1000 μm in width. The wound closure was monitored microscopically under stress-free or a compressive stress of 5.8mmHg and migration was determined as the change in wound area covered by cells 16 hr after wounding (unless specified).

Inhibition of cadherin-mediated cell-cell adhesion

To disrupt the calcium-dependent cell-cell adhesion mediated by E-cadherin, we plated MCF10A or MCF7 cells on uncoated transwell inserts (0.4um) in full-growth medium with or without a mouse anti-E-cadherin antibody (clone SHE78-7; 2ug/mL for MCF10A and 1ug/mL for MCF7; Invitrogen) (See Appendix C: Methods for determination of antibody optimum concentration). After 24 hr-incubation, we performed the in vitro

scratch wound-compression experiment and maintained the antibody-treated cells in the presence of E-cadherin antibody.

For N-cadherin blockade, we plated 67NR cells on uncoated transwell inserts (0.4um) in full-growth medium with or without a mouse anti-N-cadherin antibody (clone GC-4; 1ug/mL; Sigma) and performed the similar experiment as described earlier. (Additional methods for inhibiting cadherin-mediated cell-cell adhesion are described in Appendix C: Methods)

Forced ectopic expression of E-cadherin

The pWZL-Blast mouse E-cadherin vector was purchased from Addgene (Plasmid 18804; Cambridge, MA). The full-length murine E-cadherin cDNA was cloned into a retroviral pWZL-Blast vector backbone. The 293 cells were transfected with the vector using Lipofectamine 2000 reagent (Invitrogen Corp., Carlsbad, CA) according to the manufacturer's instruction to generate viral supernatant. The collected viral supernatant was then used to transduce the 67NR mammary carcinoma cells. The transduced cells were selected with 5ug/mL Blasticidin S (InvivoGen, San Diego, CA) 48 hr post-transduction. Expression of E-cadherin was assessed by immunofluorescence staining (see below) after 2-week antibiotic selection and the selected cells were maintained in DMEM supplemented with 10% FBS and 5ug/mL Blasticidin.

To examine the re-expression of E-cadherin in 67NR mammary carcinoma cells, cells were fixed with 4% paraformaldehyde in phosphate buffered saline (PBS), permeabilized

and blocked with 5% normal horse serum containing 0.2% Triton X-100. The cells were then incubated with a monoclonal anti-E-cadherin antibody (Clone ECCD-2, Zymed Laboratories; 1:200). The cells were mounted in Vectashield Mounting Medium containing nuclear dye DAPI and then visualized with an Olympus FluoView 500 confocal microscope system (Olympus, Center Valley, PA)

Immunofluorescence microscopy

For most of the immunostaining (except for vinculin and FAK-pY397 described below), cells were fixed with 4% paraformaldehyde in phosphate buffered saline (PBS), permeabilized and blocked with 5% normal horse serum containing 0.2% Triton X-100. The cells were then incubated with appropriate antibodies (listed in Table 4.1) for 1 hr at room temperature (unless specified), followed by 30-min incubation of appropriate secondary antibodies (e.g. anti-mouse Cy3). All the cells were mounted in Vectashield Mounting Medium containing nuclear dye DAPI and then visualized with an Olympus FluoView 500 confocal microscope system (Olympus, Center Valley, PA).

Staining	**Antibody used (clone; dilution; vendor; other info)**
N-cadherin	Clone GC-4; 1:200: Sigma
Fibronectin	Antiserum; 1:400; Sigma
Actin cytoskeleton	Alexa-Fluor-546 phalloidin; 1:200; Molecular Probe; 20-min incubation at room temperature
Phospho-FAK (Tyr 397)	Clone 18; 1:50; Millipore; see below for additional information
Vinculin	Clone hVIN-1; 1:400; Sigma; see below for additional information
Activated integrin b1 (CD29)	Clone 9EG7; 1:50; BD Pharmingen

Phospho-paxillin (Tyr 118)	1:75; Cell Signaling

Table 4.1: Antibodies used for immunofluorescence microscopy

To visualize initial adhesions with phospho-FAK (Tyr 397) antibody, the cells were fixed with cold 4% paraformaldehyde in phosphate buffered saline (PBS) containing 5mM sodium vanadate, permeabilized with cold 0.5% Triton X-100 in PBS containing 5mM sodium vanadate, and blocked with 5% normal horse serum containing 0.1% Triton X-100 and 5mM sodium vanadate. Then, the cells were incubated with anti-phospho-FAK at Tyr 397 (1:50 Millipore) at 37C for 1 hr.

To identify vinculin-containing focal adhesions, cells were permeabilized prior to fixation with 4% paraformaldehyde in cytoskeleton buffer[21], blocked with 5% normal horse serum containing 0.1% Triton and stained using a monoclonal anti-vinculin antibody (Clone hVIN-1, Sigma; 1:400).

Measurement of cell-matrix adhesion by shear distraction assay

67NR carcinoma cells plated on transwell membranes were cultured for 16 hr with or without compression and then exposed to shear forces for one minute by repeated pipetting using a 1 ml pipettor, maintained ~1 cm from the surface. (Our *in vitro* compression platform is not compatible with conventional adhesion assays so we used this alternative method to induce fluid shear stress. While we did not measure the level of shear stress we applied, we made sure that we kept the stress level consistent in both the control and compressed cultures.) Non-adherent cells were then washed away with phosphate buffered saline (PBS). The adherent cells were stained with 0.2% crystal

violet. After washing with PBS to remove excess stain, the dye was extracted from live cells by shaking in 30% acetic acid for 30mins at room temperature. The absorbance was read at 540nm on a micro-plate reader.

ECM effect on cell migration

To evaluate the role of ECM proteins in cell migration behavior, the 0.4um transwell inserts were coated with various matrix components. Transwell inserts were coated with 5ug/mL bovine fibronectin (Sigma, St. Louis, MO), rat tail collagen I (BD Biosciences, San Jose, CA) or mouse laminin (BD Biosciences, San Jose, CA). After 1-hr incubation at 37°C, the coating solution was aspirated and the coated transwell inserts were washed with PBS to remove any non-adsorbed matrix components. The ECM-coated inserts were then ready for use in the *in vitro* scratch-wound assay.

Fibronectin mRNA expression

Total RNA from control and compressed 67NR cells cultured in serum-free medium was isolated at the indicated times using the Trizol reagent (Invitrogen) according to the manufacturer's protocol. After treatment with Dnase, total RNA was reverse-transcribed using Oligo dT primers (Roche Diagnostics). Quantitative real-time PCR (ABI Prism 7300, Applied Biosystems, Foster City, CA) was used to measure fibronectin gene expression. Relative expression of fibronectin was normalized by GAPDH and then calibrated with the control (uncompressed) sample.

Quantification of cell-adhesion associated proteins (fibronectin, integrin b1, paxillin)

Confluent 67NR cells on transwell inserts were scraped with a p-200 pipette tip and then cultured for 16 hours in the compression device with or without a piston. The 67NR cells were then stained with antibodies listed in Table 4.1 for fibronectin, activated integrin b1 or phospho-paxillin (Y118), and counterstained with DAPI as described above. A z-stack (with an increment of 2mm) of 67NR cells at wound leading edges was captured from just below the transwell surface to just above the cell layer with Olympus FluoView 500 confocal microscope system (Olympus, Center Valley, PA). The images were processed and analyzed using Matlab (Mathworks, Natick, MA). The protein of interest associated with the cell-surface layer was quantified from a z-projection of 2 slices acquired closest to the transwell surface, while total level of the protein was quantified from a z-projection of all slices. Each projection image was first thresholded and then stained area was calculated and normalized to total number of DAPI-stained nuclei or total projected cell area outlined by phalloidin-stained actin.

Blocking integrin function experiment

To determine which integrin subunits could be responsible for compression-induced migration, we treated 67NR cells previously plated on fibronectin-coated surface with different anti-integrin antibodies individually or combined, each at a concentration of 50ug/mL (See Appendix C: Methods for determination of optimum concentration), and performed the scratch-wound assay. The various integrin blocking antibodies used are listed in Table 4.2.

Integrin subunit	**Blocking antibody used (clone; vendor)**
β1	Clone Ha2/5; BD Biosciences

β3	Clone 2C9.G2; BD Pharmingen
αIIb	Clone MWReg30; BD Biosciences
αv	Clone RMV-7; BD Biosciences
α6	Clone NKI-GoH3; Millipore

Table 4.2: Various integrin blocking antibodies

From the previous experiment, integrin b1 antibody was determined to be the potential integrin subunit responsible for compression-induced migration. Therefore, we blocked integrin b1 function during compression experiment. Briefly, when the 67NR cells on the 0.4um transwell inserts reached confluence, the monolayer was scraped with a p-200 pipette tip to denude a circular area of ~1000um in diameter. The cells were then treated with either 50ug/mL integrin b1 antibody (clone Ha 2/5; BD Biosciences) or 50ug/mL isotype-specific control antibody (BD Biosciences) two hours prior to compression. The wound closure was monitored microscopically under stress-free or a compressive stress of 5.8mmHg and migration was determined as the change in wound area covered by cells 16 hr after wounding. During compression, the cells were maintained in the full-growth medium containing their respective antibody.

Western blot for detection of integrin b1 and paxillin

Cell lysates were collected from the in vitro scratch wound-compression experiment at indicated time points with RIPA buffer containing phosphatase inhibitor cocktail (1:100 dilution; Sigma) and 1X protease inhibitor cocktail (Roche Biosciences). Total protein was measured with Bradford protein assay kit (BioRad). Laemmli buffer containing 5% b-mercaptoethanol was added to the protein samples and they were boiled at 100°C for 5

minutes. Samples were loaded into a 4-15% Tris-HCl gels (BioRad Ready Gel) and run at 140V for 1 hr. The proteins were transferred to polyvinylidene fluoride (PVDF) membrane at 200mA for 2 hours at room temperature. The membrane was then blocked with TBST containing 5% milk for 1 hr at room temperature with gentle agitation. After blocking, the membrane was incubated at 4°C overnight with a primary antibody for total integrin b1 (clone MB1.2; 1:100 dilution; Millipore) or phospho-paxillin at Tyr118 (polyclonal; 1:1000 dilution; Cell Signaling Technology). The following day, the membrane was washed vigorously with TBST and incubated for 1 hr at room temperature with an HRP-conjugated secondary antibody (GE Healthcare). The proteins were detected using the ECL Plus kit (GE Healthcare). After protein detection, membranes were stripped with Restore Western Blot Stripping Buffer (ThermoScientific) at 37°C and reprobed with another primary antibody for b-actin (clone AC-15; 1:5000 dilution; Sigma) or total paxillin (polyclonal; 1:1000 dilution; Cell Signaling Technology).

Inhibition of actomyosin contractility

To determine the role of actomyosin contractility in compression-induced leader-cell formation, the 67NR cells were treated with either different chemical inhibitors at specified concentrations (Rho kinase inhibitor Y-27632 from Calbiochem: 5uM and 30uM; myosin light-chain kinase inhibitor ML-7 from Sigma: 25uM or myosin II ATPase inhibitor Blebbistatin from Sigma: 50uM) or transduced with dominant negative RhoA (RhoA-T19N) retrovirus. For blocking actomyosin contractility using chemical inhibitors, the cells were pre-treated with different specified agents at appropriate concentrations two hours prior to wound-making, followed by 16-hr compression at

5.8mmHg. During compression, the cells were maintained in the full-growth medium containing the specified chemical inhibitor.

For the dominant negative RhoA experiment, the full-length RhoA DN gene was cut out from the pcDNA3-eGFP-RhoA-T19N vector purchased from Addgene (Plasmid 12967; Cambridge, MA) and cloned into retroviral pBMN-I-GFP vector backbone. 67NR cells were then transduced with the RhoT19N retrovirus particles three times. The transduction efficiency was assessed by RhoA activation pull-down experiment. Briefly, the transduced cells were serum-starved overnight and then stimulated with 10% FBS for 5 min. Cell lysates were then collected and active RhoA were pulled down using Rho Activation Assay Biochem Kit (Cytoskeleton, Denver, CO) according to the manufacturer's instruction. The pull-down proteins and total proteins were analyzed by Western Blot for active RhoA and total RhoA, respectively.

Measurement of RhoA activity with ELISA

RhoA activation in uncompressed and compressed cells was measured with an ELISA-based RhoA activation assay (RhoA G-LISA Activation Assay; Cytoskeleton, Inc), following the manufacturer's instructions. Briefly, cell lysates were collected from the in vitro scratch wound-compression experiment at indicated time points. Equal amount of protein was incubated in Rho-GTP affinity plate (binding active RhoA) for 30mins. Then antibody detection reagent was added, and signal was developed with colorimetric methods.

Statistical analysis

Quantitative data are shown as mean ± s.e.m. (unless specified), and $P \leq 0.05$ was considered significant in unpaired, two-tailed Student's t-tests.

Results

Compression-induced coordinated cell migration is independent of cadherin-mediated cell-cell adhesion

Both cell-cell coadhesion and cell-substrate interaction play an important role in modulating cell migration behavior in response to applied compressive stress (ACS). In Chapter 2, cancer cells (including normal mammary epithelial cells MCF10A) showed differential motility to ACS, and could notably be classified into two main categories: (1) E-cadherin high-expression cells (e.g. MCF10A, MCF7 mammary carcinoma cells and LS174T colon carcinoma cells), which showed reduced cell migration under ACS; and (2) E-cadherin low-expression/negative cells (e.g. 67NR and MDA-MB-231 mammary carcinoma cells), which migrated faster when they were subjected to ACS. Therefore, we first investigated whether loss of E-cadherin mediated cell-cell adhesion was required for compression-induced cell motility.

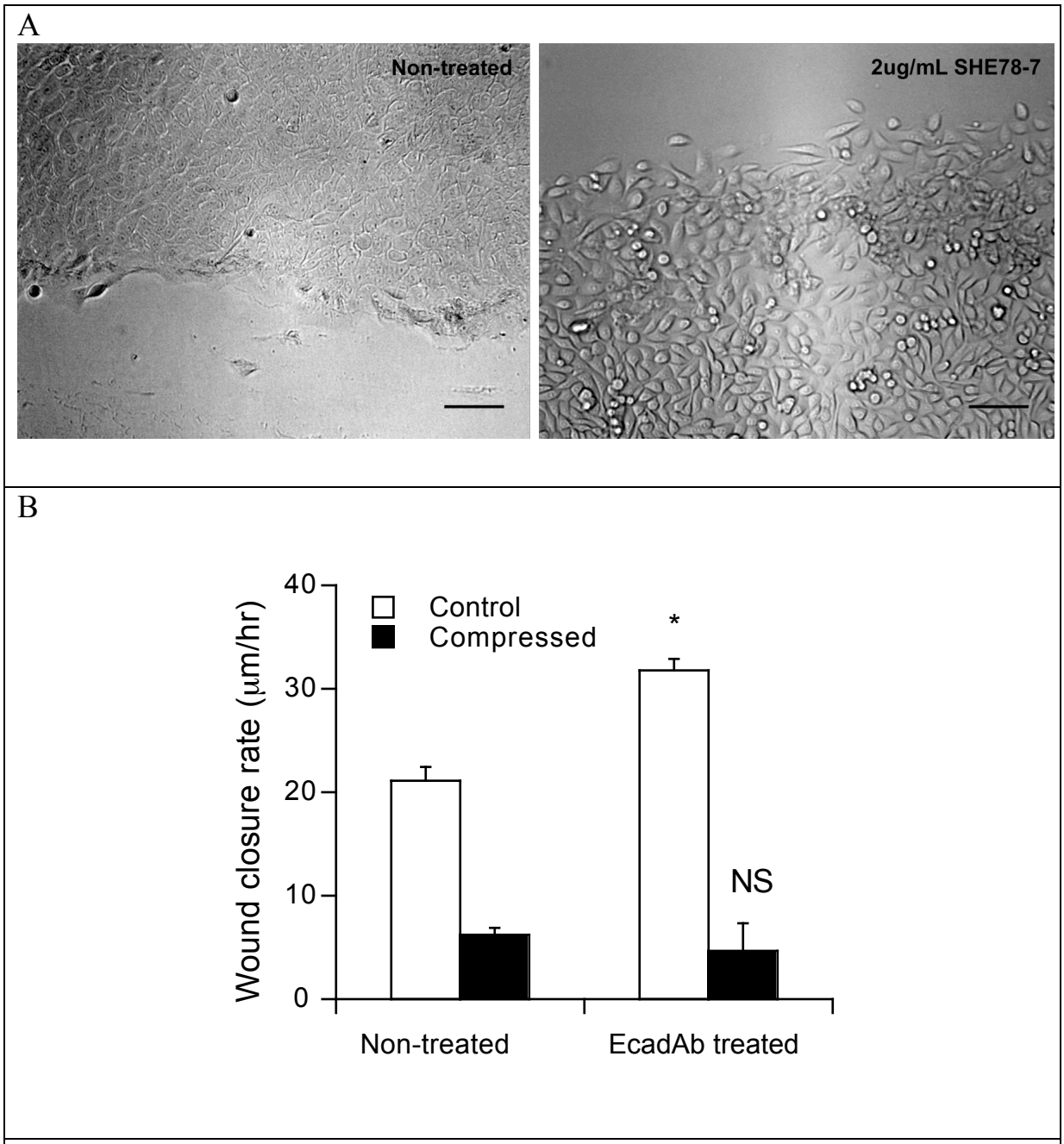

Figure 4.1. E-cadherin-mediated cell-cell adhesion in MCF10A cells does not contribute to reduced migration under compression. A, Representative images of MCF10A cell morphology showing reduced cell-cell adhesion after treatment with 2ug/mL of E-cadherin blocking antibody (SHE78-7). Scale bar, 100um. **B,** Average migration rate of MCF10A cells treated with 0 ug/mL (non-treated: n=3) or 2ug/mL of E-cadherin blocking

antibody (SHE78-7: n=6) and exposed to 0 (control) or 5.8mmHg compressive stress for 16 hrs. Compression significantly suppresses migration of MCF10A cells independent of E-cadherin-mediated cell-cell adhesion, despite elevated cell motility being observed in uncompressed MCF10A cells after treatment with E-cadherin blocking antibody. (*P<0.005 compared with the non-treated, uncompressed controls; NS=not significant compared with the non-treated, compressed cultures). Error bars represent s.e.m.

To block the cell-cell coadhesion mediated by E-cadherin, we treated mammary epithelial cell lines (normal MCF10A and breast cancer MCF7 cell lines) with an E-cadherin blocking antibody (SHE78-7) prior to compression and then assessed the migration potential via scratch-wound assay. Although treatment of both cell lines with SHE78-7 resulted in cell dissociation (Figs. 4.1A and 4.2A) and faster cell migration in uncompressed cultures, compression did not enhance cell motility in those SHE78-7-treated cells (Figs. 4.1B and 4.2B). Similar results were also observed when colon carcinoma cell lines expressing E-cadherin (LS174T and LiM6) were treated with the E-cadherin blocking antibody (Appendix Fig. C1).

A

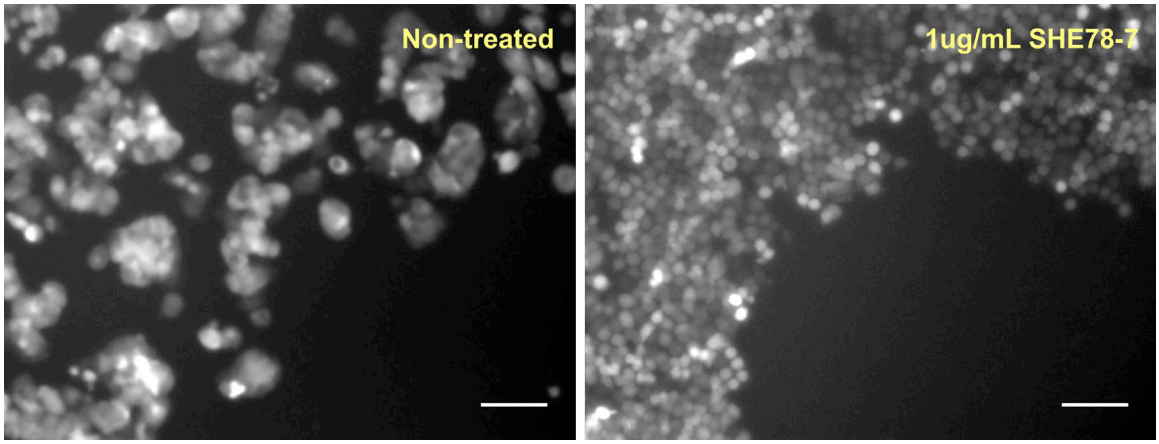

B

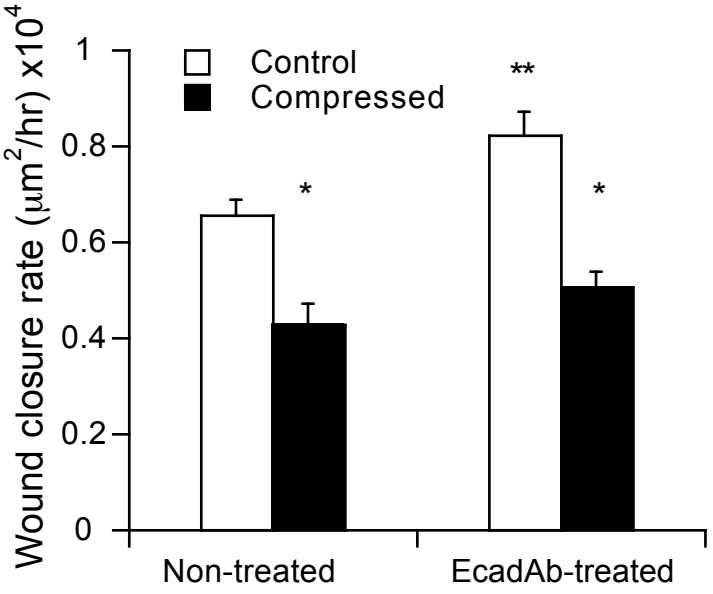

Figure 4.2. E-cadherin-mediated cell-cell adhesion in MCF7 cells does not contribute to reduced migration under compression. A, Representative images of MCF7 cells after treatment with 1ug/mL of E-cadherin blocking antibody (SHE78-7). In absence of E-cadherin blocking antibody, the cells forms small clusters and each cell border is hardly identified within the cluster because of the adheren junctions formed between cells. However, the treated cells scatter and individual cells are seen clearly.

Scale bar, 100um. **B,** Average migration rate of MCF7 cells treated with 1ug/mL IgG2a (non-treated: n=6) or 1ug/mL of E-cadherin blocking antibody (SHE78-7: n=6) and exposed to 0 (control) or 5.8mmHg compressive stress for 18 hrs. Blocking E-cadherin-mediated cell adhesion enhances migration potential of uncompressed MCF7cells, but has no significant improvement on the motility of compressed MCF7 cells. Independent of E-cadherin-mediated cell-cell adhesion, compression significantly suppresses migration of MCF7 cells. (*P<0.005 compared with their respective control; ** P<0.05 compared with the non-treated and uncompressed cultures). Error bars represent s.e.m.

As disruption of E-cadherin-mediated cell-cell adhesion in E-cadherin-expressing cell lines did not yield compression-induced aggressive phenotypes, we next sought to determine whether increased cell-cell contact in E-cadherin-negative cells would abolish compression-stimulated cell motility and leader-cell formation. The E-cadherin-negative 67NR mammary carcinoma cell line has previously shown the most pronounced morphological change and enhanced cell motility in response to mechanical compression (Chapter 2). However, increased cell cohesion by ectopic expression of E-cadherin in 67NR cells had no significant effect on compression-induced leader-cell formation or migration potential (Fig. 4.3). Taken together, our results suggest that E-cadherin is unlikely involved in ACS-modulated migration.

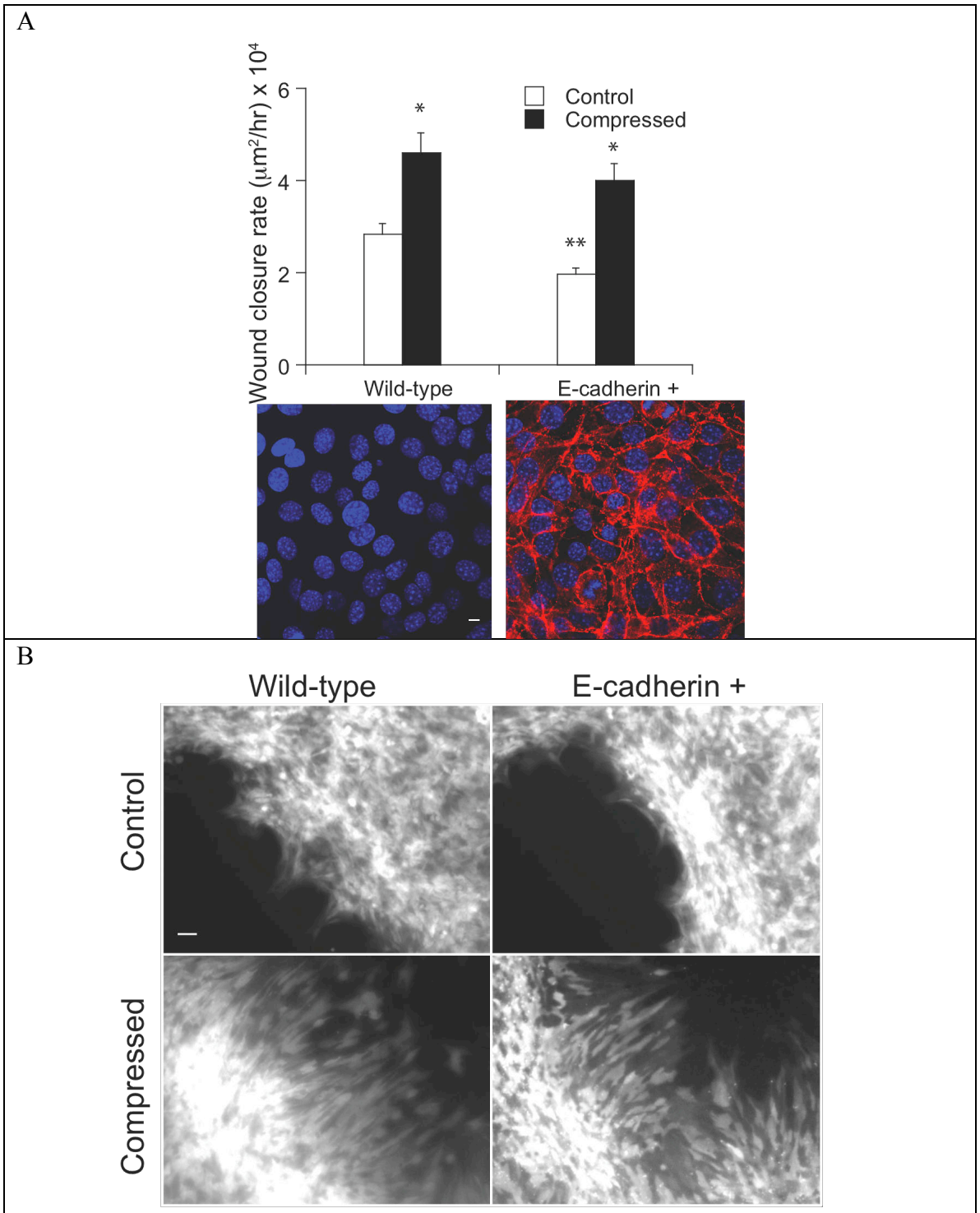

Figure 4.3. Ectopic expression of E-cadherin in 67NR mammary carcinoma cells has no effect on compression-induced migration behavior. A, Average migration rate of 67NR cells forced to re-express E-cadherin (red staining) and exposed to 0 (control) or

5.8mmHg compressive stress for 16 hrs. Compression enhances 67NR cell motility independent of its ectopic expression of E-cadherin. However, the ectopic expression of E-cadherin decreases the cell motility of the uncompressed cultures, compared to the uncompressed wild-type (n=18; *P<0.05 compared with the respective uncompressed controls; **P<0.05 compared with the uncompressed wild-type; scale bar, 10um). Error bars represent s.e.m. **B,** Representative images of the "wound" leading edge under the indicated conditions. E- cadherin re-expression does not promote or suppress leader-cell formation in control or compressed cultures (scale bar, 50um).

Although 67NR mammary carcinoma cells does not express E-cadherin, they express another member of cadherin family, N-cadherin[22], which is mostly cytoplasmic (Fig. 4.4A). Unlike E-cadherin, expression of N-cadherin has been shown to promote cell migration in breast cancer cells [23]. However, in our system, treatment of 67NR cells with a function-blocking N-cadherin antibody prior to compression had no effect on compression-induced responses (Fig. 4.4B). In addition, compressive stress did not significantly influence the transcriptional level of N-cadherin expression (data not shown), indicating that compression-induced motility is not resulted from an increased level of N-cadherin expression. Collectively, these findings suggest that compression-induced motile behavior is likely independent of expression of cadherin cell-cell adhesion molecules. However, the cells stayed connected in a sheet because there were extracellular matrix (such as fibronectin) molecules between cells (shown in Fig. 4.6A).

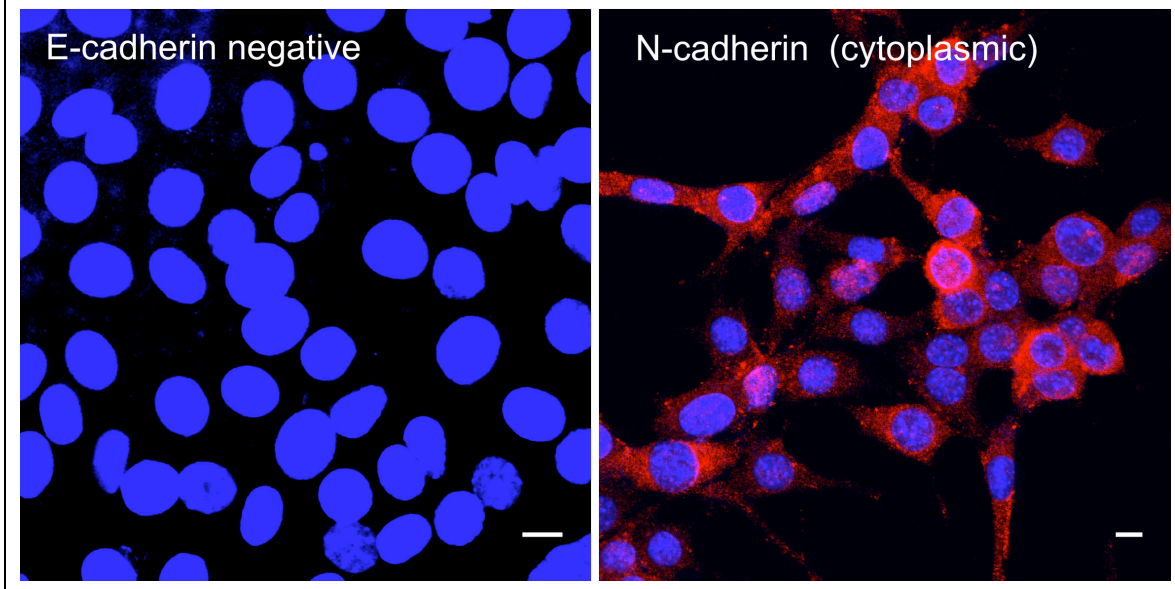

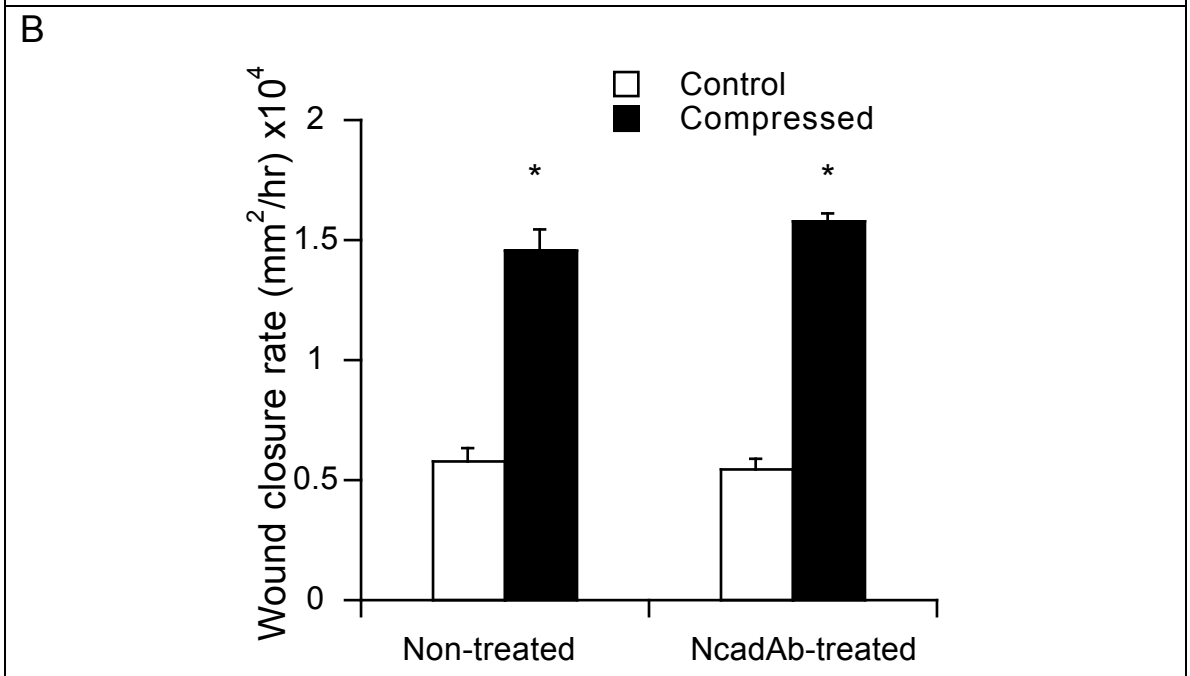

Figure 4.4. Blocking N-cadherin function does not abolish compression-induced 67NR cell migration. A, Confocal immunofluorescence microscopy of 67NR cells stained for E-cadherin (left) and N-cadherin (right), respectively. Scale bar, 10um. **B,**

Average migration rate of 67NR cells treated with 0ug/mL (non-treated: n=6-11) or 1ug/mL of N-cadherin blocking antibody (GC-4: n=9) and exposed to 0 (control) or 5.8mmHg compressive stress for 18 hrs. Disrupting N-cadherin function has no significant effect on compression-induced migration, suggesting that N-cadherin is likely not involved during compression (*P<0.005 compared to their respective control). Error bars represent s.e.m.

Compression enhances cell-substrate adhesion by shifting fibronectin balance to cell-substrate interface

To evaluate if compression affects cell-substrate adhesion strength, we performed a shear detachment assay. Compressed 67NR cells exhibited 2.5-fold higher cell-matrix adhesion than uncompressed cells on uncoated surfaces (Fig. 4.5A). Hence, we evaluated the ability of matrix-coated substrates to support migration of 67NR cells in our system. 67NR cells were seeded on fibronectin, laminin-1 and collagen I-coated surfaces and a scratch-wound assay was performed in absence of compression. Surprisingly, the uncompressed 67NR cells plated on a *fibronectin-coated* surface exhibited similar morphology and migration behavior to compressed cells on *uncoated surfaces*: cell de-clustering at the leading edge, faster wound closure (Fig. 4.5B) and increased formation of leader cells (Fig. 4.5C). This result implies that compressive stress might compensate for, or induce cell-substrate adhesions via fibronectin.

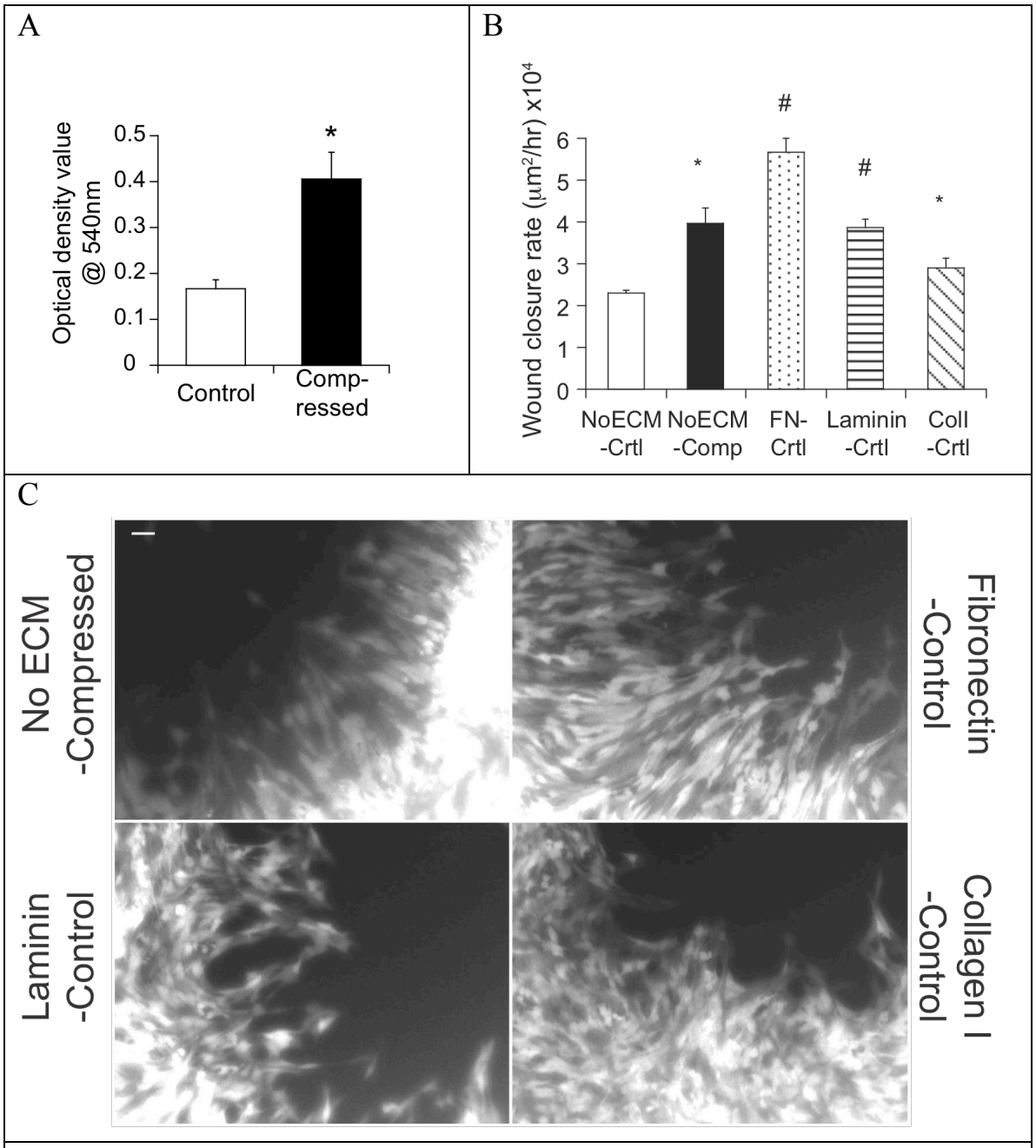

Figure 4.5. Compression-induced cell-substrate adhesion appears to be related to fibronectin. A, Uncompressed and compressed samples were exposed to fluid shear and the remaining cells were quantified using a colorimetric assay in which crystal violet stain was quantified. The number of cells remained after fluid shear in the compressed cultures is nearly doubled compared to that in the uncompressed cultures, suggesting that

compression enhances cell-substrate adhesion (n= 8; *P<0.005). **B,** Average migration rate obtained from the scratch-wound assay for 67NR cells plated on indicated extracellular matrix (ECM)-coated surfaces exposed to 0 (control) or 5.8mmHg compressive stress for 16 hrs (n=3; *P<0.05 compared with the uncompressed control on surface without ECM; #P<0.05 compared with uncompressed cells on surface without ECM; NS=not significant). Error bars represent s.d. **C,** The uncompressed 67NR cells plated on a fibronectin-coated surface exhibit similar morphology to compressed cells on an uncoated surface and had increased leader cell formation and faster wound closure (scale bar, 50um).

Since fibronectin has been shown to be regulated at the post-transcriptional level[24], and it can be deposited at the cell-substrate interface and between cells for cell-cell associations, we tested whether compression increases fibronectin deposition at the cell-substrate interface. Quantifying the spatial deposition of secreted fibronectin by confocal immunofluorescence microscopy (Fig. 4.6A), we determined that fibronectin was preferentially deposited at the compressed cell-matrix interface (Fig. 4.6B, top panel). The increased fibronectin deposit at the cell-matrix interface is apparently resulted from compression-induced cell extrusion generating additional cell adhesive contact area because the difference in fibronectin deposit between the control and compressed cultures disappeared after normalization with projected cell area (Fig. 4.6B, bottom panel). Interestingly, we observed that preferential localization of fibronectin at the compressed cell-substrate interface was oriented in the direction of migration (Fig. 4.6A). To determine whether compressive stress influences fibroectin synthesis, we isolated total

RNA from compressed or control 67NR cells and subjected them to quantitative PCR for analysis of the fibronectin mRNA level. We showed that compressive stress did not alter fibronectin transcription (Fig. 4.6C). Taken together, these findings suggest that even though compression does not alter fibronectin synthesis, it shifts the fibronectin distribution to cell-substrate interface by increasing cell-fibronectin contact areas for enhanced cell-substrate adhesion.

A

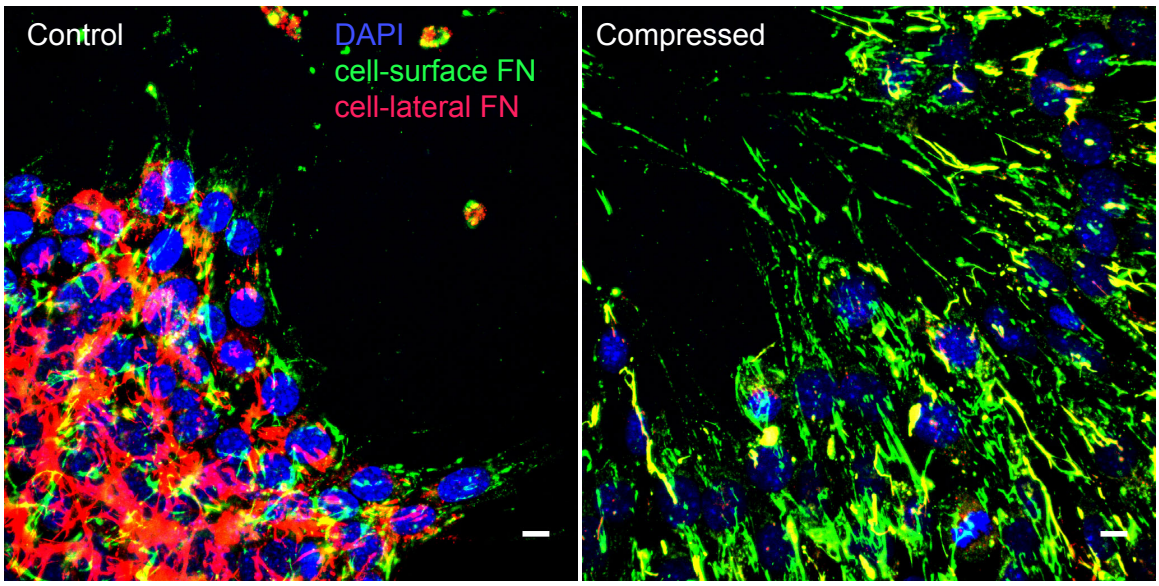

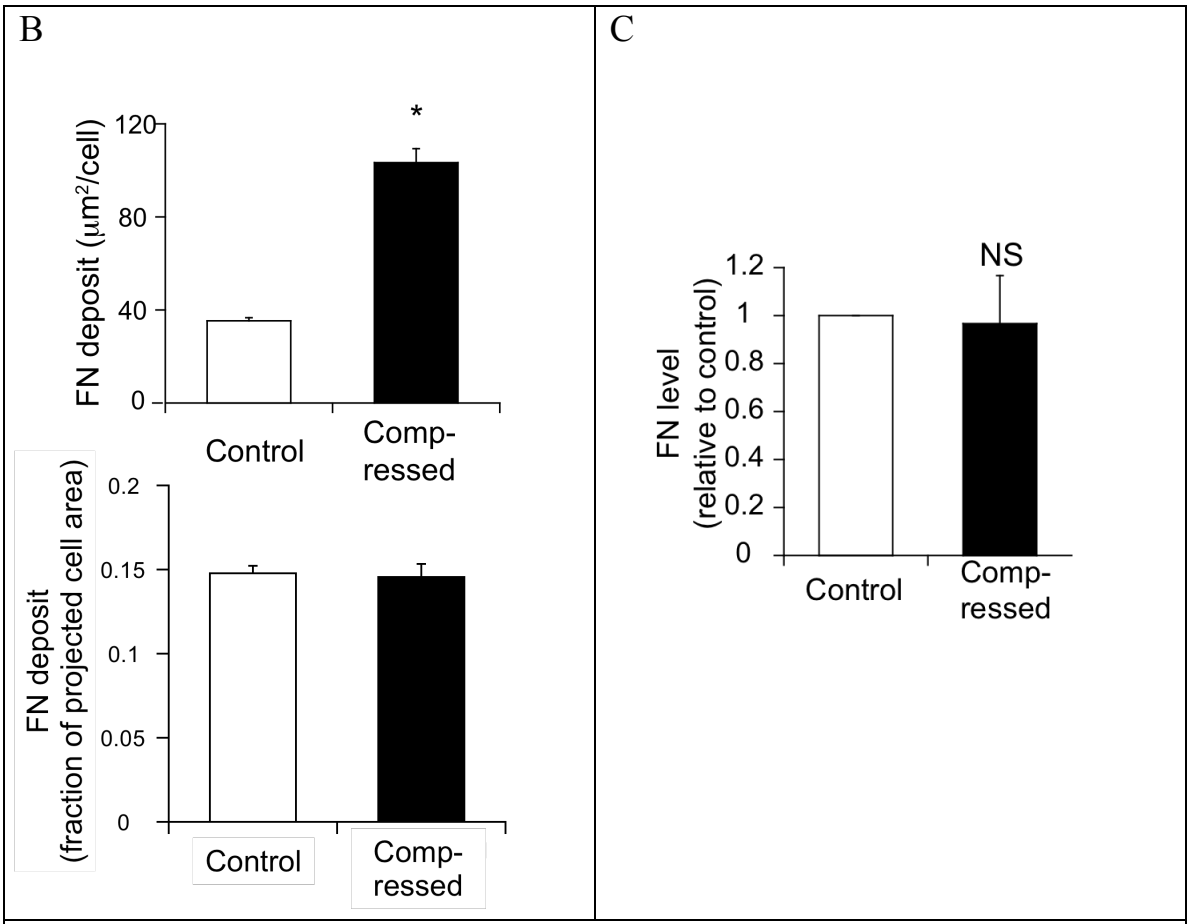

Figure 4.6. Compression increases fibronectin deposit at the cell-substrate interface independent of fibronectin synthesis. A, Fibronectin-staining of 67NR cells at the periphery of the cell-denuded area. Fibronectin at the cell-substrate interface in the compressed samples was fibrillar and orientated in the direction of migration, as opposed to the control (n=17; scale bar, 10um). **B**, Quantification of fibronectin deposition at the cell-substrate interface. Results are expressed as total fibronectin-positive pixel area relative to either total number of DAPI-stained nuclei (top panel) or projected cell area (bottom panel) (n=12; *P <0.005 compared with the control). **C**, Quantitative PCR of control and compressed 67NR cells cultured in serum-free medium for 24 hours showed no significant difference in fibronectin messenger level between the two groups. Data representative of 2 independent experiments in which 3 samples were pooled together

(NS, not significant).

Next, we investigated whether compression enhances formation of focal adhesions. For initial stage of cell adhesion to matrix, we stained the 67NR cells for phosphorylated focal adhesion kinase (FAK) [25,26] after we exposed the cells to compressive stress for a short period of time (from 5 mins to 2hrs). The compressed cells at the early stage generally showed a more diffuse and punctate (smaller) pattern at the leading edge of the cell sheet than in the uncompressed cultures (Fig. 4.7A), suggesting that compression can induce formation of small nascent adhesions to promote cell-matrix interaction and thus cell protrusion. As the maturation of those adhesions requires the recruitment of vinculin [27], we stained the 67NR cells for vinculin after the cells were subjected to 16-hr compression. Vinculin was stained in streak-like patches, extending in the direction of the filopodial protrusions on the ventral side of compressed leader cells (Fig. 4.7B). In contrast, the leading edge of uncompressed cells showed a more diffuse pattern, with vinculin in random, punctate focal adhesions. The similar patterns of fibronectin (Fig. 4.6A) and vinculin (Fig. 4.7B) in compressed cultures indicate that compression-induced filopodia act to form focal adhesions with the fibronectin substrate and sense the local environment[28] for directional migration.

A

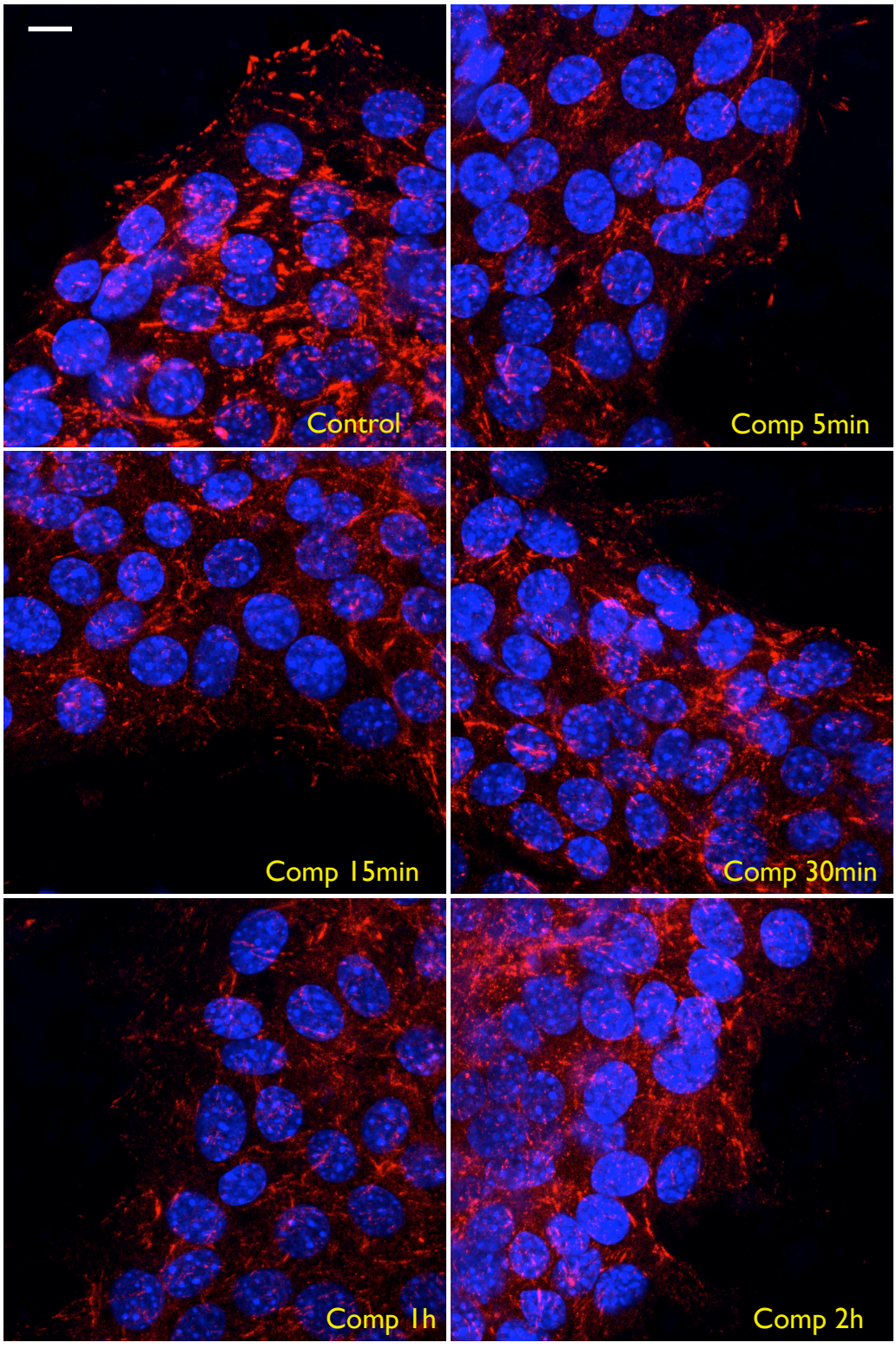

B

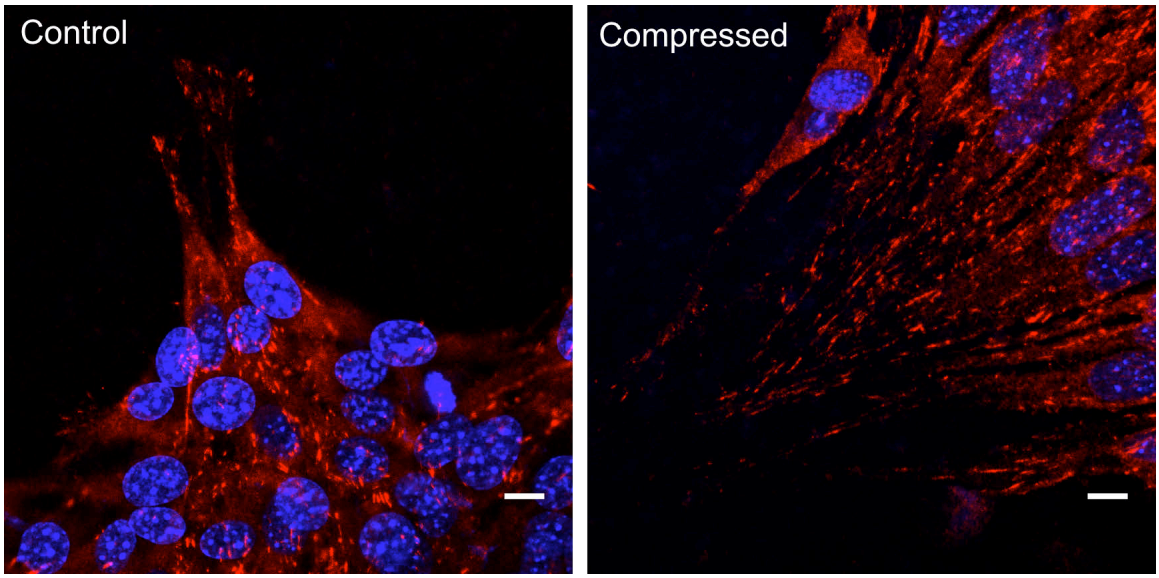

Figure 4.7. Compression promotes FAK-mediated initial adhesions, which could in turn mature into vinculin-containing focal adhesions. A, Phosphorylated FAK (Y118)-staining of 67NR cells at the periphery of the cell sheet during early stage of compression at indicated time points (n=8; scale bar, 10um). The compressed cells have a more diffuse and punctate (smaller) pattern at the leading edge of the cell sheet than in the uncompressed cultures, suggesting that external compressive stress induces formation of initial adhesion, which could mature into focal adhesions when stabilized. **B,** Vinculin-stained cells at the periphery of the cell-denuded area. 67NR cells were either uncompressed (control) or exposed to a compressive stress of 5.8mmHg for 16 hours. Vinculin-positive (red) focal adhesions were detected underneath compression-induced filopodia of elongated cells (n= 16; scale bar, 10um).

Integrin β1 *is involved in compression-induced migration, but not leader-cell formation*

The formation of focal adhesions involves the engagement of integrin receptors with the fibronectin matrix. Some of the common fibronectin-binding integrins are α5β1, αIIbβ3, αvβ1 and αvβ3. In contrast to most other fibronectin binding integrins, integrin α5β1 is specialized for binding fibronectin [10]. To determine which integrin candidate would be responsible for the compression-induced migration in our system, we screened different integrin blocking antibodies β1, β3, αIIβ, αv and α6 (non-fibronectin receptor), and assessed their effect on fibronectin-induced migration of 67NR cells via scratch-wound assay. Among all the integrin antibodies tested, wound closure rate was significantly reduced in 67NR cells treated with an anti-integrin β1 antibody alone or its combinations (Fig. 4.8A). In addition, the integrin β1 antibody-treated 67NR cells did not spread out or extend further as much as non-treated cells on fibronectin-coated surfaces (Fig. 4.8B), indicating that integrin β1 is responsible for 67NR cell attachment to fibronectin-coated surfaces and also fibronectin-mediated cell migration.

A

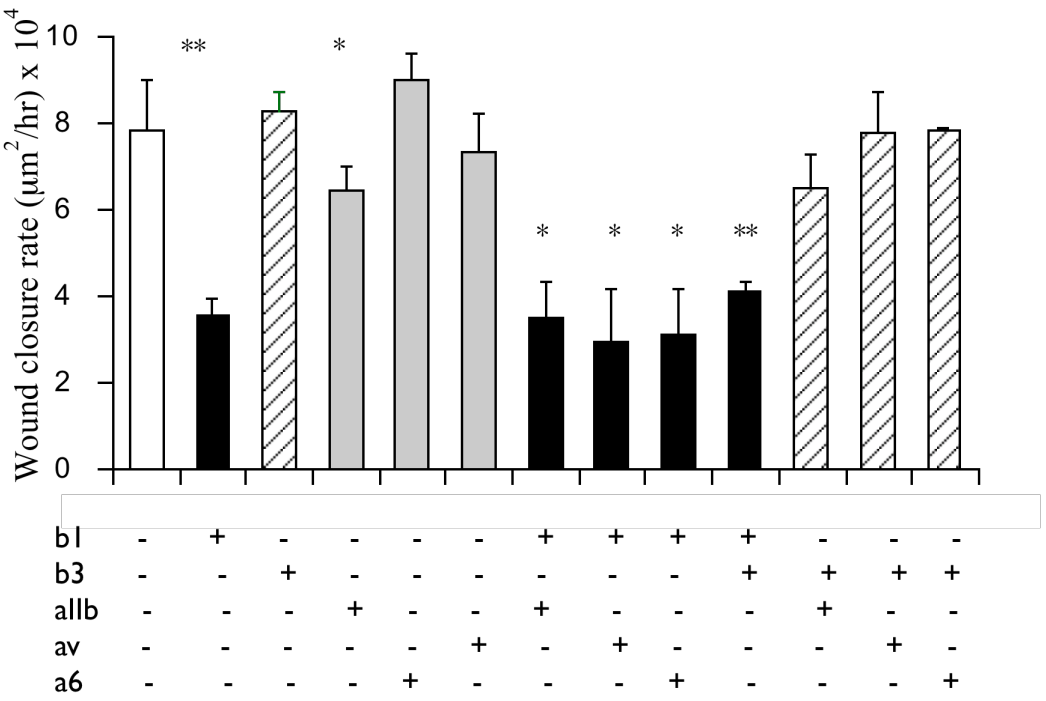
Wound closure rate (μm²/hr) x 10⁴
10
8
6
4
2
0
**
*
*
*
*
**
b1 - + - - - - + + + + - - -
b3 - - + - - - - - - + + + +
allb - - - + - - + - - - + - -
av - - - - - + - + - - - + -
a6 - - - - + - - - + - - - +

B

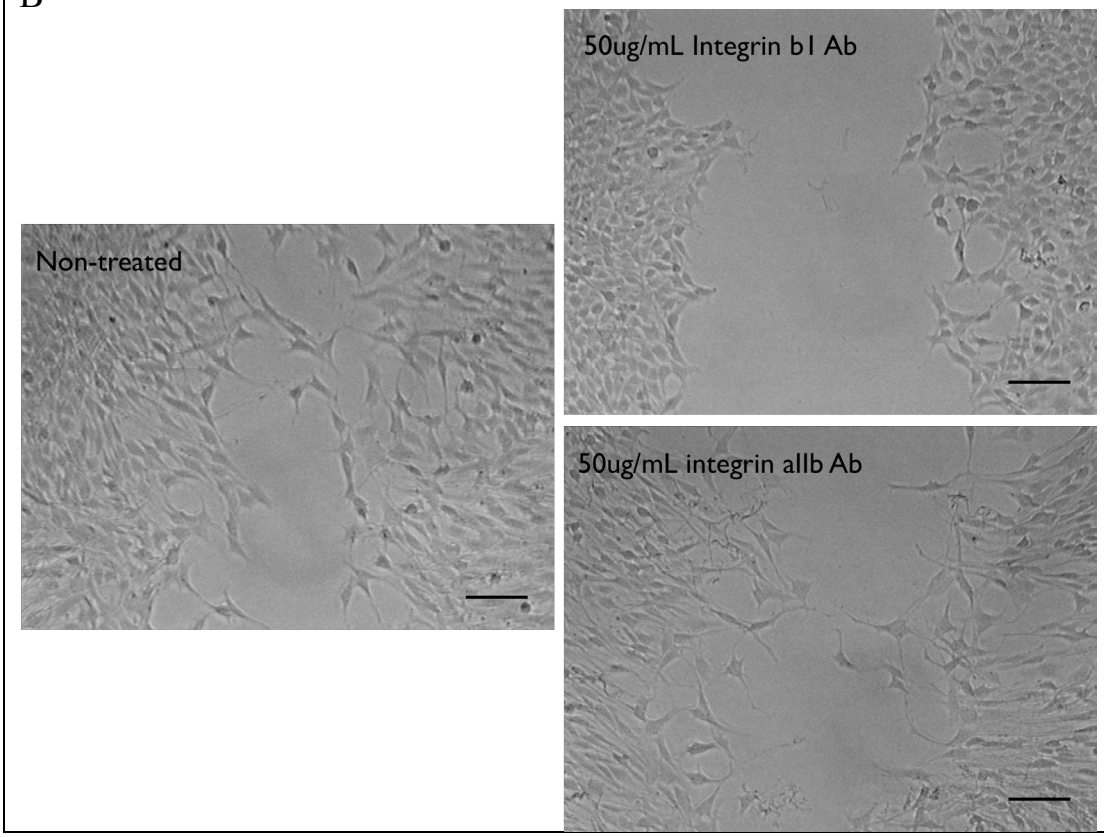
Non-treated
50ug/mL Integrin b1 Ab
50ug/mL integrin allb Ab

Figure 4.8. Integrin β1 is responsible for fibronectin-associated migration of 67NR cells. **A,** Average migration rate of 67NR cells seeded on fibronectin-coated surface and treated with either PBS (n=11) or 50ug/mL of indicated antibodies for blocking various integrins (n=2-6). Blocking integrins β1 or αIIβ (but not β3, αv or α6) with the respective antibodies reduced fibronectin-induced migration, but the effect is significantly greater in 67NR cells treated with anti-integrin β1 antibody. Combining antibodies against β1 AND αIIβ does not reduce cell migration more effectively than each antibody separately, implying that only heterodimers of integrins aIIb and b1 are present in 67NR cells (*P<0.05 and **P<0.005 compared to the non-treated control). Error bars represent s.d. **B,** Representative images of 67NR cells treated with either PBS (non-treated) or 50ug/mL anti-integrin β1 (clone Ha2/5) or αIIb antibody. The 67NR cells treated with anti-integrin β1 antibody are less elongated and more clustered than the non-treated cells. Scale bar, 100um.

As compression increased fibronectin deposit at the cell-matrix interface and in turn enhanced cell-matrix adhesion, we determined whether compression-induced cell-substrate adhesion via fibronectin could be related to expression and activation of integrin β1. Western blot analysis of lysates from 67NR cells subjected to different duration of compression time showed that the expression of integrin β1 tended to decrease after 16 hours of compression (Fig. 4.9A). However, similar to the fibronectin immunostaining shown earlier (Figs. 4.6A and 4.6B), more activated integrin β1 in streak-like patterns were localized at the cell-substrate interface in the compressed cultures (Fig. 4.9B, left) and they were aligned with the actin stress fibers (Fig. 4.9B, right). As opposed to the

punctate stains in the uncompressed cultures, the streak-like pattern of activated integrin β1 in the compressed cultures suggests that compression could induce clustering of integrin β1. Hence, we investigated the involvement of integrin β1 in compression-induced motile behavior of 67NR cells by inhibiting the binding of fibronectin to integrin β1 with an anti-integrin β1 antibody. (Synthetic peptides containing Arg-Gly-Asp (RGD) motifs [29,30] and anti-fibronectin antibody [31] were also used for inhibiting cell attachment to fibronectin but they did not impede fibronectin-mediated migration (Appendix Fig. C2)). We pre-treated the 67NR cells with 50ug/mL anti-integrin β1 antibody two hours prior to compression and the migration rate was determined by scratch-wound assay 16 hours after compression. During the 16-hr experiment, the cells were maintained in culture medium containing the anti-integrin β1 antibody. We determined that treatment of 67NR cells with anti-integrin β1 antibody decreased compression-induced migration (Fig. 4.9C, right). However, leader-cell induction by compression still occurred in presence of anti-integrin β1 antibody (Fig. 4.9C, left).

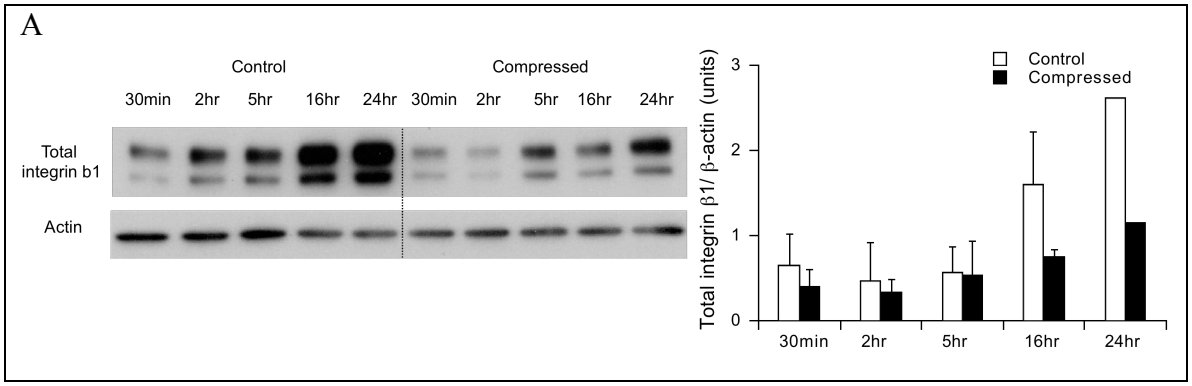

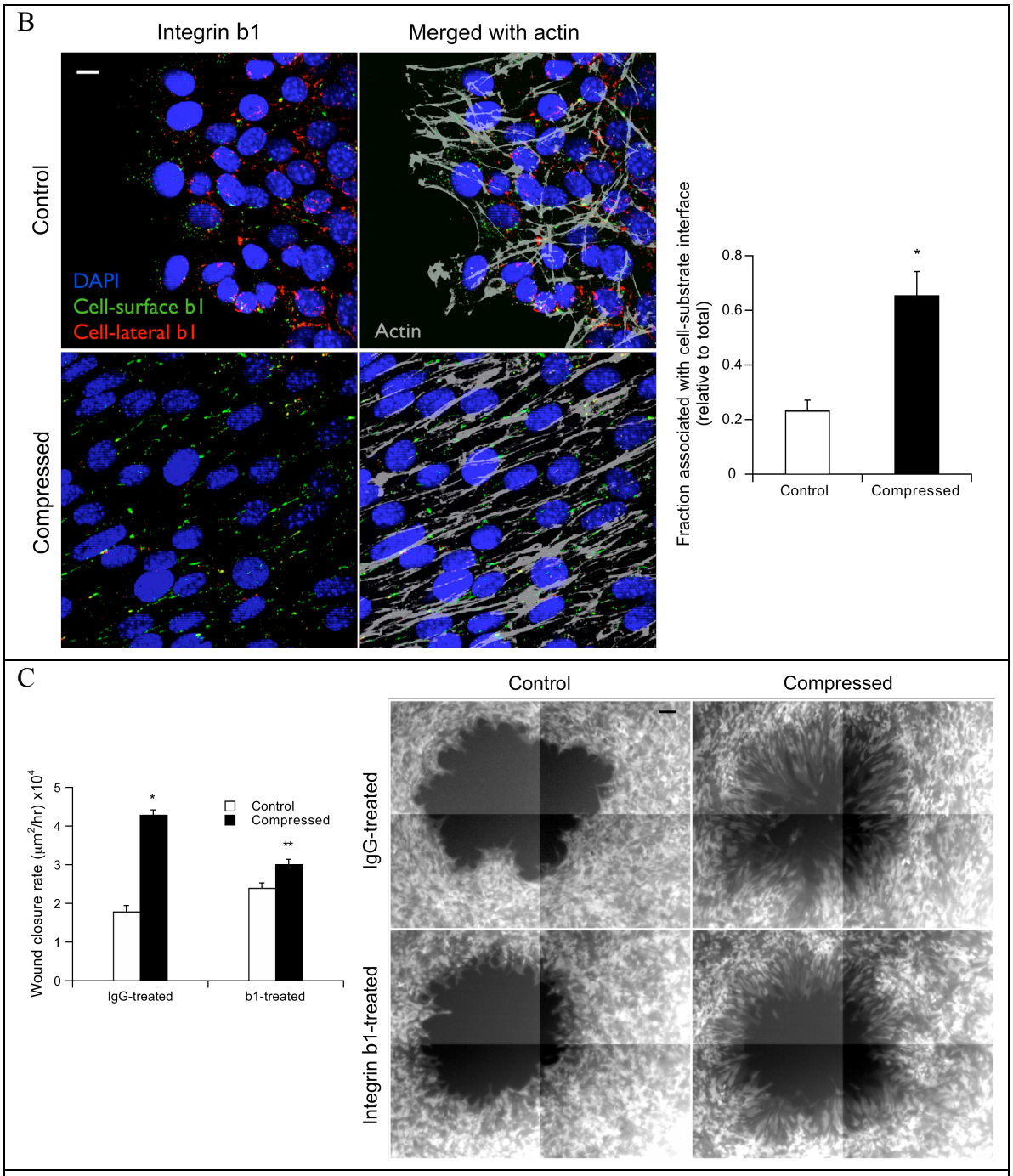

Figure 4.9. Integrin β1 is involved in compression-induced migration. A, Western blot analysis of total integrin β1 in 67NR cells subjected to stress-free or a compressive stress of 5.8mmHg for the indicated length of compression time. Data representative of 2 independent experiments in which 3 samples were pooled together. The compressed

cultures tended to express lower level of total integrin β1. Error bars presents s.d. **B**, Activated integrin β1-staining of 67NR cells at the periphery of the cell-denuded area after 16-hr wounding, and quantification results expressed as activated integrin β1-positive pixel area associated with the cell-substrate interaction relative to the total activated integrin β1-positive area (n=16-20; *P <0.005 compared with the control; scale bar, 10um). Activated integrin β1 staining at the cell-substrate interface in the compressed samples was more elongated and aligned with the actin stress fiber, as opposed to the control. Error bars represent s.e.m. **C**, Average migration rate obtained from the scratch-wound assay for 67NR cells treated with anti-integrin β1 antibody under stress-free or a compressive stress of 5.8mmHg for 16 hrs and their corresponding representative images of 67NR leader cells at the wound edge (n=8; *P<0.005 compared with the respective control; **P<0.05 compared with the respective control; scale bar, 100um). Integrin β1 inhibition reduces compression-induced migration rate but it appears that the leader-cell formation is not affected. Error bars represent s.e.m.

We then investigated integrin-associated proteins such as paxillin, which is part of the focal adhesion complex associated with the cytoplasmic domain of clustered integrins. Similar to western blot results of integrin β1, the expression levels of total paxillin was reduced in the compressed cultures. In addition, the expression levels of phosphorylated paxillin (Tyr-118) relative to that of total paxillin appeared to be lower in the compressed cultures (Figs. 4.10A). Similar western blot results were also found with focal adhesion kinase (FAK), another integrin-associated protein, and the results were shown in Appendix Figure C3. Although the expression level of paxillin was lower in the

compressed cultures, the activation of paxillin associated with cell-substrate adhesion was increased with compression (Fig. 4.10B). Moreover, the paxillin staining pattern in the compressed cultures was oriented in the direction of migration, correlated closely to fibronectin and integrin b1 staining shown earlier.

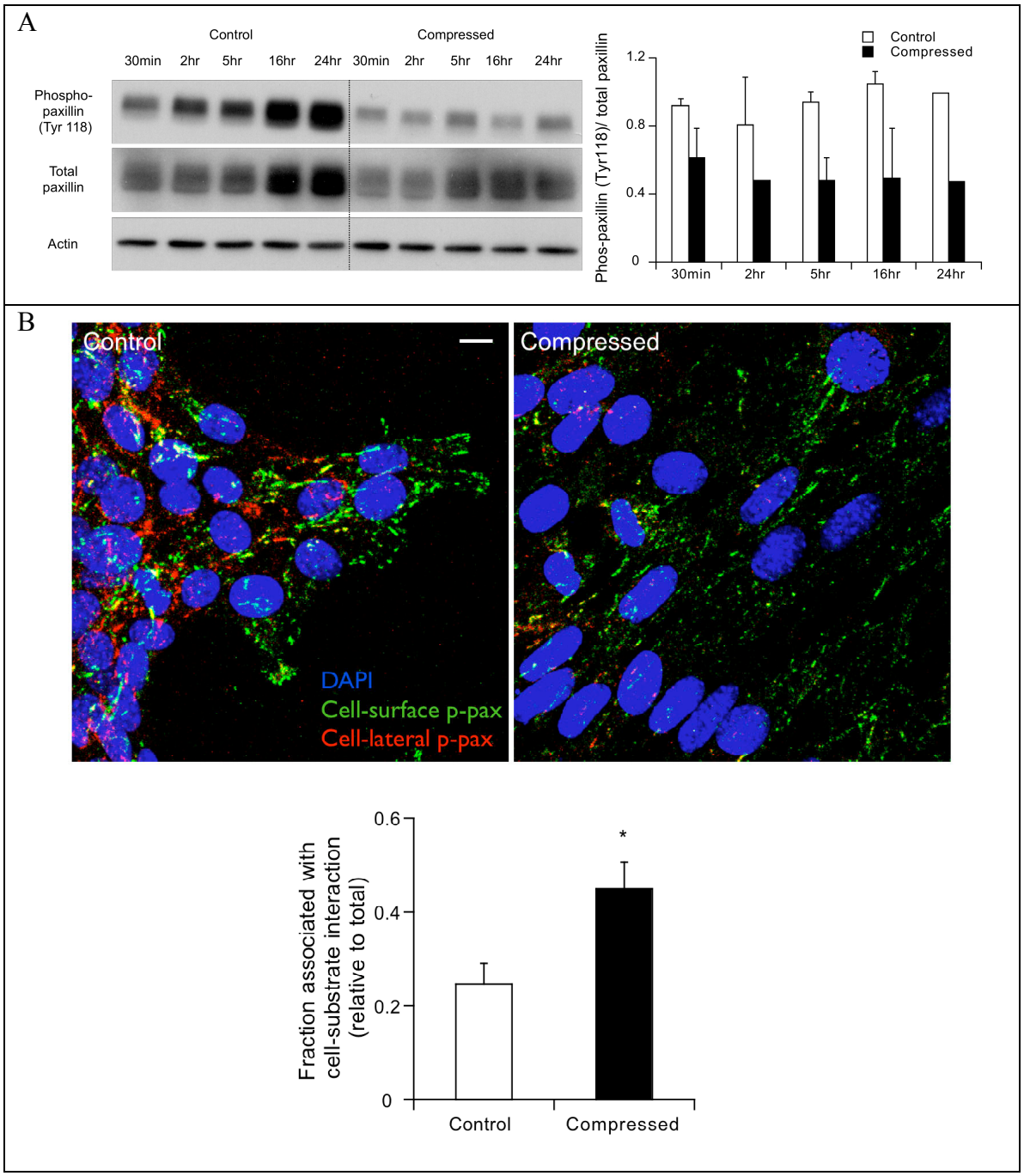

Figure 4.10. Compression reduces the total paxillin expression level, but increases the fraction of phosphorylated paxillin associated with cell-substrate interaction. A, Western blot analysis of total and phosphorylated (Y118) levels of paxillin in 67NR cells subjected to stress-free or a compressive stress of 5.8mmHg for the indicated length of compression time. Data representative of 2 independent experiments in which 3 samples were pooled together. The compressed cultures expressed lower level of total paxillin and phosphorylated tyrosine proteins. Error bars presents s.d. **B**, Phosphorylated paxillin (Y118)-staining of 67NR cells at the periphery of the cell-denuded area after 16-hr wounding, and quantification results expressed as phosphorylated paxillin (Y118)-positive pixel area associated with the cell-substrate interaction relative to the total phosphorylated paxillin (Y118)-positive area (n=16-20; *P <0.005 compared with the control; scale bar, 10um). Phosphorylated paxillin staining at the cell-substrate interface in the compressed samples contains both punctate and elongated patterns oriented in the direction of migration, as opposed to the control. Error bars represent s.e.m.

Compression-induced leader-cell formation is independent of actomyosin contractility

In the compressed cultures, enhanced integrin engagement with matrix (indicated by elongated staining of activated integrin β1) gives rise to formation of matrix adhesions, which associate with actin filaments[13]. The contractile actomyosin machinery, which is essential for maturation of focal contacts and stress fiber formation [32], could be responsible for the enhanced streak-like vinculin patterns in compressed cultures (Fig. 4.7B). We examined the requirement of actin-myosin activity in compression-induced leader cell formation using molecular and pharmacological approaches. To partially

disrupt the actin-myosin machinery, we used dominant-negative RhoA (RhoA-T19N) retrovirus [33], Rho kinase inhibitor Y-27632[34] or myosin light-chain kinase (MLCK) inhibitor ML-7[35]. Compressed samples still showed faster wound closure rates compared with controls, although they were slightly reduced (Fig. 4.11A-C). Moreover, partial inhibition did not suppress leader cell formation in the compressed cultures. Indeed, measurement of RhoA activity by enzyme-linked immunosorbent assay (ELISA) showed that compressive stress did not significantly change the RhoA activity, suggesting that the leader-cell formation is independent of RhoA-mediated actomyosin contractility (Fig. 4.11D). Furthermore, when actomyosin contractility was completely blocked by the nonmuscle myosin II ATPase inhibitor Blebbistatin[36], compressive stress was still able to induce leader-cell formation despite compromised cell motility (Fig. 4.11C). These results indicate that leader-cell formation can occur in the absence of actomyosin contractility; however, the contractile machinery is necessary for migration. This is consistent with previous studies reporting that externally-applied force induces formation of focal contacts independent of Rho-ROCK-mediated actomyosin machinery[37]. Collectively, these findings suggest that compressive stress generated in the tumor microenvironment could promote an increased number of leader cells and stabilize filopodial protrusions by enhancing cell-matrix adhesions without the involvement of actomyosin contractility.

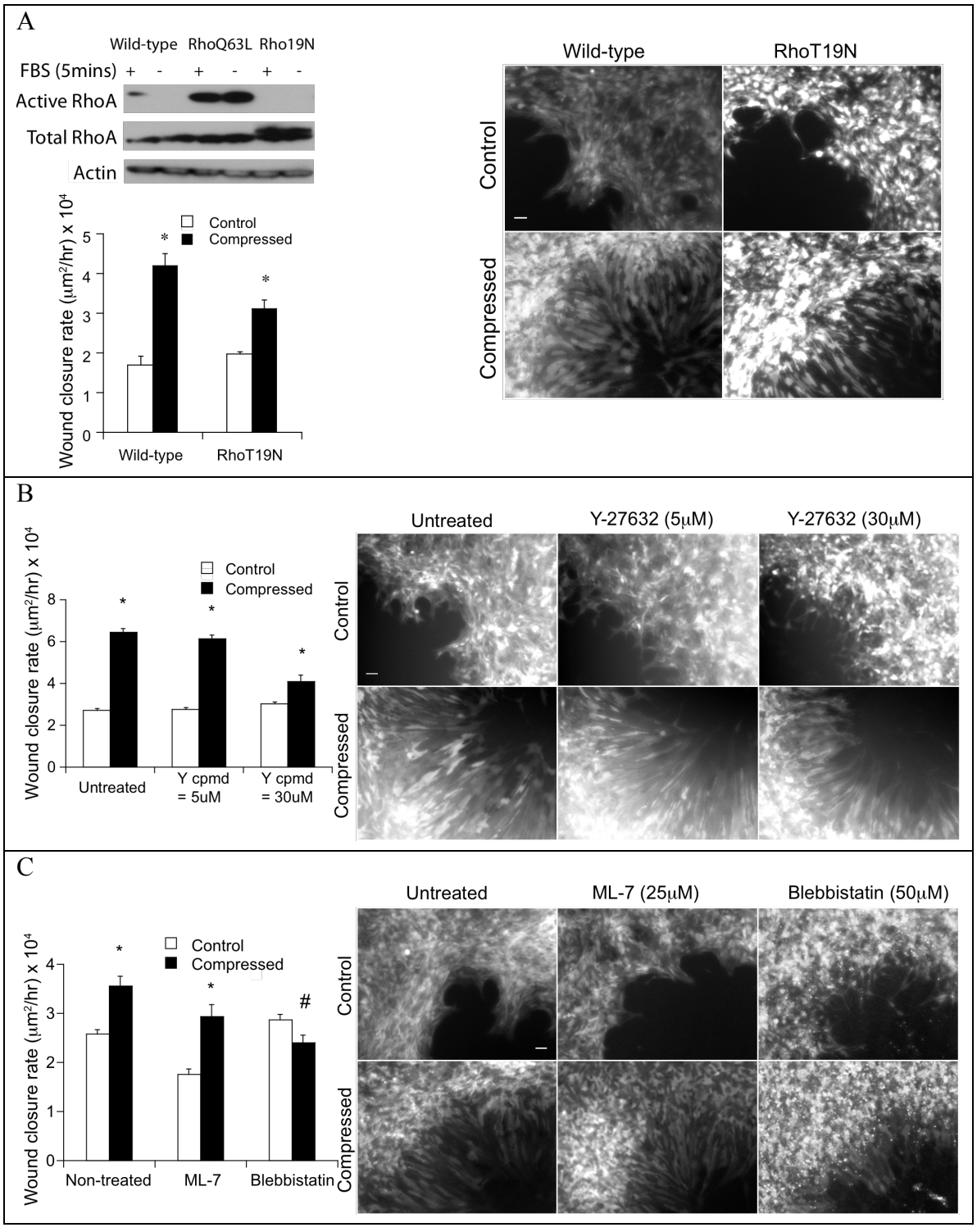
A
Wild-type
RhoQ63L
Rho19N
FBS (5mins) + - + - + -
Active RhoA
Total RhoA
Actin
Wound closure rate (μm²/hr) x 10⁴
Control
Compressed
Wild-type
RhoT19N
Wild-type
RhoT19N
Control
Compressed
B
Wound closure rate (μm²/hr) x 10⁴
Control
Compressed
Untreated
Y cpmd = 5uM
Y cpmd = 30uM
Untreated
Y-27632 (5μM)
Y-27632 (30μM)
Control
Compressed
C
Wound closure rate (μm²/hr) x 10⁴
Control
Compressed
Non-treated
ML-7
Blebbistatin
Untreated
ML-7 (25μM)
Blebbistatin (50μM)
Control
Compressed

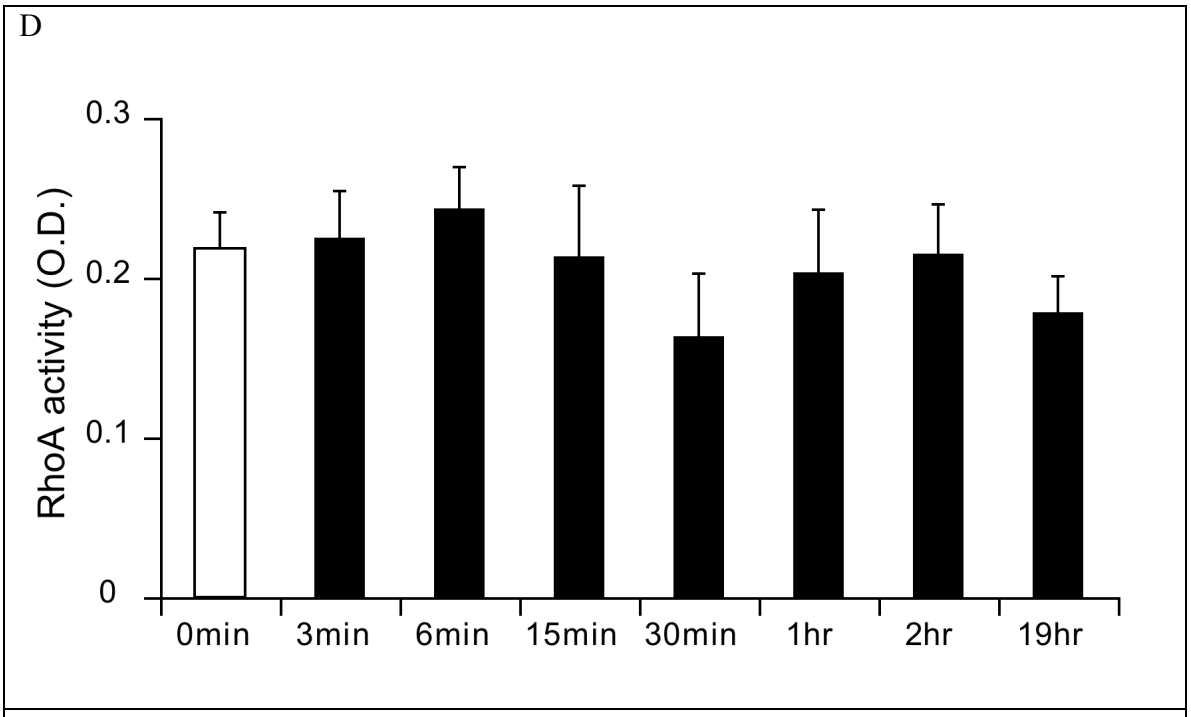

Figure 4.11. Actomyosin contractility reduces compression-induced directional cell migration. A, Western blot showing RhoA activation pull-down to analyze the transduction efficiency. **A-C,** Average migration rate obtained from the scratch-wound assay for 67NR cells transduced with dominant negative RhoT19N retrovirus (**A**; n=6), treated with Y-27632 (**B**; n=13), ML-7 (**C**; n=6) or Blebbistatin (**C**; n=6) under stress-free or a compressive stress of 5.8mmHg for 16 hrs and their corresponding representative images of 67NR leader cells at the wound edge (*P<0.005 compared with the respective control; #P<0.05 compared with the respective control; scale bar, 50um). The inhibitors of actomyosin contractility did not completely abolish compression-induced migration but at a reduced rate (except for blebbistatin). It appeared that leader-cell formation was not affected. Error bars represent s.e.m. **D,** Determination of RhoA activity in 67NR cells subjected to stress-free or a compressive stress of 5.8mmHg for the indicated length of compression time by enzyme-linked immunosorbent assay (ELISA).

Results representative of 2 independent experiments, in which 3 samples were pooled together, show that compressive stress did not significantly change the RhoA activity, supporting the notion that the leader-cell formation is independent of RhoA-mediated actomyosin contractility. Error bars represent s.d.

Discussion

In growing solid tumors, the cancer cells actively experience compressive stress generated by uncontrolled proliferation in a confined matrix. These compressive forces act at the interface between cells and their neighbors or between cells and the extracellular matrix. These cell-cell and cell-matrix interactions transmit these mechanical forces and then convert them into various intracellular chemical-signaling events [38,39]. We hypothesized that this growth-induced compressive stress could alter cell adhesion (to neighboring cells or extracellular matrix), thereby facilitating tumor progression such as leader-cell formation and enhanced cell motility (Chapter 2). In this study, using 67NR mammary carcinoma cells as a model, we found that compression-induced migration and leader-cell formation was likely cadherin-independent. Instead, compressive stress promoted cell-substrate adhesion, thus enhancing integrin b1- and myosin- dependent cell migration. Interestingly, inhibition of integrin b1 and actomyosin contractility did not abolish compression-induced leader-cell formation.

Cadherins have been implicated as mechanotransducers interacting with the dynamics of microtubules, actin and intermediate filaments for regulation of cell-cell adhesion[40]. In addition, mechanical force (intracellular contractile force) has been shown to modulate

adhesion strengthening, suggesting that cadherin-dependent cell-cell junctions exhibit similar force-dependent behavior [41]. Since previous studies have shown the inverse correlation between E-cadherin-mediated cell-cell interaction and cancer cell motility [42-45], we speculated that the reduced migration of E-cadherin-expressing cells such as MCF10A and MCF7 could be resulted from increased cell-cell adhesion strength by compression. We have shown that reduced E-cadherin cell-cell contact by an anti-E-cadherin antibody increased cell migration in absence of compression. However, the compressed cells treated with the anti-E-cadherin antibody still demonstrated suppressed cell motility. In addition, forced re-expression of E-cadherin in 67NR cells did not have significant impact on compression-induced migration or leader-cell formation. Taken together, these findings imply that that cadherin-mediated cell-cell contact is not the limiting factor in regulating compression-induced migration behavior.

Other than cell-cell cohesion, cell-matrix adhesion is critical for mediating direct interactions of cells with its extracellular environment and/or physical cues and essential for cell migration [13,26,46]. While extracellular hydrostatic pressure has been shown to increase cancer cell adhesion [4,47-49], we found that compressive stress can also up-regulate cancer cell-matrix adhesive strength. While those previous studies have shown that 30-min extracellular pressure of at least 10mmHg (maximal at 15mmHg) stimulated the adhesion of colon or breast cancer cells in suspension to collagen-coated surfaces[50], they did not investigate the effect of that stress level on cell migration. In our study, not only did we show that continuous compression of adherent 67NR cells at 5.8mmHg (equivalent to ~773 Pa, which is close to the level found in the native breast tumor

microenvironment [51]) was sufficient to promote their cell-substrate adhesion, we have also determined that such stress level enhanced cell migration and increasing the stress further would reduce cell survival and impede cell motility significantly (Chapter 2). The disparities in the stress level required to produce cell adhesion response could be caused by distinct internal prestress states of the cells prior to mechanical stimulation. The cellular tensegrity model proposed by Ingber suggested that the difference in internal prestress of a whole cell when adherent and spread on a rigid substrate (in our case) versus when it is detached and round (cell suspension) can affect initial cell stiffness and thus their sensitivity to externally-applied stress [52-54].

Furthermore, it should be noted that the level of compressive stress to produce maximal cell adhesion does not always yield highest motility. Migration potential is a biphasic function of the strength cell attachment to matrix or substrate concentration [13,55,56]. Too strong cell-substrate adhesion can impede cell retraction and detachment, thus preventing the cells from advancing forward. Hence, the reduced motility of 67NR cells that we observed under compressive stress beyond 5.8mmHg could be possibly due to the cells adhering too strongly to the surface under high stress. Similarly, compression-suppressed migration in MCF10A and MCF7 cells, independent of cadherin-mediated cell-cell adhesion, could be resulted from overly-strong cell-substrate adhesion up-regulated by compression. Since MCF10A and MCF7 cells intrinsically adhere stronger than 67NR cells on uncoated surface in absence of compression (data not shown), additional cell-substrate adhesion induced by compression at 5.8mmHg, which was shown to enhance 67NR cell migration, could have an negative effect on migration of

MCF10A and MCF7 cells. Taken together, our results suggest that the effect of compression-induced cell-matrix interaction on cell motility could be biphasic. For optimal cancer invasion *in vivo*, our results suggest a feedback regulation of stress-dependent matrix degradation and/or apoptosis as a defensive cellular response against stress. Hence, some cancer cells could respond to growth-generated compressive stress by increasing migration.

With increased cell-matrix interactions in the compressed cultures, we have observed that more elongated fibronectin fibrils (and more vinculin-containing streak-like focal adhesions) were formed under compressed cells in the direction of migration. Studies have shown that cell-generated cytoskeletal tension transmitted through integrins to the extracellular matrix (ECM) can selectively reorganize extracellular matrix proteins on substrates and assemble them into cell-surface fibrils [57,58]. Moreover, the intracellular contractility has been shown to unfold fibronectin to expose cryptic self-association sites for fibronectin fibril and matrix assembly[59-61]. In light of compression-induced cell-substrate adhesion, the streak-like vinculin staining of compressed cultures indicated the strengthening of the connection between matrix and the cytoskeleton, which in turn enabled the cell to exert force at those focal adhesions [27]. Hence, the tensional force exerted by the compressed cells to fibronectin via compression-induced focal adhesions or focal complexes [62-65] could enhance formation of fibronectin fibrils. In addition, the unfolding of fibronectin could expose more binding sites for integrins, thereby promoting formation of cell-matrix adhesion structures.

Three common types of adhesion structures have been defined, namely focal complexes, focal adhesions and fibrillar adhesions. The focal complexes are small, transient matrix contact structure that provides early attachment at the leading edge. If stabilized, they will subsequently form focal adhesions, which can in turn transition to fibrillar adhesions associated with fibrillar ECM (particularly fibronectin fibrils) in presence of intracellular tension [13,66]. In agreement with the findings on fibrillar adhesions from other studies, we observed in the compressed cells that fibronectin fibrils were aligned with cytoplasmic bundles of actin filamements[67], and vinculin were assembled into a fibrillar pattern that was correlated closely with the pattern of fibronectin fibrils beneath the surface of the leader cells, which was distinct from focal adhesions[68]. Thus, the more diffuse and punctate FAK-pY397 staining pattern in the early-stage compressed cultures suggested that compression could induce formation of small nascent focal complexes or focal adhesions, which could in turn mature into streak-like vinculin-containing fibrillar adhesions.

In addition, these three adhesion structures differ in molecular composition, such as integrin expression and the levels of tyrosine-phosphorylated proteins (including FAK and paxillin). For example, compared to focal complexes and focal adhesions, fibrillar adhesions contain abundant tensin, low levels of vinculin, protein tyrosine phosphorylation, and a5β1 instead of avb3 integrins [13,66]. Although we did not stain the cells for tensin or integrin a5β1, our results showed that the 16-hr compressed 67NR cells appeared to have less staining of the phosphorylated paxillin (and FAK) staining than the uncompressed cells, and treatment of 67NR cells with anti-integrin β1 antibody

reduced compression-induced migration, suggesting that compression might induce maturation of initial adhesions into fibrillar adhesions. Furthermore, while actomyosin contractility is required for focal adhesions, but not fibrillar adhesions, [69,70], our finding that compression-induced leader-cell formation was independent of actomyosin contractility further supports the notion that adhesion structures formed by compression could be fibrillar adhesions.

Many reports have showed that mechanical stress stimulates cell adhesion via FAK and paxillin activation [3,4,47,71] and have implicated FAK and paxillin (integrin signaling) as a positive regulator of cell motility [72-79]. In contrast to their established roles, we showed by Western blot analysis that expression levels of integrin b1 and paxillin even at early time points were not up-regulated in the compressed 67NR cultures, during which there was enhanced adhesion and motility. However, recent studies have reported that impaired FAK and paxillin signaling in HeLa cells and fibroblasts result in increased cell migration [80], and direct binding of paxillin to FAK may not be required for FAK-directed cell migration [74]. In addition, the role of FAK in generation of cell-ECM adhesive forces is time-dependent: FAK increases the initial strength of cell-ECM adhesion via integrin activation; but the presence of FAK decreases adhesive forces in the long term, steady-state cell-ECM interactions[81,82]. Consequently, the dynamic and transient interplay of paxillin and FAK with cell-ECM adhesion and migration could complicate the interpretation of the changes in these proteins. Furthermore, independent of these signaling pathways, other physical factors such as cell polarization can control directional cell migration [25]. As a cell polarizes, the molecular processes at the front

and the rear of the cell are different [83]. Hence, the fact that compression can stimulate a larger population of cells to polarize and become leader cells (Chapter 3) could also suggest that spatial localization of proteins could be more important than their expression level in regulating these cellular processes.

In conclusion, using 67NR mammary carcinoma cells as a model, we showed that compression promotes formation of new adhesions, which can in turn transition to fibrillar adhesions for enhanced cell-matrix adhesions and eventually increased migration potential. Hence, blocking integrin binding or actomyosin contractility reduces compression-stimulated cell motility (but not leader-cell formation). As adhesion is critical for metastasis related events, such as the initiation of cellular motility and subsequent invasion into the surrounding tissue [84], our results suggest that mechanical stress accumulated during tumor growth is sufficient to enhance cell-substrate adhesion and in turn stimulate cancer cell migration, without activating stroma cells to increase production of extracellular matrix. This concept would provide implications for developing new class of targets for more effective cancer therapy. Furthermore, matrix adhesion signals are also essential for regulating other biological processes involving mechanical cues such as wound healing[85], tissue maintenance[86,87], and morphogenesis [88]. Thus, elucidating the effect of mechanical stress on cell-matrix interaction provides a vantage point for understanding its relevance in tissue engineering.

References

1. Gomes, N., M. Berard, J. Vassy, N. Peyri, C. Legrand, and F. Fauvel-Lafeve. 2003. Shear stress modulates tumour cell adhesion to the endothelium. *Biorheology*. 40:41-5.
2. Benoliel, A.M., N. Pirro, V. Marin, B. Consentino, A. Pierres, J. Vitte, P. Bongrand, I. Sielezneff, and B. Sastre. 2003. Correlation between invasiveness of colorectal tumor cells and adhesive potential under flow. *Anticancer Res*. 23:4891-6.
3. Craig, D.H., C.P. Gayer, K.L. Schaubert, Y. Wei, J. Li, Y. Laouar, and M.D. Basson. 2009. Increased extracellular pressure enhances cancer cell integrin-binding affinity through phosphorylation of beta1-integrin at threonine 788/789. *Am J Physiol Cell Physiol*. 296:C193-204.
4. van Zyp, J.V., W.C. Conway, D.H. Craig, N.V. van Zyp, V. Thamilselvan, and M.D. Basson. 2006. Extracellular pressure stimulates tumor cell adhesion in vitro by paxillin activation. *Cancer Biol Ther*. 5:1169-78.
5. Conway, W.C., J.V.d.V.v. Zyp, V. Thamilselvan, M.F. Walsh, D.L. Crowe, and M.D. Basson. 2006. Paxillin modulates squamous cancer cell adhesion and is important in pressure-augmented adhesion. *Journal of Cellular Biochemistry*. 98:1507-1516.
6. Thamilselvan, V., A. Patel, J. van der Voort van Zyp, and M.D. Basson. 2004. Colon cancer cell adhesion in response to Src kinase activation and actin-cytoskeleton by non-laminar shear stress. *J Cell Biochem*. 92:361-71.
7. Ganz, A., M. Lambert, A. Saez, P. Silberzan, A. Buguin, R.M. Mege, and B. Ladoux. 2006. Traction forces exerted through N-cadherin contacts. *Biol Cell*. 98:721-30.
8. Luo, B.H., C.V. Carman, and T.A. Springer. 2007. Structural basis of integrin regulation and signaling. *Annu Rev Immunol*. 25:619-47.
9. Hynes, R. 1985. Molecular biology of fibronectin. *Annu Rev Cell Biol*. 1:67-90.
10. Johansson, S., G. Svineng, K. Wennerberg, A. Armulik, and L. Lohikangas. 1997. Fibronectin-integrin interactions. *Front Biosci*. 2:d126-46.
11. Liu, S., D.A. Calderwood, and M.H. Ginsberg. 2000. Integrin cytoplasmic domain-binding proteins. *J Cell Sci*. 113 (Pt 20):3563-71.
12. Ginsberg, M.H., A. Partridge, and S.J. Shattil. 2005. Integrin regulation. *Curr Opin Cell Biol*. 17:509-16.
13. Berrier, A.L., and K.M. Yamada. 2007. Cell-matrix adhesion. *J Cell Physiol*. 213:565-73.
14. Martin, K.H., J.K. Slack, S.A. Boerner, C.C. Martin, and J.T. Parsons. 2002. Integrin connections map: to infinity and beyond. *Science*. 296:1652-3.
15. Ilina, O., and P. Friedl. 2009. Mechanisms of collective cell migration at a glance. *J Cell Sci*. 122:3203-8.

16. Friedl, P., and D. Gilmour. 2009. Collective cell migration in morphogenesis, regeneration and cancer. *Nat Rev Mol Cell Biol*. 10:445-57.
17. Perl, A.K., P. Wilgenbus, U. Dahl, H. Semb, and G. Christofori. 1998. A causal role for E-cadherin in the transition from adenoma to carcinoma. *Nature*. 392:190-3.
18. Sloan, E.K., N. Pouliot, K.L. Stanley, J. Chia, J.M. Moseley, D.K. Hards, and R.L. Anderson. 2006. Tumor-specific expression of alphavbeta3 integrin promotes spontaneous metastasis of breast cancer to bone. *Breast Cancer Res*. 8:R20.
19. Aslakson, C.J., and F.R. Miller. 1992. Selective events in the metastatic process defined by analysis of the sequential dissemination of subpopulations of a mouse mammary tumor. *Cancer Res*. 52:1399-405.
20. Sodunke, T.R., K.K. Turner, S.A. Caldwell, K.W. McBride, M.J. Reginato, and H.M. Noh. 2007. Micropatterns of Matrigel for three-dimensional epithelial cultures. *Biomaterials*. 28:4006-16.
21. Putnam, A.J., J.J. Cunningham, B.B. Pillemer, and D.J. Mooney. 2003. External mechanical strain regulates membrane targeting of Rho GTPases by controlling microtubule assembly. *Am J Physiol Cell Physiol*. 284:C627-39.
22. Lou, Y., O. Preobrazhenska, U. auf dem Keller, M. Sutcliffe, L. Barclay, P.C. McDonald, C. Roskelley, C.M. Overall, and S. Dedhar. 2008. Epithelial-mesenchymal transition (EMT) is not sufficient for spontaneous murine breast cancer metastasis. *Dev Dyn*. 237:2755-68.
23. Hazan, R.B., G.R. Phillips, R.F. Qiao, L. Norton, and S.A. Aaronson. 2000. Exogenous expression of N-cadherin in breast cancer cells induces cell migration, invasion, and metastasis. *J Cell Biol*. 148:779-90.
24. Mourgeon, E., J. Xu, A.K. Tanswell, M. Liu, and M. Post. 1999. Mechanical strain-induced posttranscriptional regulation of fibronectin production in fetal lung cells. *Am J Physiol*. 277:L142-9.
25. Li, S., P. Butler, Y. Wang, Y. Hu, D.C. Han, S. Usami, J.L. Guan, and S. Chien. 2002. The role of the dynamics of focal adhesion kinase in the mechanotaxis of endothelial cells. *Proc Natl Acad Sci U S A*. 99:3546-51.
26. Hagerman, E.M., S.H. Chao, J.C. Dunn, and B.M. Wu. 2006. Surface modification and initial adhesion events for intestinal epithelial cells. *J Biomed Mater Res A*. 76:272-8.
27. Galbraith, C.G., K.M. Yamada, and M.P. Sheetz. 2002. The relationship between force and focal complex development. *J Cell Biol*. 159:695-705.
28. Steketee, M., K. Balazovich, and K.W. Tosney. 2001. Filopodial initiation and a novel filament-organizing center, the focal ring. *Mol Biol Cell*. 12:2378-95.
29. Ruoslahti, E. 1996. RGD and other recognition sequences for integrins. *Annu Rev Cell Dev Biol*. 12:697-715.
30. Oharazawa, H., N. Ibaraki, K. Ohara, and V.N. Reddy. 2005. Inhibitory effects of Arg-Gly-Asp (RGD) peptide on cell attachment and migration in a human lens epithelial cell line. *Ophthalmic Res*. 37:191-6.
31. Cukierman, E., R. Pankov, D.R. Stevens, and K.M. Yamada. 2001. Taking cell-matrix adhesions to the third dimension. *Science*. 294:1708-12.

32. Chrzanowska-Wodnicka, M., and K. Burridge. 1996. Rho-stimulated contractility drives the formation of stress fibers and focal adhesions. *J Cell Biol*. 133:1403-15.
33. Ridley, A.J., and A. Hall. 1992. The small GTP-binding protein rho regulates the assembly of focal adhesions and actin stress fibers in response to growth factors. *Cell*. 70:389-99.
34. Ulrich, T.A., E.M. de Juan Pardo, and S. Kumar. 2009. The Mechanical Rigidity of the Extracellular Matrix Regulates the Structure, Motility, and Proliferation of Glioma Cells. *Cancer Res*. 69:4167-4174.
35. Nelson, C.M., R.P. Jean, J.L. Tan, W.F. Liu, N.J. Sniadecki, A.A. Spector, and C.S. Chen. 2005. Emergent patterns of growth controlled by multicellular form and mechanics. *Proc Natl Acad Sci U S A*. 102:11594-9.
36. Kovacs, M., J. Toth, C. Hetenyi, A. Malnasi-Csizmadia, and J.R. Sellers. 2004. Mechanism of blebbistatin inhibition of myosin II. *J Biol Chem*. 279:35557-63.
37. Riveline, D., E. Zamir, N.Q. Balaban, U.S. Schwarz, T. Ishizaki, S. Narumiya, Z. Kam, B. Geiger, and A.D. Bershadsky. 2001. Focal contacts as mechanosensors: externally applied local mechanical force induces growth of focal contacts by an mDia1-dependent and ROCK-independent mechanism. *J Cell Biol*. 153:1175-86.
38. Bershadsky, A.D., N.Q. Balaban, and B. Geiger. 2003. Adhesion-dependent cell mechanosensitivity. *Annu Rev Cell Dev Biol*. 19:677-95.
39. Schwartz, M.A., and D.W. DeSimone. 2008. Cell adhesion receptors in mechanotransduction. *Curr Opin Cell Biol*. 20:551-6.
40. Braga, V.M. 2002. Cell-cell adhesion and signalling. *Curr Opin Cell Biol*. 14:546-56.
41. Shewan, A.M., M. Maddugoda, A. Kraemer, S.J. Stehbens, S. Verma, E.M. Kovacs, and A.S. Yap. 2005. Myosin 2 is a key Rho kinase target necessary for the local concentration of E-cadherin at cell-cell contacts. *Mol Biol Cell*. 16:4531-42.
42. Behrens, J., M.M. Mareel, F.M. Van Roy, and W. Birchmeier. 1989. Dissecting tumor cell invasion: epithelial cells acquire invasive properties after the loss of uvomorulin-mediated cell-cell adhesion. *J Cell Biol*. 108:2435-47.
43. Hirohashi, S. 1998. Inactivation of the E-cadherin-mediated cell adhesion system in human cancers. *Am J Pathol*. 153:333-9.
44. Mareel, M.M., J. Behrens, W. Birchmeier, G.K. De Bruyne, K. Vleminckx, A. Hoogewijs, W.C. Fiers, and F.M. Van Roy. 1991. Down-regulation of E-cadherin expression in Madin Darby canine kidney (MDCK) cells inside tumors of nude mice. *Int J Cancer*. 47:922-8.
45. Vleminckx, K., L. Vakaet, Jr., M. Mareel, W. Fiers, and F. van Roy. 1991. Genetic manipulation of E-cadherin expression by epithelial tumor cells reveals an invasion suppressor role. *Cell*. 66:107-19.
46. Bershadsky, A., M. Kozlov, and B. Geiger. 2006. Adhesion-mediated mechanosensitivity: a time to experiment, and a time to theorize. *Curr Opin Cell Biol*. 18:472-81.
47. Thamilselvan, V., and M.D. Basson. 2004. Pressure activates colon cancer cell adhesion by inside-out focal adhesion complex and actin cytoskeletal signaling. *Gastroenterology*. 126:8-18.

48. Downey, C., K. Alwan, V. Thamilselvan, L. Zhang, Y. Jiang, A.K. Rishi, and M.D. Basson. 2006. Pressure stimulates breast cancer cell adhesion independently of cell cycle and apoptosis regulatory protein (CARP)-1 regulation of focal adhesion kinase. *Am J Surg*. 192:631-5.
49. Downey, C., D.H. Craig, and M.D. Basson. 2008. Pressure activates colon cancer cell adhesion via paxillin phosphorylation, Crk, Cas, and Rac1. *Cell Mol Life Sci*. 65:1446-57.
50. Basson, M.D., C.F. Yu, O. Herden-Kirchoff, M. Ellermeier, M.A. Sanders, R.C. Merrell, and B.E. Sumpio. 2000. Effects of increased ambient pressure on colon cancer cell adhesion. *J Cell Biochem*. 78:47-61.
51. Butcher, D.T., T. Alliston, and V.M. Weaver. 2009. A tense situation: forcing tumour progression. *Nat Rev Cancer*. 9:108-22.
52. Ingber, D.E. 2008. Tensegrity and mechanotransduction. *J Bodyw Mov Ther*. 12:198-200.
53. Ingber, D.E. 2003. Tensegrity I. Cell structure and hierarchical systems biology. *J Cell Sci*. 116:1157-73.
54. Ingber, D.E. 1997. Tensegrity: the architectural basis of cellular mechanotransduction. *Annu Rev Physiol*. 59:575-99.
55. DiMilla, P.A., J.A. Stone, J.A. Quinn, S.M. Albelda, and D.A. Lauffenburger. 1993. Maximal migration of human smooth muscle cells on fibronectin and type IV collagen occurs at an intermediate attachment strength. *J Cell Biol*. 122:729-37.
56. Palecek, S.P., J.C. Loftus, M.H. Ginsberg, D.A. Lauffenburger, and A.F. Horwitz. 1997. Integrin-ligand binding properties govern cell migration speed through cell-substratum adhesiveness. *Nature*. 385:537-40.
57. Halliday, N.L., and J.J. Tomasek. 1995. Mechanical properties of the extracellular matrix influence fibronectin fibril assembly in vitro. *Exp Cell Res*. 217:109-17.
58. Pankov, R., E. Cukierman, B.Z. Katz, K. Matsumoto, D.C. Lin, S. Lin, C. Hahn, and K.M. Yamada. 2000. Integrin dynamics and matrix assembly: tensin-dependent translocation of alpha(5)beta(1) integrins promotes early fibronectin fibrillogenesis. *J Cell Biol*. 148:1075-90.
59. Zhong, C., M. Chrzanowska-Wodnicka, J. Brown, A. Shaub, A.M. Belkin, and K. Burridge. 1998. Rho-mediated Contractility Exposes a Cryptic Site in Fibronectin and Induces Fibronectin Matrix Assembly. *J. Cell Biol.* 141:539-551.
60. Wu, C., V.M. Keivens, T.E. O'Toole, J.A. McDonald, and M.H. Ginsberg. 1995. Integrin activation and cytoskeletal interaction are essential for the assembly of a fibronectin matrix. *Cell*. 83:715-24.
61. Schwartz, M.A. 2009. Cell biology. The force is with us. *Science*. 323:588-9.
62. Balaban, N.Q., U.S. Schwarz, D. Riveline, P. Goichberg, G. Tzur, I. Sabanay, D. Mahalu, S. Safran, A. Bershadsky, L. Addadi, and B. Geiger. 2001. Force and focal adhesion assembly: a close relationship studied using elastic micropatterned substrates. *Nat Cell Biol*. 3:466-72.
63. Beningo, K.A., M. Dembo, I. Kaverina, J.V. Small, and Y.L. Wang. 2001. Nascent focal adhesions are responsible for the generation of strong propulsive forces in migrating fibroblasts. *J Cell Biol*. 153:881-8.

64. Galbraith, C.G., and M.P. Sheetz. 1997. A micromachined device provides a new bend on fibroblast traction forces. *Proc Natl Acad Sci U S A*. 94:9114-8.
65. Harris, A.K., P. Wild, and D. Stopak. 1980. Silicone rubber substrata: a new wrinkle in the study of cell locomotion. *Science*. 208:177-9.
66. Geiger, B., A. Bershadsky, R. Pankov, and K.M. Yamada. 2001. Transmembrane crosstalk between the extracellular matrix--cytoskeleton crosstalk. *Nat Rev Mol Cell Biol*. 2:793-805.
67. Hynes, R.O., and A.T. Destree. 1978. Relationships between fibronectin (LETS protein) and actin. *Cell*. 15:875-86.
68. Burridge, K., and J.R. Feramisco. 1980. Microinjection and localization of a 130K protein in living fibroblasts: a relationship to actin and fibronectin. *Cell*. 19:587-95.
69. Zamir, E., B.Z. Katz, S. Aota, K.M. Yamada, B. Geiger, and Z. Kam. 1999. Molecular diversity of cell-matrix adhesions. *J Cell Sci*. 112 (Pt 11):1655-69.
70. Katz, B.Z., E. Zamir, A. Bershadsky, Z. Kam, K.M. Yamada, and B. Geiger. 2000. Physical state of the extracellular matrix regulates the structure and molecular composition of cell-matrix adhesions. *Mol Biol Cell*. 11:1047-60.
71. Li, C., F. Wernig, M. Leitges, Y. Hu, and Q. Xu. 2003. Mechanical stress-activated PKCdelta regulates smooth muscle cell migration. *FASEB J*. 17:2106-8.
72. Ilic, D., Y. Furuta, S. Kanazawa, N. Takeda, K. Sobue, N. Nakatsuji, S. Nomura, J. Fujimoto, M. Okada, and T. Yamamoto. 1995. Reduced cell motility and enhanced focal adhesion contact formation in cells from FAK-deficient mice. *Nature*. 377:539-44.
73. Owen, J.D., P.J. Ruest, D.W. Fry, and S.K. Hanks. 1999. Induced focal adhesion kinase (FAK) expression in FAK-null cells enhances cell spreading and migration requiring both auto- and activation loop phosphorylation sites and inhibits adhesion-dependent tyrosine phosphorylation of Pyk2. *Mol Cell Biol*. 19:4806-18.
74. Parsons, J.T., K.H. Martin, J.K. Slack, J.M. Taylor, and S.A. Weed. 2000. Focal adhesion kinase: a regulator of focal adhesion dynamics and cell movement. *Oncogene*. 19:5606-13.
75. Huang, C., Z. Rajfur, C. Borchers, M.D. Schaller, and K. Jacobson. 2003. JNK phosphorylates paxillin and regulates cell migration. *Nature*. 424:219-23.
76. Crowe, D.L., and A. Ohannessian. 2004. Recruitment of focal adhesion kinase and paxillin to beta1 integrin promotes cancer cell migration via mitogen activated protein kinase activation. *BMC Cancer*. 4:18.
77. Keely, P., L. Parise, and R. Juliano. 1998. Integrins and GTPases in tumour cell growth, motility and invasion. *Trends Cell Biol*. 8:101-6.
78. Guo, W., and F.G. Giancotti. 2004. Integrin signalling during tumour progression. *Nat Rev Mol Cell Biol*. 5:816-26.
79. Moissoglu, K., and M.A. Schwartz. 2006. Integrin signalling in directed cell migration. *Biol Cell*. 98:547-55.
80. Yano, H., Y. Mazaki, K. Kurokawa, S.K. Hanks, M. Matsuda, and H. Sabe. 2004. Roles played by a subset of integrin signaling molecules in cadherin-based cell-cell adhesion. *J Cell Biol*. 166:283-95.

81. Dumbauld, D.W., K.E. Michael, S.K. Hanks, and A.J. Garcia. 2009. Focal adhesion kinase-dependent regulation of adhesive force involves vinculin recruitment to focal adhesions. *Biol Cell*.
82. Michael, K.E., D.W. Dumbauld, K.L. Burns, S.K. Hanks, and A.J. Garcia. 2009. Focal adhesion kinase modulates cell adhesion strengthening via integrin activation. *Mol Biol Cell*. 20:2508-19.
83. Ridley, A.J., M.A. Schwartz, K. Burridge, R.A. Firtel, M.H. Ginsberg, G. Borisy, J.T. Parsons, and A.R. Horwitz. 2003. Cell migration: integrating signals from front to back. *Science*. 302:1704-9.
84. Muller, A., B. Homey, H. Soto, N. Ge, D. Catron, M.E. Buchanan, T. McClanahan, E. Murphy, W. Yuan, S.N. Wagner, J.L. Barrera, A. Mohar, E. Verastegui, and A. Zlotnik. 2001. Involvement of chemokine receptors in breast cancer metastasis. *Nature*. 410:50-6.
85. Langrana, N.A., H. Alexander, I. Strauchler, A. Mehta, and J. Ricci. 1983. Effect of mechanical load in wound healing. *Ann Plast Surg*. 10:200-8.
86. Martin, R.B., S.T. Lau, P.V. Mathews, V.A. Gibson, and S.M. Stover. 1996. Collagen fiber organization is related to mechanical properties and remodeling in equine bone. A comparison of two methods. *J Biomech*. 29:1515-21.
87. Tanne, K., T. Nagataki, S. Matsubara, J. Kato, Y. Terada, T. Sibaguchi, E. Tanaka, and M. Sakuda. 1990. Association between mechanical stress and bone remodeling. *J Osaka Univ Dent Sch*. 30:64-71.
88. Luu, Y.K., E. Capilla, C.J. Rosen, V. Gilsanz, J.E. Pessin, S. Judex, and C.T. Rubin. 2009. Mechanical stimulation of mesenchymal stem cell proliferation and differentiation promotes osteogenesis while preventing dietary-induced obesity. *J Bone Miner Res*. 24:50-61.

Chapter 5: A stochastic model of coordinated cell migration

Introduction

Collective cell migration is relevant for many processes in morphogenesis, tissue repair, and cancer invasion and metastasis. This mode of migration is different from single cell migration in that cells remain physically and functionally connected during movement and the cell cohort polarizes into "leader" cells that guide "followers" at their rear [1,2].

Different *in vitro* experimental models have been used for the study of collective migration mechanism. One of the common one is the 2D scratch-wound assay, which allows polarization and protrusions, force generation and mechanisms of cell-cell coadhesion to be studied during the movement of cell monolayer[3-5]. Existing continuum mathematical models of scratch wound assay are generally based on reaction-diffusion equations. Specifically, Fisher equation – a nonlinear parabolic partial differential equation - has been prevalently used to account for constant diffusive migration (random cell motility) in one spatial dimension and proliferation described by logistic growth [6-8].

$\frac{dn}{dt} = D\frac{d^2n}{dx^2} + \alpha n(1 - \frac{n}{n_0}),$ where n (x, t) is the cell density at time t at a given distance x from the wound edge, α is the proliferation rate of a cell and n_o is the initial cell density. The Fisher equation models the cell moving front exhibited by the cell population.

While the continuum approaches describe population-scale properties, important insights into cell-scale properties can be gained by examination of the behavior of individual migrating cells using discrete models such as cellular automata (CA)[3,9-11]. Cellular automata can be constructed on square, triangular or hexagonal grids. Each grid site is occupied by only one cell

and the simulated cells modify their behavior according to environmental variables and pre-programmed rules. In these CA models, each cell is considered as a homogenous object. However, a migrating cell is indeed a highly polarized cell with protrusions formed at the leading edge but retraction at the rear. Its cell periphery can experience different interactions such as cell-cell coadhesion or cell-open space interface, depending on the local microenvironment. Yet no discrete models are currently available to simulate the molecular steps of migration: polarization and protrusions, adhesion and rear retraction.

In Chapter 3, we have shown that free-cell perimeter influences formation of leader cells. We postulated that in the uncompressed cultures, the process of leader-cell formation depends on the geometry of the cell-neighbor contact and the extent of free-cell perimeter; but applied compression increases free-cell perimeter due to compression-induced cell distension, thereby promoting leader-cell formation. To test the hypothesis that dynamic coordination of free-cell perimeter (controlling the formation of protrusions) and cell-cell interactions determines cell migration behavior, we developed a preliminary stochastic model to simulate 2-dimensional collective migration of cells. The model simulations suggest that (1) cell distension could induce leader-cell formation; (2) induction of initial cell protrusions by compression may not be sufficient to explain enhanced coordinated cell migration; and (3) compression could induce constant, FCP-independent cell migration rate. This model provides us with insights into the physical underpinnings governing the collective migration induced by compressive stress.

Model development

Cell creation – model initialization

In the model, we first created a grid composed of 100-by-100 blocks, which provides a domain for initial cell placement and simulation of cell movement. Before introducing cells to the grid, we created a mask to define the initial geometry and size of the muticellular pattern such as squares or rosettes used in the micro-contact printing experiments (Chapter 3). In this study, we created on the grid surface a square mask containing 15 x 15 (a total of 225) blocks. We then introduced cells to the square mask without any cell overlap. Each single cell is assigned with a color and is initially composed of 3x3 (a total of 9) blocks (Fig. 5.1). The number and arrangement of the blocks within the cell reflect its overall size and shape, respectively.

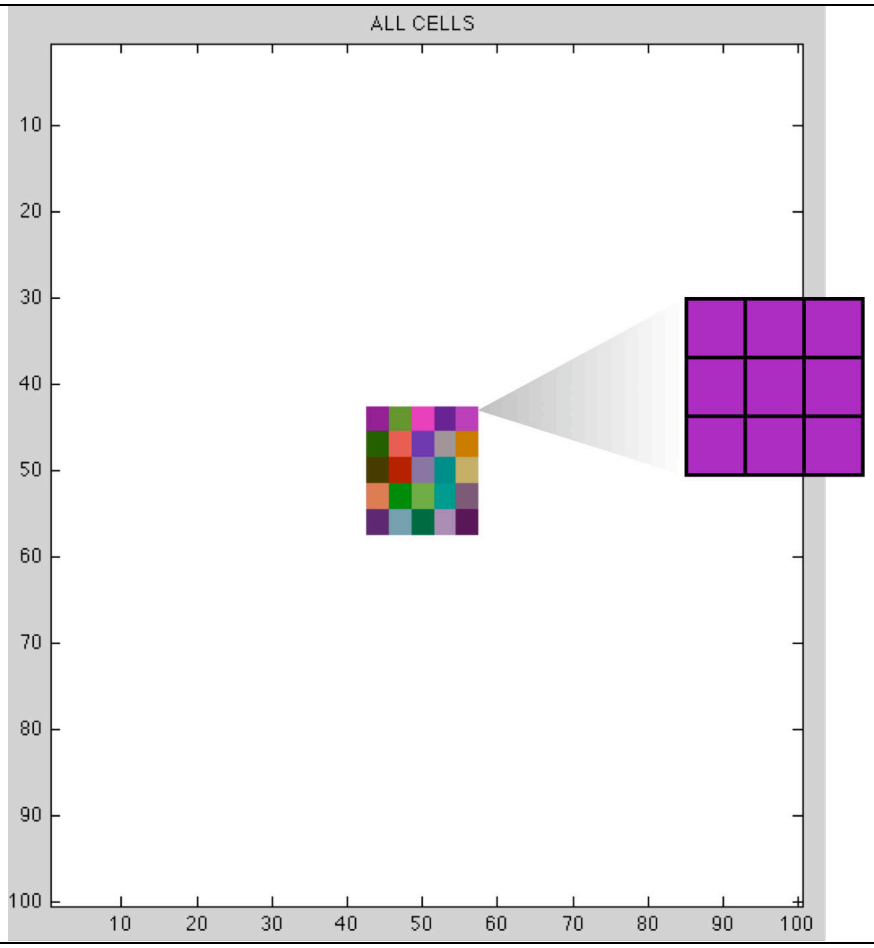

Figure 5.1. Assignment of cells to the defined square pattern on the grid surface. Each square-shaped cell is colored-coded for easy visualization and

tracking during movement and each cell initially consists of 3x3 (a total of 9) squares.

There is a set of key parameters to describe the state of each cell. The parameters (with definitions) are tabulated in Table 5.1.

Parameter	**Definition**
Cell ID	A numerical integer assigned to each cell
Cell type	An original cell or a daughter cell after proliferation
Cell location	Defined by a n-by-n zero matrix filled with 1 for the locations occupied by the cell
Cell-cell contact	The portion of cell perimeter in contact with other neighboring cells
Free-cell perimeter	The portion of cell perimeter not associated with neighboring cells, open to free space
Cell frontal length	The longest length measured from the center of mass to the tip of the cell.
Cell size	Number of squares on the grid occupied by the cells

Table 5.1: Key parameters for the cell state

Overview of the simulation

After model initialization, all cells will be selected in a random order at each time step to perform *only one* of the four actions below: (The rules for each process are described in details later.)

(1) Cell proliferation: A daughter cell will be split from the original cell. We assumed that current-migrating cells will not proliferate. If the cell has already proliferated during the current time step, then cell movement (protrusions and translocation) is aborted [12].

(2) Cell protrusion/spreading: The cell protrudes at the leading edge without rear retraction until the cell doubles in size (i.e. the maximum size set by the user) (Fig. 5.2). We assumed that (i) protrusions are stabilized by adhesions, and (ii) each protrusion generates a protrusive force measured from the tip of the protrusion to the center of mass of the cell.

(3) Cell translocation: When a cell reaches its maximum size, the cell starts to move forward. To do this, the cell protrudes at the leading edge, and then retracts at its rear (Fig. 5.3). We assumed that (i) a cell starts to translocate only when the cell spreads to its maximum size, because we speculated that sufficient tensional force generated during protrusion is required to release adhesions at the cell rear; and (ii) the rear retraction rate is same as the front protruding rate during cell translocation.

(4) No operation: The cell neither proliferates nor moves. If the cell does not fulfill the requirements for cell proliferation, it can perform either no action or protrude/spread or translocate (with an assigned probability). See Appendix D for the effect of the action probability on the simulation outcome.

The simulation result is saved as a cell-migration snapshot at the end of each time step. After all the time steps are performed, a Quick-Time movie of cell migration is generated.

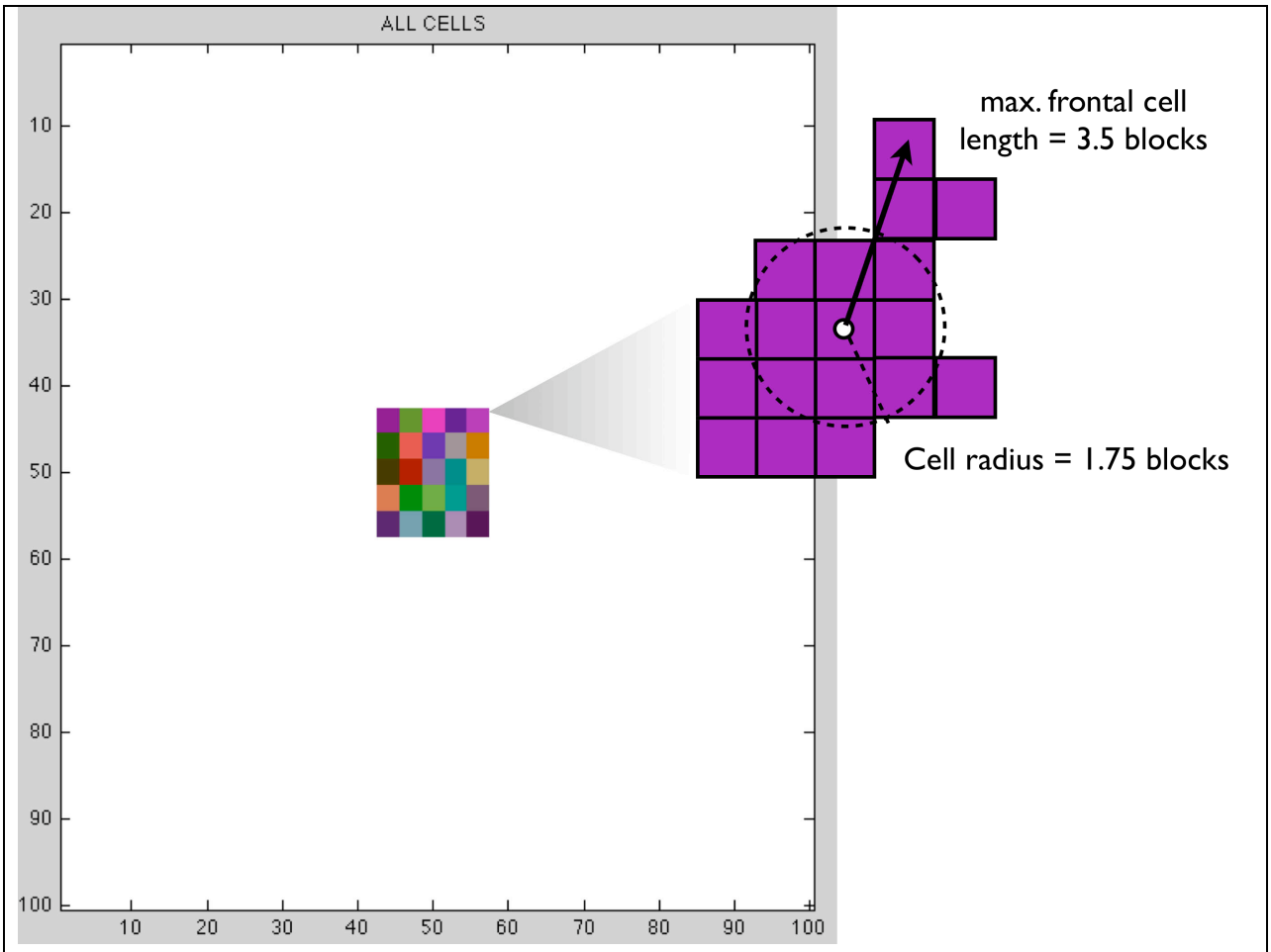

Figure 5.2. The cell protrudes at its leading edge without rear retraction until it doubles in size. During cell protrusion/spreading, block addition is performed at the leading edge of the cell until the cell reaches its maximum size (18 blocks). To maintain cell shape, block addition has to comply with these 2 rules: (1) cell core with a radius of 1.75 blocks is filled; and (2) maximum cell frontal length = 3.5 blocks.

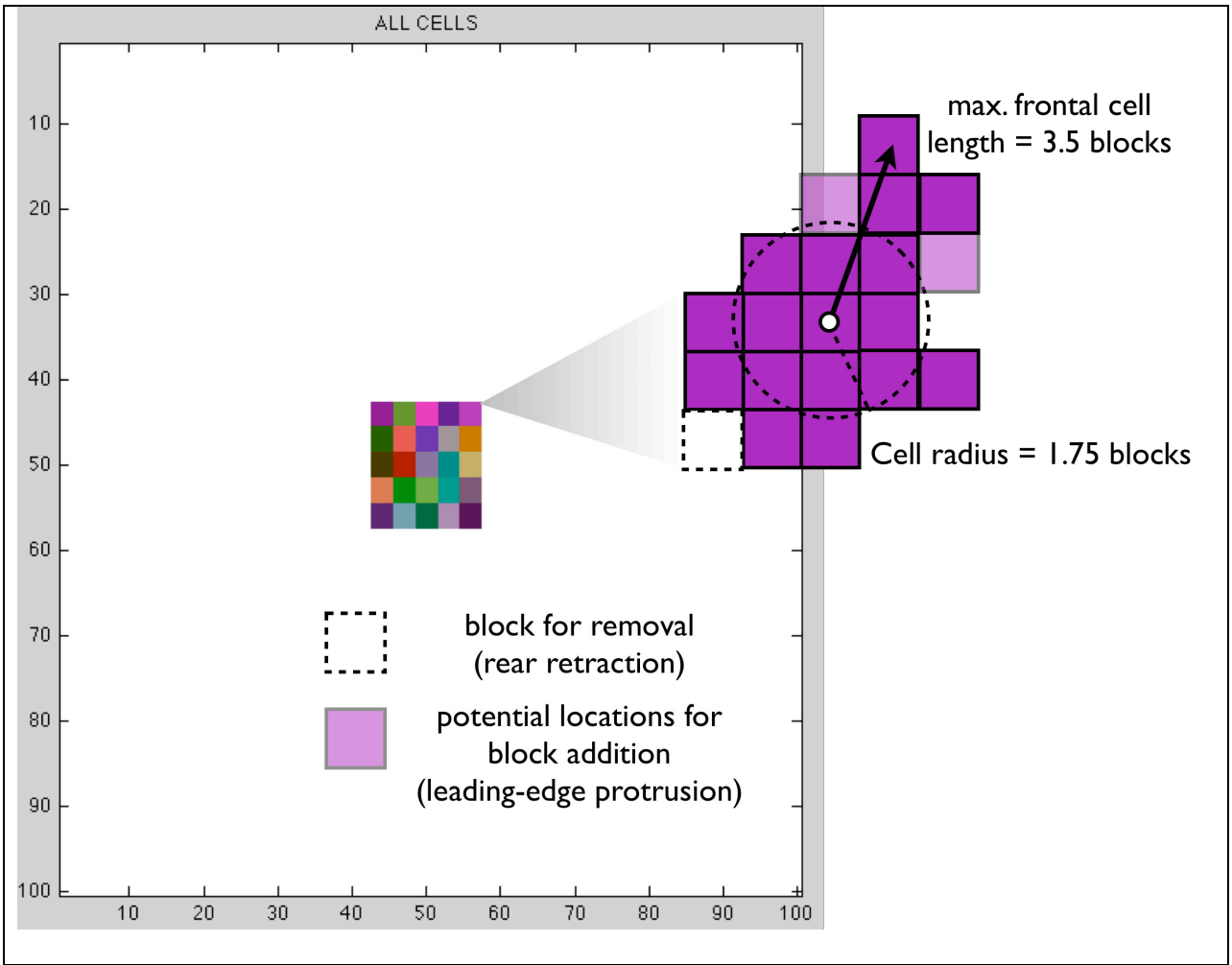

Figure 5.3. The cell protrudes at its leading edge and then retracts at the rear. During cell translocation, block addition (cell protrusion) and removal (cell retraction) are performed at the leading edge and rear of the cell, respectively. The specific rules are described in *Cellular process (I): Cell protrusion/spreading* and *Cellular process (II): Cell translocation*.

Cellular process (I): Cell protrusion/spreading

Before a cell detaches its rear from neighboring cells for cell translocation to occur, the cell will protrude and extend forward. To simulate the cell protrusion/extension, additional blocks will be added to the leading front of the cell (i.e. the cell will occupy additional squares on the grid) in the direction of migration until the maximum cell size allowed is reached.

From our time-lapse experiments (Fig. 2.8A), we observed that the leading cells at the edge of the "wound", whether they were compressed or not, migrated toward open area, suggesting that they moved toward the less populated area (*density gradient*). The leading cells also appeared to remain connected with neighboring cells and applied a *"pulling force"* on them [13]. At the same time, due to inherent cellular contractile motions, the neighboring cells could also exert a *"movement-impeding force"* on the leading cells through the cell-cell contacts. In addition, from the square micropatterning experiments (Fig. 3.5), the corner cells on the square pattern in the uncompressed cultures migrated forward more readily than the edge cells. That the corner cells have more free-cell perimeter than the edge cells suggests that the free-cell perimeter affecting the rate of cell protrusion (and hence *protrusive force*) could regulate the cell migration. Hence, for each single cell, the direction of migration $\vec{F}$ is governed by the directions of both the density gradient ∇D and the resultant force unit vector $\vec{f}_i$ calculated from a force balance comprising the three forces (protrusive, movement-impeding and pulling), which will be described further later. Applying a different weight factor w_i to each force vector $\vec{f}_i$ or ∇D controls the relative importance of each factor in determining the direction of cell migration.

$$\vec{F} = c\sum w_i \cdot \vec{f}_i + w_d \cdot \nabla D \qquad \text{Equation (1)}$$

where $w_{protrusive}$ = 1 + 0.1 * longest protrusive length

$w_{mvt-impeding}$ = 0.3 if # edges in contact with neighboring cell < 9, or else = 1

$w_{pulling}$ = 2

w_d = free-cell perimeter/ total cell perimeter

$c = 1$

The relative coefficients of each force contribution w_i were estimated by trial and error, but with rationale. In our model, there are three different forces acting on one cell: (1) positive pulling force from a moving cell, (2) protrusive force from its own self, and (3) movement-impeding force exerted by another neighboring cell via cell-cell contact. During collective migration, leader cells guide the cell cohort to move forward. Therefore, the effect of cell-cell contact force ($w_{mvt-impeding}$) was assumed to be the least among the three forces or the cell cohort would retract backward. Meanwhile, as the leading (moving) cells can direct the movement of others, the impact of the positive pulling force contributed by migrating cells was assumed to dominate over the other two forces. Thus, its coefficient value ($w_{pulling}$) is larger than that of the other two forces. As for the protrusive force, it is always present in migratory cells. Therefore, the minimum value of its coefficient ($w_{protrusive}$) is 1. However, its value also increases with protrusion length because force is generated from actin polymerization during protrusion [14]. To avoid the value of $w_{protrusive}$ from getting larger than that of $w_{pulling}$, the protrusion length is scaled down by a factor of 0.1. Lastly, cells with free edges generally migrate toward less-dense area. Therefore, the coefficient of its likelihood (w_d) is proportional to fraction of free-cell perimeter.

To determine the density gradient ∇D, the Matlab built-in gradient function is used. At the beginning of each time point, the whole grid is divided into equal partitions containing multiple squares. The cell density of each partition is determined by summing all the squares occupied by cells and then is stored in a new matrix. Applying the gradient function to this new matrix will provide a vector map representing spatial distribution of the cells. Thus, at each cell location, the

direction pointing toward the least-dense area is determined for the preferred course of cell movement

However, the density gradient is not the only factor controlling the direction of cell migration because there are cell-cell interactions. Therefore, we also performed a force balance including the three forces shown below (Fig. 5.4): (Each of the resultant force vector is normalized to a unit vector.)

1. Protrusive force – this force promoting forward cell movement is generated from protrusions by the cell itself. At t=0, the possible number of protrusions formed is proportional to the free-cell perimeter of the cell (for the uncompressed case). At t>0, the direction of the protrusive force is governed by the shift in direction of the center of mass from the previous time point.
2. "Movement-impeding" force – this cell migration-impeding force comes from any neighboring cell, which shares the same cell perimeter with the target cell. To find the resultant direction of this force, all the vectors originating from the center of mass of the target cell to its edge sharing with other neighboring cells are located and then combined.
3. "Pulling" force – this force comes from any moving cells in contact with the target cell. To determine the resultant direction of such force, all the vectors pointing from the center of mass of the target cell to the center of mass of any migrating cells are located and then combined.

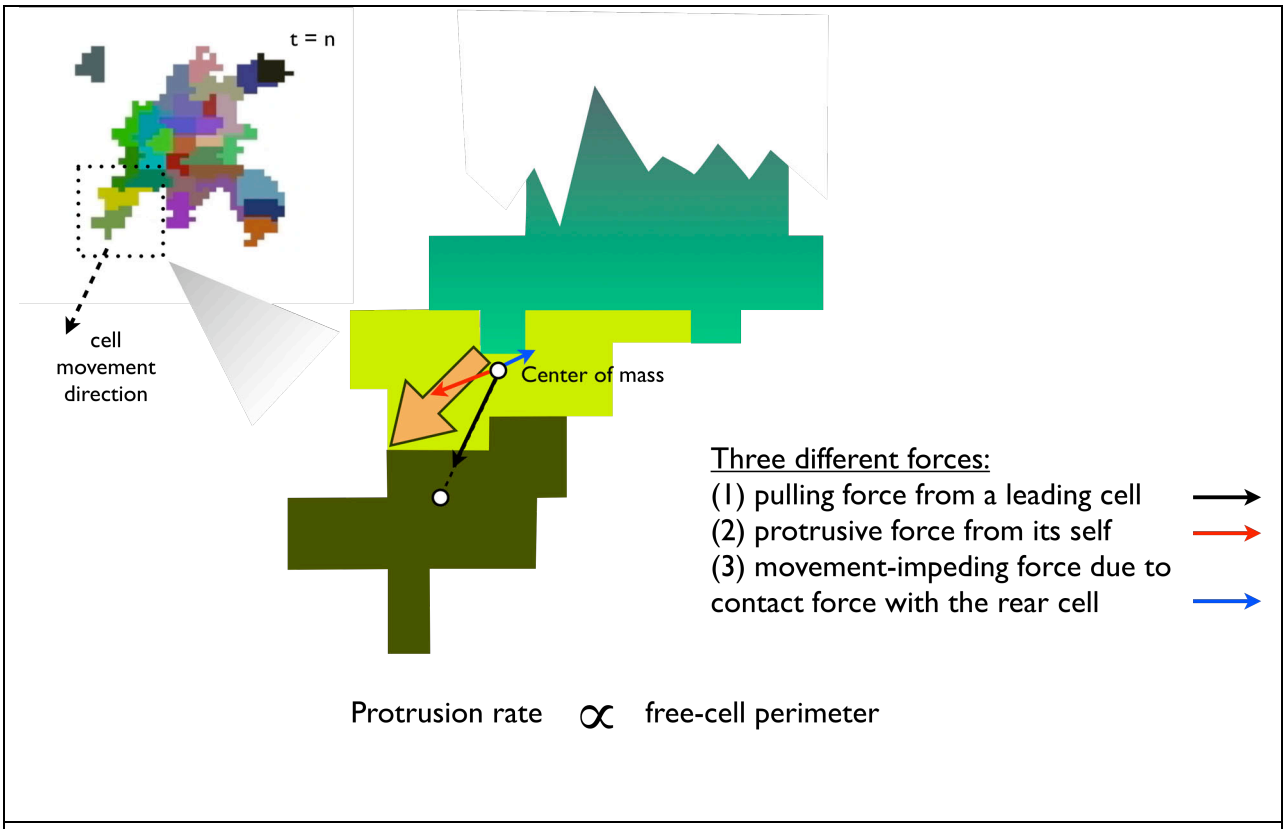

Figure 5.4. Force-body diagram of the cell being modeled. There are three different forces acting on the light-green cell: (1) pulling force from the leading cell; (2) protrusive force from its self; and (3) movement-impeding force due to cell-cell coadhesion with the rear cell. Applying a weight factor w_i to each of these unit force vectors and then combining them all together results in a resultant force vector (orange, thick arrow), of which the direction controls the protrusion direction.

After the direction of migration $\vec{F}$ (equivalent to direction of protrusion) is determined, the protrusion rate, which depends on free cell perimeter, is given by the following:

# of blocks added (protrusion rate) = CEILING (free-cell perimeter x block addition constant), where the block addition constant between 0 and 1 is a user-defined parameter that controls the protrusion rate (and the cell translocation rate described later).

To determine whether the blocks should be added, the following steps are performed:

(1) Check any free-cell perimeter of the cell. No blocks will be added if the cell has no free-cell perimeter. Otherwise, go to step (2).

(2) During block addition, the cell shape has to be maintained.

   a. To avoid the cell from becoming too thin, the blocks will be preferentially added within a region of a defined radius around the center of mass of the cell. If this is satisfied, go to step 2b.

   b. The blocks are added within (+/-) 45 degree-span from the direction of $\vec{F}$ at the protruding end of the cell. However, to avoid any cell over-stretching, the frontal cell length cannot exceed the defined maximum value after block addition.

Cellular process (II): Cell translocation

After the cell reaches the maximum cell size due to protrusion/spreading, the cell starts translocation to the direction of protrusion. For each cell migration cycle, a cell protrudes in the direction of movement, make adhesions, and then retract this rear end[15]. This translocation process is simulated in this model by a coordination of two actions: one block is *removed from the rear end* of the cell (i.e. opposite to the migration direction $\vec{F}$) for every block *added to the protruding end*. The block addition process is performed in the same manner as described in *Cellular process (II): Cell protrusion/spreading*.

Following addition of a single block, a block is selected for removal from the rear end of the cell in the opposite direction of migration. However, the following criteria have to be satisfied:

1. The cell cannot be divided into two parts after the removal of the selected block.
2. In our experiments, we observed that 67NR cells always remained connected with each other during cell movement. Hence, the removal of the selected block in contact with a third-party cell will automatically cause the third-party to take over the space to ensure the cell-cell coadhesion.

Cells can migrate randomly to explore their local environment, or in a particular direction, for example during chemotaxis. In our scratch-wound or micropatterning experiments, the cells can sense the free space created on one side and preferentially migrate to move away from the cell mass. In our model, as the process of cell translocation begins, a persistence time is assigned based on the normal distribution (assumed) of persistence times with a mean value of 2 time steps (1 hr). (The persistence time for epithelial cell migration varies from ~12 mins to ~1 hr [3]). Hence, during persistent migration, the direction of migration will be remained the same. A new direction for $\vec{F}$ will be determined only when the persistent time expires.

Cellular process (III): Cell proliferation

Each cell has the capability to proliferate, provided that the following conditions are satisfied: (1) the cell size reaches a size of 18 squares or above; and (2) the cell is surrounded by neighboring cells, i.e. the free-cell perimeter is equal to 0. (From the time lapse of 67NR migration, more round cells undergoing mitosis were found within the cell sheet.) When these conditions are satisfied, the cell will split into 2 new entities (cells). To determine how the cell is divided, the following steps are performed:

(1) Calculate the aspect ratio of the cell to determine the cell orientation (direction of elongation).
(2) Calculate the center of mass for the cell.
(3) Cut the cell into 2 halves through the center of mass in perpendicular to the direction of cell elongation.

Origin of stochasticity

The coordinated cell migration is modeled as an interrelation of random/probabilistic processes over a period of time. To introduce stochasticity into the model, some indeterminacy in future evolution is described by the following:

(1) an action probability, which allows a cell to perform no action or one of the migration steps (protrusion or translocation) during simulation. The effect of an action probability on the simulation outcomes is described in Appendix D;

(2) normal distribution of persistent time, which provides each cell with a randomized persistent time based on a probabilistic distribution. Thus, some cells display directionally persistent migration more readily than others;

(3) choice of protrusion/translocation direction: although the protrusion direction is initially determined by Equation (1), the selected course of movement can deviate within +/- 45-degrees from the pre-determined direction;

(4) choice of blocks for removal during retraction: a block is randomly selected for removal from a generated list of blocks that have shown to satisfy the requirements for removal described earlier.

This introduced randomness causes temporal changes in cell-cell spatial arrangement and cell

shape, which result in a distinct spatio-temporal pattern of forces on each cell. This in turn affects the cell migration behavior on a longer time scale: some cells are evolved to become leader cells.

Results and Discussions

We first simulated the collective migration of cells initially arranged in a square geometry under stress-free condition (Fig. 5.5), which was the base case (analogous to the experimental control). **In this model, the same set of rules was applied to all cells. There were no pre-assigned leader cells in the model.** Some cells were evolved to act like leader cells during simulation because they had higher extent of free-cell perimeter (e.g corner cells vs. edge cells in a square pattern). Since the number of protrusions is proportional to free-cell perimeter, the corner cells with more free-cell perimeter would proportionally have more protrusions than the edge cells. As a result, the corner cells generated higher tensional stress within cytoskeleton [16] and became leader cells. As the cells remained connected with each other during migration, the leader cells would pull the other cells during locomotion.

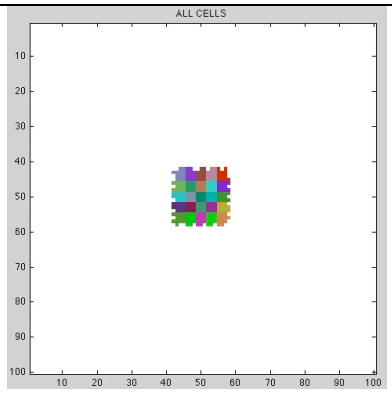

t = 0

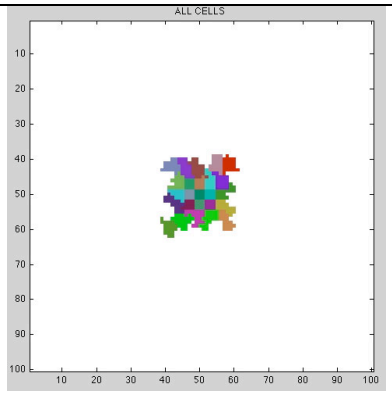

t = 10

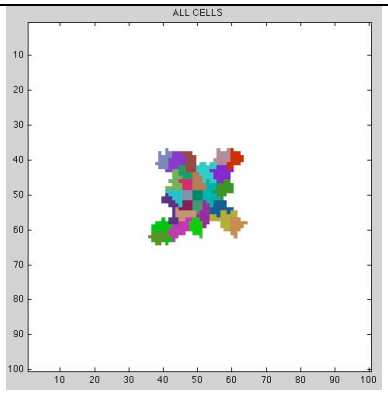

t = 20

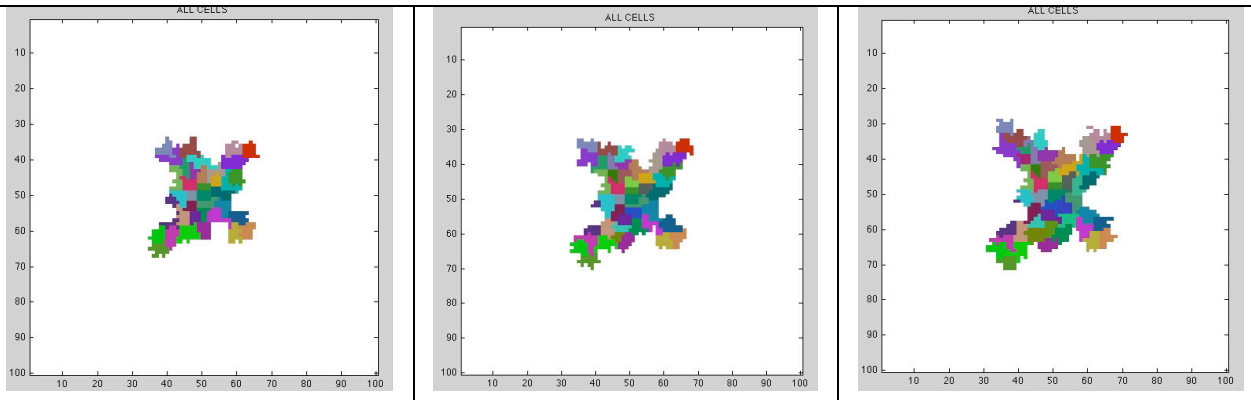

t = 30 t = 40 t = 50

Figure 5.5. Simulation of coordinated migration of cells initially arranged in a square pattern under no stress condition. The migration pattern is similar to the experimental control, where cells preferentially protrude from the corners of the square pattern than from its edges.

From our experimental study, we found that compression-induced coordinated migration of 67NR mammary carcinoma cells was geometry-independent, accompanied by cell distension, enhanced cell-matrix adhesion, increased formation of leader cells and faster migration rate. To determine which model parameter could be affected by compression, we changed one parameter of the control case at a time (Table 5.2) and then compared the resultant cell migration patterns (Figs. 5.6-5.9) with the control case (Fig. 5.5). In addition, the shape change index, which describes the shape distortion of the square pattern due to cell movement (and was previously defined in Chapter 3), was calculated for all the simulated scenarios (Fig. 5.10) and then compared with the experimental values (Fig. 3.5).

Changes in model parameters
(1) Protrusive force is increased by allowing the cell to extend further (i.e. the maximum frontal length allowed is doubled, thereby increasing free cell perimeter). The simulation result is shown in Figure 5.6.
(2) Protrusion/translocation rate is kept constant, independent of free cell perimeter

(FCP). The simulation result is shown in Figure 5.7.
(3) FCP-dependent protrusion/translocation rate is doubled. The simulation result is shown in Figure 5.8.
(4) Number of *initial* protrusions is the same for all cells around the periphery of the square pattern, regardless of initial free cell perimeter. The simulation result is shown in Figure 5.9

Table 5.2: What model parameter could be affected by compression?

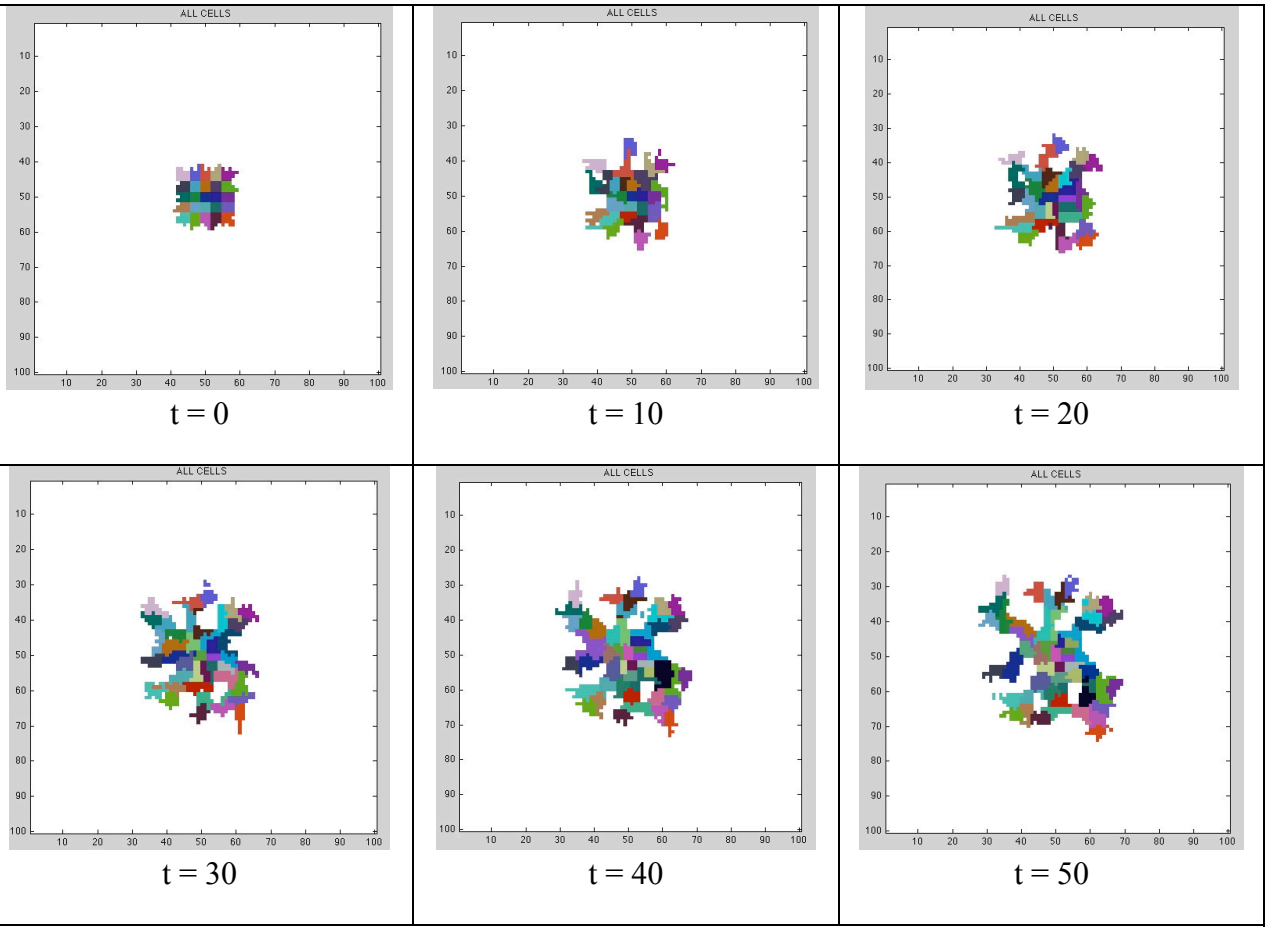

Figure 5.6. Simulation of the base condition (uncompressed case in Fig. 5.5) with the maximum frontal length allowed for each cell being doubled.

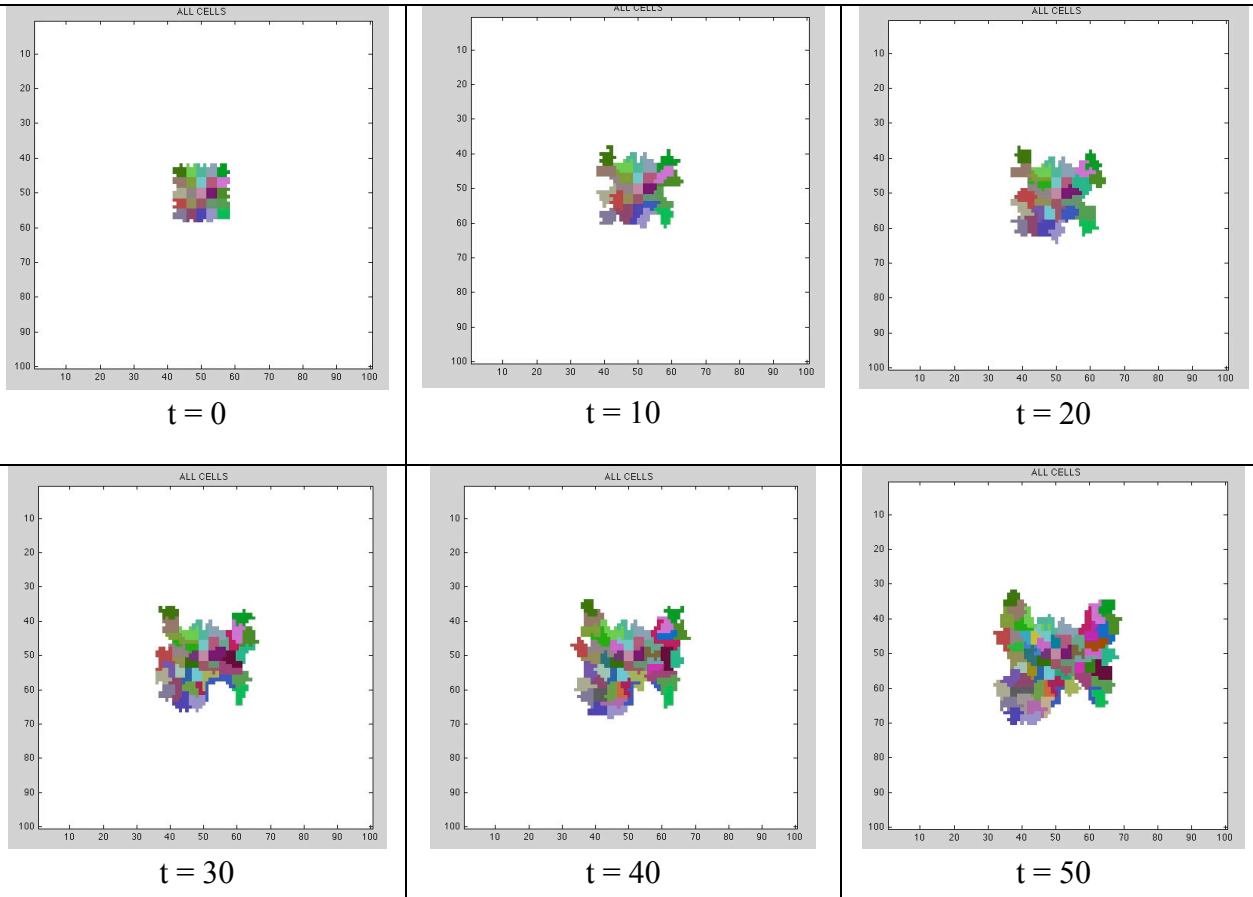

Figure 5.7. Simulation of the base condition (uncompressed case in Fig. 5.5) with the protrusion/migration rate being kept constant, independent of free cell perimeter (FCP).

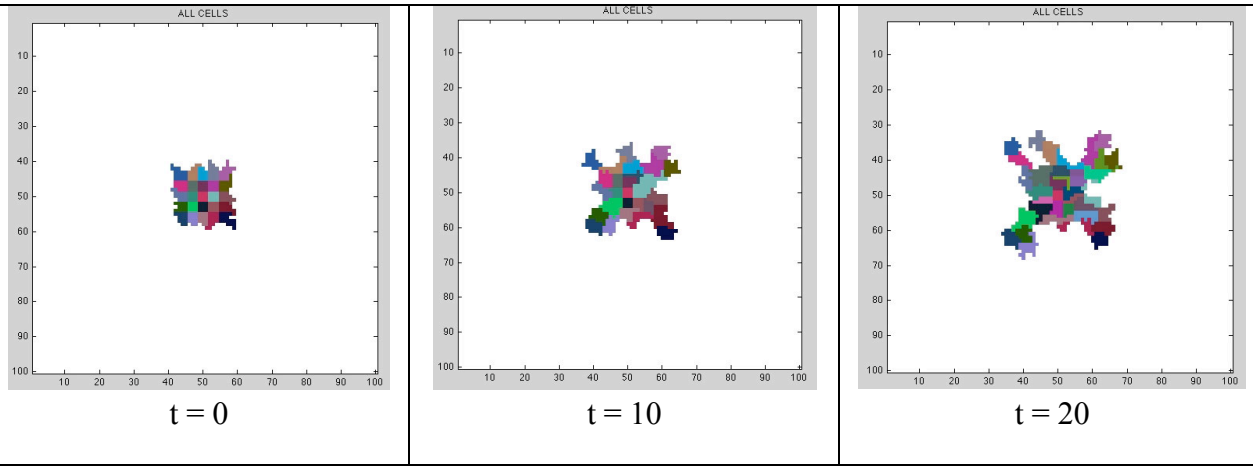

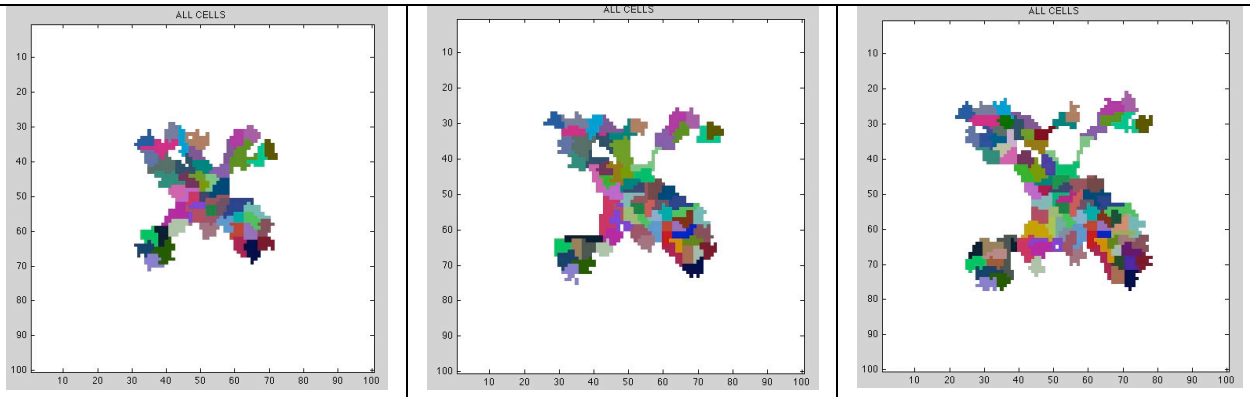

t = 30 t = 40 t = 50

Figure 5.8. Simulation of the base condition (uncompressed case in Fig. 5.5) with the FCP-dependent protrusion/migration rate being doubled.

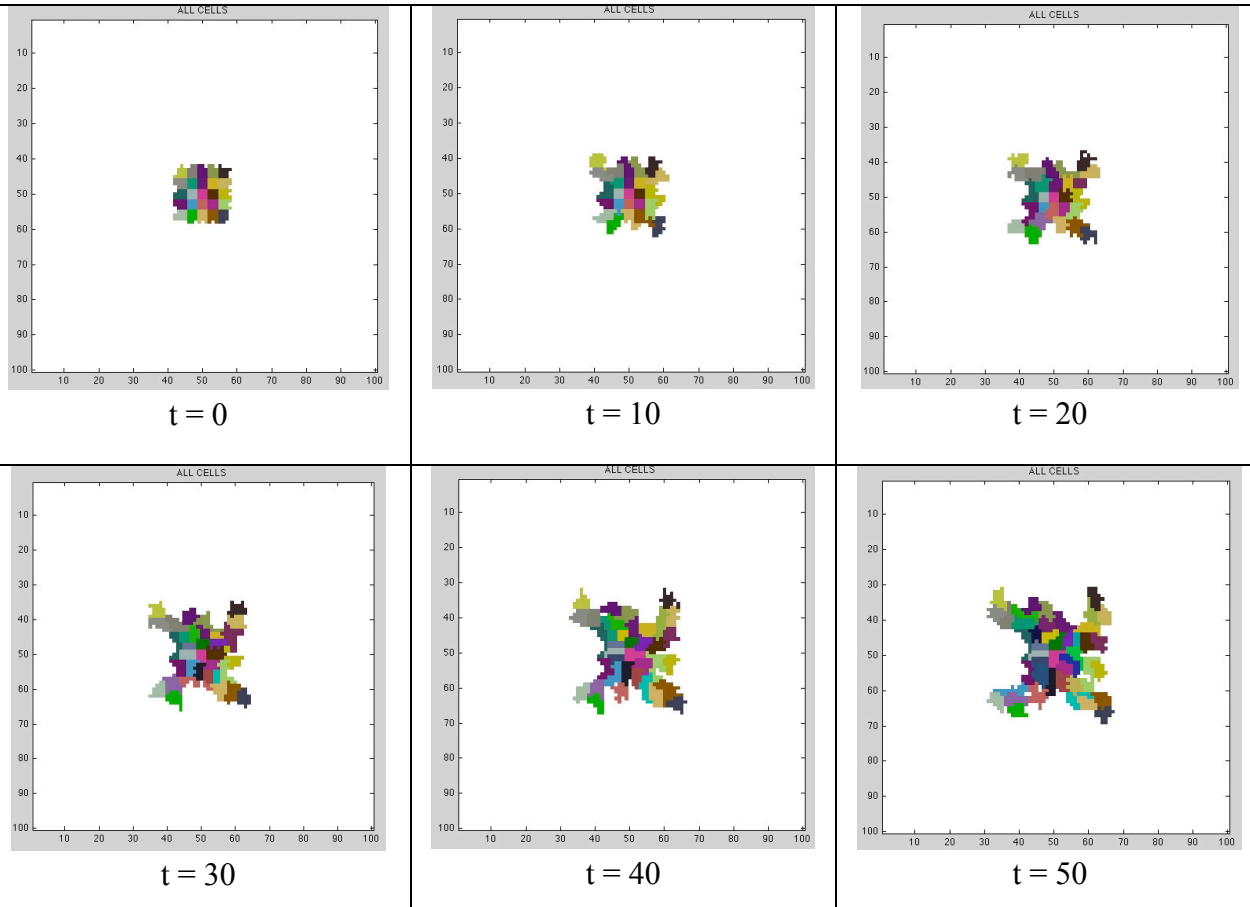

t = 0 t = 10 t = 20

t = 30 t = 40 t = 50

Figure 5.9. Simulation of the base condition (uncompressed case in Fig. 5.5) with the same

number of initial protrusions assigned for all cells around the periphery of the square pattern.

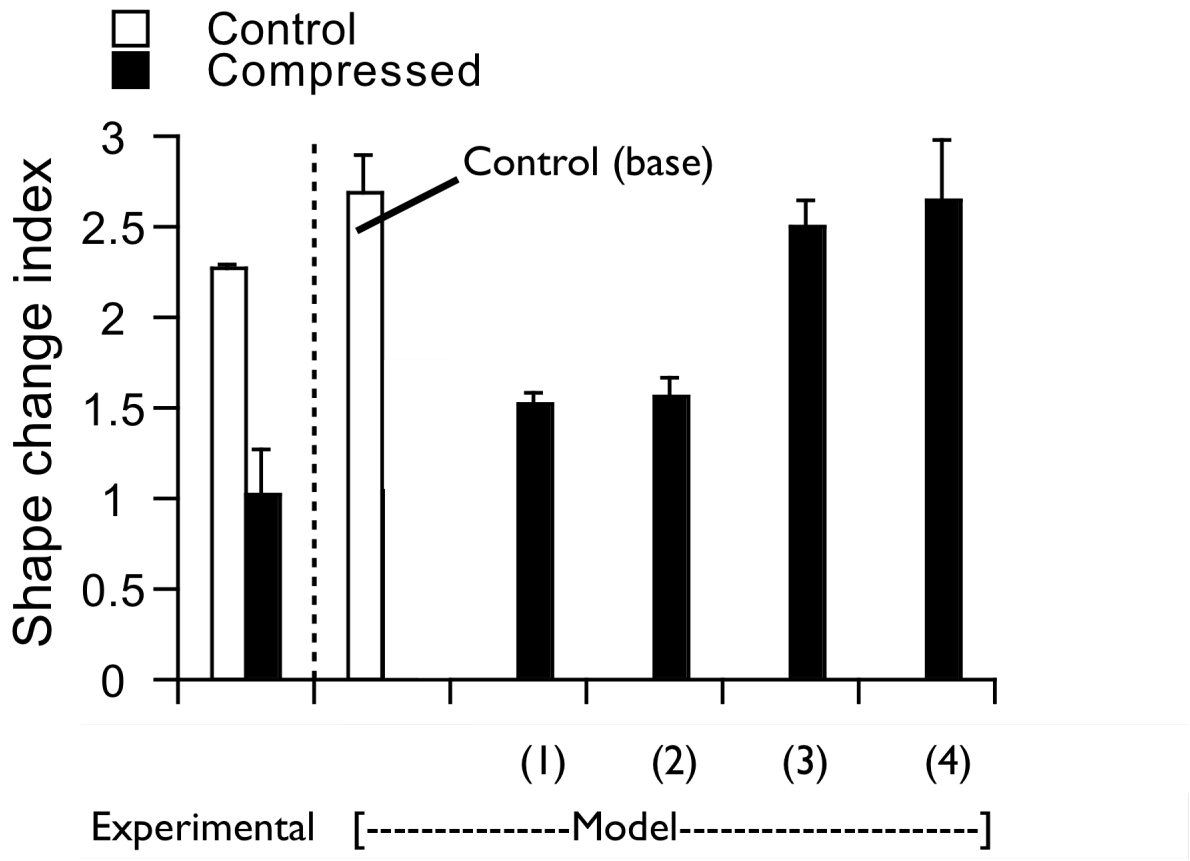

Figure 5.10. Comparison of the shape change index values between the experimental and different model conditions. The numerical values on the x-axis represent the model conditions described in Table 5.2. Unlike other model conditions (3 and 4), longer cell protrusion length (Model condition 1) and constant protrusion/migration rate independent of free cell perimeter (Model condition 2) give an value of shape change index closer to that of the experimental compressed cultures. The value of shape change index for each of the model conditions is averaged by ten simulations. Error bars represent s.e.m.

From the simulation results (Figs 5.6-5.10), we found that faster FCP-dependent protrusion/translocation rate (Fig. 5.8) and same number of *initial* protrusions (Fig 5.9) generated a cell migration pattern similar to that of the control uncompressed case (Fig. 5.5). In contrast, longer cell frontal extension (Fig. 5.6) and constant protrusion/translocation rate (independent of FCP) (Fig. 5.7) yielded a migration pattern similar to that of the experimental compressed cultures (i.e. cell movement around the periphery of the square pattern). Below is a discussion of these interesting findings:

(1) In the experiments, the compressed cells were much longer than the control cells (Fig. 3.3). In the simulation, when we doubled the maximum frontal length allowed for the cell to extend forward, more branching emerged from the original square patterns, indicating that more leaders cells were formed. When the cells extend longer, the proportion of their cell periphery in contact with neighboring cells decreases and the free-cell perimeter increases. Thus, the extended cells could behave as corner cells of the square patterns. This suggests that cell distension could induce leader-cell formation.

(2) The corner cells usually have higher free cell perimeter than that of the edge cells in a square pattern. The experimental observation that leader cells preferentially formed at the corners of the square pattern in the uncompressed cultures (Fig. 3.5) suggests that leader-cell formation is related to free cell perimeter in the absence of compression. However, in the compressed cultures, there was no preferential location for leader-cell formation as they formed ubiquitously all around the periphery of the square pattern (Fig. 3.5). As compression extended every cell around the periphery of the square pattern, the difference in the free cell perimeter between the corner and edge cells could be minimized. Hence, compression-induced leader-cell formation appeared to be

independent of free-cell perimeter. Indeed, in the simulation, constant protrusion/translocation rate independent of free cell perimeter (FCP) has generated a cell migration pattern close to that in the compressed cultures. This suggests that instead of increasing FCP-dependent cell migration, compression might facilitate uniform cell migration due to cell distension.

(3) In the experiments, compression caused initial extrusions of cells at the pattern edge (from observation). To determine if such initial extrusion would induce the migration behavior observed in the compressed cultures, we initialized each cell with the same number of protrusions. Surprisingly, we found that the simulated migration pattern was similar to the control case. For the edge cells of the square pattern, the force generated by these initial small cell extrusions might not be larger enough to overcome the high cell-cell contact force of the edges cells. Thus, they still behaved as in the control case.

These simulation results imply that (i) cell distension could polarize the cells [17], inducing leader-cell formation, and (ii) initial cell extrusions induced by compression might not be sufficient to enhance coordinated cell migration unless compression facilitates constant cell migration independent of free cell perimeter. Based on these simulation findings, when both longer cell frontal extension and constant cell migration were introduced into the base control case, the compression-induced migration was reproduced in the stimulation (Fig. 5.11A) with an R^2 value of 0.87 compared with the experimental values (Fig. 5.11B).

A

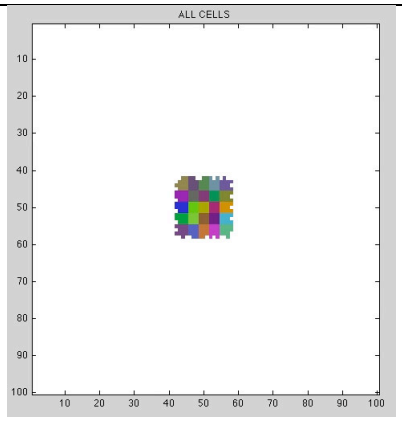

t = 0

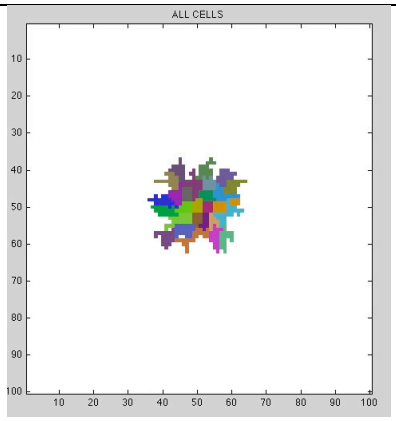

t = 10

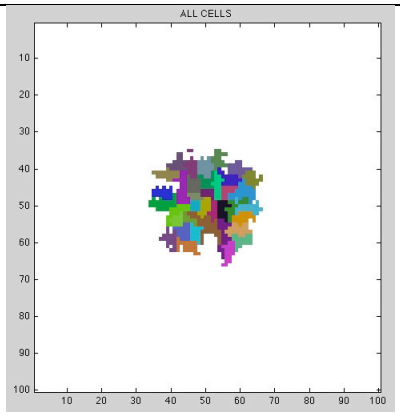

t = 20

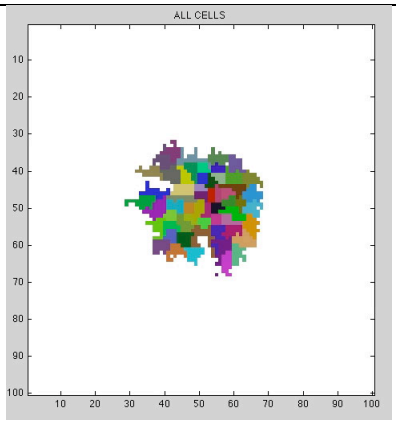

t = 30

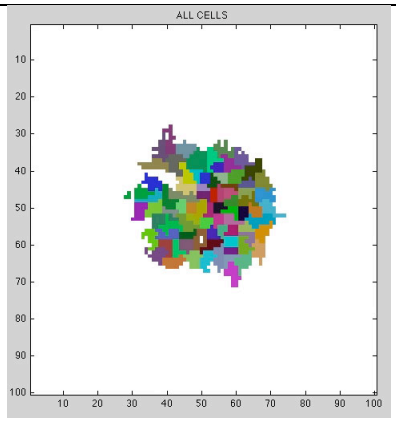

t = 40

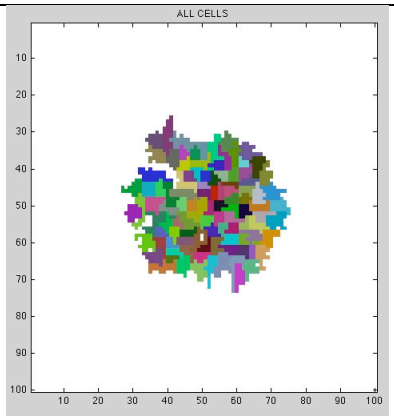

t = 50

B

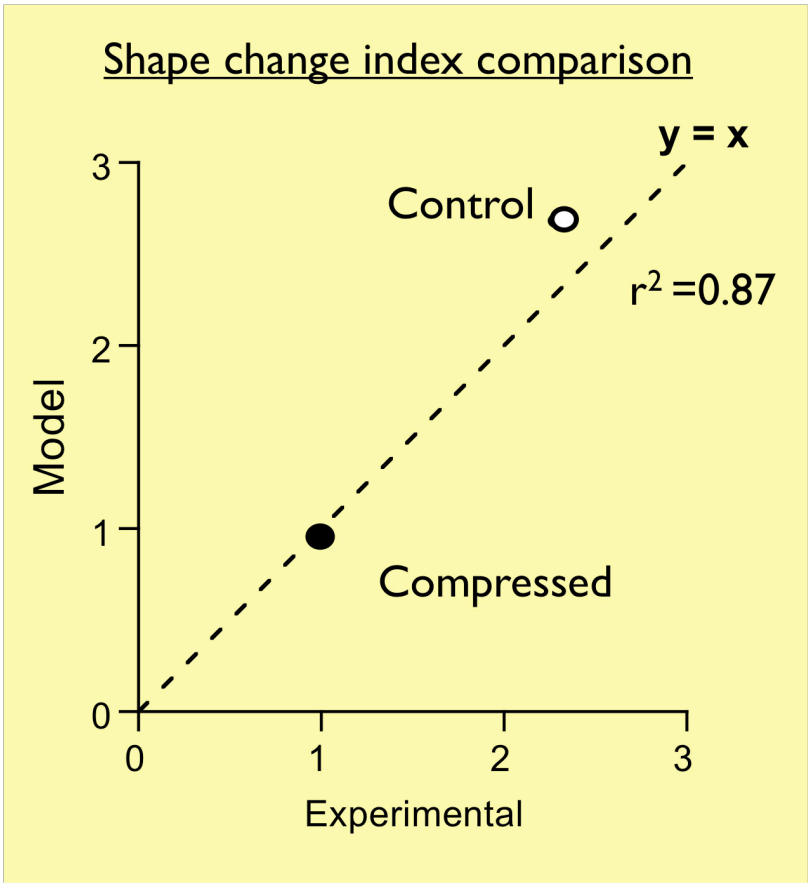

Figure 5.11. Compression could increase cell frontal extension and facilitate constant cell protrusion/translocation rate, resulting in enhanced coordinated cell migration. A, When both longer cell frontal extension and constant cell migration were introduced into the base control case, the compression-induced migration was reproduced in the stimulation. **B,** Shape change index comparison between the experimental and the model in **A** with an R^2 value of 0.87.

To determine the robustness of the model and whether the implications from the previous simulation results would be applicable to other geometries, we have also performed the simulations on the rosette and circular patterns. From the square pattern simulations, we found

that compression could increase cell frontal extension and induce constant, FCP-independent cell migration. Therefore, we simulated compressed cell migration in a rosette pattern with these changes in model parameters as well. The simulation results from the rosette pattern qualitatively matched well with the migration behavior as observed in the experiments for both the control and compressed cultures (Fig. 3.6). While leader cells mainly emerged from the tip of the rosette pattern in the control (Fig. 5.12), leader-cell formation occurred everywhere around the pattern in the compressed case (Fig. 5.13). In addition, the ratio of the migration rate of the edge cells to that of the tip cells in the experimental control was consistent with that in the simulated control ($R^2 = 0.999$), despite a higher baseline in the model simulation (Fig. 5.12: Last panel). As for the compressed cultures, the moving front of the tip cells experimentally demonstrated slower movement than that of edge cells, and our respective simulation has also *qualitatively* captured this similar phenomenon. However, the computed migration rate of the model edge cells (by tracking the initial and end points of each individual cell) was similar to that of the model tip cells instead. This quantitative analysis of the simulated migration contradicted with the experimental measurements (determined by measuring the distance travelled by the leading front, instead of individual cells) (Fig. 5.13: Last panel). This discrepancy suggests that the faster moving front of the compressed edge cells obtained from the experimental measurements could be contributed to higher cell proliferation in the more crowded (edge-cell) area.

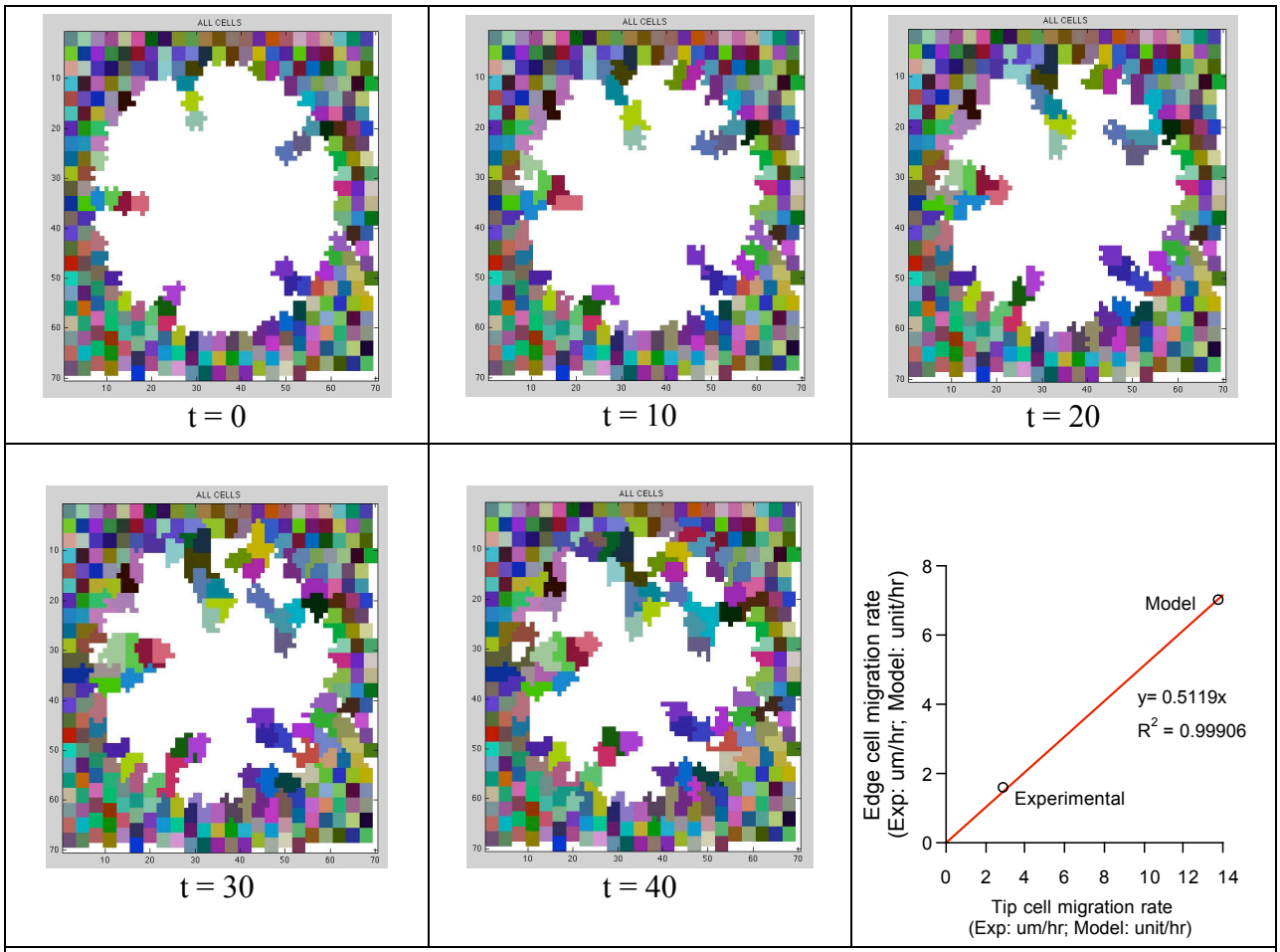

Figure 5.12. Simulation of collective cell migration in a rosette pattern under stress-free condition. The same set of rules used in the square control condition was applied to the simulation of coordinated migration in a rosette pattern. Similar to the experimental observation, the simulated cell migration demonstrates the emergence of leader cells mainly from the tip of the rosette pattern. In addition, the last panel shows that the ratio of the migration rate of the edge cells to that of the tip cells in the experimental control is consistent with that in the simulated control (R^2 = 0.999), despite a higher baseline in the model simulation.

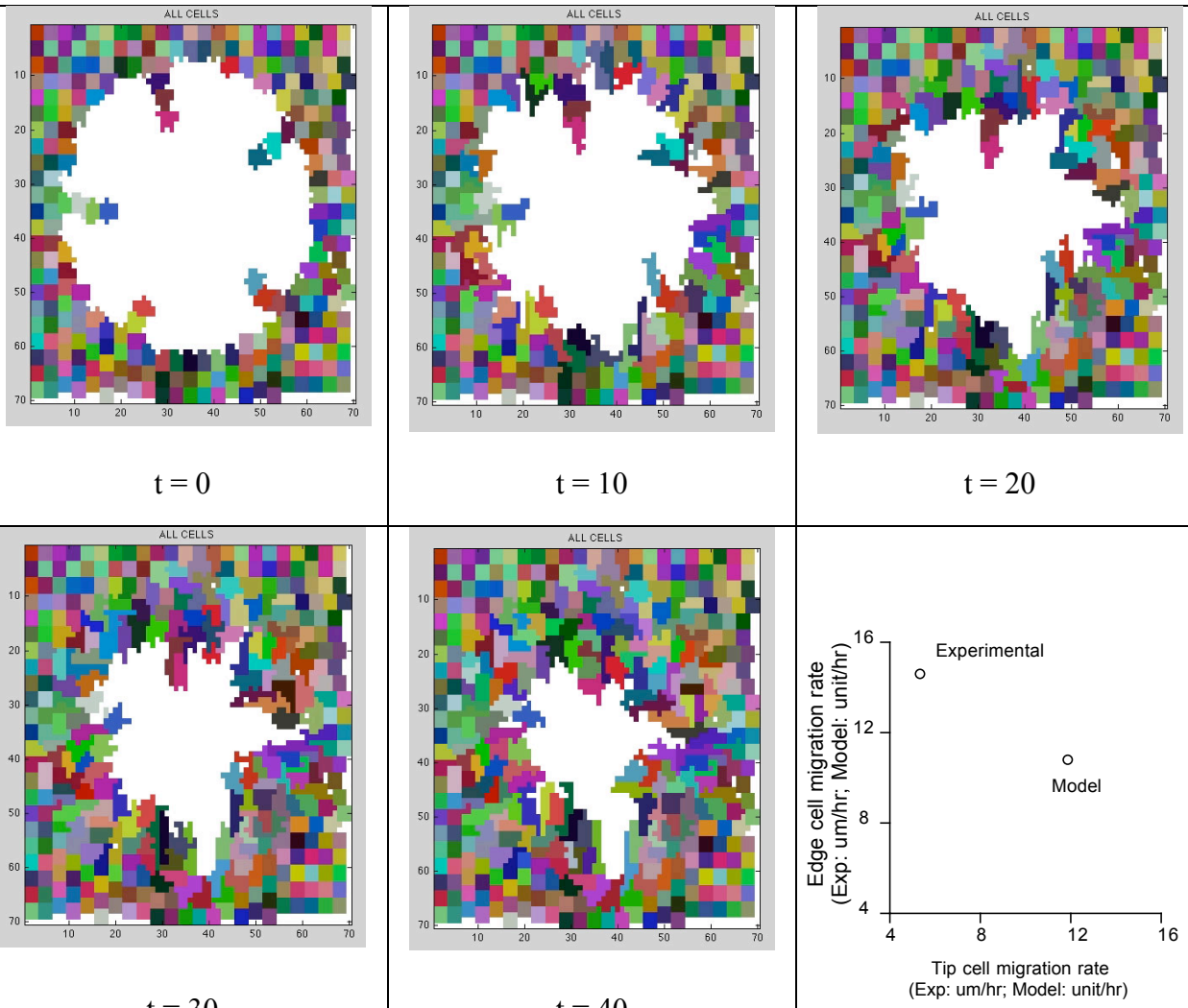

Figure 5.13. Simulation of collective cell migration in a rosette pattern under compression: increased cell frontal extension and constant, FCP-independent cell protrusion/translocation rate. Similar to the experimental observation (Fig. 3.6), the simulated cell migration qualitatively displays (1) leader-cell formation everywhere around the periphery of the rosette pattern, and (2) slower movement of tips cells that that of edge cells. However, the last panel shows that the computed migration rates of model tip and edge cells are not in agreement with that of the experimental values. Please see the main text above for discussion on such discrepancy.

For the circle case, every cell around the edge should theoretically have equivalent free-cell perimeter. Therefore, the cells should be moving outward at a similar rate, maintaining the overall pattern in a circular shape in the absence of compression. However, since the cells were modeled as squares, the resultant simulation pattern was not a perfect circle. In addition, there was no significant difference in the migration pattern between the control (Fig. 5.14) and compression (Fig. 5.15) simulations. However, in the experimental cultures, we would expect no leader cells in the control case but uniform directional leader-cell formation in the compressed case. Thus, the former should have a smoother edge than that of the compressed culture. Yet this disparity could not be distinguished by our current preliminary model.

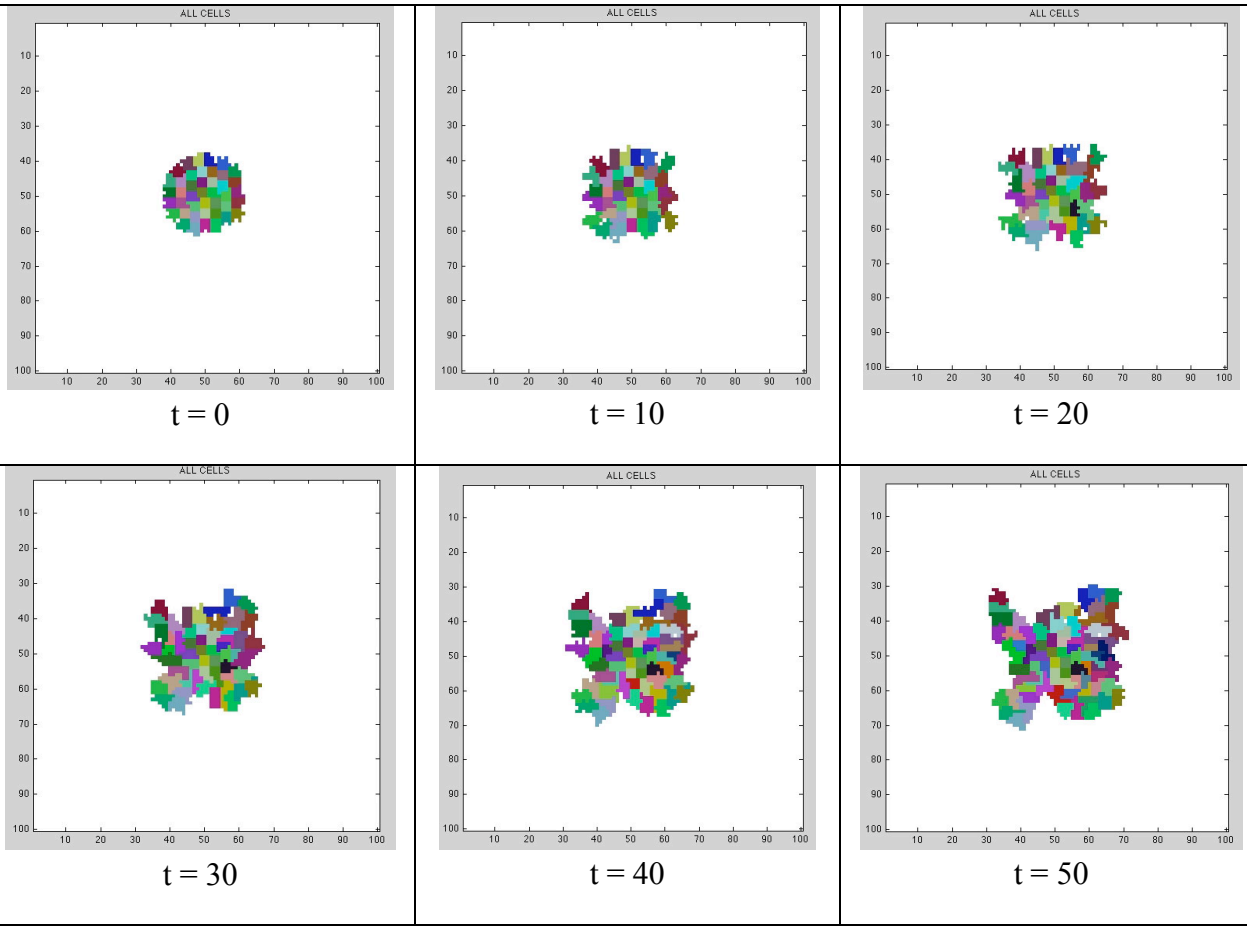

Figure 5.14. Simulation of collective cell migration in a circle pattern under stress-free

condition. The same set of rules used in the square control condition was applied to the simulation of coordinated migration in a circle pattern.

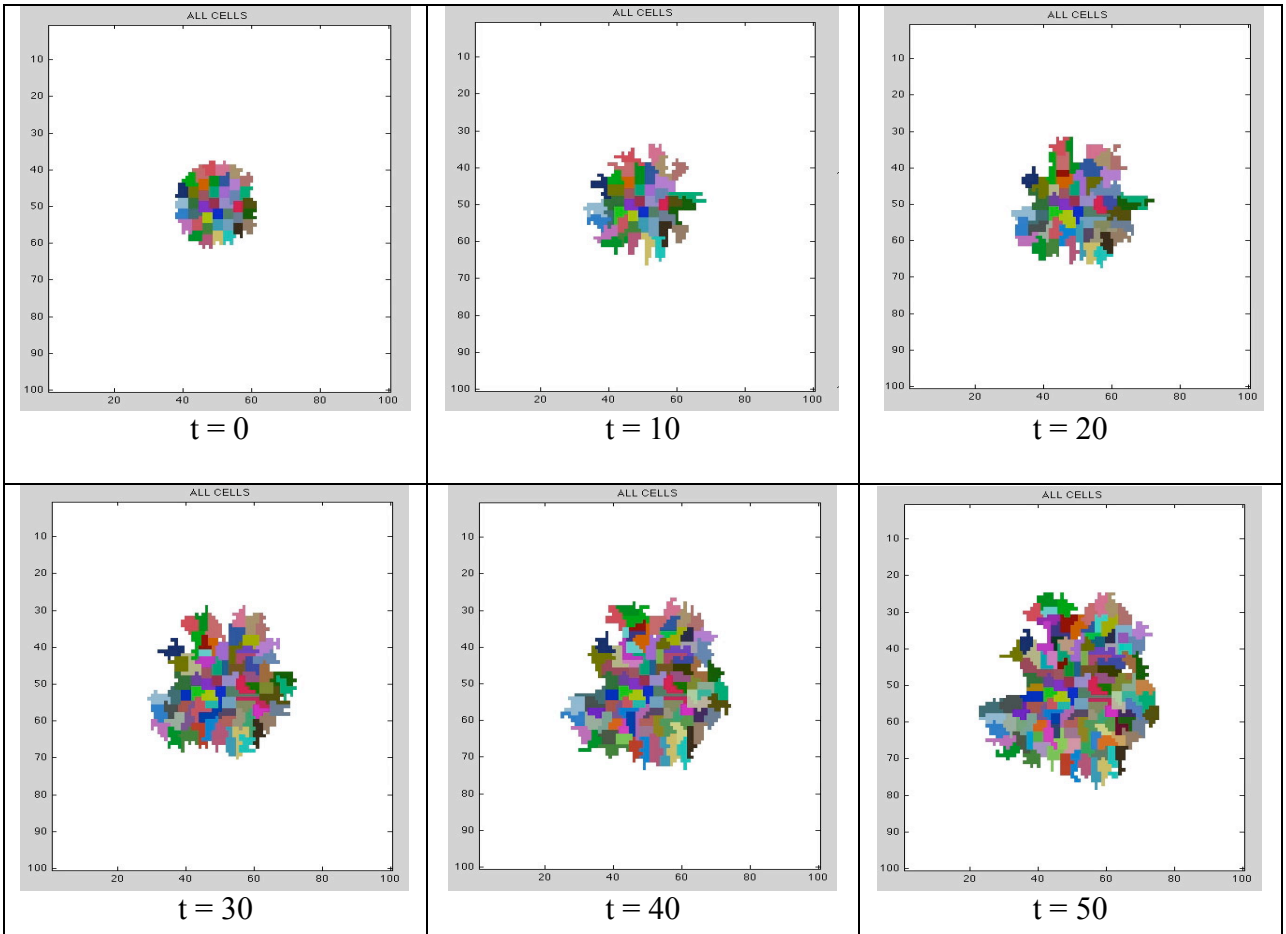

Figure 5.15. Simulation of collective cell migration in a circular pattern under compression: increased cell frontal extension and constant, FCP-independent cell protrusion/translocation rate.

Implications and Limitations

Two main limitations remain in the present model: (1) cells are modeled as squares; and (2) it lacks a complete description of cell-matrix adhesion, which is important for protrusion

stabilization and adhesion disassembly. Nevertheless, the model in general have generated simulation results that fit well with the experimental observations (square pattern in Fig. 5.11 and rosette patterns in Figs. 5.12-5.13). More importantly, it provides us with insights into the physical underpinnings governing the collective migration induced by compressive stress: (i) cell distension could polarize the cells [17], thereby inducing leader-cell formation, and (ii) compression-induced coordinated cell migration could be accompanied by constant, FCP (free cell perimeter)-independent cell migration rate.

References

1. Friedl, P., and D. Gilmour. 2009. Collective cell migration in morphogenesis, regeneration and cancer. *Nat Rev Mol Cell Biol*. 10:445-57.
2. Ilina, O., and P. Friedl. 2009. Mechanisms of collective cell migration at a glance. *J Cell Sci*. 122:3203-8.
3. Bindschadler, M., and J.L. McGrath. 2007. Sheet migration by wounded monolayers as an emergent property of single-cell dynamics. *J Cell Sci*. 120:876-884.
4. Farooqui, R., and G. Fenteany. 2005. Multiple rows of cells behind an epithelial wound edge extend cryptic lamellipodia to collectively drive cell-sheet movement. *J Cell Sci*. 118:51-63.
5. Nobes, C.D., and A. Hall. 1999. Rho GTPases control polarity, protrusion, and adhesion during cell movement. *J Cell Biol*. 144:1235-44.
6. Maini, P.K., D.L. McElwain, and D.I. Leavesley. 2004. Traveling wave model to interpret a wound-healing cell migration assay for human peritoneal mesothelial cells. *Tissue Eng*. 10:475-82.
7. Tremel, A., A. Cai, N. Tirtaatmadja, B.D. Hughes, G.W. Stevens, K.A. Landman, and A.J. O'Connor. 2009. Cell migration and proliferation during monolayer formation and wound healing. *Chemical Engineering Science*. 64:247-253.
8. Simpson, M.J., D.C. Zhang, M. Mariani, K.A. Landman, and D.F. Newgreen. 2007. Cell proliferation drives neural crest cell invasion of the intestine. *Dev Biol*. 302:553-68.
9. Hatzikirou, H., and A. Deutsch. 2008. Cellular automata as microscopic models of cell migration in heterogeneous environments. *Curr Top Dev Biol*. 81:401-34.
10. Aubert, M., M. Badoual, S. Fereol, C. Christov, and B. Grammaticos. 2006. A cellular automaton model for the migration of glioma cells. *Phys Biol*. 3:93-100.
11. Simpson, M.J., A. Merrifield, K.A. Landman, and B.D. Hughes. 2007. Simulating invasion with cellular automata: connecting cell-scale and population-scale properties. *Phys Rev E Stat Nonlin Soft Matter Phys*. 76:021918.
12. Young, H.M., A.J. Bergner, R.B. Anderson, H. Enomoto, J. Milbrandt, D.F. Newgreen, and P.M. Whitington. 2004. Dynamics of neural crest-derived cell migration in the embryonic mouse gut. *Dev Biol*. 270:455-73.
13. Vitorino, P., and T. Meyer. 2008. Modular control of endothelial sheet migration. *Genes Dev*. 22:3268-81.
14. Condeelis, J. 1993. Life at the leading edge: the formation of cell protrusions. *Annu Rev Cell Biol*. 9:411-44.
15. Ridley, A.J., M.A. Schwartz, K. Burridge, R.A. Firtel, M.H. Ginsberg, G. Borisy, J.T. Parsons, and A.R. Horwitz. 2003. Cell migration: integrating signals from front to back. *Science*. 302:1704-9.
16. Nelson, C.M., R.P. Jean, J.L. Tan, W.F. Liu, N.J. Sniadecki, A.A. Spector, and C.S. Chen. 2005. Emergent patterns of growth controlled by multicellular form and mechanics. *Proc Natl Acad Sci U S A*. 102:11594-9.
17. Chien, S. 2006. Mechanical and chemical regulation of endothelial cell polarity. *Circ Res*. 98:863-5.

Chapter 6: Conclusions and future directions

Portions of the chapter have been taken from:

J.M. Tse, G. Cheng, J.A. Tyrrell, S.A. Wilcox-Adelman, Y. Boucher, R.K. Jain, L.L. Munn, "Compression-induced cell distension and adhesion stimulate coordinated migration of mammary carcinoma cells." Submitted.

Conclusions

Uncontrolled cell proliferation within a solid tumor in a confined space not only creates oxidative stress (hypoxia) [1], but also generates mechanical compressive stress [2,3], which can influence the tumor cells and modify their interactions with neighboring cells and the extracellular matrix. Intratumoral oxidative stress has long been shown to select for aggressive cancer cells, enabling the cancer cells to metastasize- to spread to other parts of the body[1]**.** However, whether compressive stress generated by rapid cell proliferation can impose similar selection pressure remains unclear. The primary goal of this thesis is to answer the following question: can compressive stress generated by tumor growth stimulate cancer cell migration? The answer will drive our understanding of mechanical impact on solid tumor pathophysiology and open the door to a new class of targets for blocking mechanical stress pathways. Furthermore, our finding will highlight the need for integrating mechanical cues into current genetic or molecular biology approaches for drug screening as a better evaluation of drug efficacy during drug development.

To mimic the process by which cancer cells collectively experience compressive stress at the tumor margin, where rapid cell proliferation occurs[4,5], we first developed an *in vitro* compression system to apply direct and anisotropic compressive stress to cell monolayers and assess its effect on cancer cell motility with a scratch-wound assay (Chapter 2). The 2-D scratch-wound assay allows cell-cell and cell-matrix interactions that cancer cells would experience under compression to be studied during cell migration[6]. In addition, the migration rates of the uncompressed cancer cell lines

determined from the scratch-wound assay correlated reasonably with their relative inherent motility. Hence, we were confident that the scratch-wound assay provided a good measure of the effect of compressive stress on cell motility.

Our experiments showed that moderate compressive stress enhances cell migration in mammary carcinoma cells and compression-induced migration is accompanied by cell distortion regulated by cytoskeletal changes (Chapters 2). Governed by the principles of "tensegrity," cell shape can govern various cellular processes such as proliferation and directional protrusions[7,8]. As cancer cells are more deformable than normal cells[9] (also supported by our cytoskeletal immunostaining), they could impart distinct mechano-responses. Indeed, differential migratory responses to mechanical compression were obtained from various cancer cell lines and normal cells (mammary epithelial cells and fibroblasts). For example, while compression enhanced the motility of some mammary carcinoma cell lines, the migration potential of fibroblasts was not significantly affected (Appendix A). The distinct mechanosensitivities of tumor and stromal (mainly fibroblasts) cells could allow the cells to orchestrate tumor progression more effectively, as fibroblasts under mechanical stimulation have been reported to regulate the production of extracellular matrix [10], of which increasing stiffness enhances tumor malignancy. More importantly, we showed that the mechano-response was reversible. When the mechanical stress was removed, the migration potential of pre-compressed 67NR cells that previously demonstrated increased cell motility dropped significantly. Hence, compression-induced cancer cell migration is cell-distortion-dependent, implying that tumor cell motility could be modulated by the compressive

stress surrounding them. Indeed, it has been reported that altering the matrix rigidity can revert the transformed mammary epithelial cells toward a non-malignant phenotype[11].

Another intriguing result is that compression-induced leader-cell formation is independent of multicellular micro-organization (Chapter 3). Using microfabrication to control the organization of 67NR cells in a sheet, we demonstrated that emergence of leader cells corresponded to the tips or corners of the uncompressed monolayers, while externally-applied compression induced leader cell formation everywhere around the edge of the pattern. Depending on the cell's position and the overall shape of the monolayer, cytoskeletal tension generated within each cell varies[7]. For instance, the corner cells have more free-cell perimeter to interact with ECM for adhesions, and thus generate high tractional stress within the sheet[12]. Hence, multicellular spatial micro-organization could induce internal cell polarization. As a cell polarizes, distinct spatial localization of proteins occurs at the front and the rear of the cell for different molecular processes [13,14]. In a similar manner, compression-induced cell extrusion could polarize the cells [15], and affect the spatial localization of proteins such as Rho-GTPases, independent of total expression levels of the cellular proteins. Indeed, while previous work has shown that formation of leader cells is dependent on RhoA, which is responsible for contractile activity and stress fiber formation [16,17], we showed that modulating the activity of Rho-GTPases, such as RhoA, Rac and Cdc42, apparently did not affect the morphology of compression-induced leader cells (though migration rate was affected). Therefore, our findings suggest that compressive stress generated by tumor cells could mechanically polarize the cells for migratory phenotypes toward open spaces.

This could be important for local invasion and also intravasation into blood vessels, considering that loss of gap junctions within the endothelial lining of the blood vessels has been reported in metastatic tumors [18,19].

In general, it is assumed that focal adhesion formation (an indication of cell-substrate adhesion) is necessary for cell spreading. However, consistent with the finding of Chen *et. al.* that cell spreading actually controlled the amount of focal adhesions while holding the extracellular matrix density constant[20], we showed that (1) compression did not significantly increase fibronectin surface density, but (2) compression induced cell extrusion (spreading), which led to a larger fraction of fibronectin associated with cell-substrate surface for enhanced cell-substrate adhesion (supported by immunostaining of integrin, paxillin and vinculin) (Chapter 4). Different from previous studies showing that matrix rigidity enhances tumor progression[11,21], our results suggest that growth-induced compressive stress could distort cancer cells and increase their ECM adhesion for aggressive phenotypes without activation of stroma cells (fibroblasts) for extracellular matrix production.

Although compression did not increase fibronectin surface density, compression-induced cell-substrate adhesion could induce cytoskeletal tension, which has been shown to unfold fibronectin to expose cryptic self-association sites for fibronectin fibril and matrix assembly[22-24]. Hence, consistent with the previous report that persistent movement of leader cells results from cell adhesion to fibronectin[25], we found that elongated fibronectin fibrils were formed under compressed leading cells in the direction of

migration. Meanwhile, as fibronectin fibrils could expose more binding sites for cell integrin-matrix interactions, higher intracellular cytoskeletal force could be generated to pull the cell sheet forward and thereby enhance coordinated cell migration. Since formation of fibronectin fibrils is a cell-mediated process involving interactions with integrins and actin cytoskeleton [26], blocking the dynamic interactions between fibronectin, integrin and actin cytoskeleton would hinder formation of fibronectin fibrils for enhanced coordinated migration. Indeed, when we performed integrin b1 blocking and inhibition of actomyosin contractility on 67NR cells, compression-induced coordinated migration rate was reduced but the leading edge of the cell sheet remained morphologically the same (Chapter 4). Taken together, our findings suggest that changes in internal cytoskeletal tension that result from large-scale changes in cell shape (e.g compression-induced cell distortion) can lead to enhanced cell-matrix adhesions.

From our experimental study, we found that compression-induced coordinated migration of 67NR mammary carcinoma cells was geometry-independent, accompanied by cell distension, enhanced cell-matrix adhesion, increased formation of leader cells and faster migration rate. To experimentally decouple each parameter from one another and identify the factor(s) governing compression-induced collective migration was challenging. Hence, we developed a preliminary and simple stochastic model to simulate 2-D collective migration of cells initially arranged in a square geometry (Chapter 5). As each cell was composed of multiple blocks, its cell periphery could undergo different processes, such as protrusions on one side while maintaining cell-cell contact with another neighboring cell on a different side. The model simulations suggest that (1) cell

distension generated by compression could induce leader-cell formation, (2) initial cell extrusions induced by compression may not be sufficient to enhance coordinated cell migration, and more importantly, (3) constant cell migration rate independent of free cell perimeter (FCP) could be responsible for compression-induced coordinated migration.

Combining both experimental and theoretical approaches, our work suggests that anisotropic compression may be able to promote coordinated cell migration (independent of the geometric determinant of directional cell protrusions[27,28]) by affecting the free-cell perimeter and also the number of cell-substrate adhesions, or the rate at which they form (Fig. 6.1). This is consistent with the observation from the micropatterning experiment that leader cells form at the square corners or rosette tips in uncompressed samples, which have greater free perimeter. Thus, more protrusions/adhesions are formed, generating tension on the actin cytoskeleton and enhancing force transmission and mechano-sensing at the focal adhesions [29]. It is also consistent with the induction of leader cells by compression, which forces cell distension, and thus increases free-cell membrane available for protrusions and adhesion sites. The compression-induced cell distortion can increase cytoskeletal tension, affecting local changes in focal adhesion assembly [7,20] and the rate of adhesive contact formation. The resultant cell-matrix adhesion induced by compressive stress might facilitate more uniform cell migration, resulting in geometry-independent and thus more effective coordinated migration.

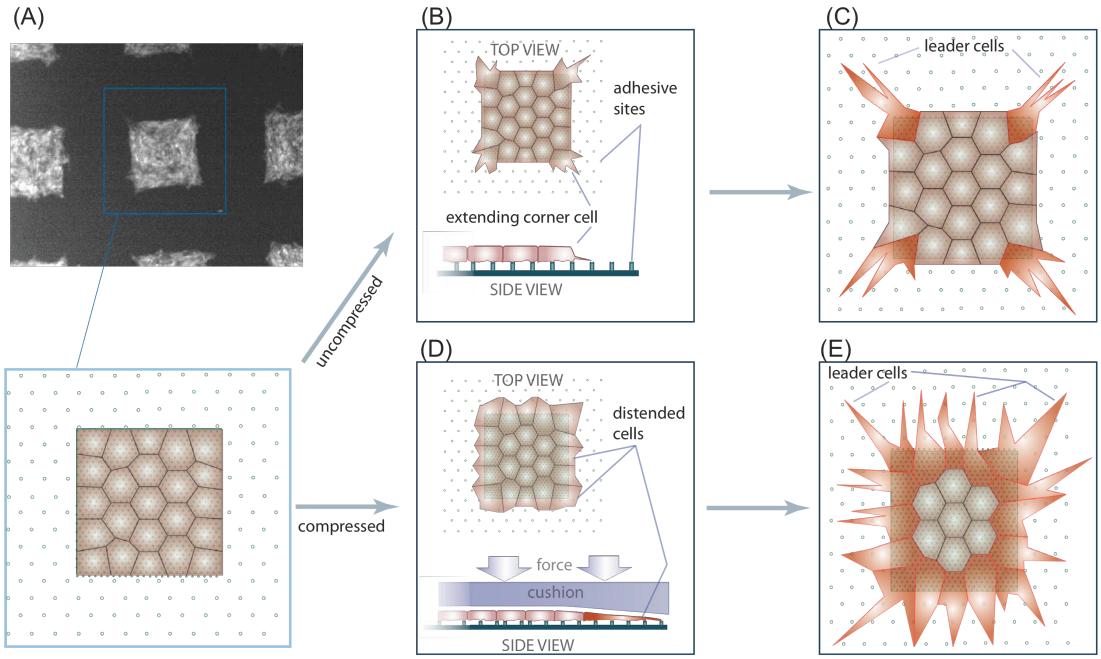

Figure 6.1. Conceptual model of compression-modulated coordinated cell migration. Cells seeded in square islands have different extents of free perimeter, depending on location (**A**). In uncompressed cultures, free perimeter affects leader cell formation (**B**). On average, the corner cells in the square islands have more free cell perimeter than the edge cells, and are therefore able to extend more protrusions than the edge cells. The rate at which these protrusions form adhesions – or the resulting change in force balance within the cell – likely causes their phenotypic change into "leader" cells (**C**). In our system, cell-cell adhesion is maintained, so cells adjacent to the leader cells (either behind or on the sides) appear to be pulled in the coordinated migration. As a result, the

sheet preferentially extends from the corners of the square pattern. In contrast, when the culture is compressed, all cells around the periphery of the island are deformed, or extruded, against the surface, into the empty space (**D**). Similar to the case of the active extension of the uncompressed corner cells, cell extrusion or "reaching" directed by asymmetric neighbors has the effect of increasing cell-surface contact and formation of new adhesion contacts with the substrate. Hence, all cells around the periphery of the square pattern become leader cells (**E**).

In the classical view of metastasis – a process of tumor cells spreading to other parts of the body, transformation of epithelial-like tumor cells to become mesenchymal is thought to be required for them to migrate as single cells[30]. However, it has been found recently that tumor cells can also invade the surrounding environment in clusters or strands guided by leader cells (collective/coordinated cell migration) [31]. The work presented in this thesis serves as the first evidence of the mechanical impact in cancer coordinated cell migration. It suggests that compressive stress generated by proliferating cancer cells can distort their cell shapes, enhance their cell-substrate adhesion and stimulate formation of leader cells responsible for collective cell migration, potentially leading to metastasis. In addition, the phenotypic characteristics of compression-induced leader cells are: (1) polarized; (2) enhanced directional migration with extended protrusions; (3) stress fiber formation; and (4) increased fibronectin deposition at the cell-substrate interface. The unsuccessful attempt to identify the regulatory molecule controlling compression-induced migration and leader-cell formation apparently implies that such compressive stress activates cancer cells via another adaptive mechanism

independent of the conventional pathways responsible for migration and adhesion. Nevertheless, our work provides novel insight into how physical determinants trigger leader-cell formation in coordinated migration, which is relevant in many other physiological processes, such as vascular sprouting and wound healing[32,33]. These small steps forward in the field of cancer mechano-biology help to propel research in discovering mechanical-stress pathways and improved strategies for cancer treatment.

Future Directions

As a tumor contains both cancer cells and stromal cells including fibroblasts and macrophages, *it is important to understand the effect of compressive stress on stromal cells* as well. Although we have shown that mechanical compression did not affect fibroblast migration (Appendix A), mechanical stress has been shown to influence the production of extracellular matrix by fibroblasts[10]. In addition, we have shown that different extracellular matrix/substrate can have distinct effect on leader-cell formation in our 2-D *in vitro* model (Fig. 4.5, B-C). Therefore, it is possible that compression induces synthesis or deposition of extracellular matrix molecules by fibroblasts, which in turn enhances leader-cell formation in cancer cells. To test this possibility, we will first use the current 2D *in vitro* compression platform to apply mechanical stress to fibroblast monoculture and then measure the transcriptional and post-translational changes in expression of extracellular matrix molecules or growth factors with gene arrays and Western blots, respectively. We can also perform similar experiments to evaluate the effect of compression stress on other stromal cells such as macrophages in terms of the production of inflammation-associated molecules.

With a better understanding of the role of mechanical compression in stroma component, *we will then determine if the cancer-stromal cell interaction augments compression-induced migratory phenotypes.* To do this, we will co-culture stromal cells such as fibroblasts with cancer cells by seeding a mixed population of cancer cells labeled with green fluorescent proteins (GFP) and fibroblasts labeled with red fluorescent protein from Discosoma sp. reef coral (DsRed) onto the transwell surface. A scratch-wound assay is then performed to measure the migration potential of GFP-cancer cells under compression. To control the spatial localization of different cell types, alternate rings of cancer cells and fibroblasts can be patterned on transwell surfaces by micro-contact printing techniques.

If compression-induced migratory response of cancer cells is enhanced in the presence of fibroblasts, we will next investigate whether the physical contact between cancer cells and fibroblasts is required. We can pre-treat the transwell surface with fibroblasts (which will deposit matrix and secrete growth factors) and compress them. After compression of fibroblast monoculture, we will collect the conditioned culture medium and remove the cells from the transwell surface. Then, cancer cells are seeded on the conditioned surface and cultured in the collected conditioned medium for the *in vitro* scratch wound-compression experiment.

Active migration of cancer cells is necessary at the initiation of the metastatic cascade, at which time the cancer cells leave the primary site and gain access to the circulation, and

also at the end of cell invasion when they enter the secondary site[34]. My 2D work has shown that compression can enhance migration of cancer cells. Next, *we will extend my 2D work to a 3D in vitro compression model.* Development of a 3D model by incorporating matrix rigidity and structure into the current 2D model would allow us to investigate the effect of compressive stress on invasive potential of cancer cells. In the preliminary experiments, we have compressed mammary epithelial cells in the Matrigel using the *in vitro* compression device. Enhanced cell invasion and more pronounced fibronectin expression near the migrating cells were observed in the compressed 3D cultures. In addition, continuous compression was also required in the 3D model to induce those invasive phenotypes (Data not shown). These initial studies suggest that the results from my 2D work are still applicable for migration in 3D. However, higher stress may be required to yield comparable cell strain on a gel substrate rather than on a rigid 2D surface. Next, we will introduce cancer-stromal cell interaction into a 3D co-culture-compression model. Eventually, we attempt to discover the molecular mechanism responsible for compression-induced invasive phenotypes using this 3D model.

Toward the end of my PhD project, we have started to develop a preliminary stochastic model of coordinated cell migration to explain the experimental results (Chapter 5). In the current model, the direction of cell migration was determined by considering all the cell-cell interaction forces and self-protrusive forces with the relative contribution of each force estimated by trial and error (but with rationale). The current model is able to qualitatively reproduce the experimental observations of coordinated migration in both the control and compressed cultures. *To validate the parameters in the stochastic model,*

various experiments will be performed, such as determination of various force magnitudes by traction force microscopy [35] and optical tweezers, and measurement of cell migration persistence time by time-lapse microscopy. In addition, *we want to introduce into the model a description of the biochemical environment*, in which cells can secrete growth factors and sense gradients of soluble factors for directional migration. Such a model combining both biophysical and biochemical components of the cell microenvironment would provide us with insights into their interplay during coordinated cell migration.

References

1. Bernards, R. 2003. Cancer: cues for migration. *Nature*. 425:247-8.
2. Helmlinger, G., P.A. Netti, H.C. Lichtenbeld, R.J. Melder, and R.K. Jain. 1997. Solid stress inhibits the growth of multicellular tumor spheroids. *Nat Biotechnol*. 15:778-83.
3. Cheng, G., J. Tse, R.K. Jain, and L.L. Munn. 2009. Micro-environmental mechanical stress controls tumor spheroid size and morphology by suppressing proliferation and inducing apoptosis in cancer cells. *PLoS ONE*. 4:e4632.
4. Roose, T., P.A. Netti, L.L. Munn, Y. Boucher, and R.K. Jain. 2003. Solid stress generated by spheroid growth estimated using a linear poroelasticity model small star, filled. *Microvasc Res*. 66:204-12.
5. Sarntinoranont, M., F. Rooney, and M. Ferrari. 2003. Interstitial stress and fluid pressure within a growing tumor. *Ann Biomed Eng*. 31:327-35.
6. Liang, C.-C., A.Y. Park, and J.-L. Guan. 2007. In vitro scratch assay: a convenient and inexpensive method for analysis of cell migration in vitro. *Nat. Protocols*. 2:329-333.
7. Ingber, D.E. 2008. Tensegrity-based mechanosensing from macro to micro. *Prog Biophys Mol Biol*. 97:163-79.
8. Ingber, D.E. 2003. Tensegrity II. How structural networks influence cellular information processing networks. *J Cell Sci*. 116:1397-408.
9. Suresh, S. 2007. Biomechanics and biophysics of cancer cells. *Acta Biomater*. 3:413-38.
10. Chiquet, M., A.S. Renedo, F. Huber, and M. Fluck. 2003. How do fibroblasts translate mechanical signals into changes in extracellular matrix production? *Matrix Biol*. 22:73-80.
11. Paszek, M.J., N. Zahir, K.R. Johnson, J.N. Lakins, G.I. Rozenberg, A. Gefen, C.A. Reinhart-King, S.S. Margulies, M. Dembo, D. Boettiger, D.A. Hammer, and

V.M. Weaver. 2005. Tensional homeostasis and the malignant phenotype. *Cancer Cell*. 8:241-254.
12. Nelson, C.M., R.P. Jean, J.L. Tan, W.F. Liu, N.J. Sniadecki, A.A. Spector, and C.S. Chen. 2005. Emergent patterns of growth controlled by multicellular form and mechanics. *Proc Natl Acad Sci U S A*. 102:11594-9.
13. Ridley, A.J., M.A. Schwartz, K. Burridge, R.A. Firtel, M.H. Ginsberg, G. Borisy, J.T. Parsons, and A.R. Horwitz. 2003. Cell migration: integrating signals from front to back. *Science*. 302:1704-9.
14. Verkhovsky, A.B., T.M. Svitkina, and G.G. Borisy. 1999. Self-polarization and directional motility of cytoplasm. *Curr Biol*. 9:11-20.
15. Chien, S. 2006. Mechanical and chemical regulation of endothelial cell polarity. *Circ Res*. 98:863-5.
16. De Smet, F., I. Segura, K. De Bock, P.J. Hohensinner, and P. Carmeliet. 2009. Mechanisms of vessel branching: filopodia on endothelial tip cells lead the way. *Arterioscler Thromb Vasc Biol*. 29:639-49.
17. Omelchenko, T., J.M. Vasiliev, I.M. Gelfand, H.H. Feder, and E.M. Bonder. 2003. Rho-dependent formation of epithelial "leader" cells during wound healing. *Proc Natl Acad Sci U S A*. 100:10788-93.
18. Carter, B., ;, G. Small, M. Ward, and J. Hahn. 2006. Her2 signaling in breast cancer induces dissociation of adherens junction porteins in endothelial cell monolayers. *Journal of Surgical Research*. 130:216-216.
19. Donahue, H.J., M.M. Saunders, Z. Li, A.M. Mastro, C.V. Gay, and D.R. Welch. 2003. A potential role for gap junctions in breast cancer metastasis to bone. *J Musculoskelet Neuronal Interact*. 3:156-61.
20. Chen, C.S., J.L. Alonso, E. Ostuni, G.M. Whitesides, and D.E. Ingber. 2003. Cell shape provides global control of focal adhesion assembly. *Biochem Biophys Res Commun*. 307:355-61.
21. Paszek, M.J., and V.M. Weaver. 2004. The tension mounts: mechanics meets morphogenesis and malignancy. *J Mammary Gland Biol Neoplasia*. 9:325-42.
22. Zhong, C., M. Chrzanowska-Wodnicka, J. Brown, A. Shaub, A.M. Belkin, and K. Burridge. 1998. Rho-mediated Contractility Exposes a Cryptic Site in Fibronectin and Induces Fibronectin Matrix Assembly. *J. Cell Biol.* 141:539-551.
23. Wu, C., V.M. Keivens, T.E. O'Toole, J.A. McDonald, and M.H. Ginsberg. 1995. Integrin activation and cytoskeletal interaction are essential for the assembly of a fibronectin matrix. *Cell*. 83:715-24.
24. Schwartz, M.A. 2009. Cell biology. The force is with us. *Science*. 323:588-9.
25. Biname, F., P. Lassus, and U. Hibner. 2008. Transforming growth factor beta controls the directional migration of hepatocyte cohorts by modulating their adhesion to fibronectin. *Mol Biol Cell*. 19:945-56.
26. Mao, Y., and J.E. Schwarzbauer. 2005. Fibronectin fibrillogenesis, a cell-mediated matrix assembly process. *Matrix Biol*. 24:389-99.
27. Brock, A., E. Chang, C.C. Ho, P. LeDuc, X. Jiang, G.M. Whitesides, and D.E. Ingber. 2003. Geometric determinants of directional cell motility revealed using microcontact printing. *Langmuir*. 19:1611-7.
28. Parker, K.K., A.L. Brock, C. Brangwynne, R.J. Mannix, N. Wang, E. Ostuni, N.A. Geisse, J.C. Adams, G.M. Whitesides, and D.E. Ingber. 2002. Directional

control of lamellipodia extension by constraining cell shape and orienting cell tractional forces. *FASEB J*. 16:1195-204.
29. Bershadsky, A., M. Kozlov, and B. Geiger. 2006. Adhesion-mediated mechanosensitivity: a time to experiment, and a time to theorize. *Curr Opin Cell Biol*. 18:472-81.
30. Thiery, J.P. 2002. Epithelial-mesenchymal transitions in tumour progression. *Nat Rev Cancer*. 2:442-54.
31. Christiansen, J.J., and A.K. Rajasekaran. 2006. Reassessing epithelial to mesenchymal transition as a prerequisite for carcinoma invasion and metastasis. *Cancer Res*. 66:8319-26.
32. Friedl, P., and D. Gilmour. 2009. Collective cell migration in morphogenesis, regeneration and cancer. *Nat Rev Mol Cell Biol*. 10:445-57.
33. Ilina, O., and P. Friedl. 2009. Mechanisms of collective cell migration at a glance. *J Cell Sci*. 122:3203-8.
34. Joyce, J.A., and J.W. Pollard. 2009. Microenvironmental regulation of metastasis. *Nat Rev Cancer*. 9:239-52.
35. Trepat, X., M.R. Wasserman, T.E. Angelini, E. Millet, D.A. Weitz, J.P. Butler, and J.J. Fredberg. 2009. Physical forces during collective cell migration. *Nature Physics*. 5:426-430.

Appendix A

Results

Porous membranes vs. non-porous surfaces on compression-induced migration

Despite no forced cell-extrusion through the 0.4um porous membrane in the compressed cultures (Fig. 2.2), it is not clear whether the mere presence of pores on the membranes could contribute to compression-induced migration in mammary carcinoma cells. In Figure 2.3, 67NR mammary carcinoma cells showed the most pronounced increase in migration potential under compression. Therefore, we compared the migration response of 67NR cells to mechanical compressive stress on a 0.4um porous membrane and a nonporous plastic surface. In spite of overall slower migration on the plastic surfaces, the cell migration enhanced by compression on 0.4um porous membrane was reproduced in a similar manner on the plastic surfaces (Appendix Fig. A1). It should be noted that nonporous membranes of the same material as 0.4um membranes should be ideally used but they were not found available. Hence, the surface material difference could contribute to discrepancies in cell migration enhanced by compression. Taken together, our finding confirmed that the presence of pores on the transwell membranes were not accountable for compression-induced migration.

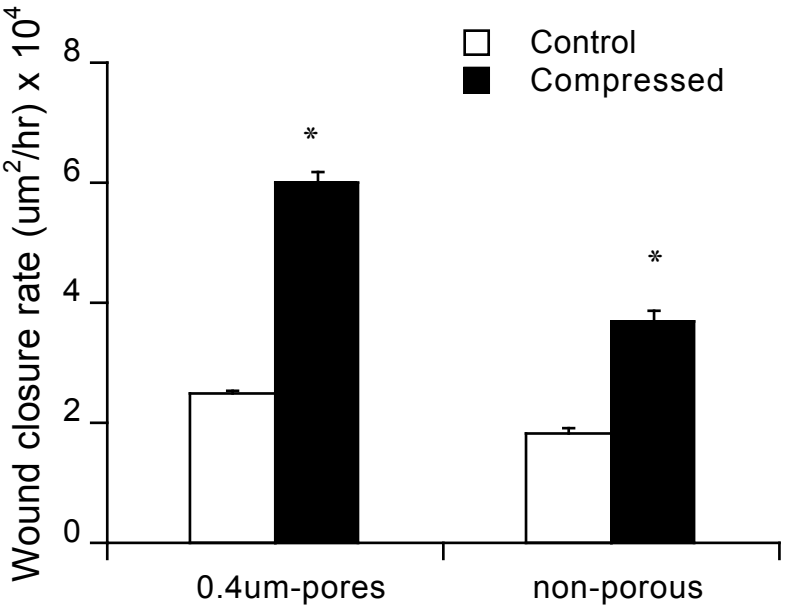

Appendix Figure A1. Compression-induced 67NR migration is observed on both porous and nonporous surfaces. Average migration rate obtained from the scratch-wound assay for the 67NR cells subjected to either stress-free (control) or a compressive stress of 5.8mmHg for 16 hrs. The cells were plated on 0.4um porous membranes or plastic surfaces, respectively (n=6-9; *P<0.05 compared with their individual control). Error bars represent s.e.m.

Gene tables for pathway-focused microarray used in the study

Two different microarrays (from SABiosciences) were used to study the effect of compressive stress on gene expression related to migratory phenotype. They were tumor metastasis microarray and extracellular matrix (ECM) and adhesion molecules array. Their gene tables are displayed in Appendix Figure A2. The tumor metastasis microarray includes genes encoding several classes of protein factors such as cell adhesion, ECM components, cell cycle, cell growth and proliferation, apoptosis, transcription factors and

regulators and other gens related to tumor metastasis. The ECM and adhesion molecules array contains ECM proteins including basement membrane constituents, collagens, and genes playing a role in ECM structure such as ECM proteases and their inhibitors. It also includes molecules important to cell-cell and cell-matrix adhesions such as transmembrane molecules and integrin subunits.

A

Array Layout

Gapdh 1	Apc 2	Bai1 3	Brms1 4	Ctnna1 5	Ctnnb1 6	Cav1 7	Ccl7 8
Cd44 9	Cdh1 10	Cdh11 11	Cdh6 12	Cdh8 13	Cdk4 14	Cdkn2a 15	Chd4 16
Col4a2 17	Csf1 18	Cst7 19	Ctbp1 20	Ctsk 21	Ctsl 22	Cxcl12 23	Cxcr4 24
Denr 25	Ela2 26	Ephb2 27	Etv4 28	Etv6 29	Ewsr1 30	Fat1 31	Fgfr4 32
Flt4 33	Fn1 34	Fxyd5 35	Gpnmb 36	Kiss1r 37	Gzma 38	Hdac1 39	Hgf 40
Hpse 41	Hras1 42	Htatip2 43	Igf1 44	Il18 45	Il1b 46	Il8rb 47	Itga7 48
Itgb3 49	Cd82 50	Kiss1 51	Kras 52	Lamb1-1 53	Rpsa 54	Mycl1 55	Mcam 56
Mdm2 57	Met 58	Metap2 59	Mgat5 60	Mmp10 61	Mmp11 62	Mmp13 63	Mmp2 64
Mmp3 65	Mmp7 66	Mmp9 67	Mta1 68	Mta2 69	Mtss1 70	Myb 71	Myc 72
Nf2 73	Nme1 74	Nme2 75	Nme4 76	Nr4a3 77	P2ry5 78	Chmp1a 79	Plaur 80
Pnn 81	Prkar1a 82	Pten 83	Pthlh 84	Ptp4a3 85	Rb1 86	Reck 87	Rhoc 88
Rorb 89	S100a4 90	Serpinb5 91	Set 92	Slpi 93	Smad2 94	Smad4 95	Src 96
Sstr2 97	Syk 98	Tcf20 99	Tgfb1 100	Tiam1 101	Tiam2 102	Timp2 103	Timp3 104
Timp4 105	Tmprss4 106	Tnfsf10 107	Tpbg 108	Trp53 109	Trpm1 110	Tshr 111	Twist1 112
Vegfa 113	Ezr 114	PUC18 115	Blank 116	Blank 117	AS1R2 118	AS1R1 119	AS1 120
Rps27a 121	B2m 122	Hsp90ab1 123	Hsp90ab1 124	Ppia 125	Ppia 126	BAS2C 127	BAS2C 128

B

Array Layout

Gapdh 1	Adamts1 2	Adamts2 3	Adamts5 4	Adamts8 5	Ctnna1 6	Ctnna2 7	Ctnnb1 8
Cd44 9	Cdh1 10	Cdh2 11	Cdh3 12	Cdh4 13	Cdh5 14	Cntn1 15	Col11a1 16
Col11a2 17	Col18a1 18	Col1a1 19	Col24a1 20	Col27a1 21	Col2a1 22	Col3a1 23	Col4a1 24
Col4a2 25	Col4a3 26	Col4a6 27	Col5a1 28	Col5a3 29	Col6a1 30	Col6a2 31	Col8a1 32
Col9a1 33	Vcan 34	Ctgf 35	Ecm1 36	Emilin1 37	Entpd1 38	Fbln1 39	Fn1 40
Hapln1 41	Hc 42	Icam1 43	Itga2 44	Itga2b 45	Itga3 46	Itga4 47	Itga5 48
Itga6 49	Itga7 50	Itga8 51	Itgae 52	Itgal 53	Itgam 54	Itgav 55	Itgax 56
Itgb1 57	Itgb2 58	Itgb3 59	Itgb4 60	Itgb5 61	Itgb6 62	Itgb7 63	Lama1 64
Lama2 65	Lama3 66	Lama4 67	Lama5 68	Lamb1-1 69	Lamb2 70	Lamb3 71	Lamc1 72
Mmp10 73	Mmp11 74	Mmp12 75	Mmp13 76	Mmp14 77	Mmp15 78	Mmp16 79	Mmp17 80
Mmp19 81	Mmp1a 82	Mmp2 83	Mmp20 84	Mmp23 85	Mmp24 86	Mmp3 87	Mmp7 88
Mmp8 89	Mmp9 90	Ncam1 91	Ncam2 92	Pecam1 93	Postn 94	Sele 95	Sell 96
Selp 97	Sgce 98	Sparc 99	Spock1 100	Spp1 101	Syt1 102	Tgfbi 103	Thbs1 104
Thbs2 105	Thbs3 106	Thbs4 107	Timp1 108	Timp2 109	Timp3 110	Timp4 111	Tnc 112
Vcam1 113	Vtn 114	PUC18 115	Blank 116	Blank 117	AS1R2 118	AS1R1 119	AS1 120
Rps27a 121	B2m 122	Hsp90ab1 123	Hsp90ab1 124	Ppia 125	Ppia 126	BAS2C 127	BAS2C 128

Appendix Figure A2. Gene tables for SABiosciences microarrays. A, Tumor metastasis array. **B,** Extracellular matrix and adhesion molecules array. Additional information can be found from SABiosciences website: http://www.sabiosciences.com.

Effect of compressive stress on nuclear localization of beta-catenin

Nuclear localization of beta-catenin is one of molecular markers for epithelial-to-mesenchymal transition (EMT) – a transformation process of an epithelial cell to a mesenchymal cell with increased migratory and invasion potentials[1]. In addition, high activity of beta-catenin has been shown as a poor prognostic marker for breast cancer patients[2]. To examine whether compressive stress induces translocation of beta-catenin to nuclei, we fixed the 67NR cells at the end of the in vitro scratch wound-compression experiment, and then performed immunofluorescent staining using anti-beta-catenin antibody (Clone 14; BD Transduction Laboratories).

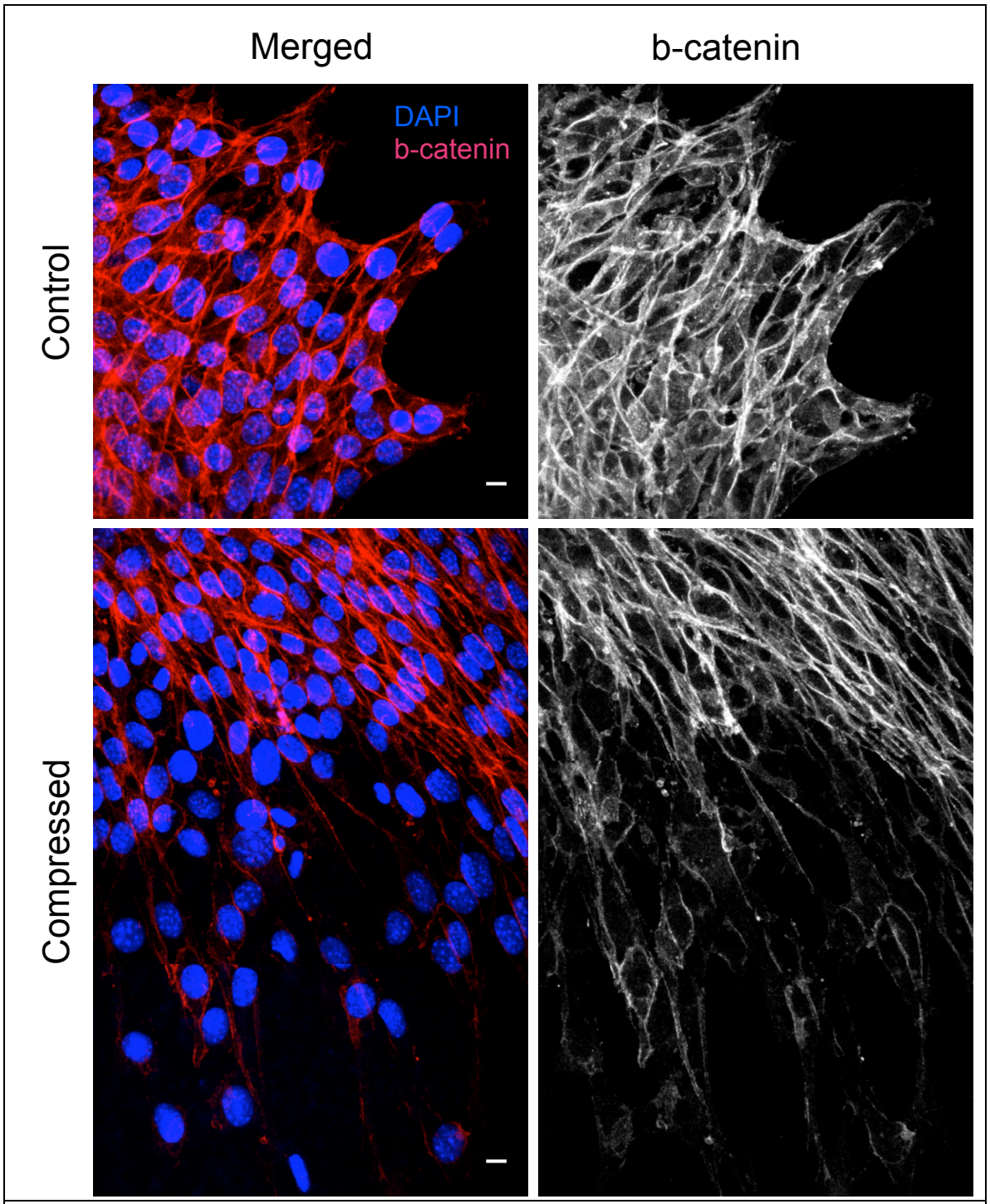

Appendix Figure A3. Compressive stress does not induce nuclear localization of beta-catenin. Immunostaining of beta-catenin (Cy3; red) of 67NR cells at the periphery of the cell-denuded area after 20 hours. Fluorescent staining of beta-catenin is localized

between cell-cell borders in both control and compressed cultures. No beta-catenin staining is found in the nuclei of the compressed cells (n=12; scale bar, 10um).

Effect of compressive stress on fibroblasts

As a tumor grows in a confined matrix, the stroma (mainly consisted of fibroblasts) of the tumor also gets compressed. To gain insight into the effects of compressive stress on normal cells, we compressed normal fibroblasts (CRL-2575 from ATCC) and performed *in vitro* scratch wound assay. Interestingly, compressive stress did not affect the migration rate of normal fibroblasts.

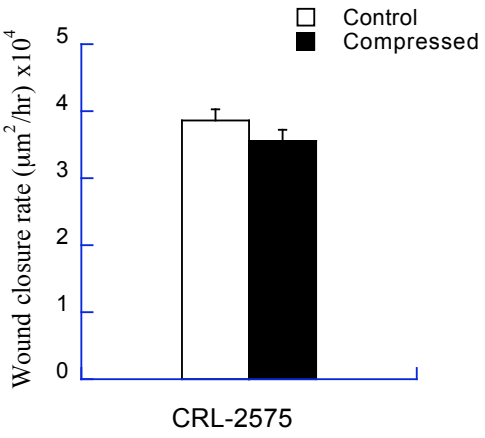

Appendix Figure A4. Compressive stress has no significant effect on fibroblast migration. Average migration rate obtained from the scratch-wound assay for normal fibroblasts (CRL-2575) subjected to stress-free (control) or a compressive stress of 5.8mmHg for 16 hrs using the device described in **Figure 2.1** (n=9). Error bars represent s.e.m.

References

1. Lee, J.M., S. Dedhar, R. Kalluri, and E.W. Thompson. 2006. The epithelial-mesenchymal transition: new insights in signaling, development, and disease. *J Cell Biol*. 172:973-81.
2. Lin, S.Y., W. Xia, J.C. Wang, K.Y. Kwong, B. Spohn, Y. Wen, R.G. Pestell, and M.C. Hung. 2000. Beta-catenin, a novel prognostic marker for breast cancer: its roles in cyclin D1 expression and cancer progression. *Proc Natl Acad Sci U S A*. 97:4262-6.

Appendix B

Results

Compression-induced lamellipodial protrusions in LS174T colon carcinoma cells

The human colon cancer cell line LS174T was obtained from Dr. R. Bresalier (Henry Ford Hospital, Detroit, Michigan). The cells were cultured in DMEM supplemented with 10% fetal bovine serum (FBS), and incubated at 37°C with 5%CO_2.

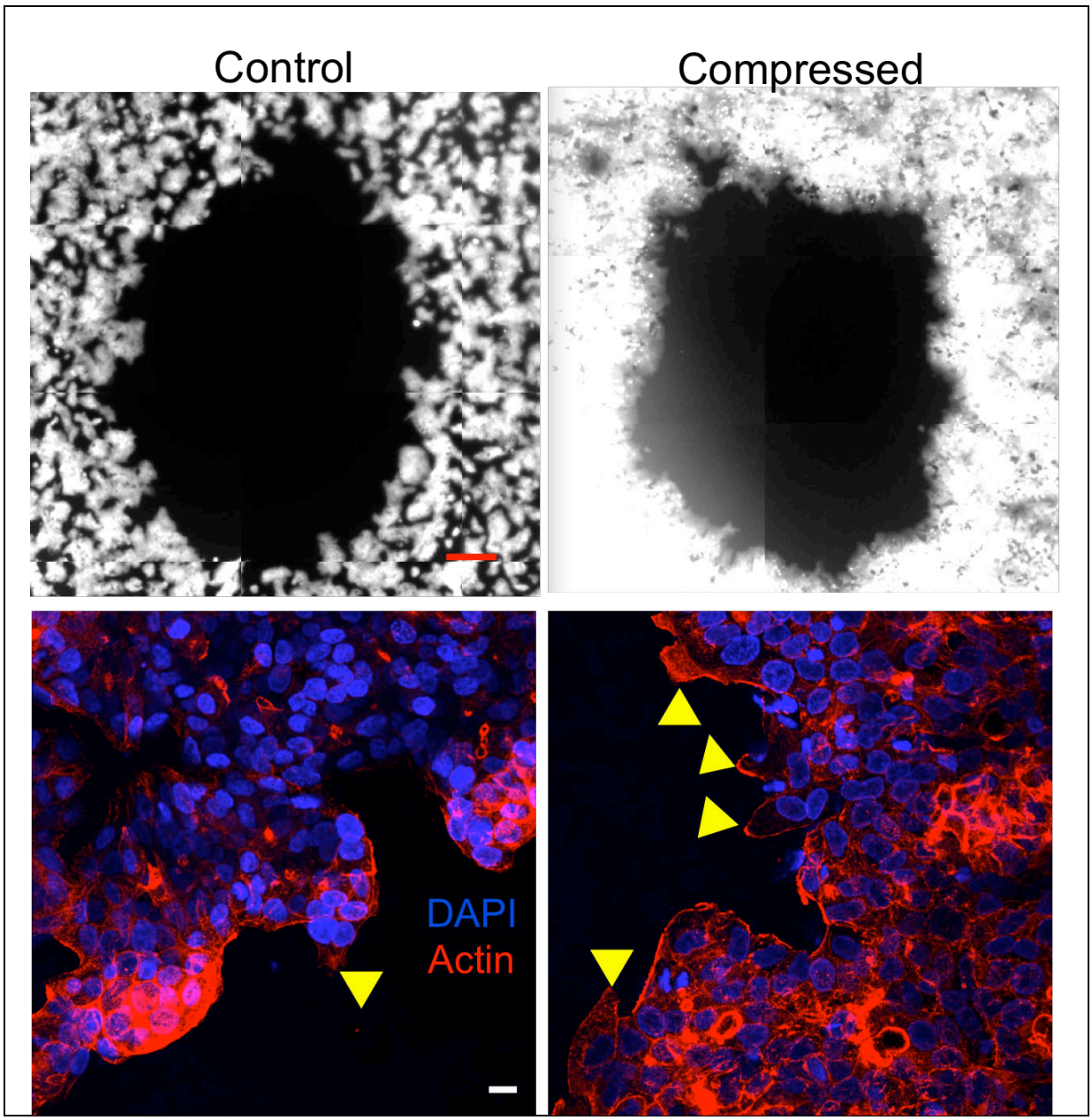

Appendix Figure B1. Compression induces lamellipodial protrusions in LS174T colon carcinoma cells. Representative images of control (left side) and compressed LS174T cells (right side) closing the "wound" after 16 hrs. The top panel shows the wound closure of LS174T-GFP cells under 16-hr stress-free (control) or compressive stress of 5.8mmHg, visualized by fluorescent microscopy. The cells were then fixed for phalloidin staining for actin microfilaments (bottom panel; red: actin microfilaments; blue: nuclei) and imaged by confocal microscopy. The compressed cells at the leading edge showed increased formation of lamellipodia indicated by the yellow triangles. Scale bar, 200um (top) and 10um (bottom).

Fluorescent images of the fibronectin-coated patterns created with polydimethylsiloxane (PDMS) stamps

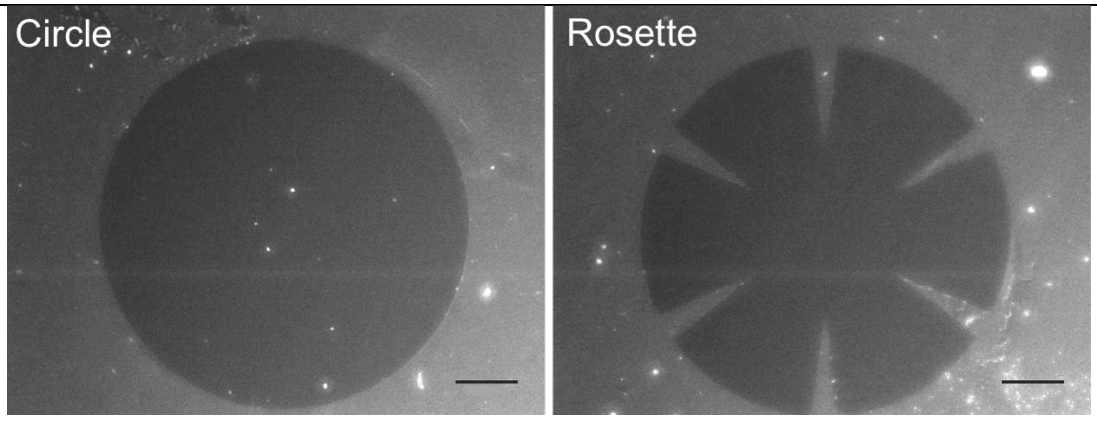

Appendix Figure B2. Fibronectin-coated patterns created with PDMS stamps. Rhodamine-conjugated fibronectin mixed in equal parts with unconjugated fibronectin was used to create fibronectin-coated patterns by adsorbing the protein on a PDMS pattern, and transferring it onto the transwell membranes. Using this stamping procedure, the 67NR cells could be patterned on fibronectin-coated areas, generating different geometric patterns, such as circular voids (left) or rosette-void areas (right). Scale bar,

100um.

Appendix C

Methods

Inhibition of cadherin-mediated cell-cell adhesion

To disrupt the calcium-dependent cell-cell adhesion mediated by cadherins, a chelating agent, ethylenediaminetetraacetic acid (EDTA), at various concentrations (1, 3, 5, 8, 10mM) or calcium-free medium were used but in vain, because divalent ions are important for both cadherin-based and integrin signaling. As a result, when too high concentration of EDTA (>3mM) or calcium-free medium was used, clumps of cells started to detach from the culture plates after 6 hours. However, too low concentration of EDTA (≤1mM) could not segregate the cells effectively. Similarly, calcium-depleted medium affect 67NR cell spreading and cell viability.

To determine the optimum concentration for the E-cadherin blockade experiment, the E-cadherin antibody effect on cell migration was titrated at concentrations ranging from 1 to 10ug/mL, using the scratch-wound assay. The wound closure rate increased with the antibody concentration, and the optimum concentration was determined when a plateau was reached.

Screening of integrins responsible for fibronectin-induced migration

To determine the optimum concentration for blocking integrin function, we cultured 67NR cells on fibroenctin-coated surface in the presence of various integrin antibodies ($\beta1$, $\beta3$, αIIb, αv, and $\alpha6$) at three different concentrations (10, 50, and 200 ug/mL) and performed the scratch-wound experiment. The αv integrin antibody did not have any

effect on wound closure rate at any concentrations. Despite the reduced wound closure rate, the αIIb or α6 integrin antibodies at a concentration of 200ug/mL might cause non-specific blocking because some cell debris was observed (data not shown). Therefore, we decided to use the concentration of 50ug/mL, which is a typical concentration shown in literature.

Results

Treatment of colon carcinoma cells with anti-E-cadherin antibody

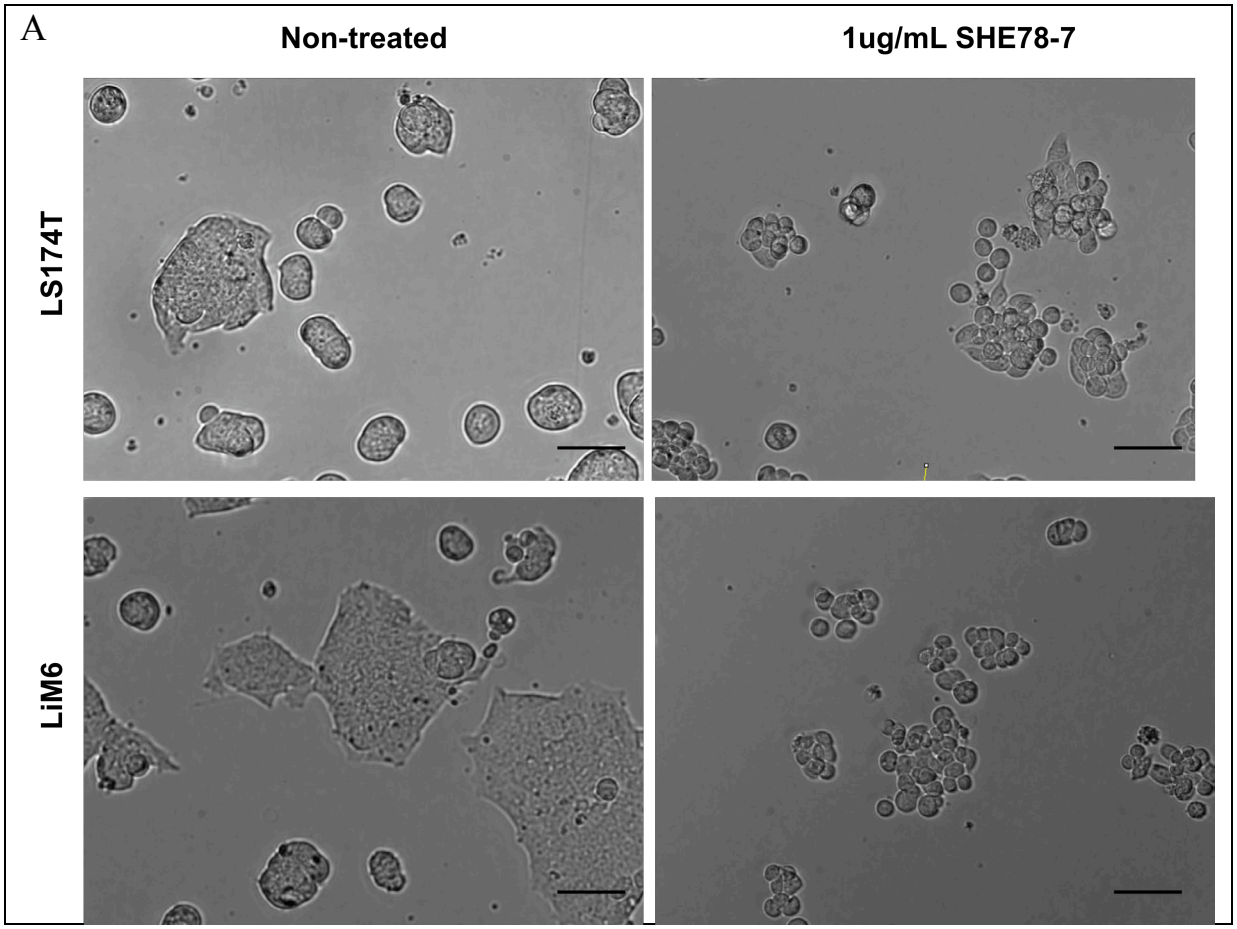

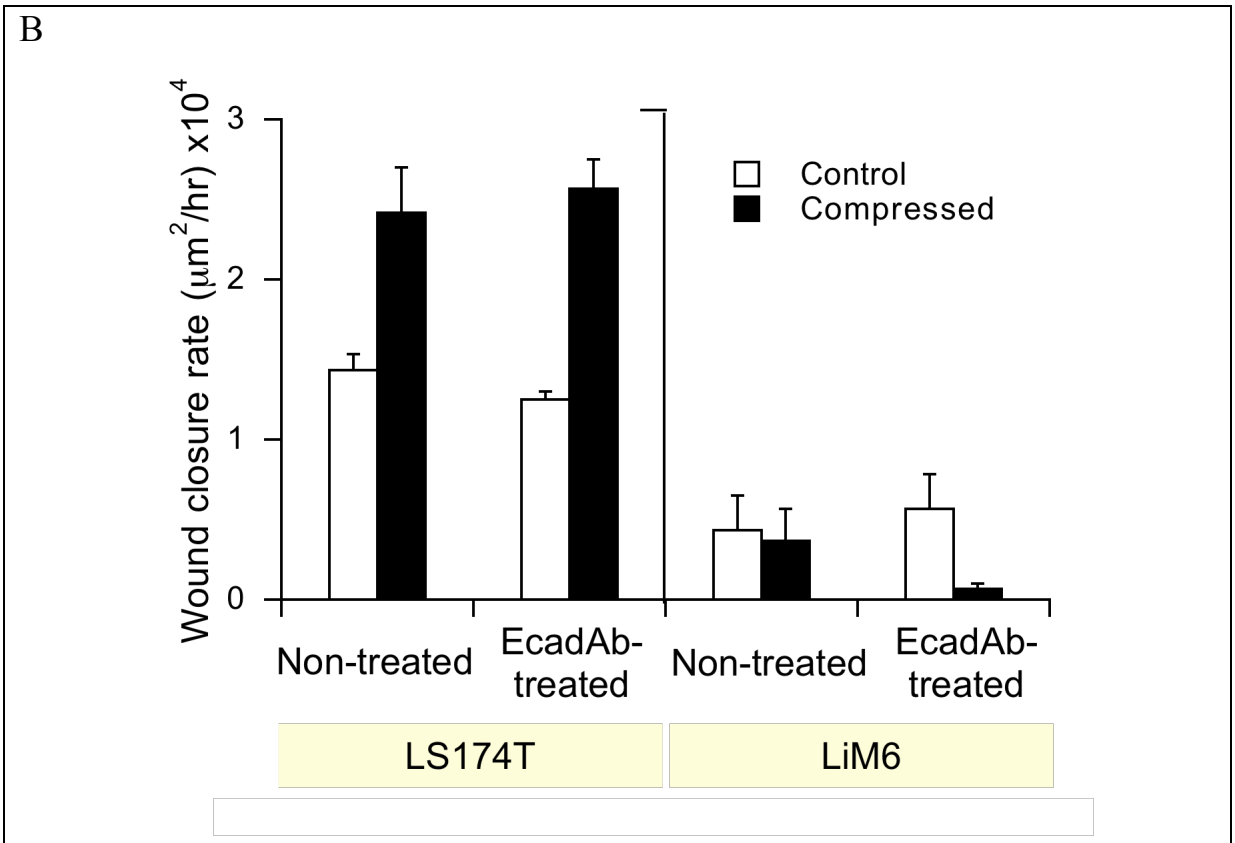

Appendix Figure C1. Loss of E-cadherin-mediated cell adhesion has no effect on LS174T or LiM6 colon carcinoma cell migration. A, Representative images of LS174T and LiM6 cells with reduced cell-cell adhesion after treatment with 1ug/mL of E-cadherin blocking antibody (SHE78-7). In absence of E-cadherin blocking antibody, each cell border was hardly identified because of the adheren junctions formed between cells (Scale bar, 100um). **B,** Average migration rate of LS174T and LiM6 cells treated with 1ug/mL IgG2a (non-treated: n=4-5) or 1ug/mL of E-cadherin blocking antibody (SHE78-7: n=4-6) and exposed to 0 (control) or 5.8mmHg compressive stress for 18 hrs. Blocking E-cadherin-mediated cell adhesion caused LS174T and LiM6 cells to segregate, but did not significantly influence their motility, either under stress-free or compressed conditions. Error bars represent s.e.m.

Synthetic RGD peptides and anti-fibronectin antibody

The primary sequence motif of fibronectin for integrin binding is a tripeptide, Arg-Gly-Asp (RGD) [1]. Synthetic peptides containing the RGD motifs have been used extensively as inhibitors of integrin-ligand interactions in studies of cell adhesion and migration [2,3]. However, in our study, the two peptides (RGDS and RGDTP) at concentrations up to 1mM did not significantly reduce migration of 67NR cells on fibronectin-coated surfaces (Appendix Fig. C2). It has been shown that the affinity for short peptides containing the RGD sequence varies significantly among these integrins [1]. For example, the area in the vinicity of the RGD site (synergy site PHSRN) is required for high affinity binding with integrin $\alpha 5\beta 1$, but not with integrin $\alpha v\beta 3$ [1]. Therefore, if integrin $\alpha 5\beta 1$ is involved in compression-induced migration, short synthetic peptides might not be effective to block the integrin function.

In another experiment using antibody to fibronectin, which has been shown to inhibit cell attachment to 2D fibronectin by 95% [4], fibronectin-mediated cell migration appeared to be dose-dependent in a bell-shaped curve (Appendix Fig. C2). We speculated that at low concentrations, the anti-fibronectin antibody could decrease cell-cell adhesion mediated by fibronectin, resulting in increased migration. However, increasing antibody concentrations could eventually hinder cell-fibronectin interactions and in turn negatively affect cell migration.

A

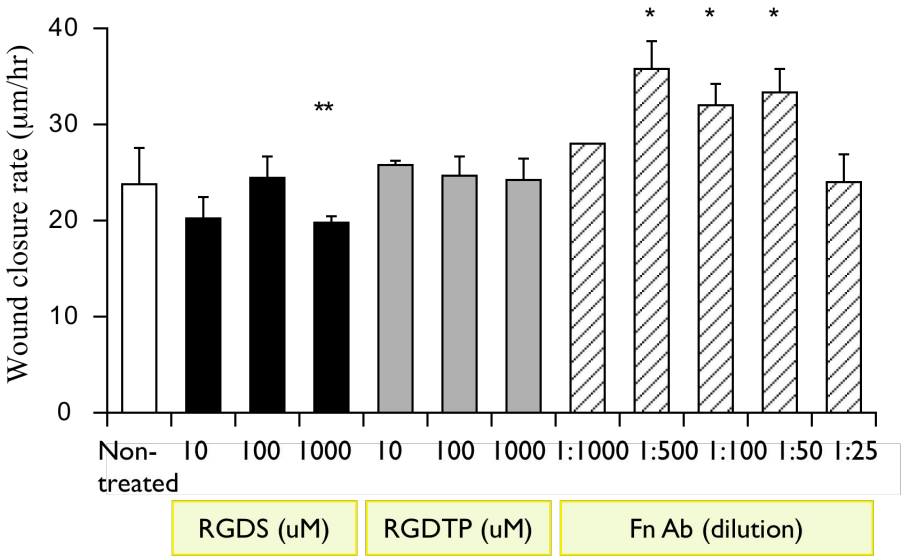
Wound closure rate (μm/hr)
40
30
20
10
0
**
* * *
Non-treated
10
100
1000
10
100
1000
1:1000
1:500
1:100
1:50
1:25
RGDS (uM)
RGDTP (uM)
Fn Ab (dilution)

B

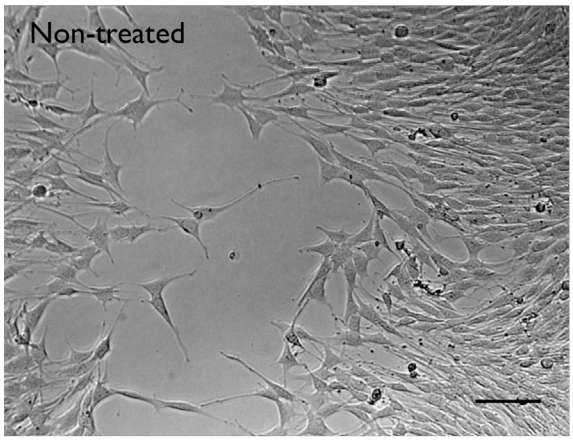
Non-treated

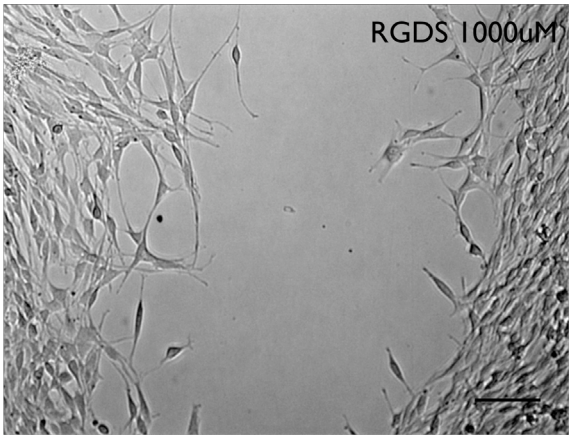
RGDS 1000uM

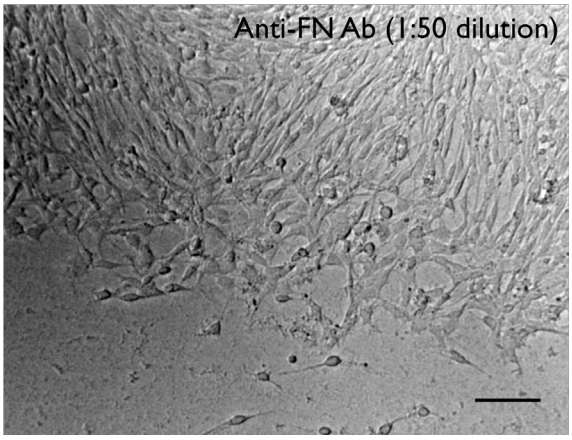
Anti-FN Ab (1:50 dilution)

Appendix Figure C2. Blocking fibronectin-integrin interaction with RGD peptides or an antibody to fibronectin does not necessarily reduce fibronectin-induced migration. A, Average migration rate of 67NR cells seeded on fibronectin-coated surface and either non-treated (n=9) or treated with indicated concentrations of RGD peptides or anti-fibronectin antibody (n=3) over 16 hours. Blocking RGD sequence on fibronectin using two different sequences of RGD short peptides has no significant effect on fibronectin-induced migration. Even at very high concentration (1mM), the effect is minimal. The dose effect of anti-fibronectin antibody on 67NR cell migration follows a bell-shape response. (**P<0.05 and *P<0.005 compared to the non-treated control.) Error bars represent s.d. **B,** Representative images of 67NR cells either non-treated or treated with (1000uM RGDS peptides or 1:50 dilution of antiserum against fibronectin). There are no significant changes in 67NR cell morphology after culturing them with RGDS peptides or anti-fibronectin antibodies, suggesting that the treatment does not affect the cell attachment to fibronectin substrate. Scale bar, 100um.

Effect of compressive stress on expression of focal adhesion kinase (FAK)

Focal adhesion kinase (FAK) is a cytoplasmic tyrosine kinase that colocalizes with integrins at focal adhesions. Phosphorylation of FAK at Tyr-397 upon cell adhesion allows FAK to regulate tyrosine phosphorylation of downstream substrate such as paxillin[5]. Previous studies have shown that FAK signaling modulates cell adhesion[6,7]and migration [8]. Appendix Figure C3 shows that compressed 67NR cells appeared to have lower level of FAK(Y397) phosphorylation than that of the control cells, despite enhanced cell migration induced by compressive stress. However, a

previous report has demonstrated that cell polarization induced by shear stress is more important than the total level of FAK(Y397) phosphorylation for directional cell migration[5]. Similarly, in our study, compression-induced cell polarization (Chapter 3) could play a dominant role in modulating directional cell migration rather than the FAK signaling.

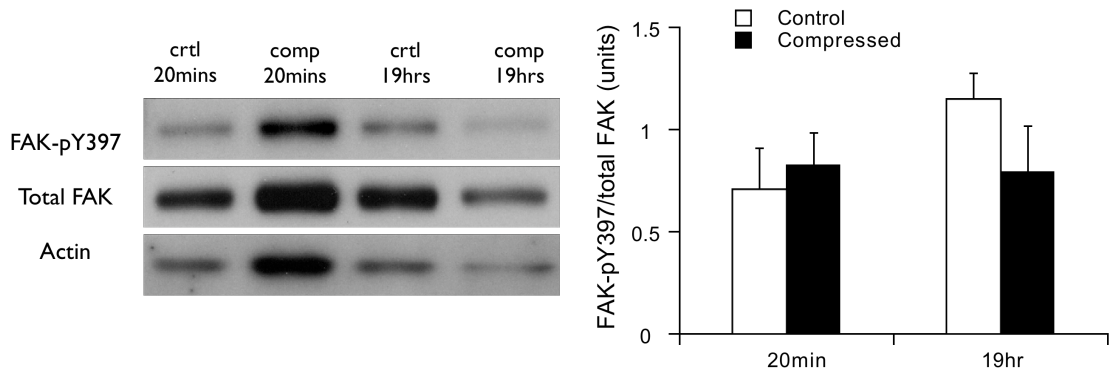

Appendix Figure C3. Compression appears to reduce the phosphorylated level of focal adhesion kinase (FAK). Western blot analysis of total and phosphorylated (Y397) levels of FAK in 67NR cells subjected to stress-free or a compressive stress of 5.8mmHg for the indicated length of compression time. Data representative of 2 independent experiments in which 3 samples were pooled together. The compressed cultures expressed lower fraction of phosphorylated FAK after 16-hr compression. Error bars presents s.d. Primary antibodies used were: anti-FAK-pY397 (clone 18; 1:500 dilution; Millipore); total FAK (polyclonal; 1:1000 dilution; Millipore); b-actin (clone AC-14; 1:5000 dilution: Sigma).

References

1. Johansson, S., G. Svineng, K. Wennerberg, A. Armulik, and L. Lohikangas. 1997. Fibronectin-integrin interactions. *Front Biosci*. 2:d126-46.
2. Ruoslahti, E. 1996. RGD and other recognition sequences for integrins. *Annu Rev Cell Dev Biol*. 12:697-715.
3. Oharazawa, H., N. Ibaraki, K. Ohara, and V.N. Reddy. 2005. Inhibitory effects of Arg-Gly-Asp (RGD) peptide on cell attachment and migration in a human lens epithelial cell line. *Ophthalmic Res*. 37:191-6.
4. Cukierman, E., R. Pankov, D.R. Stevens, and K.M. Yamada. 2001. Taking cell-matrix adhesions to the third dimension. *Science*. 294:1708-12.
5. Li, S., P. Butler, Y. Wang, Y. Hu, D.C. Han, S. Usami, J.L. Guan, and S. Chien. 2002. The role of the dynamics of focal adhesion kinase in the mechanotaxis of endothelial cells. *Proc Natl Acad Sci U S A*. 99:3546-51.
6. Dumbauld, D.W., K.E. Michael, S.K. Hanks, and A.J. Garcia. 2009. Focal adhesion kinase-dependent regulation of adhesive force involves vinculin recruitment to focal adhesions. *Biol Cell*.
7. Michael, K.E., D.W. Dumbauld, K.L. Burns, S.K. Hanks, and A.J. Garcia. 2009. Focal adhesion kinase modulates cell adhesion strengthening via integrin activation. *Mol Biol Cell*. 20:2508-19.
8. Crowe, D.L., and A. Ohannessian. 2004. Recruitment of focal adhesion kinase and paxillin to beta1 integrin promotes cancer cell migration via mitogen activated protein kinase activation. *BMC Cancer*. 4:18.

Appendix D

Effect of action probability on cell migration

At each time step, each non-proliferating cell could choose to perform no action, or either protrude or translocate, based on an action probability. Using the base condition, we experimented with different values of the action probability to determine its effect on cell migration. The action probability did not affect the overall migration pattern, but the overall migration rate was lower (Appendix Fig. D1, A-D). In addition, when the probability was set at 0.5 or lower, about 42% of the cells did not move (Appendix Fig. D2). In order to have more cells involved in migration simulation while introducing some randomness, we set the probability at 0.7.

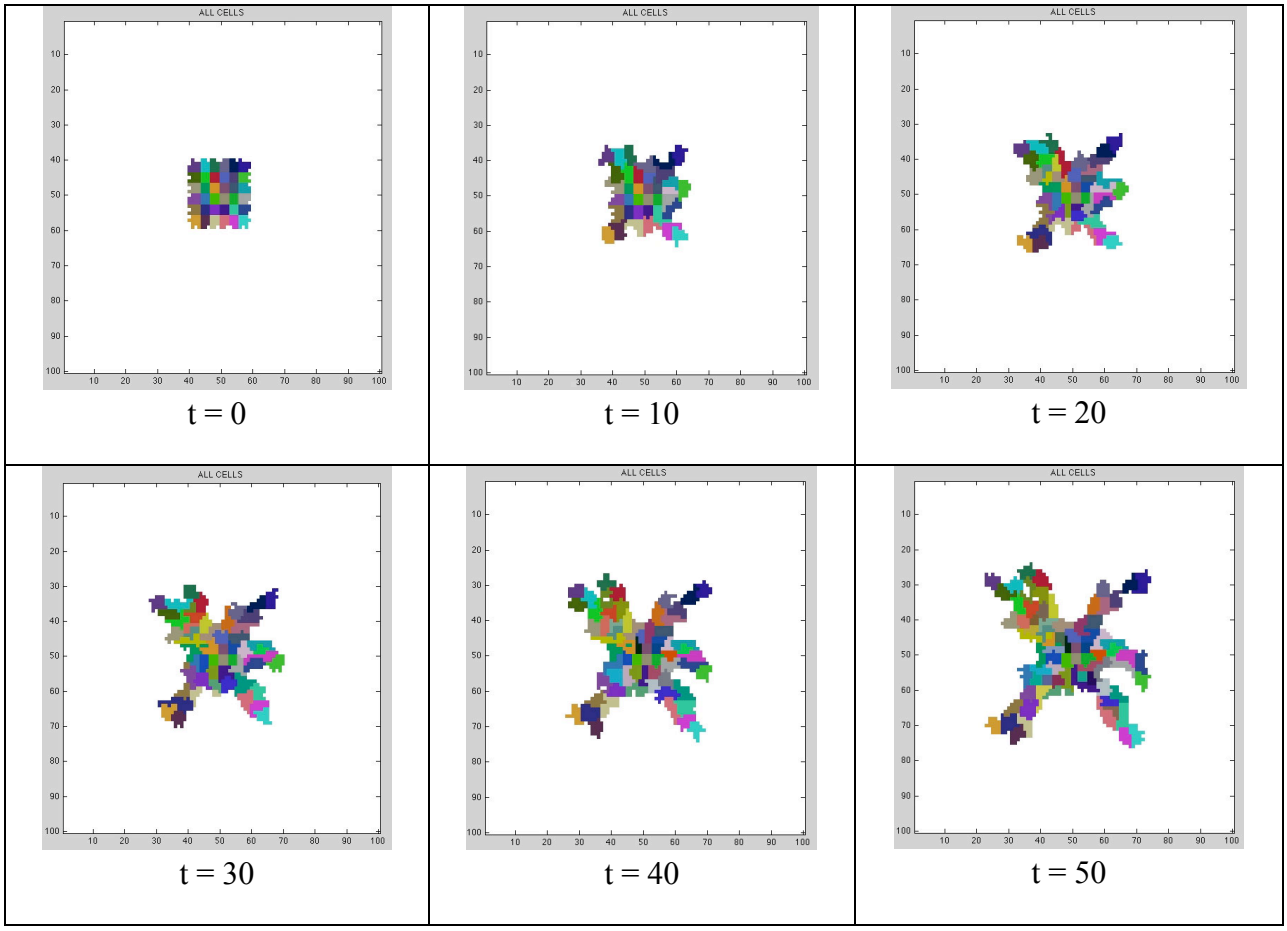

Appendix Figure D1, A: Simulation of collective migration under stress-free condition with an action probability of 1.

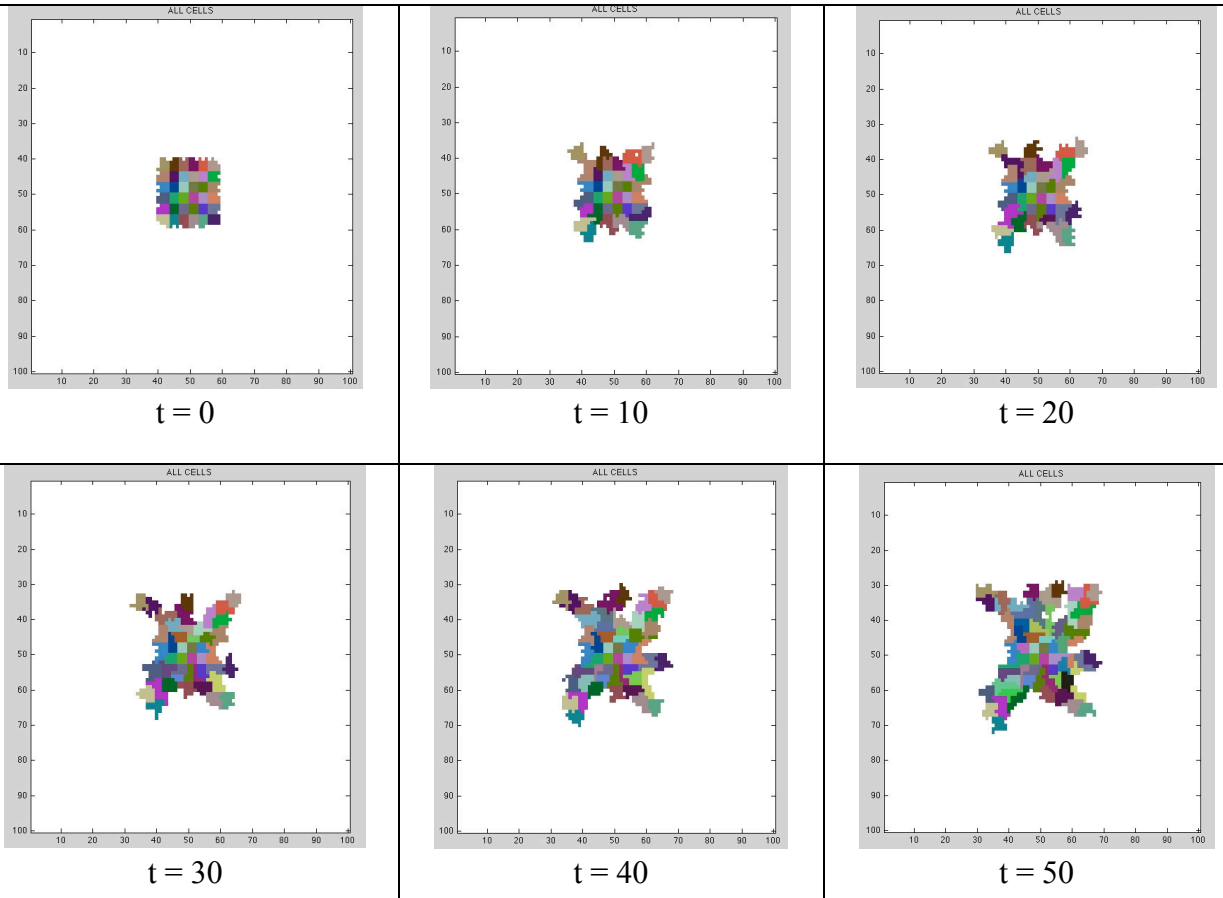

Appendix Figure D1, B: Simulation of collective migration under stress-free condition with an action probability of 0.7.

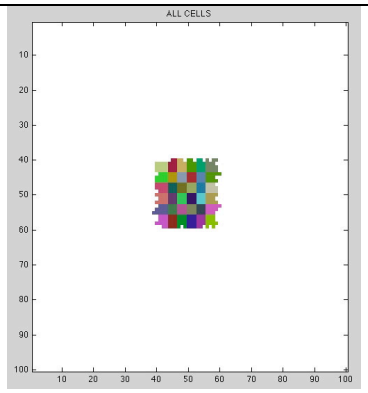

t = 0

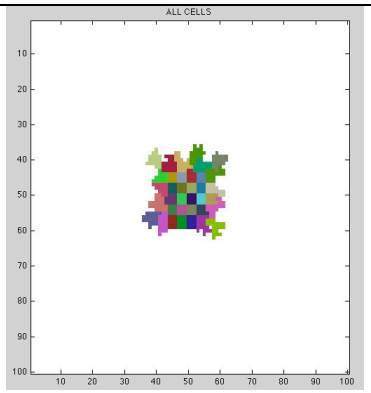

t = 10

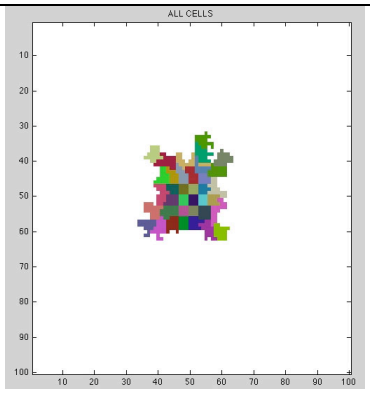

t = 20

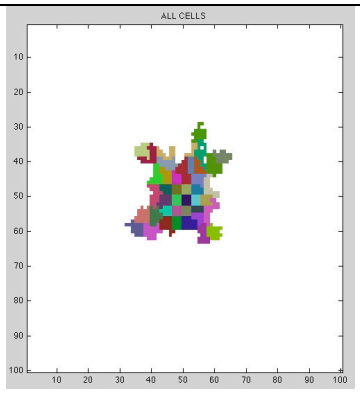

t = 30

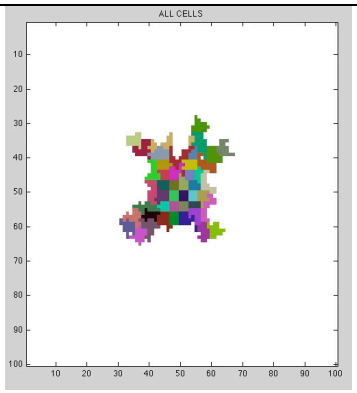

t = 40

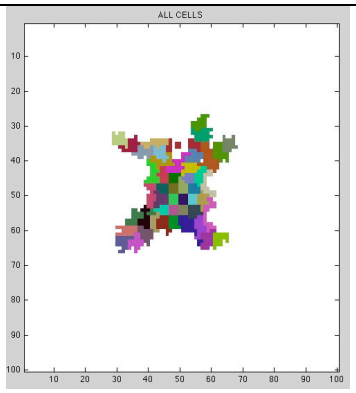

t = 50

Appendix Figure D1, C: Simulation of collective migration under stress-free condition with an action probability of 0.5.

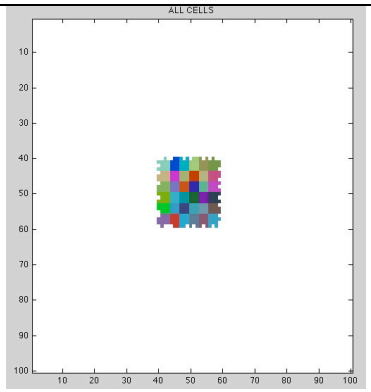

t = 0

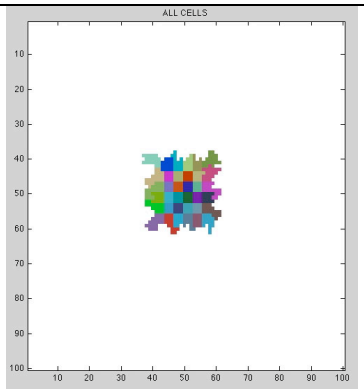

t = 10

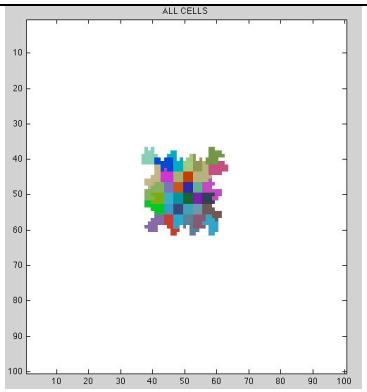

t = 20

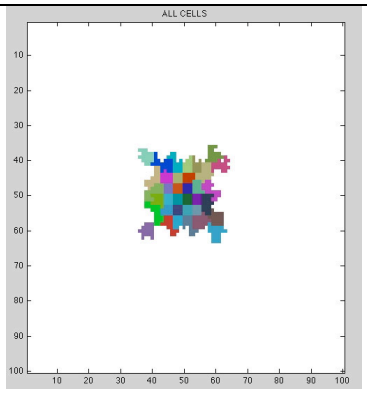

t = 30

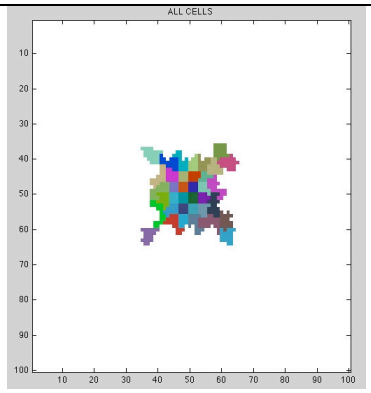

t = 40

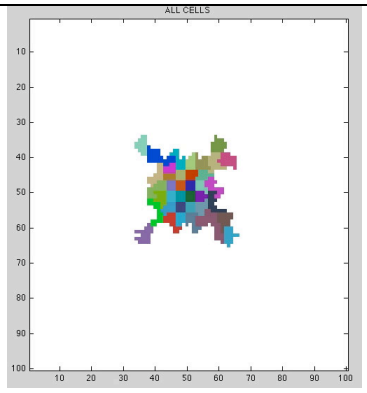

t = 50

Appendix Figure D1, D: Simulation of collective migration under stress-free condition with an action probability of 0.3.

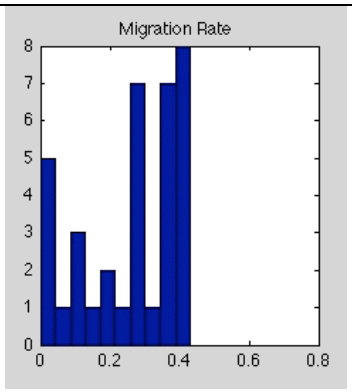

Probability = 1

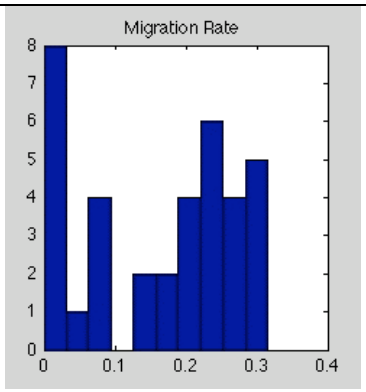

Probability = 0.7

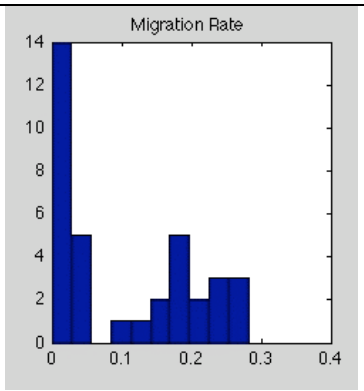

Probability = 0.5

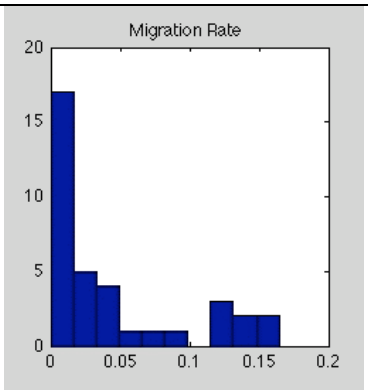

Probability = 0.3

Appendix Figure D2: Histogram of migration rates for simulations in Appendix Figure D1.